

**A STUDY OF METHANE-RELATED PROCESSES IN FRESHWATER
ECOSYSTEMS: METHANOGENESIS, ANAEROBIC METHANE OXIDATION,
AND INTERACTIONS WITH OTHER TERMINAL METABOLISMS**

by

KATHERINE EOWYN SEGARRA

(Under the Direction of Samantha B. Joye)

ABSTRACT

This dissertation seeks to understand the seasonal controls of methane cycling in freshwater sediments. Using a combination of field measurements, radiotracer incubations, porewater characterization, lipid biomarker analysis, and stable carbon isotopes, pronounced seasonal variations in microbial carbon turnover were documented in a freshwater sediment and in two peat wetlands. Constraints of the methane budget in shallow (< 40 cm) sediments revealed a seasonal imbalance between methane fluxes and methane production that may be relieved through tidal pumping of methane-laden porewaters derived from adjacent high marsh through the creekbank. Rate measurements of sulfate reduction and the anaerobic oxidation of methane (AOM), two processes not typically considered relevant in low salinity habitats, revealed their importance in freshwater settings. Seasonal variations in AOM may be driven by fluctuations in hydrogen and acetate dynamics generated by variations in other microbial metabolisms (e.g. sulfate reduction and methanogenesis). Lipid biomarker analysis revealed the presence of sulfate-reducing bacteria and archaea associated with methane cycling.

However, seasonal variations in microbial metabolisms were not associated with changes in the lipid distribution. Stable carbon isotope analyses revealed the imprint of AOM on the signatures of methane and dissolved inorganic carbon. The influence of methanotrophy, however, was not as pronounced in the microbial lipid signatures. A potential AOM isotopic signal may have been diluted by methanogenesis and other autotrophic and heterotrophic processes, which may mask a clear methanotrophic signature. While sulfate reduction activity is sufficient to support all observed AOM activity, no conclusive evidence was found to link these processes. Long-term enrichments of coastal sediments with various electron acceptors demonstrated a positive influence of sulfate and ferric citrate additions on AOM. Other electron acceptors such as nitrate and manganese may also support AOM in these coastal settings. These studies advance the understanding of the seasonal controls on methane emissions, methane production, and methane consumption via AOM in freshwater ecosystems. Future efforts are aimed at closer examinations of these mediating factors, especially temperature changes and substrate availability.

INDEX WORDS: methane, sulfate, biogeochemistry, AOM, methanogenesis,
freshwater, wetland, lipid

**A STUDY OF METHANE-RELATED PROCESSES IN FRESHWATER
ECOSYSTEMS: METHANOGENESIS, ANAEROBIC METHANE OXIDATION,
AND INTERACTIONS WITH OTHER TERMINAL METABOLISMS**

by

KATHERINE EOWYN SEGARRA

BS, Brown University, 2002

A Dissertation Submitted to the Graduate Faculty of The University of Georgia in Partial

Fulfillment of the Requirements for the Degree

DOCTOR OF PHILOSOPHY

ATHENS, GEORGIA

2012

© 2012

Katherine Eowyn Segarra

All Rights Reserved

**A STUDY OF METHANE-RELATED PROCESSES IN FRESHWATER
ECOSYSTEMS: METHANOGENESIS, ANAEROBIC METHANE OXIDATION,
AND INTERACTIONS WITH OTHER TERMINAL METABOLISMS**

by

KATHERINE EOWYN SEGARRA

Major Professor:	Samantha B. Joye
Committee:	Christof Meile
	Vladimir Samarkin
	Kai-Uwe Hinrichs
	William 'Barny' Whitman

Electronic Version Approved:

Maureen Grasso
Dean of the Graduate School
The University of Georgia
May 2012

ACKNOWLEDGEMENTS

Above all I must thank my advisor, Mandy Joye. Her support, both intellectual and financial, made this work possible. I am in her debt for her guidance, for providing quality feedback and insight, and for always challenging me to reach beyond my limits.

I would also like to thank my other committee members, for whom I have a great deal of respect and admiration. Vladimir Samarkin, who was very giving of his time and knowledge, always had a kind face and a good joke. I appreciate the intellectual and emotional support he has provided over the years. Christof Meile has been very supportive during my PhD tenure. He is a wonderful editor and provided creative solutions to problems I faced. William ‘Barny’ Whitman was both a great teacher and committee member. I appreciate his wisdom and thoughtful comments. And last, but not least, I thank Kai-Uwe Hinrichs, who is both a great scientist and a great advisor. I am so grateful to him for making my time in Bremen an unforgettable experience.

Working in the Joye Lab has been an amazing experience and I wish to thank all of its members, both past and present, especially Laura Polomo, Christelle Hyacinthe, Melitza Crespo-Medina, Charles Schutte, Chris Comerford, and Julia Slaughter. Thanks to Kim Hunter for keeping things running smoothly and efficiently. Special thanks to Bill Porubsky for getting my feet wet in the field of biogeochemistry and navigating the science world. A big thank you to my undergraduate helpers, especially Ruthie Taylor, Laura Potter, Leia Edenfelder, and Will Spence.

There is a small but special community of people in Athens that made this journey all the better. A big hug to Megan ‘Chubi’ Machmuller, Peter Baas, and Andrew Binderup – thanks for the camaraderie and love. I am grateful to Beth! Orcutt for being a real friend in the science world. You are an inspiration to me – kein Fleisch! Eric King was an invaluable colleague whether we were pondering data or driving up and down the east coast in a windowless van. Thanks for all the Dexters and the Weezer snuggie.

My time at the MARUM in Bremen, Germany were the most rewarding months of my PhD program. I thank the A.G. Hinrichs for making me feel very welcome and for their generosity of knowledge, time, and energy. I especially thank Florence Schubotz for her tireless enthusiasm, and for her wonderful analytical and editorial assistance. A big thanks to my other Bremen-based co-authors, Marcos Yoshinaga, and Verena Heuer. A special thanks to Julius Lipp, Matthias Kellerman, Marcus Elvert, Xavier Prieto, Eoghan Reeves, and Travis Meador for teaching me the ins and outs of lipid analysis, for hot mensa dates, and for making those long days huffing solvents even more enjoyable.

I thank my family (Mom, Dad, and Ben), whose generosity, support, and unconditional love have been wondrous gifts that I may never repay. And finally, I thank Noah, my light when all other lights have gone out.

This dissertation project was primarily funded by a NSF DEB award. The LTER sites at the Georgia Coastal Ecosystems and the Florida Coastal Everglades provided field support and personnel. I especially want to thank Daniel Saucedo and Franco Tobias, two very capable and hardworking captains. Additional financial support was provided by a Boyd Scholarship, The Alfred E. Brown Scholarship, and a recruitment fellowship from the Graduate School at the University of Georgia.

TABLE OF CONTENTS

	Page
ACKNOWLEDGEMENTS	iv
CHAPTER	
1 INTRODUCTION	1
2 SEASONAL VARIATIONS OF METHANE FLUXES FROM A TIDAL, FRESHWATER WETLAND (HAMMERSMITH CREEK, GA)	11
3 TIDAL, FRESHWATER SEDIMENTS SUPPORT HIGH RATES OF ANAEROBIC OXIDATION OF METHANE.....	44
4 SEASONAL PATTERNS IN METHANE CYCLING IN FLORIDA AND MAINE PEAT WETLANDS	94
5 IMPACT OF ELECTRON ACCEPTOR AVAILABILITY ON THE ANAEROBIC OXIDATION OF METHANE IN COASTAL FRESHWATER AND BRACKISH INTERTIDAL SEDIMENTS	186
6 CONCLUSIONS AND OUTLOOK	250

CHAPTER 1

INTRODUCTION

“There is something fascinating about science. One gets such wholesale returns of conjecture out of such a trifling investment of fact.

— Mark Twain, *Life on the Mississippi*

Despite anthropogenic changes, microbial processes continue to play a key role in regulating the Earth’s atmosphere and climate. This PhD dissertation explored pathways of microbially-mediated carbon flow in freshwater environments. In these chapters, I examined the factors, both biotic (e.g., microbial community composition) and abiotic (e.g., temperature), that regulate terminal metabolism of organic carbon in anoxic sediments, with a specific focus on seasonal variations on rates and pathways of methane (CH₄) cycling in wetland ecosystems.

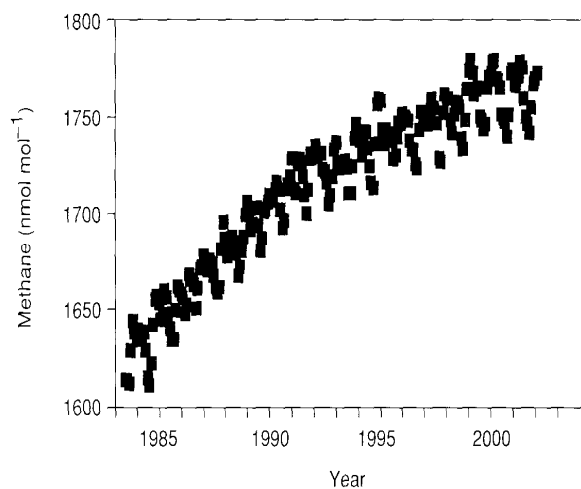


Figure 1.1: Atmospheric methane concentrations at the Mona Loa, Hawaii observatory from 1983 to 2002. From Canfield *et al.* (2005).

CH₄, a very potent greenhouse gas, has a heat-trapping potential twenty-five times that of carbon dioxide (BLAKE and ROWLAND, 1988). Increases of global atmospheric

methane levels (about 1% per year) contribute to present-day global warming (Fig. 1.1; IPCC, 2007; KHALIL and RASMUSSEN, 1990). Atmospheric methane concentrations are currently estimated at 1.8 ppm (IPCC, 2007). Sources of this methane include a variety of natural and anthropogenic (Fig. 1.2), the largest of which is natural wetlands (BROOK et al., 2008). A large uncertainty is associated with this source due to the high spatial variability of these systems and uncertainties of their area (BARTLETT and HARRISS, 1993). Methane emissions from wetlands have been implicated in both past (KAPLAN, 2002) and contemporary climate change (IPCC, 2007). In the face of rising global temperatures, further constraint of the sources and sinks of methane in freshwater wetlands is warranted.

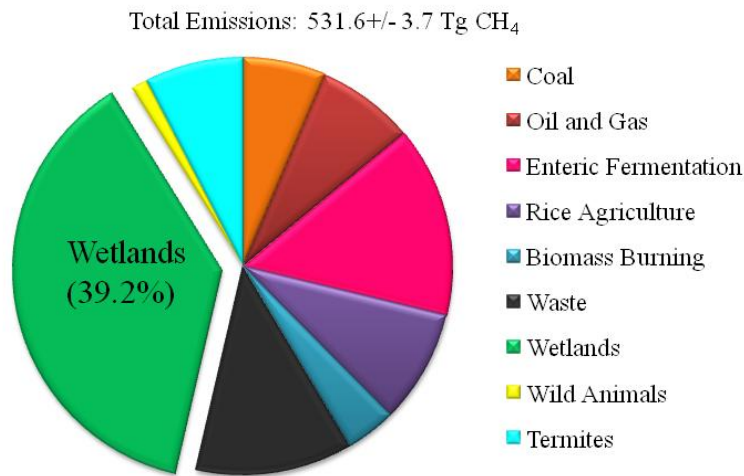


Figure 2. Sources of atmospheric methane (CH₄) presented as relative contribution to annual emissions (as reviewed by Brook et al. 2008).

In anoxic environments, the conversion of organic carbon to terminal products like carbon dioxide and CH₄ is accomplished by a series of interdependent microbial processes. CH₄

producers, or methanogens, are the largest and most diverse physiological group in the domain *Archaea* (WHITMAN et al., 1992). Whether organic carbon is converted to CH₄ or carbon dioxide often depends on whether sulfate is present: sulfate-reducing bacteria may outcompete methanogens for substrates (LOVLEY et al., 1982). Therefore, substantial CH₄

production occurs mainly in sulfate-limited environments (e.g. freshwater ecosystems or sulfate-depleted marine sediments).

Chapter 2 describes seasonal methane fluxes from a tidal, freshwater sediment (Hammersmith Creek) in coastal Georgia (Fig. 1.3). Methane fluxes were compared to rates of methane production, methane saturation state, and temperature. A 1D sediment model was employed to constrain the methane sources which support methane emissions from these sediments.

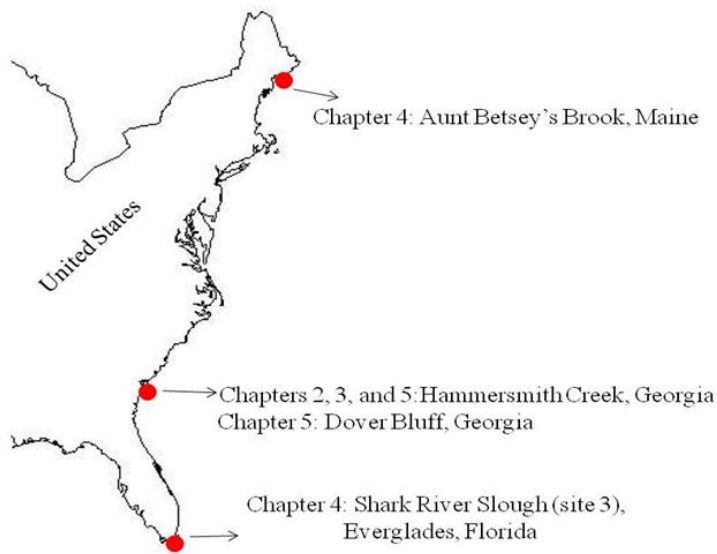


Figure 1.3. Map of study sites for chapters 2-5.

The primary precursors of CH_4 are either carbon dioxide and hydrogen (hydrogenotrophic methanogenesis) or acetate (acetoclastic methanogenesis; ZEIKUS, 1977). Other substrates for methane production include alcohols, methanol, formate, carbon monoxide, and methylated compounds (e.g.

dimethylsulfide, methylamines; SCHINK, 1997). In addition to primary fermentation of organic matter, the formation of acetate in sediments may be derived from carbon dioxide reduction with hydrogen (homoacetogenesis); homoacetogenesis-derived acetate may then serve as a substrate for acetoclastic methanogenesis. Conversely, under appropriate conditions, acetate may be syntrophically oxidized to CO_2 and H_2 , which may thereby provide substrates to hydrogenotrophic methanogens (ZINDER, 1994). The microorganisms

mediating the processes resulting in CH₄ production are often operating near or at minimum energy requirements to support growth; if environmental conditions are unfavorable, a given process may be inhibited or, in some cases, the reverse process may proceed (HOEHLER et al., 2001).

An important component of methane cycling in soils and sediments is methane oxidation. In oxic environments, aerobic methane-oxidizing bacteria consume large quantities of methane produced in the lower, anoxic horizons (SEGERS, 1998). The consumption of methane in anoxic settings is a widespread phenomenon in marine settings (as reviewed by VALENTINE, 2002). This process, dubbed AOM (anaerobic oxidation of methane), is believed to be performed by anaerobic methanotrophs (ANMEs) in the domain Archaea (HINRICHS and BOETIUS, 2002). However, recent studies indicate that at least one type of bacteria (phylum NC10) may oxidize methane anaerobically using non-sulfate electron acceptors (ETTWIG et al., 2010; HU et al., 2009).

In marine settings, AOM is believed to be mediated by a consortium of ANME archaea and sulfate-reducing bacteria (BOETIUS et al., 2000). Four major lines of evidence are used to support sulfate-dependent AOM: 1) concave porewater concentration profiles of sulfate and methane in marine sediments (BARNES and GOLDBERG, 1976; IVERSEN and JORGENSEN, 1985; MARTENS and BERNER, 1974; REEBURGH, 1976), 2) the concurrence of rate increases in sulfate reduction and AOM in the sulfate-methane transition zone (SMTZ; DEVOL, 1983; IVERSEN and JORGENSEN, 1985), 3) highly depleted isotopic signatures of archaeal and bacterial lipids (HINRICHS et al., 1999; HINRICHS et al., 2000; ORPHAN et al., 2001; PANCOST et al., 2000) and 4) high densities of methanogen-like archaea and sulfate-

reducing bacteria (TESKE et al., 2002), often in close physical association (BOETIUS et al., 2000; ORPHAN et al., 2001) in the SMTZ.

Until recently, AOM in low-sulfate, freshwater environments was largely ignored. However, mounting evidence of sulfate-independent AOM (ETTWIG et al., 2010; RAGHOEBARSING et al., 2006) and AOM in freshwater environments (ELLER et al., 2005; SIVAN et al., 2011; SMEMO and YAVITT, 2011) is quickly changing this paradigm. *Chapter 3* explored the importance of AOM in Hammersmith Creek, a small, tidal river in coastal Georgia (Fig. 1.3). Rates of AOM, methane production, and other relevant terminal metabolisms (e.g. sulfate reduction and homoacetogenesis), as well as porewater geochemistry, stable isotopes, and lipid biomarkers were analyzed across several seasons in this two-year study. The pathways of methane cycling depended on a host of environmental and microbiological parameters. Many of these factors, though well studied individually, are not collectively understood. *Chapter 4* continued the themes of *Chapter 3* with a comparative, seasonal study of two freshwater peat wetlands from distinct climate regimes (Fig. 1.3). This study explored interactions between the methane and sulfur-cycling community. Microbial transformations of sulfate, methane, hydrogen, and acetate were constrained with porewater geochemistry and microbial rate activity measurements. Seasonal variations in carbon flow were compared with the lipid distribution and stable isotopic signatures of the microbial community.

The anaerobic oxidation of methane has been linked to the reduction of sulfate (NAUHAUS et al., 2002), nitrite (ETTWIG et al., 2008), iron (BEAL et al., 2009; SIVAN et al., 2011), and manganese (BEAL et al., 2009). Chapter 5 describes a laboratory-based experiment that explored possible electron acceptors for AOM in coastal marine and

freshwater sediments (Fig. 1.3). The influence of various oxidants on rates of AOM was evaluated in long-term AOM enrichments. The response between the low-sulfate (freshwater) and high-sulfate (brackish) communities were compared through rates of AOM, geochemical characterization, and thermodynamic calculations.

Finally, Chapter 6 summarizes the findings of this dissertation and suggests avenues of future research.

REFERENCES

- Barnes, R. O. and Goldberg, E. D. (1976) Methane production and consumption in anoxic marine sediments. *Geology* **4**, 297-300.
- Bartlett, K. B. and Harriss, R. C. (1993) Review and assessment of methane emissions from wetlands. *Chemosphere* **26**, 261-320.
- Beal, E. J., House, C. H., and Orphan, V. J. (2009) Manganese- and Iron-Dependent Marine Methane Oxidation. *Science* **325**, 184-187.
- Blake, D. R. and Rowland, F. S. (1988) Continuing Worldwide Increase in Tropospheric Methane, 1978 to 1987. *Science* **239**, 1129-1131.
- Boetius, A., Ravenschlag, K., Schubert, C. J., Rickert, D., Widdel, F., Gieseke, A., Amann, R., Jorgensen, B. B., Witte, U., and Pfannkuche, O. (2000) A marine microbial consortium apparently mediating anaerobic oxidation of methane. *Nature* **407**, 623-626.
- Brook, E., Archer, D., Dlugokencky, E., Frolking, S., and Lawrence, D. (2008) Potential for abrupt changes in atmospheric methane, *Abrupt Climate Change. A report by the U.S. Climate Change Science Program and the Subcommittee on Global Change Research.* . U.S. Geological Survey, Reston, VA.

- Canfield, D. E., E. Kristensen, and B. Thamdrup. 2005. *Aquatic Geomicrobiology*.
Amerstam: Elsevier, 640 pp.
- Devol, A. H. (1983) Methane Oxidation Rates in the Anaerobic Sediments of Saanich
Inlet. *Limnology and Oceanography* **28**, 738-742.
- Eller, G., Känel, L., and Krüger, M. (2005) Cooccurrence of Aerobic and Anaerobic
Methane Oxidation in the Water Column of Lake Plußsee. *Applied and
Environmental Microbiology* **71**, 8925-8928.
- Ettwig, K. F., Butler, M. K., Le Paslier, D., Pelletier, E., Mangenot, S., Kuypers, M. M.
M., Schreiber, F., Dutilh, B. E., Zedelius, J., de Beer, D., Gloerich, J., Wessels, H.
J. C. T., van Alen, T., Luesken, F., Wu, M. L., van de Pas-Schoonen, K. T., Op
den Camp, H. J. M., Janssen-Megens, E. M., Francoijs, K.-J., Stunnenberg, H.,
Weissenbach, J., Jetten, M. S. M., and Strous, M. (2010) Nitrite-driven anaerobic
methane oxidation by oxygenic bacteria. *Nature* **464**, 543-548.
- Ettwig, K. F., Shima, S., Van De Pas-Schoonen, K. T., Kahnt, J., Medema, M. H., Op
Den Camp, H. J. M., Jetten, M. S. M., and Strous, M. (2008) Denitrifying bacteria
anaerobically oxidize methane in the absence of Archaea. *Environmental
Microbiology* **10**, 3164-3173.
- Hinrichs, K.-U. and Boetius, A. (2002) The anaerobic oxidation of methane: new insights
in microbial ecology and biogeochemistry. In: Wefer, G., Billett, D. Hebbeln, BB
Jorgensen, M. Schluter, T. Van Weering (eds). *Ocean Margin System.s*
- Hinrichs, K.-U., Hayes, J. M., Sylva, S. P., Brewer, P. G., and DeLong, E. F. (1999)
Methane-consuming archaeobacteria in marine sediments. *Nature* **398**, 802-805.

- Hinrichs, K.-U., Summons, R. E., Orphan, V., Sylva, S. P., and Hayes, J. M. (2000) Molecular and isotopic analysis of anaerobic methane-oxidizing communities in marine sediments. *Organic Geochemistry* **31**, 1685-1701.
- Hoehler, T. M., Alperin, M. J., Albert, D. B., and Martens, C. S. (2001) Apparent minimum free energy requirements for methanogenic Archaea and sulfate-reducing bacteria in an anoxic marine sediment. *FEMS Microbiology Ecology* **38**, 33-41.
- Hu, S., Zeng, R. J., Burow, L. C., Lant, P., Keller, J., and Yuan, Z. (2009) Enrichment of denitrifying anaerobic methane oxidizing microorganisms. *Environmental Microbiology Reports* **1**, 377-384.
- IPCC, I. P. o. C. C. (2007) Climate Change 2007: The physical science basis. Contribution of working group I to the fourth assessment report of the intergovernmental panel on climate change. . In: Solomon, S., D. Qin, M. Manning, Z. Chen, M. Marquis, K. B. Averyt, M. Tignor, and H. L. Miller (Ed.).
- Iversen, N. and Jorgensen, B. B. (1985) Anaerobic Methane Oxidation Rates at the Sulfate-Methane Transition in Marine Sediments from Kattegat and Skagerrak (Denmark). *Limnology and Oceanography* **30**, 944-955.
- Kaplan, J. O. (2002) Wetlands at the Last Glacial Maximum: distribution and methane emissions. *Geophys. Res. Lett.* **29**.
- Khalil, M. A. K. and Rasmussen, R. A. (1990) Atmospheric methane: recent global trends. *Environmental Science & Technology* **24**, 549-553.

- Lovley, D. R., Dwyer, D. F., and Klug, M. J. (1982) Kinetic Analysis of Competition Between Sulfate Reducers and Methanogens for Hydrogen in Sediments. *Appl. Environ. Microbiol.* **43**, 1373-1379.
- Martens, C. S. and Berner, R. A. (1974) Methane Production in the Interstitial Waters of Sulfate-Depleted Marine Sediments. *Science* **185**, 1167-1169.
- Nauhaus, K., Boetius, A., Krüger, M., and Widdel, F. (2002) In vitro demonstration of anaerobic oxidation of methane coupled to sulphate reduction in sediment from a marine gas hydrate area. *Environmental Microbiology* **4**, 296-305.
- Orphan, V. J., Hinrichs, K.-U., Ussler, W., III, Paull, C. K., Taylor, L. T., Sylva, S. P., Hayes, J. M., and Delong, E. F. (2001) Comparative Analysis of Methane-Oxidizing Archaea and Sulfate-Reducing Bacteria in Anoxic Marine Sediments. *Appl. Environ. Microbiol.* **67**, 1922-1934.
- Pancost, R. D., Sinninghe Damsté, J. S., de Lint, S., van der Maarel, M. J. E. C., Gottschal, J. C., and Party, T. M. S. S. (2000) Biomarker Evidence for Widespread Anaerobic Methane Oxidation in Mediterranean Sediments by a Consortium of Methanogenic Archaea and Bacteria. *Applied and Environmental Microbiology* **66**, 1126-1132.
- Raghoebarsing, A. A., Pol, A., van de Pas-Schoonen, K. T., Smolders, A. J. P., Ettwig, K. F., Rijpstra, W. I. C., Schouten, S., Damste, J. S. S., Op den Camp, H. J. M., Jetten, M. S. M., and Strous, M. (2006) A microbial consortium couples anaerobic methane oxidation to denitrification. *Nature* **440**, 918-921.
- Reeburgh, W. S. (1976) Methane consumption in Cariaco Trench waters and sediments. *Earth and Planetary Science Letters* **28**, 337-344.

- Schink, B. (1997) Energetics of syntrophic cooperation in methanogenic degradation. *Microbiol. Mol. Biol. Rev.* **61**, 262-280.
- Segers, R. (1998) Methane Production and Methane Consumption: A Review of Processes Underlying Wetland Methane Fluxes. *Biogeochemistry* **41**, 23-51.
- Sivan, O., Alder, M., Pearson, A., Gelman, F., Bar-Or, I., John, S., and Eckert, W. (2011) Geochemical evidence for iron-mediated anaerobic oxidation of methane. *Limnology and Oceanography* **56**, 1536-1544.
- Smemo, K. A. and Yavitt, J. B. (2011) Anaerobic oxidation of methane: an underappreciated aspect of methane cycling in peatland ecosystems? *Biogeosciences* **8**, 779-793.
- Teske, A., Hinrichs, K.-U., Edgcomb, V., de Vera Gomez, A., Kysela, D., Sylva, S. P., Sogin, M. L., and Jannasch, H. W. (2002) Microbial Diversity of Hydrothermal Sediments in the Guaymas Basin: Evidence for Anaerobic Methanotrophic Communities. *Applied and Environmental Microbiology* **68**, 1994-2007.
- Valentine, D. (2002) Biogeochemistry and microbial ecology of methane oxidation in anoxic environments: a review. *Antonie van Leeuwenhoek* **81**, 271-282.
- Whitman, W. B., Bowen, T. L., and Boone, D. R. (1992) The methanogenic bacteria. In: Balows, A., Truper, H. G., Dworkin, M., Harder, W., and Schleifer, K.-H. (Eds.), *The Prokaryotes*. Springer-Verlag, Berlin.
- Zeikus, J. G. (1977) The biology of methanogenic bacteria. *Bacteriol. Rev.* **41**, 514-541.
- Zinder, S. H. (1994) Syntrophic acetate oxidation and "Reversible acetogenesis. In: Drake, H. L. (Ed.), *Acetogenesis*. Chapman and Hall, London.

CHAPTER 2

SEASONAL VARIATIONS OF METHANE FLUXES FROM A TIDAL, FRESHWATER WETLAND (HAMMERSMITH CREEK, GA)

Running title: Methane fluxes from tidal, freshwater sediments

K. E. A. Segarra, V. Samarkin, E. King, C. Meile, and S. B. Joye*

To be submitted to *Biogeochemistry*

Department of Marine Sciences, The University of Georgia, Athens, GA 30602

* Corresponding Author: Dr. Samantha Joye, Room 200 Marine Sciences Building,
Athens, GA, USA, 30602-3636; Tel: 706-542-5893; Fax: 706-542-5888; electronic mail:
mjoye@uga.edu

ACKNOWLEDGMENTS

We would like to thank the Georgia Coastal Ecosystems LTER, J. Shalack, D. Saucedo, M. Machmuller for assistance in the field. This work was funded by the National Science Foundation (DEB 0717189).

ABSTRACT

Wetlands are estimated to contribute nearly 40% of global methane emissions to the atmosphere. However, because methane fluxes from these systems vary spatially, seasonally, and by wetland type, there is a large uncertainty associated with these estimates. We monitored seasonal patterns of methane cycling from the tidally-flooded, unvegetated sediments adjacent to a coastal Georgia freshwater wetland between 2008 and 2009. Methane emissions correlated with methane production and sediment saturation state but not temperature. Methane cycling in these intertidal sediments displayed distinct seasonal patterns. Winter months were characterized by low methane production and emissions. During the spring, summer and fall, methane fluxes exceeded methane production in the top 40 cm, highlighting a strong imbalance in the methane budget. Comparison of methane sources and sinks in conjunction with the results of a 1D model indicated that methane delivered via lateral tidal pumping provided additional methane to the upper sediment column. Seasonally high methane ebullition rates reflected increased methane production and decreased methane solubility. Modeled annual methane fluxes were $12.2 \text{ mol CH}_4 \text{ m}^{-2} \text{ yr}^{-1}$. Though intertidal, unvegetated freshwater sediments represent a small global area, the environments may sustain large annual fluxes of methane to the atmosphere. This study highlights the importance of these dynamic environments to the global methane cycle and their relevance to climate dynamics.

1. INTRODUCTION

Methane (CH_4) is a dominant product of terminal metabolism in freshwater sediments. The production and subsequent emission of this greenhouse gas has important implications for climate change prediction. Recent estimates of the annual CH_4 emissions from wetlands at 209 Tg CH_4 makes them the single largest source of methane to the atmosphere (Brook et al., 2008). The release of CH_4 from wetlands drove global climate perturbations in the geologic past (Chappellaz et al., 1993; Pancost et al., 2007).

Although annual accumulation rates of atmospheric CH_4 declined from a steady 1% between the 1970's and 1999 to essentially zero between 1999 and 2006 (Bousquet et al., 2006; Dlugokencky et al., 1998; Simpson et al., 2002), more recent data demonstrates that concentrations are once again increasing (Dlugokencky et al., 2009). These recent variations in atmospheric concentrations are driven, in part, by changes in wetland emissions (Bousquet, 2011; Chen and Prinn, 2006; Morimoto et al., 2006).

Various CH_4 sources and sinks are not well constrained (Bastviken et al., 2011; Bousquet, 2011; Crutzen, 1995), and the range in annual emission rates for wetlands alone (100-231 Tg CH_4 ; as reviewed in Denman et al., 2007) demonstrates the complex factors regulating CH_4 dynamics in these widespread habitats. Furthermore, wetlands account for about 40% of total annual CH_4 emissions (Brook et al., 2008) but this number is heavily based on data from inland wetlands, such as bogs and peatlands (Anselman and Crutzen, 1989; Matthews and Fung, 1987; Walter et al., 2001). Tidal freshwater wetlands have the capacity for considerable CH_4 production and atmospheric emission (Bartlett et al., 1987; Chanton et al., 1989) but their area extent and the variability of methane emissions and hence their impact on global budgets is poorly known (Bridgham et al.,

2006). The bulk of studies on gaseous carbon emissions from these environments have focused on vegetated marshes (e.g., Middelburg et al. 1996; Van Der Nat and Middelburg 2000; Bridgham et al. 2006), with only few from unvegetated, intertidal sediments (Chanton et al., 1989; Sorrell and Boon, 1992; Middelburg et al., 1996a).

Here, we present a seasonal survey of sediment biogeochemistry and gaseous carbon emissions from unvegetated sediments of a tidal creek in coastal Georgia. Seasonal patterns in the fluxes of methane are related to methane production and solubility, and 1D sediment model is employed to simulate the observed methane dynamics and explain the methane budget imbalances observed during the study.

2. METHODS

2.1 Study Site

The study site was located in coastal Georgia along the Hammersmith Creek (31°20' N, 81°28' W), a tidal, freshwater (salinity of 0-2 PSU) creek that feeds into the Altamaha River. The sediments at Hammersmith Creek are fine-grained silt and clays with an average organic carbon content of 5%. Diurnal tides result in a range of maximum water depth at high tide from about 0.5 (neap) to 2 m (spring). Our sampling efforts focused on the unvegetated, intertidal creek bank sediments where oxygen was consumed within the top 3 mm of sediment as evidenced by O₂ microelectrode measurements. Above this zone is vegetated marsh, dominated by *Zizaniopsis miliacea*; the *Zizaniopsis* zone is partially inundated at high tide. Wooden boardwalks were installed to minimize sediment disturbance from repeat sampling.

2.2 Sediment Collection and Methane Analysis

In the winter, spring, and summer of 2008 and again in the winter, summer, and fall of 2009, several replicate cores 40 cm in length and 7.5 cm in diameter were collected and stored at *in situ* temperature until processing. Three replicate cores were processed for geochemical analyses with 24 hours of collection. Cores were extruded and sectioned at 3-5 cm intervals under a stream of argon to minimize oxygen contamination. Subsamples for CH₄ and porosity were collected from each depth interval. For CH₄, a 6 cm³ subsample was collected and preserved in a helium-purged 20 mL glass headspace vial that contained 2 mL of 2 mol L⁻¹ NaOH. The vial was crimp-sealed with a butyl rubber stopper and CH₄ was analyzed subsequently using a Shimadzu GC-2014 gas chromatograph equipped a flame-ionization detector and a CarbosphereTM column. Saturated CH₄ concentrations were calculated according to Yamamoto et al. (1976) using *in situ* temperature and salinity (0 PSU). Porosity was determined on a 1 cm³ subsample placed in a tared weigh-dish (Joye et al., 2004).

2.3 Methanogenesis

On each sampling expedition, three additional sediment cores were processed within 36 hours of collection to quantify rates of methanogenesis (MOG). These cores were sectioned under argon into the same depth horizons as those for geochemical analyses. Assays for hydrogenotrophic MOG (bic-MOG; ¹⁴CH₄ from H¹⁴CO₃⁻) and acetoclastic MOG (ace-MOG; ¹⁴CH₄ from ¹⁴CH₃COO⁻) were performed, and rates calculated using the methods of Orcutt et al. (2005). The rates of these two processes were summed to estimate the *total* MOG rate as bicarbonate and acetate are assumed to be the major substrates of CH₄ production in freshwater sediments (Winfrey and Zeikus,

1979). Depth-integrated rates were calculated via trapezoidal integration of the volumetric rates.

In the winter, spring, and summer of 2008, net CH₄ production was measured by monitoring CH₄ accumulation from sediment sub-samples over time. These samples were processed (from triplicate sub-cores) in parallel with samples for the radiotracer rate measurements. 6 cm³ sub-samples were placed into helium-purged 20 mL gas vials and sealed with butyl rubber stoppers. Each vial was immediately purged with helium; vials were re-purged after 12 hours and then incubated in the dark at *in situ* temperature for 3-4 days. The concentration of CH₄ in the headspace was monitored every 24 hours by injecting a 500 μL headspace subsample into the GC-FID. Rates of MOG were calculated from the increase of CH₄ concentration over time (average R^2 of 0.89). Blanks (sediment-free vials) and killed-controls (sediment plus 100 μM NaOH) run simultaneously with the live incubations confirmed that no abiotic CH₄ production occurred.

2.4 Flux Measurements and Calculations

At each sampling date, fluxes of CH₄ across the sediment surface were quantified. Fluxes from exposed sediment to the atmosphere were measured with a cylindrical plexiglass chamber (diameter = 25 cm, height = 20.5 cm) that was gently placed on the sediment-atmosphere interface and attached to a trace gas analyzer (TGA; Europa Scientific). A small battery-operated fan homogenized the atmosphere within the chamber. A stopcock at the top of the chamber remained open to the atmosphere during all flux measurements. All fluxes were performed in the dark by blocking light with a Mylar sheet to reduce changes in temperature within the chamber. CH₄ concentrations were measured in 1 minute intervals for 45 to 60 minutes using a base trap (sodium

hydroxide pellets) at the inlet line of the TGA to avoid interference of the methane signal by carbon dioxide. Due to tidal constraints, flux measurements (n=3 to 5) were taken at low tide within 1 to 3 days of each core sampling date. Air, water, and sediment temperature was measured using a K-type temperature probe (Fluke) connected to a hand-held thermometer (Fluke 53 II).

Gas fluxes were calculated as,

$$F = dC/dt * V / SA \quad (1)$$

where F is the flux in $\text{mmol m}^{-2} \text{d}^{-1}$, dC/dt is the change in CH_4 concentration with time in $\text{mmol m}^{-3} \text{d}^{-1}$, V is the volume of the flux chamber in m^3 , and SA is the surface area of the sediment in m^2 . A linear fit was not appropriate for all CH_4 measurements as these concentrations were, at times, reflecting ebullition. Therefore, total CH_4 fluxes were calculated using a method similar to Middelburg et al. (1996) wherein diffusive exposed CH_4 fluxes were calculated from the linear, diffusive portions of the methane time course, total flux was determined as the total accumulation of methane over time, and ebullition flux was calculated as the difference in the total flux and the diffusive flux.

In January and April 2008 and in July and November 2009, fluxes of CH_4 from the sediment to the overlying water were measured over a tidal cycle using cylindrical, opaque chambers (20 cm in height by 12 cm in diameter) with removable lids which had been cleaned with 10% HCl and rinsed 5x with MQ water. An initial sampling was performed after the tide filled the chambers (time zero) and then the chambers were closed. At high-tide 3 of the 6 chambers were sampled and the other half were sampled at low tide just as the chambers were exposed. This design allowed us to determine fluxes as the tide flooded the sediment and during inundation.

Samples taken from each chamber were immediately preserved for CH₄ analysis in helium-purged headspace vials and fixed with 100 µL of HCl and headspace concentrations of CH₄ were determined using a GC-FID. Benthic CH₄ fluxes were calculated according to equation 1.

To estimate the total sediment flux of CH₄ on a daily basis, benthic fluxes and exposed fluxes were time-averaged according to the time the sediment was inundated or exposed. For our study site, we estimated that the sediment was exposed for 8 hours per day and inundated for 16 hours per day.

2.5 Statistical Calculations

Comparisons of means were performed with ANOVA followed by Tukey HSD post-hoc testing. To evaluate seasonal differences, measurements from replicate seasonal sampling (i.e. the winters and summers of 2008 and 2009) were pooled. Correlations were determined using Spearman's rank correlation coefficients (ρ). All tests were carried out with SPSS 15.0 and were evaluated using a significance level (α) of 0.05.

2.6 Modeling Approach

A 1D sediment model was designed to simulate CH₄ dynamics in the sediment. Dissolved CH₄ profiles were computed by considering degassing, biological production, diffusion, and input through alternate sources according to:

$$\frac{dC}{dt} = \frac{d}{dx} \left(D \frac{dC}{dx} \right) - E_{gas} + R_{prod} + Q \quad (2)$$

where C is the concentration of methane, x is depth, D is the diffusion coefficient, and E_{gas} , R_{prod} , and Q refer to loss of CH₄ through degassing and inputs through biological production and alternate sources, respectively. E_{gas} is defined by:

$$E_{gas} = k_{gas} \cdot (C - C_{sat}) \cdot \delta \quad (3)$$

where k_{gas} is the CH₄ gas exchange coefficient, C_{sat} is the CH₄ saturation (Yamamoto et al. 1976) and δ is equal to 1 if the dissolved CH₄ concentration exceeds saturation, else it is 0. Additional sources of CH₄ (Q) are defined as:

$$Q = k_Q C^* \quad (4)$$

where the source strength k_Q is assumed constant over the seasons ($5 \times 10^7 \text{ s}^{-1}$), while C^* reflects the methane concentration in the source fluid. The source is set to saturation levels for spring, summer, and fall but because of lower CH₄ production rates, it was set to 0 for winter.

Measurements for sediment temperature, biological production, total CH₄ flux, and CH₄ concentrations taken over 4 seasons were used to parameterize the model. Biological production and temperature were linearly interpolated over time. CH₄ was set to a concentration of 0 at the sediment surface, and at 40 cm, a no gradient condition was imposed $dC/dx = 0$. The CH₄ profile measured in winter 2008 was used as initial condition, and simulations were run for sufficient time such that a repetitive pattern was seen from year to year. In additional simulations assessing the possibility of a deep methane source advecting vertically into the domain, the advective flux at the bottom boundary was imposed, $F = v * C_{sat}$, where v was set to match the missing methane source, $\int_{0cm}^{40cm} Q dx$, and Q in Eq. 2 was replaced by advection, $-v \frac{dC}{dx}$.

3. RESULTS

3.1 Porewater Methane

CH₄ concentrations typically increased with depth to a mid-depth maximum (between 9 and 25 cm) after which point concentrations gradually decreased (Fig. 2.1). Porewater CH₄ concentrations ranged from 18 to 4200 μmol L⁻¹. Though some temporal variation in the shape of the CH₄ profile was observed, the depth integrated CH₄ inventory (0-40 cm) varied only slightly (Table 2.1). Surficial (0-3 cm) CH₄ concentrations (Fig. 2.1) and CH₄ percent saturation were significantly higher during spring and fall than during summer and winter (Table 2.1; $p < 0.05$). From 2008 to 2009, depth-integrated CH₄ concentrations did not vary significantly during replicate seasonal sampling (winter and summer), despite differences in the shape of the profiles, surface concentrations, and differences in sediment temperature (Table 2.1). Concentrations of CH₄ were significantly correlated with temperature ($\rho = 0.50$).

3.2 Methane Production

Rates of total MOG ranged from 0.1 to 148 nmol cm⁻³ d⁻¹ (Fig. 2.2). Methane production profiles mimicked the CH₄ concentration profiles, though the seasonal variability was more pronounced: areal rates of total MOG in the top 40 cm were significantly lower during winter and rates during fall and spring were higher than those observed in summer ($p < 0.05$; Table 2.1). Surficial (0-3 cm) rates of MOG were significantly higher during spring (Fig. 2.2).

Net CH₄ production rates ranged from below detection to 159 nmol cm⁻³ d⁻¹. Generally, net MOG rates were lower than or similar to total MOG rates except in summer 2008, when the observed CH₄ accumulation rates in some depth horizons were significantly higher than combined hydrogenotrophic and acetoclastic CH₄ production (Fig. 2.2).

3.3 Methane Fluxes

Exposed CH₄ fluxes ranged from 0 to 6.4 mmol m⁻² hr⁻¹ and were maximal during spring (Table 2.1). CH₄ fluxes were dominated by ebullition, except for winter, when diffusion is a large component of the total flux (Table 2.1). Diffusive CH₄ fluxes did not vary significantly with season and the exposed fluxes of CH₄ observed during replicate seasons (summer and winter) were not significantly different.

Inundated fluxes of CH₄ were extremely variable both spatially and seasonally (Table 2.1). Inundated CH₄ fluxes ranged from below detection to 1.1 mmol m⁻² hr⁻¹ and were generally lower than exposed CH₄ fluxes, significantly so during fall.

The total daily sediment CH₄ fluxes (time-averaged cumulative inundated and exposed fluxes) ranged from 0.1 mmol m⁻² d⁻¹ to 55.8 mmol m⁻² d⁻¹ and were significantly higher during spring and fall compared to winter ($p < 0.05$; Table 2.1). Fluxes were dominated by exposed (low-tide) fluxes except during winter, when inundated CH₄ fluxes were much higher than exposed fluxes.

Neither exposed nor inundated fluxes of CH₄ were significantly correlated with temperature (Fig. 2.3) or CH₄ concentrations; however, fluxes of CH₄ and percent CH₄ saturation in surface (0-3 cm) sediment were significantly correlated ($\rho = 0.48$ for exposed fluxes, $\rho = 0.74$ during inundation, $\rho = 0.65$ for total CH₄ fluxes; Fig. 2.4A).

Rates of total CH₄ production in the top 40 cm were positively correlated with exposed ($\rho = 0.70$), inundated ($\rho = 0.63$), and total CH₄ fluxes ($\rho = 0.79$; Fig. 2.4B).

Methane production rates in the top 40 cm influenced the degree of CH₄ saturation in the surface sediments (Fig. 2.5), indicating that CH₄ production influenced both CH₄

saturation and CH₄ fluxes. However, total CH₄ loss due to fluxes exceeded CH₄ production rates in the top 40 cm in all seasons except the winter.

3.4 Residence times

The seasonal variability in methane emissions impacted the residence time of CH₄ in the upper 40 cm of sediment: low methane fluxes led to long turnover times for CH₄ in the winter (Table 2.1). Conversely, the shortest residence times were observed in the spring, which coincided with CH₄ flux and production maxima. When CH₄ fluxes were highest and dominated by ebullition (spring, summer, and fall), the residence time of CH₄ was relatively short (2-5 weeks) and controlled by exposed, rather than inundated, fluxes.

3.5 Modeled methane dynamics

Results from the 1D sediment model were compared to measurements of exposed gas flux and integrated methane concentrations for all four seasons (Table 2.1). The model parameters k_Q and k_{gas} were set to $5 \times 10^{-7} \text{ s}^{-1}$ and $1 \times 10^{-5} \text{ s}^{-1}$, respectively, chosen such that the misfit between measured and calculated exposed gas fluxes was at a minimum for all seasons. Assuming saturated methane concentrations (equation 4), the additional source term (Q) was substantial in spring, summer, and fall (Table 2.1).

When taking into account the additional source term (Q), a relatively good match between the measured and predicted depth-integrated concentrations of methane was observed in all seasons, with an approximately $\pm 15\%$ difference at each time point. There was also about a 1-10% difference between the measured and predicted exposed methane fluxes in all seasons except for the spring. For spring of 2008, methane emission was predicted to emit a little less than half of what was measured. The annual modeled methane loss to the atmosphere was $1.4 \text{ mmol CH}_4 \text{ m}^{-2} \text{ hr}^{-1}$ or $12.2 \text{ mol CH}_4 \text{ m}^{-2} \text{ yr}^{-1}$.

Simulations results using a vertical advective flow of methane rich fluids rising from below 40 cm did not match concentration and flux measurements simultaneously (not shown).

4. DISCUSSION

4.1 Comparison of Unvegetated, Intertidal Sediments to Global Wetland Emissions

Methane cycling in the unvegetated, intertidal sediments of Hammersmith Creek displayed strong seasonality, with very low production and emission rates in the winter months. Yet, on an annual scale these sediments support substantial methane fluxes to the atmosphere. CH₄ fluxes from wetlands range from 100-231 Tg CH₄ yr⁻¹ (as reviewed by Brook et al., 2008). Using an estimated area of global wetlands of 5.3x10¹² m², the average areal flux from wetlands is 19-44 g CH₄ m⁻² per year. Modeled annual fluxes of CH₄ from Hammersmith Creek's banks (195 g CH₄ m⁻² yr⁻¹) are 4 to 10 times this global average and more closely resembled those from non-vegetated Virginia swamp sediments (Wilson et al., 1989) vegetated and unvegetated sediments of an Australian billabong (Sorrell and Boon, 1992), and brackish sites along an estuary (Middelburg et al., 1996).

Methane emissions from vegetated sites typically exceed those from unvegetated areas (Laanbroek, 2010). However, the annual methane fluxes presented in this study are between 2 and nearly 200 times higher than fluxes from vegetated tidal wetlands along the east coast (Kelley et al., 1995; Megonigal and Schlesinger, 2002; Neubauer et al., 2000). As this study suggests, unvegetated, intertidal, freshwater wetlands may be 'hot spots' of methane emission to the atmosphere.

4.2 Controls on Methane Emissions

Fluxes of CH₄ displayed pronounced seasonality as observed in previous studies of freshwater wetlands (Chanton et al., 1989; Middelburg et al., 1996; Wilson et al., 1989). Seasonality in CH₄ emissions from wetlands has been linked to water table fluctuations (Christensen et al., 2003; Devol et al., 1990; Sebacher et al., 1986), temperature (Sorrell and Boon, 1992; Van der Nat and Middelburg, 2000; Wilson et al., 1989), methane production (Sorrell and Boon, 1992), methane solubility (Chanton et al., 1989), and plant physiology (Bellisario et al., 1999; Bubier et al., 1995; King et al., 1998). Water table fluctuations and plant physiology are not relevant for the unvegetated banks of Hammersmith Creek, which are inundated by diurnal tides. The remaining factors are discussed below.

4.2.1 Temperature

Temperature may affect the activity of methanogenic processes (Zeikus and Winfrey, 1976), solubility (Yamamoto et al., 1976), and may indirectly influence methane emissions via controls on net ecosystem production (Whiting and Chanton, 1993) and competing terminal metabolisms (Kotsyurbenko, 2005). Increases in global temperatures are expected to fuel higher wetland methane fluxes (Cao et al., 1998; Gedney et al., 2004), and in predictive climate models, methane emissions from wetlands are usually driven by enhanced precipitation and temperature increases (Christensen and Cox, 1995; Shindell et al., 2004). However, we found no relationship between CH₄ fluxes, production, or concentrations and temperature during this study. Other studies which explored methane emissions and temperature in temperate, freshwater systems have produced varied results (Bartlett et al., 1985; Sorrell and Boon, 1992; Wilson et al., 1989). Studies in freshwater lakes (Barber et al., 1988), rice paddy soils (Schütz et al.,

1990), and freshwater wetlands (Kelley et al., 1995; Middelburg et al., 1996) noted no relationship between temperature and methane fluxes. CH₄ emissions from several east coast wetlands displayed a weak reliance on temperature (Wilson et al., 1989). Still, a few studies documented a link between temperature and methane emissions in temperate wetlands (Bartlett et al., 1985; Sorrell and Boon, 1992; Van der Nat and Middelburg, 2000).

4.2.2 Ebullition and seasonal changes in solubility

Loss via ebullition dominates global CH₄ fluxes from freshwater environments (Bastviken et al., 2011; Chanton et al., 1989; Middelburg et al., 1996) and Hammersmith Creek is no exception. Here, exposed fluxes via ebullition were often several times higher than diffusive fluxes. The seasonal high of ebullition contribution to measured methane fluxes (up to 99% of the exposed flux) is among the highest reported.

Exposed CH₄ fluxes were dominated by ebullition during all seasons except winter. This likely reflects the significantly lower MOG rates in the winter; a strong correlation between CH₄ flux and MOG (Fig. 2.4B) has also been documented in previous studies of seasonal CH₄ fluxes (Crill and Martens, 1983; Kelley et al., 1995; Sorrell and Boon, 1992) In addition to seasonal production maxima, higher ebullition in the warmer months may be explained by CH₄ solubility. In the White Oak River (a tidal, freshwater wetland), seasonally-related increases in temperature caused CH₄ to shift from the dissolved phase in the winter to a higher contribution of the bubble phase in the summer (Chanton et al., 1989). The actual concentration of CH₄ varied very little during this phase shift. The methane stocks in the sediments of Hammersmith Creek also did not vary with season. However, the seasonal variations in methane saturations likely

produced a larger inventory of CH₄ bubbles in the sediment in the warmer months. Gas pockets were observed throughout the length of the sediment cores collected during this study, especially in the spring and summer months. Though the composition of these gas bubbles was not determined, previous studies have found the CH₄ inventory in gas bubbles to increase in warmer months (Chanton et al., 1989).

4.3 Methane Production

A strong correlation between CH₄ flux and MOG (Fig. 2.4B) has also been documented in previous studies of seasonal CH₄ fluxes (Crill and Martens, 1983; Kelley et al., 1995; Sorrell and Boon, 1992). Ultimately, CH₄ production controls the CH₄ inventory, which regulates the CH₄ flux. A variety of environmental parameters may indirectly influence CH₄ emissions by affecting methanogenesis rates. Substrate availability, primary production, temperature, microbial community structure, and competition with other microbial groups may control methane production (as reviewed in Segers, 1998). The data available for HC do not clarify which, if any of these factors, influence seasonal patterns of methane production. Substrate concentrations (e.g., DIC, acetate, H₂, and others) do not correlate with CH₄ production (this study and *Chapter 3*). Though DIC concentrations varied significantly with season, it is unlikely that DIC concentration limited methanogens at any time point. Other terminal metabolizers (e.g. denitrifiers, sulfate reducers, and metal reducers) may outcompete methanogens for substrates such as H₂ (Chidthaisong and Conrad, 2000; Lovley et al., 1982). In Hammersmith Creek sediments, sulfate reduction rates typically exceed methanogenesis rates (*Chapter 3*) and denitrification and metal reduction account for up to 20% of anaerobic terminal metabolism (Weston et al., 2006). It is possible that the seasonality in

methane production was driven by competition with other terminal metabolizers, as found by Neubauer et al. (2005).

In vegetated wetlands, net ecosystem production and primary production exert a major control on CH₄ emissions (Bellisario et al., 1999; Joabsson and Christensen, 2001; Kankaala et al., 2003; Whiting and Chanton, 1996; Wilson et al., 1989). This relationship is thought to be driven by stimulation of the methanogenic community by root exudates and other labile organic compounds released by plants (Joabsson et al., 1999; Kankaala et al., 2003; King and Reeburgh, 2002) and by enhanced CH₄ emissions via plant roots and stems which act as a conduit for CH₄ from the sediments to the atmosphere (King et al., 1998; Sebacher et al., 1985). Thus methane emissions from vegetated sediment usually exceed those from unvegetated sediments (Laanbroek, 2010).

The intertidal creek bank sediments at Hammersmith Creek are free of vegetation. However, directly upslope from the study site is a marsh densely vegetated with *Zizaniopsis miliacea*. At high tide, portions of this marsh are inundated and falling tides may deliver organic material out of the marsh and onto the intertidal creek bank. With these regular inputs of organic material to the creek bank it is conceivable that the seasonality we observed in CH₄ fluxes is related to marsh productivity cycles. In lake sediments the addition of plant detritus and leaves, which mimic marsh inputs to the system, stimulated potential methane production (Kankaala et al., 2003). In this study, the lowest methane production rates were measured in the winter, when marsh productivity is at a minimum (Neubauer et al., 2000). Influence of such externally sourced organic material on methane production and fluxes has been proposed in other tidal, freshwater wetlands (Kelley et al. 1995). In addition to external influences of

primary production, benthic macroalgae are present on the surface sediments of Hammersmith creek, as evidenced by a green film (*pers. obs*). In addition to inputs of organic material from the adjacent marsh, seasonal methane production patterns may be driven by benthic macroalgae, which have also been shown to stimulate potential methanogenesis (Kankaala et al., 2003).

4.4 Methane budget

Regardless of what controls CH₄ production rates, methanogenesis alone cannot explain the observed seasonality in CH₄ emissions from Hammersmith Creek sediments. In three of four seasons CH₄ emission from surface sediments exceeded CH₄ production in the top 40 cm. While there was a strong correlation between CH₄ emission and CH₄ production (Fig. 2.4), there was also a pronounced deficit in the CH₄ budget in the spring, summer, and fall when CH₄ fluxes were high. Though we did not measure net CH₄ production at all time points (Table 2.1), the close agreement of total and net rates of MOG for the available time points suggest that CH₄ produced from ‘alternative substrates’, such as methanol and methylamines (King, 1984), is inconsequential. Therefore, though methane emissions and production are related, there appears to be an imbalance in the sources and sinks of methane in the top 40 cm of sediment.

Previous studies that compared wetland CH₄ production and flux often reveal an imbalance between these two terms (Sorrell and Boon 1992; Kelley et al. 1995). Kelley et al. (1995) examined several sites in the White Oak River estuary and found both CH₄ deficits (due to excess flux) and surpluses (due to excess production) depending on the site and the season. Comparison of CH₄ production and CH₄ fluxes is not straightforward and the methods used to measure these processes vary within the literature. The bulk of

studies that compare CH₄ fluxes with production report *potential* rather than *in situ* methanogenesis rates because it is more difficult to measure *in situ* rates of CH₄ production. The assays of CH₄ production reported here were conducted *ex situ* with minimally disturbed cores, so as to approximate *in situ* rates.

The seasonally high methane fluxes from the creek bank may be supported by external methane sources. To assess lateral or vertical inputs as alternative methane sources, a 1D sediment model that takes into account biological production, diffusion, and degassing was employed wherein an additional input of dissolved methane via advection was added.

Though MOG rates decrease with depth, there was still measurable CH₄ production at the bottom horizons of our sediment cores throughout the year (Fig. 2.2). However, if one assumes that the measured methane production at 40 cm continues in the deeper sediment, this production must remain constant for more than 2 meters for each of the seasons in order to support the observed sediment efflux. Thus, while it is feasible that a portion of the CH₄ produced below 40 cm may contribute to the CH₄ pools in the shallow sediments, it is unlikely that this would account for the large differences seen in the mass balance, a finding further corroborated by the poor fit of model simulations that include vertically advective movement of methane towards the sediment surface (not shown).

Methane produced in the adjacent sediments (e.g. high marsh) could introduce methane into the unvegetated creek banks at a concentration near saturation levels to creekbank sediments. At high tide, portions of this marsh are inundated and falling tides may deliver methane downslope, possibly delivering methane to our study site.

Simulations with lateral inputs of fluids enriched in CH₄ resulted in a relatively good fit between the measured and predicted gas flux (Table 2.1) and the methane budget. Such inputs may be derived from tidal forcing (Deborde et al., 2010; Ferrón et al., 2007; Kelley et al., 1995; Kim and Hwang, 2002). Methane inputs to coastal waters can vary with the tidal stage, especially with the spring/neap cycle (Kim and Hwang, 2002). Tidal pumping was a major source of CH₄ to the Archachon lagoon (Deborde et al., 2010) and it is plausible that tidal inputs of CH₄ from the adjacent intertidal high marsh at HC are important sources of porewater CH₄. As most measurements were conducted during a spring tide, the large volume of tidal flushing during these sampling periods may have delivered CH₄ from sediments within the marsh to the creek bank. The close agreement between the measured CH₄ fluxes and those which were modeled including an external source of methane via lateral input reinforces this scenario.

4.5 Seasonal methane budget

Methane cycling in the intertidal sediments of Hammersmith Creek differs distinctly between the winter (Fig. 2.6A) and the rest of the year (Fig. 2.6B). In the winter, low, diffusive methane fluxes were accompanied by low methane production rates which resulted in long residence times for methane in the top 40 cm of sediment. Methane fluxes were dominated by diffusion; no ebullition was detected. For the remainder of the year, high, ebullition-dominated methane fluxes exceeded measured methane sources. Modeled methane concentrations and fluxes which assumed a seasonally-large input of methane-saturated waters closely matched the field data. Inequalities in methane sources and losses may be balanced by tidally-derived lateral

advection of methane-rich waters from the surrounding marsh and subtidal sediments.4.6

Conclusions

The intertidal sediments of Hammersmith Creek support high annual CH₄ fluxes (12.2 mol CH₄ m⁻² y⁻¹). Despite significant fluctuations in methane saturation, methane production, and methane fluxes, there was no observable variation in the porewater methane pool during the study. Methane production and methane fluxes were highly correlated; however, the high methane fluxes during the spring, summer, and fall months exceeded methane production rates within the top 40 cm. Externally-sourced methane delivered via lateral advection may provide additional CH₄ to support seasonally-high fluxes, a finding supported by the model results (Fig. 2.6). However, future study is necessary to affirm this mechanism.

Future gaseous carbon budgets should include fluxes from intertidal freshwater sites such as Hammersmith Creek, which have been underrepresented in the literature but which may support substantial trace gas fluxes. Tidal freshwater marshes are dynamic systems with physical, biological, and chemical parameters that change on a daily, tidal, and seasonal scale. Our data supports previous studies which have found a strong seasonal variability in the biogeochemistry of freshwater wetlands. CH₄ fluxes were dominated by ebullition and exceeded CH₄ production rates during most of the year. Both of these findings underscore the strong role that tides play in these complex systems, whereby tidal pumping and tide-related pressure changes likely affect non-diffusive CH₄ fluxes. This three-dimensional scheme distinguishes tidal freshwater wetlands from their non-tidal counterparts. Though small in total area, further study of the role of these systems in the global methane budget is warranted.

REFERENCES

- Barnes, R. O. and Goldberg, E. D. (1976) Methane production and consumption in anoxic marine sediments. *Geology* **4**, 297-300.
- Bartlett, K. B. and Harriss, R. C. (1993) Review and assessment of methane emissions from wetlands. *Chemosphere* **26**, 261-320.
- Beal, E. J., House, C. H., and Orphan, V. J. (2009) Manganese- and Iron-Dependent Marine Methane Oxidation. *Science* **325**, 184-187.
- Blake, D. R. and Rowland, F. S. (1988) Continuing Worldwide Increase in Tropospheric Methane, 1978 to 1987. *Science* **239**, 1129-1131.
- Boetius, A., Ravensschlag, K., Schubert, C. J., Rickert, D., Widdel, F., Gieseke, A., Amann, R., Jorgensen, B. B., Witte, U., and Pfannkuche, O. (2000) A marine microbial consortium apparently mediating anaerobic oxidation of methane. *Nature* **407**, 623-626.
- Brook, E., Archer, D., Dlugokencky, E., Frohking, S., and Lawrence, D. (2008) Potential for abrupt changes in atmospheric methane, *Abrupt Climate Change. A report by the U.S. Climate Change Science Program and the Subcommittee on Global Change Research.* . U.S. Geological Survey, Reston, VA.
- Canfield, D. E., Kristensen, E., and Thamdrup, B. (2005) *Aquatic Geomicrobiology.* . Elsevier, Amsterdam.
- Devol, A. H. (1983) Methane Oxidation Rates in the Anaerobic Sediments of Saanich Inlet. *Limnology and Oceanography* **28**, 738-742.

- Eller, G., Känel, L., and Krüger, M. (2005) Cooccurrence of Aerobic and Anaerobic Methane Oxidation in the Water Column of Lake Plußsee. *Applied and Environmental Microbiology* **71**, 8925-8928.
- Ettwig, K. F., Butler, M. K., Le Paslier, D., Pelletier, E., Mangenot, S., Kuypers, M. M. M., Schreiber, F., Dutilh, B. E., Zedelius, J., de Beer, D., Gloerich, J., Wessels, H. J. C. T., van Alen, T., Luesken, F., Wu, M. L., van de Pas-Schoonen, K. T., Op den Camp, H. J. M., Janssen-Megens, E. M., Francoijs, K.-J., Stunnenberg, H., Weissenbach, J., Jetten, M. S. M., and Strous, M. (2010) Nitrite-driven anaerobic methane oxidation by oxygenic bacteria. *Nature* **464**, 543-548.
- Ettwig, K. F., Shima, S., Van De Pas-Schoonen, K. T., Kahnt, J., Medema, M. H., Op Den Camp, H. J. M., Jetten, M. S. M., and Strous, M. (2008) Denitrifying bacteria anaerobically oxidize methane in the absence of Archaea. *Environmental Microbiology* **10**, 3164-3173.
- Hinrichs, K.-U. and Boetius, A. (2002) The anaerobic oxidation of methane: new insights in microbial ecology and biogeochemistry. . *Ocean Margin Systems*.
- Hinrichs, K.-U., Hayes, J. M., Sylva, S. P., Brewer, P. G., and DeLong, E. F. (1999) Methane-consuming archaeobacteria in marine sediments. *Nature* **398**, 802-805.
- Hinrichs, K.-U., Summons, R. E., Orphan, V., Sylva, S. P., and Hayes, J. M. (2000) Molecular and isotopic analysis of anaerobic methane-oxidizing communities in marine sediments. *Organic Geochemistry* **31**, 1685-1701.
- Hoehler, T. M., Alperin, M. J., Albert, D. B., and Martens, C. S. (2001) Apparent minimum free energy requirements for methanogenic Archaea and sulfate-

- reducing bacteria in an anoxic marine sediment. *FEMS microbiology ecology* **38**, 33-41.
- Hu, S., Zeng, R. J., Burow, L. C., Lant, P., Keller, J., and Yuan, Z. (2009) Enrichment of denitrifying anaerobic methane oxidizing microorganisms. *Environmental Microbiology Reports* **1**, 377-384.
- IPCC, I. P. o. C. C. (2007) Climate Change 2007: The physical science basis. Contribution of working group I to the fourth assessment report of the intergovernmental panel on climate change. . In: Solomon, S., D. Qin, M. Manning, Z. Chen, M. Marquis, K. B. Averyt, M. Tignor, and H. L. Miller (Ed.).
- Iversen, N. and Jorgensen, B. B. (1985) Anaerobic Methane Oxidation Rates at the Sulfate-Methane Transition in Marine Sediments from Kattegat and Skagerrak (Denmark). *Limnology and Oceanography* **30**, 944-955.
- Kaplan, J. O. (2002) Wetlands at the Last Glacial Maximum: distribution and methane emissions. *Geophys. Res. Lett.* **29**.
- Khalil, M. A. K. and Rasmussen, R. A. (1990) Atmospheric methane: recent global trends. *Environmental Science & Technology* **24**, 549-553.
- Lovley, D. R., Dwyer, D. F., and Klug, M. J. (1982) Kinetic Analysis of Competition Between Sulfate Reducers and Methanogens for Hydrogen in Sediments. *Appl. Environ. Microbiol.* **43**, 1373-1379.
- Martens, C. S. and Berner, R. A. (1974) Methane Production in the Interstitial Waters of Sulfate-Depleted Marine Sediments. *Science* **185**, 1167-1169.

- Nauhaus, K., Boetius, A., Krüger, M., and Widdel, F. (2002) In vitro demonstration of anaerobic oxidation of methane coupled to sulphate reduction in sediment from a marine gas hydrate area. *Environmental Microbiology* **4**, 296-305.
- Orphan, V. J., Hinrichs, K.-U., Ussler, W., III, Paull, C. K., Taylor, L. T., Sylva, S. P., Hayes, J. M., and Delong, E. F. (2001) Comparative Analysis of Methane-Oxidizing Archaea and Sulfate-Reducing Bacteria in Anoxic Marine Sediments. *Appl. Environ. Microbiol.* **67**, 1922-1934.
- Pancost, R. D., Sinninghe Damsté, J. S., de Lint, S., van der Maarel, M. J. E. C., Gottschal, J. C., and Party, T. M. S. S. (2000) Biomarker Evidence for Widespread Anaerobic Methane Oxidation in Mediterranean Sediments by a Consortium of Methanogenic Archaea and Bacteria. *Applied and Environmental Microbiology* **66**, 1126-1132.
- Raghoebarsing, A. A., Pol, A., van de Pas-Schoonen, K. T., Smolders, A. J. P., Ettwig, K. F., Rijpstra, W. I. C., Schouten, S., Damste, J. S. S., Op den Camp, H. J. M., Jetten, M. S. M., and Strous, M. (2006) A microbial consortium couples anaerobic methane oxidation to denitrification. *Nature* **440**, 918-921.
- Reeburgh, W. S. (1976) Methane consumption in Cariaco Trench waters and sediments. *Earth and Planetary Science Letters* **28**, 337-344.
- Schink, B. (1997) Energetics of syntrophic cooperation in methanogenic degradation. *Microbiol. Mol. Biol. Rev.* **61**, 262-280.
- Segers, R. (1998) Methane Production and Methane Consumption: A Review of Processes Underlying Wetland Methane Fluxes. *Biogeochemistry* **41**, 23-51.

- Sivan, O., Alder, M., Pearson, A., Gelman, F., Bar-Or, I., John, S., and Eckert, W. (2011) Geochemical evidence for iron-mediated anaerobic oxidation of methane. *Limnology and Oceanography* **56**, 1536-1544.
- Smemo, K. A. and Yavitt, J. B. (2011) Anaerobic oxidation of methane: an underappreciated aspect of methane cycling in peat and ecosystems? *Biogeosciences* **8**, 779-793.
- Teske, A., Hinrichs, K.-U., Edgcomb, V., de Vera Gomez, A., Kysela, D., Sylva, S. P., Sogin, M. L., and Jannasch, H. W. (2002) Microbial Diversity of Hydrothermal Sediments in the Guaymas Basin: Evidence for Anaerobic Methanotrophic Communities. *Applied and Environmental Microbiology* **68**, 1994-2007.
- Valentine, D. (2002) Biogeochemistry and microbial ecology of methane oxidation in anoxic environments: a review. *Antonie van Leeuwenhoek* **81**, 271-282.
- Whitman, W. B., Bowen, T. L., and Boone, D. R. (1992) The methanogenic bacteria. In: Balows, A., Truper, H. G., Dworkin, M., Harder, W., and Schleifer, K.-H. (Eds.), *The Prokaryotes*. Springer-Verlag, Berlin.
- Zeikus, J. G. (1977) The biology of methanogenic bacteria. *Bacteriol. Rev.* **41**, 514-541.
- Zinder, S. H. (1994) Syntrophic acetate oxidation and "Reversible acetogenesis. In: Drake, H. L. (Ed.), *Acetogenesis*. Chapman and Hall, London.

Table 2.1. Seasonal variations in methane cycling within the to 40 cm of sediment. Concentrations of methane (measured and predicted) are depth-integrated (0-40 cm). The percent saturation of methane is within the top 3 cm of sediment. Sediment temperature is an average of measurements taken within the top 40 cm. Measured concentration and flux values are an average of replicate measurements ($n=3-4$) +/- the standard error. Percentages are calculated from these averages. Total MOG is the sum of methane produced from radiolabeled acetate and bicarbonate. Net MOG is the slope of methane production over time during 6 day incubations. Turnover times (τ), in days, of methane in the top 40 cm of sediment due to total methane flux. Abbreviations: MOG, methanogenesis, Q_e external methane source (see method for details).

	Winter 2008	Winter 2009	Spring 2008	Summer 2008	Summer 2009	Fall 2009
Temperature (°C)	8.7 ± 1.0	13.5 ± 0.2	21.5 ± 0.7	28.3 ± 1.4	30.1 ± 0.5	18.8 ± 0.5
CH ₄ (mmol m ⁻²)	590.7 ± 132.7	476.1 ± 75.0	554.3 ± 27.3	578.2 ± 28.9	550.0 ± 8.6	683.6 ± 59.5
Surface Saturation (%)	10.3 ± 6.0	10.7 ± 1.3	46.0 ± 11.3	17.4 ± 7.3	16.0 ± 0.8	39.6 ± 4.7
MOG (mmol m ⁻² d ⁻¹)	0.5 ± 2.0x10 ⁻²	3.7 ± 0.4	17.6 ± 1.4	3.7 ± 0.8	10.8 ± 1.4	16.9 ± 0.8
Net MOG	0.65 ± 0.2	na	3.16 ± 0.3	7.34 ± 1.6	na	na
Exposed Flux (mmol m ⁻² hr ⁻¹)	1.9x10 ⁻² ± 2.2x10 ⁻³	3.0x10 ⁻² ± 3.0x10 ⁻²	1.6 ± 0.9	2.9 ± 0.9	1.6 ± 0.9	2.1 ± 0.5
% ebullition	0	51	92	99	87	90
Inundated Flux (mmol m ⁻² hr ⁻¹)	7.5x10 ⁻² ± 6.5x10 ⁻³	na	0.26 ± 0.31	na	0.14 ± 0.12	0.72 ± 0.19
Total Flux (mmol m ⁻² d ⁻¹)	0.1 ± 0.1	na	41.3 ± 7.7	na	15.4 ± 9.3	27.9 ± 7.0
% exposed	11	na	90	na	85	59
τ (days)	4,359	na	13	na	36	25
Predicted CH ₄ (mmol m ⁻²)	572.3	na	584.0	na	501.6	611.2
Predicted Exposed Flux (mmol m ⁻² yr ⁻¹)	0	na	1.9	na	1.7	2.1
Q_e (mmol m ⁻² s ⁻¹)	0	na	7263	na	5999	7341

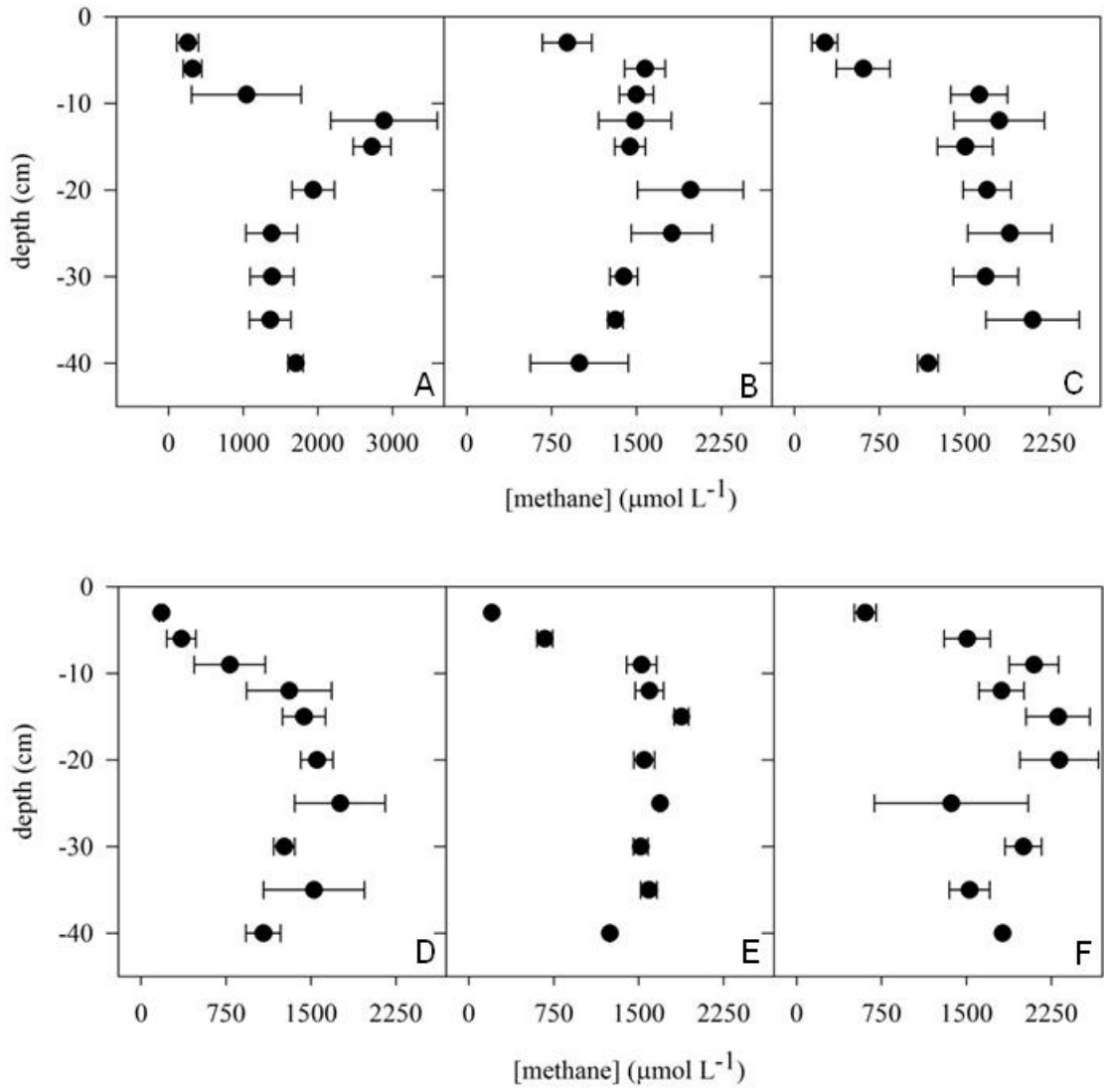


Figure 2.1. Depth profiles of porewater methane (filled circles) at Hammersmith Creek, GA in Winter 2008 (A), Spring 2008 (B), Summer 2008 (C), Winter 2009 (D), Summer 2009 (E), and Fall 2009 (F). Values are an average of 3 sediment cores and error bars represent the standard error.

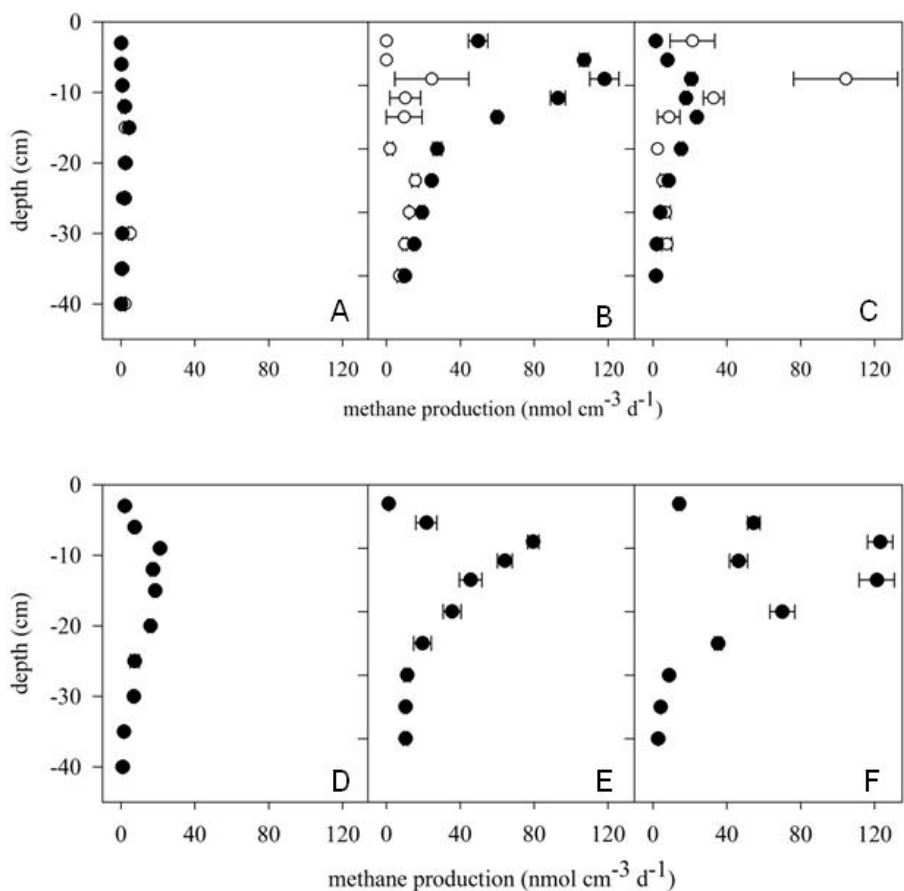


Figure 2.2. Seasonal depth profiles of total (black circles) and net (open circles) methane production at Hammersmith Creek, GA in the Winter 2008 (A), Spring 2008 (B), Summer 2008 (C), Winter 2009 (D), Summer 2009 (E), and Fall 2009 (F). Net methane production rates are only available for Winter, Spring, and Summer of 2008. Rates of total methane production are calculated as the sum of methane produced from $\text{H}^{14}\text{CO}_3^-$ and $^{14}\text{CH}_3\text{COO}^-$ and net methane production rates were calculated as the production of methane over time (see methods for calculation details). Values are an average of 3 sediment cores and error bars represent the standard error. Some error bars are smaller than the data marker.

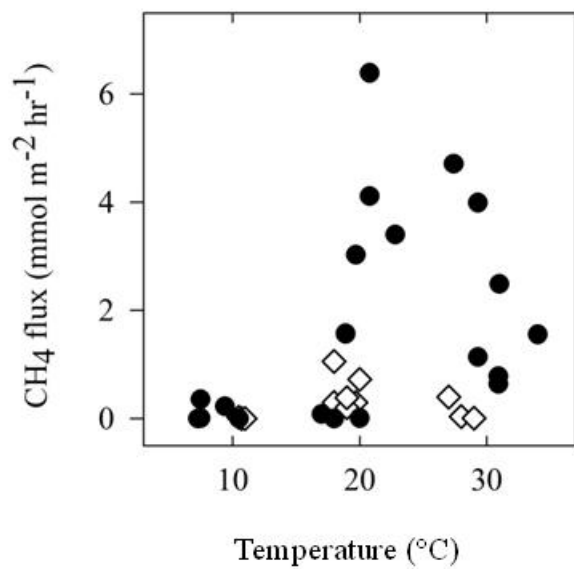


Figure 2.3. Methane (CH₄) fluxes as a function of surface sediment temperature. Filled circles represent atmospheric fluxes and open diamonds represent benthic fluxes.

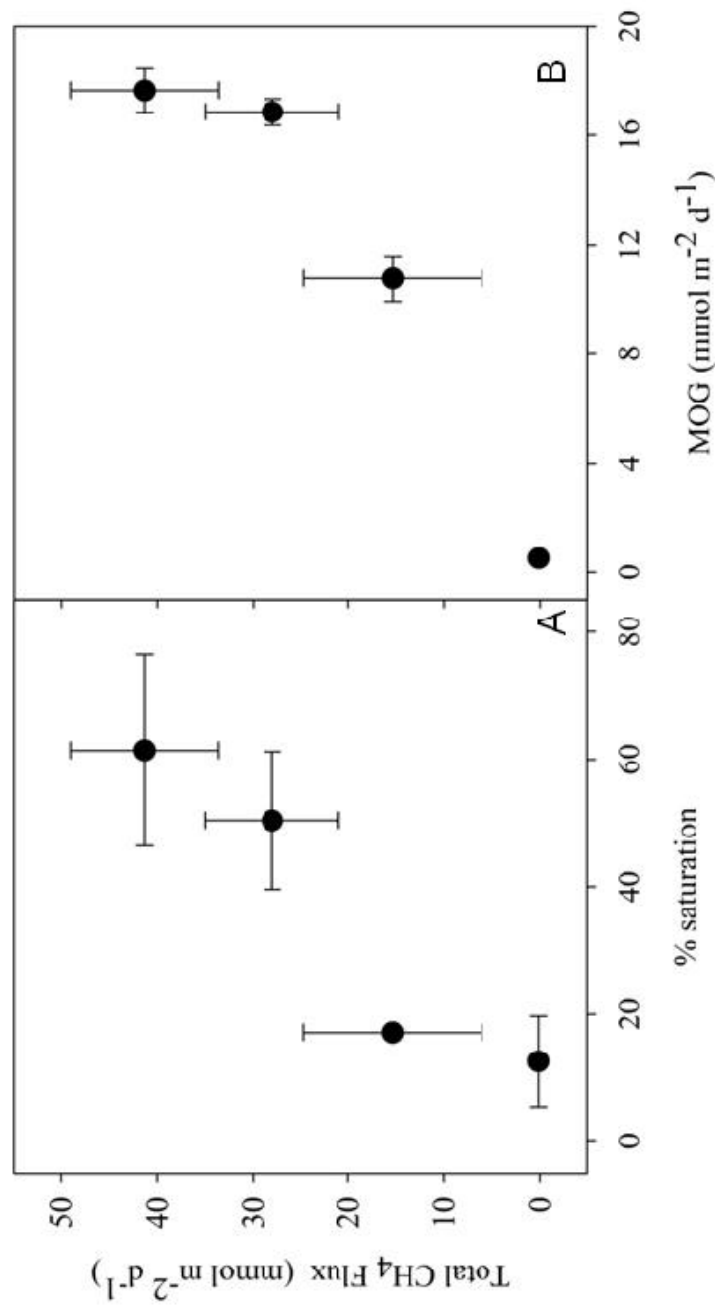


Figure 2.4 A&B. Total methane flux with methane saturation in the surface sediments (A) and with methane production rates in the top 40 cm (MOG; B). Values are an average (n= 3-4) +/- the standard error. See methods for calculation details.

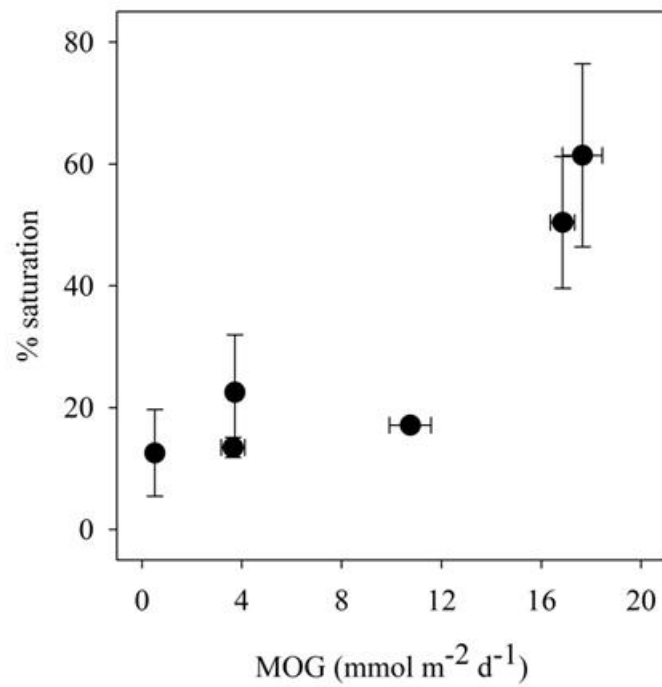


Figure 2.5. Relationship between methane saturation in the surface sediments with methane production in the top 40 cm (MOG). Values are an average of triplicate cores and error bars represent the standard error. See methods for calculation details.

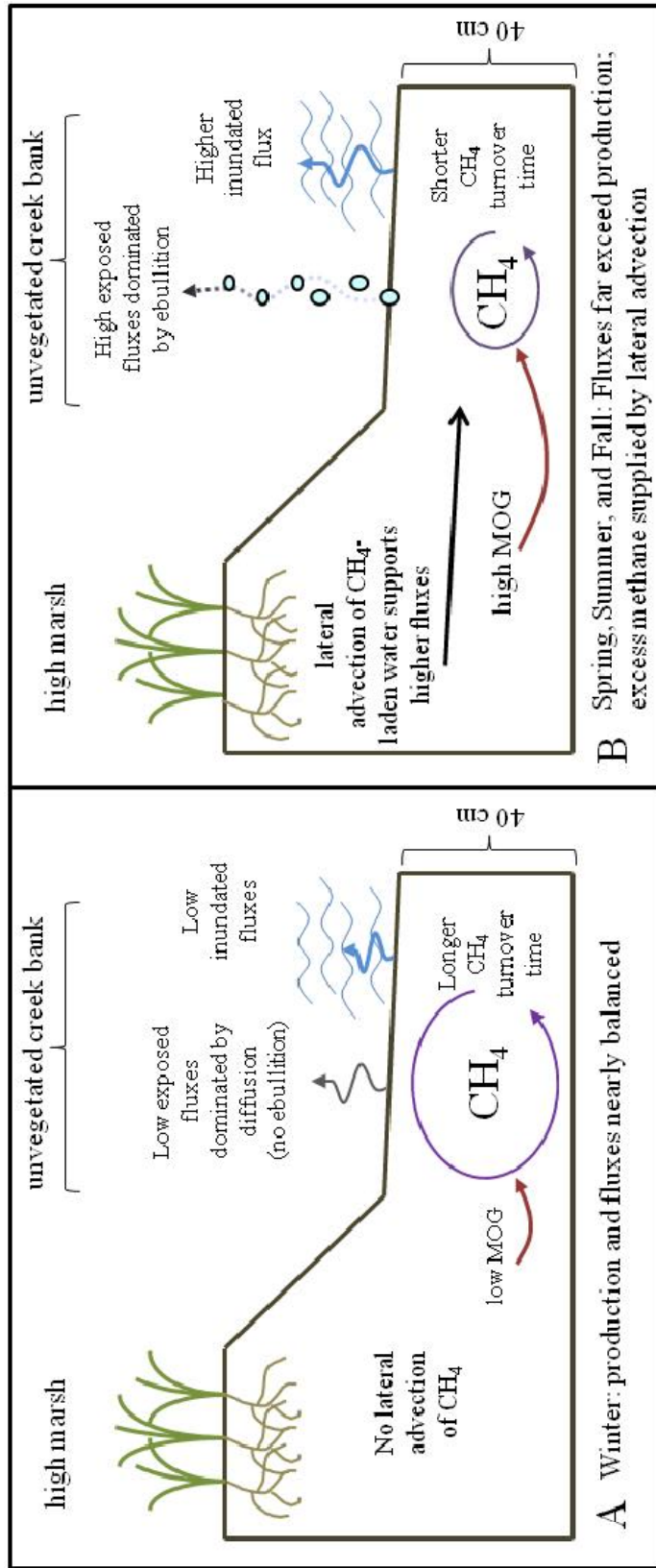


Figure 2.6. Proposed schematic diagram of methane cycling in the top 40 cm of the unvegetated creek bank of Hammersmith Creek, GA in the winter (A) and the other three seasons (B). Depicted are losses of methane from the sediment directly to the atmosphere via ebullition and diffusion during low tide as well as methane loss from inundated sediment to the overlying water. Methane sources include methanogenesis (MOG) and lateral advection from the surrounding marsh.

CHAPTER 3

TIDAL, FRESHWATER SEDIMENTS SUPPORT HIGH RATES OF ANAEROBIC OXIDATION OF METHANE

K. E. A. Segarra¹, V. Samarkin¹, F. Schubotz², M. Y. Yoshinaga³, V. Heuer³,
K.-U. Hinrichs³, and S. B. Joye^{1*}.

To be submitted to *The ISME Journal*

* Corresponding Author

1 Department of Marine Sciences, University of Georgia, Athens, GA

2 Department of Earth, Atmospheric and Planetary Sciences, MIT, Cambridge, MA

3 MARUM Center for Marine Environmental Sciences and Department of Geosciences,
University of Bremen, 28359 Bremen, Germany

ABSTRACT

Freshwater wetlands are characterized by high rates of methanogenesis and support a major portion of global methane emissions. Anaerobic oxidation of methane (AOM), a previously underappreciated process in these systems, may be an important component in freshwater methane budgets. Here we report some of the first direct measurements of AOM in wetland sediments. Rates of AOM were high (up to $286 \text{ nmol cm}^{-3} \text{ d}^{-1}$) and varied on a seasonal basis. Variations in methane production and oxidation were not reflected in variations in archaeal intact polar membrane lipids. Despite low sulfate concentrations, rates of sulfate reduction were sufficient to support all the observed AOM activity, though rates of these two processes were not correlated. The zone of AOM activity was marked by enriched stable carbon isotopic signatures ($\delta^{13}\text{C}$) of methane and depleted signatures of DIC. However, the $\delta^{13}\text{C}$ of archaeal and bacterial lipids were not indicative of methanotrophy. On an annual basis, AOM may consume some $3.3 \text{ mol CH}_4 \text{ m}^{-2}$ which is nearly balanced with measured methane production rates ($4.0 \text{ mol CH}_4 \text{ m}^{-2} \text{ yr}^{-1}$). This study highlights the importance of AOM in freshwater sediments, where this process may control emissions of methane to the atmosphere.

1. INTRODUCTION

Freshwater wetlands are the single largest source of methane (CH₄) to the atmosphere (BROOK et al., 2008). While its concentration in the atmosphere is lower than carbon dioxide, CH₄ is a more powerful greenhouse gas due to its higher radiative forcing capacity (RAMASWAMY, 2001). Thus, the study of CH₄ cycling in freshwater wetlands has important implications for climate change. Methane cycling is mediated by a complex suite of microorganisms spanning anaerobic methanogenic archaea, anaerobic methanotrophic microorganisms, and aerobic methanotrophic bacteria (SEGERS, 1998; SMEMO and YAVITT, 2011). While methane production and aerobic oxidation processes are well studied in wetlands, the process of the anaerobic oxidation of methane (AOM) has received little attention.

In marine settings, AOM is well described (as reviewed by VALENTINE, 2002) and the process certainly mitigates oceanic methane emissions to the atmosphere (REEBURGH, 1996). Previous studies of freshwater CH₄ cycling have overlooked this potential major sink of methane. The reason for this is clear: sulfate is the most commonly asserted to be electron acceptor for AOM (HINRICHS and BOETIUS, 2002; KNITTEL and BOETIUS, 2009) and sulfate concentrations in freshwater environments are typically low. In marine settings, AOM is believed to be mediated by anaerobic methanotrophic archaea (ANMEs), which are often found in close association with sulfate-reducing bacteria (BOETIUS et al., 2000; HINRICHS et al., 1999; ORPHAN et al., 2001). Evidence for this ANME-SRB consortium is based on genetic probing (BOETIUS et al., 2000; ORPHAN et al., 2001), mesocosm experiments (NAUHAUS et al., 2005), and lipid biomarkers for both SRB and archaea which are heavily depleted in ¹³C (ELVERT et al., 1999; HINRICHS et al., 2000;

PANCOST et al., 2001). Still, the biogeochemical controls on AOM in marine environments remain elusive.

Recently, the dogma of sulfate-dependent AOM has been challenged with mounting evidence of AOM coupled to alternative electron acceptors such as nitrite and manganese and iron oxides (BEAL et al., 2009; BOETIUS et al., 2000; ETTWIG et al., 2008; RAGHOEBARSING et al., 2006; SIVAN et al., 2011). Nonetheless, reports of AOM in freshwater settings are scarce. The majority of these studies have been focused in lake water and sediments (CROWE et al., 2011; ELLER et al., 2005; SCHUBERT et al., 2011; SIVAN et al., 2011). Far fewer studies of AOM in wetlands exist (SMEMO and YAVITT, 2007; SMEMO and YAVITT, 2011). The bulk of these previous studies have relied on water chemistry profiles, stable isotope geochemistry, and potential methane oxidation assays as evidence for AOM activity in freshwater; few direct measurements of AOM in wetlands exist (SIVAN et al., 2011).

In this study we assessed the seasonal variations in methanogenic carbon cycling in the unvegetated, intertidal sediments of a freshwater creek. We examined the importance of AOM through sediment geochemistry, direct measurements of microbial activities, stable carbon isotopes, and lipid biomarkers. We discuss AOM in relation to methane production, sulfate reduction, and other biogeochemical processes.

2. METHODS

2.1 Study Site Description

This study was conducted in coastal Georgia along Hammersmith Creek (31°20' N, 81°28' W), a tidal, freshwater (salinity of 0-2 PSU) creek that feeds into the Altamaha River. Adjacent to the creek bank is a marsh dominated by *Zizaniopsis miliacea*. The

sediments at Hammersmith Creek are fine-grained silt and clays with an average carbon content of 5% and C to N ratios around 12. Maximum water depths at high tide range from about 0.5 (neap) to 2 m (spring) and oxygen is consumed within the top 3 mm of sediment (Pers. Obs.).

2.2 Sediment and Porewater Collection and Analyses

At each sampling point (Table 1) several replicate cores were collected as described in *Chapter 3*. Three replicate cores were processed to obtain porewater and solid phase data. These cores were extruded and sectioned at 3-5 cm intervals under a stream of argon to minimize oxygen contamination. Methane and porosity sampling techniques were previously described in *Chapter 3*. Subsamples for hydrogen were collected from each depth interval. Steady-state hydrogen concentrations were determined using a method similar to Hoehler et al. (1998). Briefly, 3 cm³ of sediment were incubated in a helium-purged, sealed 20 mL glass headspace vial at *in situ* temperature for 5 days whereupon the headspace H₂ concentration was quantified with a Peak Performer 1 reduced-gas analyzer (Peak Laboratories).

After gas and porosity samples were collected, the porewater from each core section was extracted using an argon-purged Reeburgh-type squeezer (JOYE et al., 2004; REEBURGH, 1967). The porewater was collected in an argon-purged syringe and filtered (0.2 μm) to halt microbial activity. Prior to use each filter was pre-rinsed with deionized water twice and dried by pushing 10 to 15 mL of air through it to prevent DOC contamination. A 10 mL volume of porewater was preserved for sulfate, phosphate, iron (II), and manganese (II) by addition of 100 μL concentrated trace-metal grade nitric acid to reduce the sample to pH < 2. Samples for hydrogen sulfide (HS⁻) were preserved by

adding 200 μL 20% zinc acetate to 2 mL of pore water and analyzed according to Cline (1969). Samples for ammonium were preserved with 200 μL phenol reagent per mL sample (SOLORZANO, 1969). Samples for DOC, acetate, nitrate, and nitrite analysis were stored frozen. For dissolved inorganic carbon (DIC) analysis, an unfiltered 2 mL sample was injected into a helium-purged headspace vial fitted with a butyl rubber septum and fixed with 100 μL of HCl. Subsequently, the headspace concentration of CO_2 was determined using a GC-FID outfitted with a methanizer to convert CO_2 to CH_4 for detection via the FID.

Sulfate was analyzed via ion chromatography with a Dionex ICS-2000 RFIC. Dissolved iron (II) and manganese (II) were analyzed colorimetrically using the methods of Stookey (1970) and Armstrong (1979), respectively. Combined NO_x species were analyzed with an Antek Instruments model 745 vanadium reduction manifold and model 7050 nitric oxide detector. Nitrite, ammonium, and phosphate were determined colorimetrically using the methods of Parsons et al. (1984), Soloranzo (1969), and Strickland and Parsons (1972), respectively. Nitrate was determined by as the difference between NO_x and NO_2^- . DOC was analyzed with a Shimadzu TOC-V equipped with a NDIR detector. Salinity was measured on unfiltered, extracted porewater with a refractometer and was confirmed by IC chloride analysis. See methods below for acetate analysis.

2.3 Rate Measurements

Incubations with radiolabeled substrates were used to measure microbial activities in replicated samples. Three cores were sectioned under a stream of argon and intact sediment subcores were collected from the sections for rate assays. Microbial activities

were calculated as a volume-specific rate ($\text{nmol cm}^{-3} \text{ d}^{-1}$) and as depth-integrated ($\text{mmol m}^{-2} \text{ d}^{-1}$) [via trapezoidal integration of the volume-specific rates in the top 40 cm of sediment] bases. Rates were porosity corrected when appropriate. Controls (killed with base) for each activity measurement were incubated in parallel with live samples to correct for abiotic transformations of the labeled substrates.

Rates of hydrogenotrophic MOG (bic-MOG; $^{14}\text{CH}_4$ from $\text{H}^{14}\text{CO}_3^-$) and acetoclastic MOG (ace-MOG; $^{14}\text{CH}_4$ from $^{14}\text{CH}_3\text{COO}^-$) were performed, processed, and calculated using the methods of Orcutt et al. (2005). Activities of the injected $\text{H}^{14}\text{CO}_3^-$ and $^{14}\text{CH}_3\text{COO}^-$ were $\sim 2.6 \times 10^7$ dpm and 1.6×10^7 dpm, respectively. The specific activity of the tracers were $50\text{-}60 \text{ Ci mol}^{-1}$ and $45\text{-}60 \text{ Ci mol}^{-1}$, respectively, which increased *in situ* concentrations of DIC by $42 \mu\text{mol L}^{-1}$ and concentrations of acetate by an average of $28 \mu\text{mol L}^{-1}$. Rates of acetate oxidation were quantified as $^{14}\text{CO}_2$ production from $^{14}\text{CH}_3^{14}\text{COO}^-$ (activity $\sim 1 \times 10^7$ dpm, increased *in situ* concentrations by an average of $17 \mu\text{mol L}^{-1}$) according to Orcutt et al. (2010) except that sample distillation proceeded at a low boil for 1 hour with sulfuric acid, not HCl and $^{14}\text{CO}_2$ was trapped into a 15 mL centrifuge tube containing 2 mL of Carbosorb. Rates of acetate oxidation were calculated as per Orcutt et al. (2010).

Rates of homoacetogenesis (AOG; ^{14}C -acetate production from $\text{H}^{14}\text{CO}_3^-$) were determined in the same incubations as bic-MOG. Samples were spiked with 5 mL of 20% zinc acetate to increase the concentration of the product to be collected. Samples were transferred to 125 mL flasks and connected to a soxhlet device and condenser. Samples were brought to a low boil for 45 minutes to separate the volatile fatty acids (VFAs; including acetate) from the rest of the organics and these VFAs were subsequently

collected into the soxhlet reservoir. After separation the condensate from the soxhlet reservoir was transferred to a 50 mL centrifuge tube and 1% of the final volume was mixed with Scintisafe Gel in a 20 mL glass vial and counted with a scintillation counter. In-house recovery rates of acetate standards were on average 97% (unpublished data). Rates of homoacetogenesis were calculated as:

$$\text{AOG} = [\text{DIC}] \times \alpha_{\text{AOG}} \times \frac{a^{14}\text{C-Acetate}}{\text{time} \times a\text{H}^{14}\text{CO}_3^-} \quad (1)$$

Here, [DIC] is the concentration of dissolved inorganic carbon in the porewater (mM), α_{AOG} is the isotope fractionation factor for homoacetogenesis (1.12; Gelwicks 1989), time is the incubation time in days, $a^{14}\text{C-Acetate}$ is the activity of the product, and $a\text{H}^{14}\text{CO}_3^-$ is the activity of the injected tracer.

For anaerobic methane oxidation (AOM), approximately 7×10^5 DPM of $^{14}\text{CH}_4$ tracer was injected and live samples were incubated for 24 hours alongside killed-controls for each depth interval. To terminate activity and preserve produced $^{14}\text{CO}_2$ as carbonate, 5 mL of 2 N NaOH was injected through the rubber septum. The product ($^{14}\text{CO}_2$) was recovered by acid digestion and the activity of both the product and tracer were determined via liquid scintillation counting (JOYE et al., 1999). The rate of AOM was calculated as:

$$\text{AOM rate} = [\text{CH}_4] \times \frac{\alpha_{\text{AOM}} \times a^{14}\text{CO}_2}{\text{time} \times a^{14}\text{CH}_4} \quad (2)$$

Here, $[\text{CH}_4]$ is the concentration of methane in the sediment (nmol cm^{-3} wet sediment), α_{AOM} is the isotope fractionation factor for AOM (1.018 ALPERIN et al., 1988), time is the incubation time in days, $a^{14}\text{CO}_2$ is the activity of the product, and $a^{14}\text{CH}_4$ is the activity of the substrate.

Methods for SR sample preparation and rate assays were identical to those of Orcutt et al. (2010; adapted from Canfield et al. 1986 and Fossing and Jorgensen 1989).

Lipid Extraction and IPL analysis

For lipid analysis between 5 and 33 grams of sediment were homogenized by hand while still frozen with a Teflon spatula. Larger amounts of sediment were extracted from lower depths than the surface due to the generally lower lipid yields at these depths. Sediment lipids were extracted using a modified Bligh-Dyer extraction protocol (LIPP and HINRICHS, 2009; STURT et al., 2004). The polar, intact lipid fraction was separated from the non-polar fraction of the resultant total lipid extract using preparative high-performance liquid chromatography (HPLC) with a fraction collector using methods similar to Kellermann et al. (2012). After prep-HPLC separation the two fractions (polar and apolar) were analyzed by mass-spectrometry (see method below) to ensure complete separation. The IPLs within the polar fraction were then analyzed using an HPLC coupled to a ThermoFinnigan LCQ DecaXP Plus ion-trap mass spectrometer via electrospray interface (HPLC-ESI-MSⁿ) using previously described conditions (SCHUBOTZ et al., 2009; STURT et al., 2004). Identification of IPLs was based on interpretation of mass spectral data as described previously (ROSSEL et al., 2011; ROSSEL et al., 2008; STURT et al., 2004; YOSHINAGA et al., 2011). Quantification of the IPLs was achieved by a comparison of the response of individual IPLs to the response of an injection standard (C₁₉-phosphatidylcholine) followed by a correction for the relative response factors of the injection standard relative to the various IPL standards which were run in parallel to the samples (SCHUBOTZ et al., 2011b).

2.4 Core GDGT Analysis

The core GDGTs of IPLs were produced by acid hydrolysis of the head group (Lipp and Hinrichs, 2009) and subsequently analyzed using an HPLC system coupled to a ion trap mass spectrometer via an electrospray ionization (ESI) source (HPLC-ESI-MS; LIU, 2011).

2.5 Stable Isotope Analyses

The stable carbon isotopic signature of CH₄, DIC, acetate, and particulate organic carbon (POC), and various microbial core lipids were determined using GC-isotope ratio mass spectrometer (GC-IRMS). Carbon isotope results are reported in the $\delta^{13}\text{C}$ notation (‰) relative to V-PBD standard. The isotopic composition of CH₄ and DIC were determined using a Thermo Scientific Delta V plus IRMS. Measurements were performed in duplicate on each triplicate sub-sample. For POC, replicate (n=3) sediment horizons were dried, homogenized, and combined prior to analysis with an elemental analyzer coupled to an IRMS. The concentration and carbon isotope composition of acetate were analyzed simultaneously by irm-LC/MS as reported previously (HEUER et al., 2006; HEUER et al., 2010; LEVER et al., 2010).

Apolar derivatives of the IPLs were analyzed for ¹³C content using a ThermoFinnigan GC coupled to a ThermoFinnigan Delta-plus SP IRMS. Selected samples were run in duplicate and the analytical precision was better than 1 ‰. Prior to isotope analysis, apolar derivatives were produced using standard protocols and analyzed with GC-MS for identification of the compounds. Polar-lipid fatty acids (PLFA) and polar neutral lipids were obtained via saponification of an aliquot of the polar lipid fraction (ELVERT et al., 2003; SCHUBOTZ et al., 2011a). The PLFA products were then derivatized with BBr₃ and analyzed as fatty acid methyl esters (JAHNKE et al., 2002). The

neutral lipid fraction, (which includes monoacyl glycerol ethers or MAGEs and diacyl glycerol ethers or DAGEs) were derivitized with bis-(trimethylsilyl)trifluoroacetamide (BSTFA) at 70°C for 1 hr. Ether-cleavage (JAHNKE et al., 2002; SCHUBOTZ et al., 2011a) of ether-bound IPLs produced apolar phytanes and biphytanes which were analyzed without further derivatization.

2.6 Statistics

Statistical differences were determined using ANOVA with Tukey posthoc testing and Bonferroni corrections. Spearman's rank correlation coefficients were calculated to determine dependence between variables. All tests were conducted in SPSS (SPSS Inc., Chicago, IL) with a significance level of 0.05.

The relationships between geochemical species and archaeal IPLs were assessed using ordination techniques performed with the statistical package CANOCO for Windows 4.5 (Microcomputer Power, Ithaca, NY). Rare archaeal IPLs were removed from the data set prior to a Hellinger transformation (LEGENDRE and GALLAGHER, 2001; RAMETTE, 2007) and where appropriate, highly similar IPL classes were combined (e.g. 2 and 3 Gly-GDGT). All other data was log transformed ($X' = \log[X+10]$) prior to analysis. Within CANOCO all species were centered and standardized. We employed an indirect linear method (principle components analysis; PCA) with a scaling focus on sample distances to explore the distribution of individual samples and their relation to different variables. We used canonical redundancy analysis (RDA) with a focus on species correlations to explore multiple correlations among the microbial and geochemistry data sets. Forward selection with a Monte Carlo permutation test (499 permutations,

significance level $\alpha=0.05$) was used to select minimal sets of variables that significantly explained variation in the data for each RDA.

3. RESULTS

3.1 Porewater Geochemistry

Porewater methane concentrations and temperature (Table 3.1; Fig. 3.1) have been previously reported (Chapter 2) but will be described here as they relate to other variables reported. Generally, DIC profiles mimicked the shape of the CH₄ profiles with a mid-depth maximum between 9 and 15 cm (Fig. 3.1). Concentrations ranged from 0.2 to 7.9 mmol L⁻¹ and were significantly higher during summer and fall than during spring and winter ($p < 0.05$). Additionally, spring DIC concentrations were significantly higher than those observed in winter ($p < 0.05$; Table 3.1). Hydrogen concentrations ranged from below detection limit to 650 nM (Fig. 3.1) and were significantly higher in the summer ($p < 0.05$). DOC concentrations varied significantly with season: fall and winter DOC concentrations were higher than those in spring and summer (Table 3.1). Depth-integrated concentrations were correlated negatively with temperature ($\rho = -0.50$; Table 3.1). Acetate concentrations ranged from below detection to 116 μ M and were significantly higher in the spring than during winter and summer (Fig. 3.1). Sulfate concentrations varied significantly with depth and temperature and concentrations ranged from below detection limit to 1.3 mM, significantly decreasing with depth (Fig. 3.1) and were maximal during summer (Table 3.1). Dissolved sulfide was below detection limits throughout the study.

Dissolved iron II concentrations ranged from $<1 \mu$ M to 1 mM with highest concentrations observed during the winter of 2009 (Table 3.1). Dissolved manganese II

concentrations ranged from 30 μM to over 1 mM with maximum concentrations observed during the summer of 2008 (Table 3.1).

3.2 Microbial Activities

Maximum rates of AOM were observed in the surface sediments and decreased with depth (Fig. 3.2; range of 0.7 to 330 $\text{nmol cm}^{-3} \text{d}^{-1}$). AOM activity was significantly higher in spring and summer (Table 3.2) and there was substantial interannual variability in summertime AOM rates. The ratio of depth-integrated AOM to depth-integrated MOG (ace-MOG + bic-MOG) varied from 0.2 to 25 with highest ratios observed in the winter of 2008 (Table 3.2).

Both pathways of methane production were highest in the upper sediments (3-12 cm) and were only weakly correlated with temperature (Fig. 3.2; bic-MOG: $\rho=0.49$; ace-MOG: $R^2=0.20$). Bic-MOG rates ranged from 0.03 to 140 $\text{nmol cm}^{-3} \text{d}^{-1}$ and were highest in the spring (Table 3.2). Bic-MOG rates were positively but weakly correlated with hydrogen ($\rho=0.21$) and DIC ($\rho=0.36$). Acetoclastic MOG rates were highest in the fall and ranged from below detection to 132 $\text{nmol cm}^{-3} \text{d}^{-1}$.

Sulfate reduction (SR) rates ranged from non-detectable to 6.4 $\mu\text{mol cm}^{-3} \text{d}^{-1}$ (Fig. 3.2) and were significantly highest in the fall and lowest in the spring (Table 3.2). Sulfate reduction rates were negatively correlated with hydrogen ($\rho=-0.47$) and positively correlated with DOC concentration ($\rho=0.60$). The ratio of depth-integrated SR to depth-integrated AOM was greater than 1 at all time points, negatively correlated with hydrogen ($\rho =0.56$), and positively correlated with DOC ($\rho =0.49$).

Rates of homoacetogenesis (AOG) ranged from below detection to 11.5 $\text{nmol cm}^{-3} \text{d}^{-1}$ and varied significantly with season: maximum rates were measured in the spring

and rates in summer and spring were significantly higher than those in winter and fall (Fig. 3.2). Acetate oxidation rates ranged from below detection to $105 \text{ nmol cm}^{-3} \text{ d}^{-1}$ and rates were positively correlated with temperature ($\rho = 0.63$), DIC ($\rho = 0.50$), and AOM ($\rho = 0.61$). Maximum rates were always detected in surface sediments and decreased significantly with depth; activity was significantly highest in summer and lowest in spring and fall (Table 3.2).

3.3 IPLs

Concentrations of total IPLs decreased as the contribution of archaeal IPLs to the total pool increased with depth (Fig. 3.3). Concentrations of total IPLs ranged from 3 to $80 \mu\text{g g dry sediment}^{-1}$, with highest concentrations measured in winter of 2008 and in summers of 2008 and 2009. These seasonal variations were only evident in the surface sediments, however, and concentrations in deeper horizons were fairly uniform. The contribution of archaea to total IPLs ranged from less than 1 to 11%.

The concentration of archaeal IPLs ranged from 148 to 1051 ng g^{-1} dry sediment (Fig. 3.3). Archaeal biomass typically decreased, although slightly, with depth while the contribution of archaeal lipids to the total IPL pool increased. Archaeal IPLs were comprised mainly of glycosidic (Gly) headgroups with archaeol (AR) and glyceroldietherglyceroltetraether(GDGT) core lipids (Table 3.3). The most prevalent archaeal IPL was diglycosyl-archaeol (2Gly-AR), which was present at concentrations up to $470 \text{ ng g dry sediment}^{-1}$. 2Gly-GDGT was the second most prevalent archaeal IPL, though 3 Gly-GDGT also comprised a significant portion of the archaeal lipids. Phosphatidylmethylethanolamine hydroxyarchaeol (PME-OH-AR) contributed an average of 20% of the archaeal lipids. These ubiquitous archaeal lipids were detected at

all depths in all samples. Some of lipids present at lower concentration were found in only a few samples. These include hydroxy-GDGTs with one and two sugars as a head group (2 and 3 Gly-OH-GDGT), 1 Gly-GDGT, a mixed glycol-phospho GDGT with a PI and a monoglycosidic headgroup (PI-GDGT-Gly) and a hydroxyarchaeol with 2 unsaturations and a PG headgroup (PG-di-unsat-OH-AR).

Core lipid analysis of the GDGTs revealed a predominance of GDGT-0 and GDGT-1 (78% of GDGTs on average; not shown). The remainder was comprised of GDGT-2 along with small percentages of crenarchaeol (GDGT-3; average of 6%).

3.4 Stable Isotopes

The stable carbon isotopic signature of methane generally became lighter with depth, although this pattern was most pronounced in spring and summer (Fig. 3.1). Values of $\delta^{13}\text{C-CH}_4$ were significantly heavier (less depleted) in the fall and summer than in the spring and winter. The $\delta^{13}\text{C-DIC}$ values were significantly heavier in the fall than the rest of the seasons ($p < 0.05$) and values generally increased with depth in all seasons (Fig. 3.1). The stable isotopic composition of acetate and POC did not vary seasonally (Table 3.4). Depth-averaged $\delta^{13}\text{C-DIC}$ values decreased with depth-integrated rates of AOM (Fig. 3.4).

The $\delta^{13}\text{C}$ values for archaeal-derived phytanes (from archaeol and hydroxyarchaeol) and biphytanes (from GDGTs) ranged from -30 ‰ to -59.5 ‰, with the lightest values observed in biphytane 2 (Table 3.4). PLFAs derived from bacterial IPLs ranged from -25.4 to -48.5 ‰. The monounsaturated fatty acids C16:1 ω 7 and C16:1 ω 5 were consistently the lightest bacterial lipids detected. No clear patterns with respect to depth or season were observed in the stable isotope values of the microbial core lipids.

Monoacylglycerolethers (MAGEs) and diacylglycerolethers (DAGEs) were not abundant enough to generate a signal on the GC-IRMS.

3.5 Ordinations

The composition of the archaeal lipids was examined through a principal component and redundancy analysis. The PCA (Fig. 3.5) explained most of the variation in the data (78.1 % explained by the first two axes). The associations between the samples and individual IPLs did not display any distinct groupings by depth or season. Glycosidic GDGTs and glycosidic OH-GDGTs were correlated in the PCA and negatively correlated with glycosidic archaeols. The phosphohydroxyarchaeols plotted separately from the other IPL groups.

Relationships between porewater geochemistry (Table 3.1) and microbial activities (Table 3.2) were explored with RDA (Fig. 3.6). Forward selection in CANOCO revealed that a few variables (depth, sulfate, DOC, C:N, DIC, hydrogen, and methane) explained 63.9 % of the variation in the data and the first two axes explained 72.4 % of the variance in the relationship between the rates and geochemical variables.

4. DISCUSSION

4.1 Importance of AOM in tidal, freshwater sediments

Freshwater wetlands are major sources of methane to the atmosphere; therefore, processes that limit methane emissions from these environments directly affect the global climate. Methane production and oxidation were comparable in the investigated sediments (Table 3.1), although AOM was seasonally more important than methane production via acetate or hydrogen. Additional methane may have been sourced from alternative substrates, such as methanethiols and methylated amines (OREMLAND and

POLCIN, 1982). However, previous estimates of net methane production in these sediments suggest that production of methane from alternative substrates is not important (*Chapter 2*). Seasonally-averaged rates of AOM provide an annual estimate of 3.3 mol CH₄ m⁻² consumed in the top 40 cm of anoxic sediments. This is about 83% of methane produced from acetate and bicarbonate, the dominant pathways of methane production (WINFREY and ZEIKUS, 1979), a comparison which demonstrates the importance of AOM in this freshwater system.

The rates of AOM in these sediments are the highest reported for freshwater settings (SIVAN et al., 2011), although only a few studies are available for comparison. Previous reports of AOM rates in freshwaters have been based on potential AOM activity assays under laboratory conditions (DEUTZMANN and SCHINK, 2011; ELLER et al., 2005; RAGHOEBARSING et al., 2006; SMEMO and YAVITT, 2007). The AOM rates for Hammersmith Creek are similar to those reported for deep sea methane seeps and inner shelf sediments (as reviewed by HINRICHS and BOETIUS, 2002; HOEHLER et al., 1994; ORCUTT et al., 2005).

4.2 Sulfate Reduction and AOM

The sulfate-methane transition zone fluctuated seasonally (Fig. 3.1), mirroring seasonal variations in the depth of maximum SR activity. However, maximum AOM activity was always observed in surface sediments (0-3 cm), suggesting that AOM and SR may not be linked in these sediments. However, SR rates exceeded AOM rates at nearly all depths and therefore is of sufficient magnitude to support the measured methane oxidation activity. The sulfate concentrations in these sediments are low (average of 100 μM), and high SR rates led to rapid sulfate turnover times on the order of

hours to days. The sulfate pool is likely replenished by the reoxidation of reduced sulfur species (RODEN and TUTTLE, 1993) and diurnal tides which may deliver low inputs of sulfate via tidal pumping.

While it is conceivable that methane was oxidized by sulfate in these sediments, rates of AOM and SR were not correlated and demonstrated different seasonal patterns. The consumption of oxygen within the top 3 mm of sediment in conjunction with anoxic incubations confirm that methane oxidation was anaerobic. Other electron acceptors linked to AOM, such as iron oxides, manganese oxides, nitrate, and nitrite are readily available in these sediments (Table 3.1; BEAL et al., 2009; ETTWIG et al., 2010; SIVAN et al., 2011). Nitrogen, iron, and manganese reduction rates were not directly measured during the study, however, the substantial concentrations of reduced iron and manganese which accumulated in the sediments with depth indicate active metal reduction throughout the year. The mechanism of AOM in these and other freshwater sediments is unclear (*Chapter 5*). The oxidation of methane with sulfate in these sediments is feasible, although the data does not preclude the involvement of one or more alternative electron acceptors.

4.3 Controls of AOM and Interactions with Other Metabolisms

As in this study, rates of AOM have been shown to vary on a seasonal basis in other coastal sediments, where peak AOM activity coincided with warm summer temperatures (IVERSEN and BLACKBURN, 1981). In HC, AOM was highest in the spring and therefore temperature does not appear to be the major driver of AOM seasonality. Modeled seasonal variations of AOM in coastal sediments suggest a thermodynamic control on AOM (DALE et al., 2006). The mechanism proposed involved seasonal

variations in the demand for hydrogen, which was assumed to be a product of AOM (HOEHLER et al., 1994). Hydrogen and acetate have both been proposed as intermediates produced by methane oxidizers in the AOM consortium (HOEHLER et al., 1994; VALENTINE and REEBURGH, 2000). These two species are also key intermediates in organic matter degradation and each may thermodynamically influence the dominant pathways of terminal metabolism (HOEHLER et al., 1998; LOVLEY and GOODWIN, 1988; SCHINK, 1997).

In these sediments, AOM was significantly correlated with acetate oxidation, as corroborated by the RDA (Fig. 3.6), suggesting a linkage between AOM and acetate cycling. Acetate produced as an AOM intermediate could be coupled to acetate oxidation. Acetate produced via AOM could support the majority of the observed acetate oxidation activity measured in these sediments, as evidenced by a comparison of acetate turnover times (Table 3.5). Although AOM was not correlated with ace-MOG or SR (which may use acetate; SCHÖNHEIT et al., 1982), multiple other acetate-consuming processes likely occur in these sediments, including heterotrophic nitrogen and metal reduction (WESTON et al., 2006). Assuming a syntrophic arrangement between methane oxidizers and consumers of the intermediate, acetate produced by AOM would be consumed quickly. Radiotracer experiments have indicated that a portion of porewater acetate may be recalcitrant and not available to microorganisms (PARKES et al., 1984; WELLSBURY and PARKES, 1995). However, if acetate is produced during AOM, it may support multiple pathways of mineralization by the delivery of fresh, labile substrate. Differences in acetate availability may also explain why concentrations of porewater acetate did not mirror variations in measured acetate-consuming and producing processes.

In aquatic sediments hydrogen concentrations are typically very low, which suggests a tight coupling between hydrogen production by hydrolytic and fermentative processes and consumption by terminal metabolizers (HOEHLER et al., 1998). The short turnover times of hydrogen (minutes to hours; Table 3.5) due to bic-MOG and AOG in Hammersmith Creek sediments necessitates significant hydrogen production. Although our data suggests that SR rates were influenced by DOC and hydrogen concentrations, autotrophic SR would lead to even greater hydrogen demand in these sediments (Table 3.5). Models suggest that AOM may be an important hydrogen-producing process in coastal sediments (DALE et al., 2006). Therefore, AOM may be an important producer of substrates for other terminal metabolizing groups in these sediments.

4.4 Composition of Archaeal IPLs

The microbial community that mediates AOM in freshwaters is undescribed. Some studies have suggested the process is mediated entirely by bacteria (ETTWIG et al., 2008; NIEMANN et al., 2009). Still, other freshwater-based studies have detected both ANMEs (ELLER et al., 2005) and members of the clade AAA (AOM-associated archaea; SCHUBERT et al., 2011). Here, we examined the IPLs of the archaeal community in attempt to link AOM activity with biomarkers for archaeal methanotrophs. In contrast to traditional lipid-based techniques, IPLs provide an estimate of the viable microbial community (BIDDLE et al., 2006; RÜTTERS et al., 2001; STURT et al., 2004), as the polar head group is lost quickly after cell death (WHITE et al., 1979). Our estimates of biomass are lower than those reported for some peats (LIU et al., 2010) and similar to those reported in the sediments of the Black Sea (SCHUBOTZ et al., 2009).

The archaeal lipids were comprised of a diverse collection of GDGTs with mainly glycosidic headgroups and several archaeol and hydroxyarchaeol-based lipids. All of these lipids are diagnostic for the archaeal kingdom (KATES, 1993; KOGA et al., 1993), but specific assignment to particular archaeal groups was based on previous environmental studies and ordination analysis (Table 3.4). Glycosidic GDGTs have been detected in many marine settings where they have been attributed to both methanogenic and methanotrophic archaea (ROSSEL et al., 2011; ROSSEL et al., 2008; SCHUBOTZ et al., 2009). The glycosidic OH-GDGTs observed in these sediments are a relatively newly identified lipid class (Liu et al. 2011). Glycosidic OH-GDGTs have been found to date both in one member of the crenarchaea and euryarchaea, within the ammonia oxidizing *Candidatus Nitrosopumilus maritimus* (SCHOUTEN et al., 2008) and the methanogen *Methanococcus thermolithotrophicus* (LIU, 2011), respectively. The close association of these lipids with the other glycosidic GDGTs in the PCA (Fig. 3.5) suggests similar sources and/or niches of source organisms. Di- and triglycosidic archaeols are found in the deep subsurface (BIDDLE et al., 2006; LIPP et al., 2008), marine seep sites (ROSSEL et al., 2011; ROSSEL et al., 2008; YOSHINAGA et al., 2011), and in cultured methanogens (STURT et al., 2004). These lipids were the most prevalent and are likely attributed to generic archaea as well as methanogens. PME-OH-AR, which was uncorrelated with the other archaeal lipids in the PCA (Fig. 3.5), was documented previously in freshwater lake sediments (YOSHINAGA et al., 2011). Other phospho-hydroxyarchaeols have been identified in cultured methanogens (KOGA et al., 1993). Its arrangement in the PCA plot suggests a niche distinct from those organisms which produce GDGTs and archaeol-

based lipids. As this particular IPL has only been reported in freshwater environments, it may be a biomarker for freshwater methane-cycling organisms.

The composition of the archaeal lipids varied slightly with season. In the warmer months, especially the summer of 2009, the contribution of OH-GDGTs increased. The presence of PG-di-unsat-OH-AR, an IPL previously identified in cold seeps (YOSHINAGA et al., 2011), and PI-GDGT-Gly, coincided with the coldest sampling temperatures at Hammersmith Creek, suggesting that these biomarkers may be produced by cold-adapted organisms (NICHOLS et al., 2004). These seasonal changes in the archaeal lipid profiles indicate that the turnover of the microbial community occurs quickly enough, and is of sufficient magnitude, to be captured through IPL analysis.

Observed temporal variations in the contribution of archaeol-based IPLs to GDGTs were likely due to variations in the archaeal community structure. The ratio of archaeol- versus GDGT-based archaeal lipids has been used as an indicator for different ANME communities (ROSSEL et al., 2008). Variations in the lipid profiles could explain seasonal changes in methane cycling in these sediments. For example, the low ratio of AOM:MOG in summer of 2009 may be attributed a shift in the archaeal community which produced a relatively larger contribution of OH-GDGTs at this time point. Concentrations of total archaeal IPLs did not correspond with maxima in methanogenic or AOM activity in most samples. For example, the highest rates of AOM and MOG were measured in the spring of 2008, yet the archaeal biomass is no higher at this time point than in the winter of 2008, when MOG was at a minimum. This indicates that a major portion of the archaeal biomass might not be involved in methane cycling, but rather other, heterotrophic processes, such as observed for the deep biosphere (BIDDLE et al.,

2006). However, in the fall of 2009, the high archaeal biomass at 6-9 cm was matched by maximum rates of methanogenesis. Methane cycling is likely not the only trophic role of Archaea in these sediments, and changes in microbial activity need not be associated with changes in biomass (BLUME et al., 2002). Modeling efforts have suggested that seasonal changes in SR and AOM are not controlled by biomass, which remained constant throughout the year, but rather changes in cell-specific rate (DALE et al., 2006).

4.5 Stable isotopes

Typically, lipids associated with methanotrophic archaea are more depleted than their purported carbon source of methane and highly depleted lipids have been used as indicators of AOM in a variety of marine environments (HINRICHS et al., 1999; HINRICHS et al., 2000; PANCOST et al., 2000; SCHUBOTZ et al., 2011a). In contrast to marine-based studies of AOM, few studies have examined microbial lipids in relation to AOM in freshwater (NIEMANN et al., 2009; SIVAN et al., 2011). For example, a slight depletion in the $\delta^{13}\text{C}$ of the total lipid extract in the sediments of Lake Kinneret was attributed to AOM (SIVAN et al., 2011); however, the isotopic composition of the individual lipids was not reported.

While the influence of AOM on the $\delta^{13}\text{C}$ of methane and DIC is clear (both in profile, Fig. 3.1, and on a depth-integrated basis, Fig. 3.4), the isotopic evidence for AOM in the archaeal lipids is less evident (Table 3.4). Minimum signatures of -59.5 ‰ were measured in the zone of maximum AOM activity, suggesting the incorporation of depleted methane-sourced carbon. These values are much heavier than those reported for ANME-dominated settings (HINRICHS and BOETIUS, 2002). Hence, the observed archaeal stable carbon isotope values may be derived from a mixed signal of methanotrophic and

methanogenic pathways. Reported fractionation between methanogenic substrates and lipids vary from -6.6 (enriched) to 47.0 ‰ for hydrogenotrophic and acetoclastic methanogenesis, depending upon growth conditions (LONDRY et al., 2008). The range in ^{13}C content of the archaeal lipids of this study (-30.0 to -59.5 ‰) could result purely from methanogenic activity, as revealed by a comparison of the stable isotopic composition of acetate and carbon dioxide (derived from DIC; MOOK et al., 1974) to archaeal lipids (Table 3.4). The wide range of values for the archaeal lipids could be attributed to variations in methanogenic substrates (e.g. hydrogen and acetate) and with fluctuations in the dominant methanogenic pathway (acetoclastic versus hydrogenotrophic MOG) both with depth and season (Fig. 3.1 and 3.2). These findings are in accord with a recent review of isotopic evidence surrounding AOM in vent and seep communities which argued the high depletions in lipids in excess of the methane isotope signature in these environments may be entirely due to autotrophic methanogenesis (ALPERIN and HOEHLER, 2009).

In addition to the depleted archaeal lipids, slightly depleted monounsaturated fatty acids (C16:1 ω 7 and C16:1 ω 5) were detected in these sediments. These lipids are associated with sulfate-reducing bacteria and relatively high amounts of these lipids have been found with depleted isotopic signatures in AOM-dominated settings such as cold seeps and vent sites (ELVERT et al., 2003; NIEMANN and ELVERT, 2008; ORCUTT et al., 2005). The isotopic signatures of these two lipids may indicate the involvement of SRB in AOM in the sediments of Hammersmith Creek. It is also conceivable that utilization of carbon dioxide or acetate (both known substrates of SRBs) could produce these observed depletions. Evidence suggests that unlike marine sediments, freshwater anaerobic

methanotrophs are not found in close association with SRB (ELLER et al., 2005; SCHUBERT et al., 2011). Furthermore, SRBs in AOM-enrichments assimilated bicarbonate and not methane-derived carbon (WEGENER et al., 2008). Thus, the detection of highly depleted bacterial lipids may not be an appropriate diagnostic for AOM in these environments.

Sulfate-independent AOM may involve one or more groups of bacteria. For example, the novel bacterial phylum NC10, isolated from freshwater batch reactors, is capable of oxidizing methane with nitrite (ETTWIG et al., 2010). Diagnostic lipids of the NC10 bacteria have not yet been reported; however, bacterial fatty acids implicated in earlier reports of denitrification coupled to AOM (RAGHOEBARSING et al., 2006), were either not detected in the sediments of Hammersmith Creek or found in non-depleted forms (Table 3.4). Thus, while our data do not necessarily link SRB to the oxidation of AOM in these sediments, other bacterial groups are likewise not supported by our data.

The isotopic signatures of the archaeal and bacterial lipids in these sediments are likely the result of a range of metabolic processes, including methanotrophy. Carbon inputs from heterotrophic and autotrophic processes would dilute a potential signal of 'pure' methanotrophy. Thus, elucidation of the microorganisms involved in AOM in this setting is inconclusive based on stable isotope data alone.

4.6 Conclusions

The freshwater, tidal sediments of Hammersmith Creek support substantial rates of AOM that are comparable to the measured methane production rates. Rates varied seasonally, with significantly higher rates in spring and summer. Sulfate reduction may support all of the observed methane oxidation in these sediments, notwithstanding low *in*

situ sulfate concentrations. Archaeal biomarkers for AOM and methanogenesis were abundantly found in the sediments. Small temporal variations in the archaeal biomass and lipid profiles may indicate seasonal variations in the archaeal community. However, despite high methane oxidation activity, no highly depleted carbon isotopic signatures of archaeal or bacterial lipids were detected. The results highlight the importance of AOM in methane cycling in this system. However, no conclusions may be made about the mechanism of the process or the organisms involved. This work adds to the increasing evidence of the importance of AOM in freshwater settings. As these ecosystems are responsible for a major portion of global emissions, an understanding of this methane-consuming process deserves further attention.

ACKNOWLEDGEMENTS

We wish to thank D. Saucedo, J. Shalack, and the GCE-LTER for valuable field assistance and site access. We thank K. Hunter for analytical assistance. J. Chanton kindly provided methane isotope standards. This research was funded by an NSF DEB award (DEB 0717189).

REFERENCES

- Alperin, M. J. and Hoehler, T. M. (2009) Anaerobic methane oxidation by archaea/sulfate-reducing bacteria aggregates: 2. Isotopic constraints. *American Journal of Science* **309**, 958-984.
- Alperin, M. J., Reeburgh, W. S., and Whiticar, M. J. (1988) Carbon and hydrogen isotope fractionation resulting from anaerobic methane oxidation. *Global Biogeochem. Cycles* **2**, 279-288.

- Armstrong, P. B., Lyons, W. B., and Gaudette, H. E. (1979) Application of Formaldoxime Colorimetric Method for the Determination of Manganese in the Pore Water of Anoxic Estuarine Sediments. *Estuaries* **2**, 198-201.
- Beal, E. J., House, C. H., and Orphan, V. J. (2009) Manganese- and Iron-Dependent Marine Methane Oxidation. *Science* **325**, 184-187.
- Biddle, J. F., Lipp, J. S., Lever, M. A., Lloyd, K. G., Sørensen, K. B., Anderson, R., Fredricks, H. F., Elvert, M., Kelly, T. J., Schrag, D. P., Sogin, M. L., Brenchley, J. E., Teske, A., House, C. H., and Hinrichs, K.-U. (2006) Heterotrophic Archaea dominate sedimentary subsurface ecosystems off Peru. *Proceedings of the National Academy of Sciences of the United States of America* **103**, 3846-3851.
- Blume, E., Bischoff, M., Reichert, J. M., Moorman, T., Konopka, A., and Turco, R. F. (2002) Surface and subsurface microbial biomass, community structure and metabolic activity as a function of soil depth and season. *Applied Soil Ecology* **20**, 171-181.
- Boetius, A., Ravenschlag, K., Schubert, C. J., Rickert, D., Widdel, F., Gieseke, A., Amann, R., Jorgensen, B. B., Witte, U., and Pfannkuche, O. (2000) A marine microbial consortium apparently mediating anaerobic oxidation of methane. *Nature* **407**, 623-626.
- Brook, E., Archer, D., Dlugokencky, E., Frohling, S., and Lawrence, D. (2008) Potential for abrupt changes in atmospheric methane, *Abrupt Climate Change. A report by the U.S. Climate Change Science Program and the Subcommittee on Global Change Research.* . U.S. Geological Survey, Reston, VA.

- Canfield, D. E., Raiswell, R., Westrich, J. T., Reaves, C. M., and Berner, R. A. (1986) The use of chromium reduction in the analysis of reduced inorganic sulfur in sediments and shales. *Chemical Geology* **54**, 149-155.
- Cline, J. D. (1969) Spectrophotometric Determination of Hydrogen Sulfide in Natural Waters. *Limnology and Oceanography* **14**, 454-458.
- Crowe, S. A., Katsev, S., Leslie, K., Sturm, A., Magen, C., Nomosatryo, S., Pack, M. A., Kessler, J. D., Reeburgh, W. S., Roberts, J. A., Gonzalez, L., Douglas Haffner, G., Mucci, A., Sundby, B., and Fowle, D. A. (2011) The methane cycle in ferruginous Lake Matano. *Geobiology* **9**, 61-78.
- Dale, A. W., Regnier, P., and Van Cappellen, P. (2006) Bioenergetic Controls on Anaerobic Oxidation of Methane (AOM) in Coastal Marine Sediments: A Theoretical Analysis. *American Journal of Science* **306**, 246-294.
- Deutzmann, J. S. and Schink, B. (2011) Anaerobic Oxidation of Methane in Sediments of an Oligotrophic Freshwater Lake (Lake Constance). *Appl. Environ. Microbiol.*, AEM.00340-11.
- Eller, G., Känel, L., and Krüger, M. (2005) Cooccurrence of Aerobic and Anaerobic Methane Oxidation in the Water Column of Lake Plußsee. *Applied and Environmental Microbiology* **71**, 8925-8928.
- Elvert, M., Boetius, A., Knittel, K., and Jørgensen, B. B. (2003) Characterization of Specific Membrane Fatty Acids as Chemotaxonomic Markers for Sulfate-Reducing Bacteria Involved in Anaerobic Oxidation of Methane. *Geomicrobiology Journal* **20**, 403-419.

- Elvert, M., Suess, E., and Whiticar, M. J. (1999) Anaerobic methane oxidation associated with marine gas hydrates: superlight C-isotopes from saturated and unsaturated C20 and C25 irregular isoprenoids. *Naturwissenschaften* **86**, 295-300.
- Ettwig, K. F., Butler, M. K., Le Paslier, D., Pelletier, E., Mangenot, S., Kuypers, M. M. M., Schreiber, F., Dutilh, B. E., Zedelius, J., de Beer, D., Gloerich, J., Wessels, H. J. C. T., van Alen, T., Luesken, F., Wu, M. L., van de Pas-Schoonen, K. T., Op den Camp, H. J. M., Janssen-Megens, E. M., Francoijs, K.-J., Stunnenberg, H., Weissenbach, J., Jetten, M. S. M., and Strous, M. (2010) Nitrite-driven anaerobic methane oxidation by oxygenic bacteria. *Nature* **464**, 543-548.
- Ettwig, K. F., Shima, S., Van De Pas-Schoonen, K. T., Kahnt, J., Medema, M. H., Op Den Camp, H. J. M., Jetten, M. S. M., and Strous, M. (2008) Denitrifying bacteria anaerobically oxidize methane in the absence of Archaea. *Environmental Microbiology* **10**, 3164-3173.
- Fossing, H. and Jørgensen, B. B. (1989) Measurement of bacterial sulfate reduction in sediments: Evaluation of a single-step chromium reduction method. *Biogeochemistry* **8**, 205-222.
- Heuer, V., Elvert, M., Tille, S., Krummern, M., Mollar, X. P., Hmelo, L., and Hinrichs, K.-U. (2006) Online d13C analysis of volatile fatty acids in sediment/porewater systems by liquid chromatography-isotope ratio mass spectrometry. *Limnology and Oceanography: Methods* **4**, 346-357.
- Heuer, V. B., Krüger, M., Elvert, M., and Hinrichs, K.-U. (2010) Experimental studies on the stable carbon isotope biogeochemistry of acetate in lake sediments. *Organic Geochemistry* **41**, 22-30.

- Hinrichs, K.-U. and Boetius, A. (2002) The anaerobic oxidation of methane: new insights in microbial ecology and biogeochemistry. *Ocean Margin Systems*.
- Hinrichs, K.-U., Hayes, J. M., Sylva, S. P., Brewer, P. G., and DeLong, E. F. (1999) Methane-consuming archaeobacteria in marine sediments. *Nature* **398**, 802-805.
- Hinrichs, K.-U., Summons, R. E., Orphan, V., Sylva, S. P., and Hayes, J. M. (2000) Molecular and isotopic analysis of anaerobic methane-oxidizing communities in marine sediments. *Organic Geochemistry* **31**, 1685-1701.
- Hoehler, T. M., Alperin, M. J., Albert, D. B., and Martens, C. S. (1994) Field and laboratory studies of methane oxidation in an anoxic marine sediment: Evidence for a methanogen-sulfate reducer consortium. *Global Biogeochem. Cycles* **8**, 451-463.
- Hoehler, T. M., Alperin, M. J., Albert, D. B., and Martens, C. S. (1998) Thermodynamic control on hydrogen concentrations in anoxic sediments. *Geochimica et Cosmochimica Acta* **62**, 1745-1756.
- Iversen, N. and Blackburn, T. H. (1981) Seasonal Rates of Methane Oxidation in Anoxic Marine Sediments. *Appl. Environ. Microbiol.* **41**, 1295-1300.
- Jahnke, L. L., Embaye, T., and Summons, R. E. (2002) Lipid biomarkers for methanogens in hypersaline cyanobacterial mats for Guerro Negro, Baja California Sur. In: NASA (Ed.).
- Joye, S. B., Boetius, A., Orcutt, B. N., Montoya, J. P., Schulz, H. N., Erickson, M. J., and Lugo, S. K. (2004) The anaerobic oxidation of methane and sulfate reduction in sediments from Gulf of Mexico cold seeps. *Chemical Geology* **205**, 219-238.

- Joye, S. B., Connell, T. L., Miller, L. G., Oremland, R. S., and Jellison, R. S. (1999) Oxidation of Ammonia and Methane in an Alkaline, Saline Lake. *Limnology and Oceanography* **44**, 178-188.
- Kates, M. (1993) Chapter 9 Membrane lipids of archaea. In: M. Kates, D. J. K. and Matheson, A. T. (Eds.), *New Comprehensive Biochemistry*. Elsevier.
- Kellermann, M. Y., Schubotz, F., Elvert, M., Lipp, J. S., Birgel, D., Prieto-Mollar, X., Dubilier, N., and Hinrichs, K.-U. (2012) Symbiont–host relationships in chemosynthetic mussels: A comprehensive lipid biomarker study. *Organic Geochemistry* **43**, 112-124.
- Knittel, K. and Boetius, A. (2009) Anaerobic Oxidation of Methane: Progress with an Unknown Process. *Annual Review of Microbiology* **63**, 311-334.
- Koga, Y., Nishihara, M., Morii, H., and Akagawa-Matsushita, M. (1993) Ether polar lipids of methanogenic bacteria: structures, comparative aspects, and biosyntheses. *Microbiological Reviews* **57**, 164-182.
- Legendre, P. and Gallagher, E. (2001) Ecologically meaningful transformations for ordination of species data. *Oecologia* **129**, 271-280.
- Lever, M. A., Heuer, V. B., Morono, Y., Masui, N., Schmidt, F., Alperin, M. J., Inagaki, F., Hinrichs, K.-U., and Teske, A. (2010) Acetogenesis in Deep Subseafloor Sediments of The Juan de Fuca Ridge Flank: A Synthesis of Geochemical, Thermodynamic, and Gene-based Evidence. *Geomicrobiology Journal* **27**, 183-211.
- Lipp, J. S. and Hinrichs, K.-U. (2009) Structural diversity and fate of intact polar lipids in marine sediments. *Geochimica et Cosmochimica Acta* **73**, 6816-6833.

- Lipp, J. S., Morono, Y., Inagaki, F., and Hinrichs, K.-U. (2008) Significant contribution of Archaea to extant biomass in marine subsurface sediments. *Nature* **454**, 991-994.
- Liu, X.-L. (2011) Glycerol ether lipids in sediments: sources, diversity and implications
University of Bremen.
- Liu, X.-L., Leider, A., Gillespie, A., Gröger, J., Versteegh, G. J. M., and Hinrichs, K.-U. (2010) Identification of polar lipid precursors of the ubiquitous branched GDGT orphan lipids in a peat bog in Northern Germany. *Organic Geochemistry* **41**, 653-660.
- Londry, K. L., Dawson, K. G., Grover, H. D., Summons, R. E., and Bradley, A. S. (2008) Stable carbon isotope fractionation between substrates and products of *Methanosarcina barkeri*. *Organic Geochemistry* **39**, 608-621.
- Lovley, D. R. and Goodwin, S. (1988) Hydrogen concentrations as an indicator of the predominant terminal electron-accepting reactions in aquatic sediments. *Geochimica et Cosmochimica Acta* **52**, 2993-3003.
- Mook, W. G., Bommerson, J. C., and Staverman, W. H. (1974) Carbon isotope fractionation between dissolved bicarbonate and gaseous carbon dioxide. *Earth and Planetary Science Letters* **22**, 169-176.
- Nauhaus, K., Treude, T., Boetius, A., and Krüger, M. (2005) Environmental regulation of the anaerobic oxidation of methane: a comparison of ANME-I and ANME-II communities. *Environmental Microbiology* **7**, 98-106.
- Nichols, D. S., Miller, M. R., Davies, N. W., Goodchild, A., Raftery, M., and Cavicchioli, R. (2004) Cold Adaptation in the Antarctic Archaeon

- Methanococcoides burtonii Involves Membrane Lipid Unsaturation. *Journal of Bacteriology* **186**, 8508-8515.
- Niemann, H. and Elvert, M. (2008) Diagnostic lipid biomarker and stable carbon isotope signatures of microbial communities mediating the anaerobic oxidation of methane with sulphate. *Organic Geochemistry* **39**, 1668-1677.
- Niemann, H., Hitz, C., Schubert, C., Veronesi, M., Simona, M., and Lehmann, M. (2009) Biogeochemical signatures of the anaerobic oxidation of methane in a south alpine lake (Lake Lugano). *Geophysical Reserach Abstracts* **11**, EGU2009-11652.
- Orcutt, B., Boetius, A., Elvert, M., Samarkin, V., and Joye, S. B. (2005) Molecular biogeochemistry of sulfate reduction, methanogenesis and the anaerobic oxidation of methane at Gulf of Mexico cold seeps. *Geochimica et Cosmochimica Acta* **69**, 4267-4281.
- Orcutt, B. N., Joye, S. B., Kleindienst, S., Knittel, K., Ramette, A., Reitz, A., Samarkin, V., Treude, T., and Boetius, A. (2010) Impact of natural oil and higher hydrocarbons on microbial diversity, distribution, and activity in Gulf of Mexico cold-seep sediments. *Deep Sea Research Part II: Topical Studies in Oceanography* **57**, 2008-2021.
- Oremland, R. S. and Polcin, S. (1982) Methanogenesis and Sulfate Reduction: Competitive and Noncompetitive Substrates in Estuarine Sediments. *Applied and Environmental Microbiology* **44**, 1270-1276.
- Orphan, V. J., Hinrichs, K.-U., Ussler, W., III, Paull, C. K., Taylor, L. T., Sylva, S. P., Hayes, J. M., and Delong, E. F. (2001) Comparative Analysis of Methane-

- Oxidizing Archaea and Sulfate-Reducing Bacteria in Anoxic Marine Sediments. *Appl. Environ. Microbiol.* **67**, 1922-1934.
- Pancost, R. D., Hopmans, E. C., and Sinninghe Damsté, J. S. (2001) Archaeal lipids in Mediterranean cold seeps: molecular proxies for anaerobic methane oxidation. *Geochimica et Cosmochimica Acta* **65**, 1611-1627.
- Pancost, R. D., Sinninghe Damsté, J. S., de Lint, S., van der Maarel, M. J. E. C., Gottschal, J. C., and Party, T. M. S. S. (2000) Biomarker Evidence for Widespread Anaerobic Methane Oxidation in Mediterranean Sediments by a Consortium of Methanogenic Archaea and Bacteria. *Applied and Environmental Microbiology* **66**, 1126-1132.
- Parkes, R. J., Taylor, J., and Jørck-Ramberg, D. (1984) Demonstration, using *Desulfobacter* sp., of two pools of acetate with different biological availabilities in marine pore water. *Marine Biology* **83**, 271-276.
- Parsons, T. R., Maita, Y., and Lalli, C. (1984) *A manual of chemical and biological methods for seawater analysis*. Pergamon Press, Oxford Oxfordshire.
- Raghoebarsing, A. A., Pol, A., van de Pas-Schoonen, K. T., Smolders, A. J. P., Ettwig, K. F., Rijpstra, W. I. C., Schouten, S., Damste, J. S. S., Op den Camp, H. J. M., Jetten, M. S. M., and Strous, M. (2006) A microbial consortium couples anaerobic methane oxidation to denitrification. *Nature* **440**, 918-921.
- Ramaswamy, V., O. Boucher, J. Haigh, D. Hauglustaine, J. Haywood, G. Myhre, T. Nakajima, G.Y. Shi, S. Solomon, R. Betts, R. Charlson, C. Chuang, J.S. Daniel, A. Del Genio, R. van Dorland, J. Feichter, J. Fuglestvedt, P.M. de F. Forster, S.J. Ghan, A. Jones, J.T. Kiehl, D. Koch, C. Land, J. Lean, U. Lohmann, K.

- Minschwaner, J.E. Penner, D.L. Roberts, H. Rodhe, G.J. Roelofs, L.D. Rotstayn, T.L. Schneider, U. Schumann, S.E. Schwartz, M.D. Schwarzkopf, K.P. Shine, S. Smith, D.S. Stevenson, F. Stordal, I. Tegen, Y. Zhang (2001) Radiative forcing of climate change. In: J. T Houghton, Y. D., D. J. Griggs, M. Noguer, P. J. van der Linden, X. Dai, K. Maskell, C. A. Jonson (Ed.), *Climate Change 2001: The Scientific Basis. Contribution of Working Group I to the Third Assessment Report of the Intergovernmental Panel on Climate Change*. Cambridge University Press, Cambridge, United Kingdom and New York, NY, USA.
- Ramette, A. (2007) Multivariate analyses in microbial ecology. *FEMS microbiology ecology* **62**, 142-160.
- Reeburgh, W. S. (1967) An Improved Interstitial Water Sampler. *Limnology and Oceanography* **12**, 163-165.
- Reeburgh, W. S. (1996) "Soft spots" in the global methane budget. In: Lindstrom, M. E. and Tabita, F. F. (Eds.), *Microbial growth on Cl compounds*. Kluwer Academic Publishers, Dordrecht.
- Roden, E. and Tuttle, J. (1993) Inorganic sulfur turnover in oligohaline estuarine sediments. *Biogeochemistry* **22**, 81-105.
- Rossel, P. E., Elvert, M., Ramette, A., Boetius, A., and Hinrichs, K.-U. (2011) Factors controlling the distribution of anaerobic methanotrophic communities in marine environments: Evidence from intact polar membrane lipids. *Geochimica et Cosmochimica Acta* **75**, 164-184.

- Rossel, P. E., Lipp, J. S., Fredricks, H. F., Arnds, J., Boetius, A., Elvert, M., and Hinrichs, K.-U. (2008) Intact polar lipids of anaerobic methanotrophic archaea and associated bacteria. *Organic Geochemistry* **39**, 992-999.
- Rütters, H., Sass, H., Cypionka, H., and Rullkötter, J. (2001) Monoalkylether phospholipids in the sulfate-reducing bacteria *Desulfosarcina variabilis* and *Desulforhabdus amnigenus*. *Archiv für Hydrobiologie* **176**, 435-442.
- Schink, B. (1997) Energetics of syntrophic cooperation in methanogenic degradation. *Microbiol. Mol. Biol. Rev.* **61**, 262-280.
- Schönheit, P., Kristjansson, J. K., and Thauer, R. K. (1982) Kinetic mechanism for the ability of sulfate reducers to out-compete methanogens for acetate. *Archives of Microbiology* **132**, 285-288.
- Schouten, S., Hopmans, E. C., Baas, M., Boumann, H., Standfest, S., Könneke, M., Stahl, D. A., and Sinninghe Damsté, J. S. (2008) Intact Membrane Lipids of “*Candidatus Nitrosopumilus maritimus*,” a Cultivated Representative of the Cosmopolitan Mesophilic Group I Crenarchaeota. *Applied and Environmental Microbiology* **74**, 2433-2440.
- Schubert, C. J., Vazquez, F., Lösekann-Behrens, T., Knittel, K., Tonolla, M., and Boetius, A. (2011) Evidence for anaerobic oxidation of methane in sediments of a freshwater system (Lago di Cadagno). *FEMS microbiology ecology* **76**, 26-38.
- Schubotz, F., Lipp, J. S., Elvert, M., and Hinrichs, K.-U. (2011a) Stable carbon isotopic compositions of intact polar lipids reveal complex carbon flow patterns among hydrocarbon degrading microbial communities at the Chapopote asphalt volcano. *Geochimica et Cosmochimica Acta* **75**, 4399-4415.

- Schubotz, F., Lipp, J. S., Elvert, M., Kasten, S., Mollar, X. P., Zabel, M., Bohrmann, G., and Hinrichs, K.-U. (2011b) Petroleum degradation and associated microbial signatures at the Chapopote asphalt volcano, Southern Gulf of Mexico. *Geochimica et Cosmochimica Acta* **75**, 4377-4398.
- Schubotz, F., Wakeham, S. G., Lipp, J. S., Fredricks, H. F., and Hinrichs, K.-U. (2009) Detection of microbial biomass by intact polar membrane lipid analysis in the water column and surface sediments of the Black Sea. *Environmental Microbiology* **11**, 2720-2734.
- Segers, R. (1998) Methane Production and Methane Consumption: A Review of Processes Underlying Wetland Methane Fluxes. *Biogeochemistry* **41**, 23-51.
- Sivan, O., Alder, M., Pearson, A., Gelman, F., Bar-Or, I., John, S., and Eckert, W. (2011) Geochemical evidence for iron-mediated anaerobic oxidation of methane. *Limnology and Oceanography* **56**, 1536-1544.
- Smemo, K. A. and Yavitt, J. B. (2007) Evidence for Anaerobic CH₄ Oxidation in Freshwater Peatlands. *Geomicrobiology Journal* **24**, 583-597.
- Smemo, K. A. and Yavitt, J. B. (2011) Anaerobic oxidation of methane: an underappreciated aspect of methane cycling in peatland ecosystems? *Biogeosciences* **8**, 779-793.
- Solorzano, L. (1969) Determination of Ammonia in Natural Waters by the Phenolhypochlorite Method. *Limnology and Oceanography* **14**, 799-801.
- Stookey, L. L. (1970) Ferrozine---a new spectrophotometric reagent for iron. *Analytical Chemistry* **42**, 779-781.

- Strickland, J. D. H. and Parsons, T. R. (1972) A manual of seawater analysis *Bulletin of the Fisheries Research Board Canada*, Ottawa.
- Sturt, H. F., Summons, R. E., Smith, K., Elvert, M., and Hinrichs, K.-U. (2004) Intact polar membrane lipids in prokaryotes and sediments deciphered by high-performance liquid chromatography/electrospray ionization multistage mass spectrometry—new biomarkers for biogeochemistry and microbial ecology. *Rapid Communications in Mass Spectrometry* **18**, 617-628.
- Valentine, D. (2002) Biogeochemistry and microbial ecology of methane oxidation in anoxic environments: a review. *Antonie van Leeuwenhoek* **81**, 271-282.
- Valentine, D. L. and Reeburgh, W. S. (2000) New perspectives on anaerobic methane oxidation. *Environmental Microbiology* **2**, 477-484.
- Wegener, G., Niemann, H., Elvert, M., Hinrichs, K.-U., and Boetius, A. (2008) Assimilation of methane and inorganic carbon by microbial communities mediating the anaerobic oxidation of methane. *Environmental Microbiology* **10**, 2287-2298.
- Wellsbury, P. and Parkes, R. J. (1995) Acetate bioavailability and turnover in an estuarine sediment. *FEMS microbiology ecology* **17**, 85-94.
- Weston, N. B., Dixon, R. E., and Joye, S. B. (2006) Ramifications of increased salinity in tidal freshwater sediments: Geochemistry and microbial pathways of organic matter mineralization. *J. Geophys. Res.* **111**, G01009.
- White, D. C., Davis, M., Nickels, J. S., King, J. D., and Bobbie, R. J. (1979) Determination of the sedimentary microbial biomass by extractible lipid phosphate. *Oecologia* **40**, 51-62.

- Winfrey, M. R. and Zeikus, J. G. (1979) Microbial Methanogenesis and Acetate Metabolism in a Meromictic Lake. *Appl. Environ. Microbiol.* **37**, 213-221.
- Yoshinaga, M. Y., Kellermann, M. Y., Rossel, P. E., Schubotz, F., Lipp, J. S., and Hinrichs, K.-U. (2011) Systematic fragmentation patterns of archaeal intact polar lipids by high-performance liquid chromatography/electrospray ionization ion-trap mass spectrometry. *Rapid Communications in Mass Spectrometry* **25**, 3563-3574.

Table 3.1. Seasonal variations in geochemical species in the top 40 cm of sediment of Hammersmith Creek, GA. All species are reported as average (n=3) areal, depth-integrated concentrations except C:N ratios, %C, and temperature, which are reported as average measurements in the top 40 cm. Error terms are the standard error. Abbreviations: %C, percent organic carbon by weight; C:N, carbon to nitrogen ratios by weight, CH₄, methane; DIC, dissolved inorganic carbon, H₂, steady-state hydrogen concentrations; DOC, dissolved organic carbon, Mn²⁺, dissolved, reduced manganese, Fe²⁺, dissolved, reduced iron, NH₄⁺, ammonium, NO_x, nitrate + nitrite, PO₄²⁻, phosphate.

* Previously reported in Chapter 2

** Measurement of a pooled replicate

	January 2008	April 2008	August 2008	February 2009	July 2009	November 2009
Organic C (%)	5.1	5.3	5.0	5.2	5.0	5.5
C:N (wt:wt)	13.2	12.6	12.4	10.2	10.4	13.5
Temperature (°C)	8.7 ± 1.0	21.5 ± 0.7	28.3 ± 1.4	13.5 ± 0.2	30.1 ± 0.5	18.8 ± 0.5
*CH ₄ (mmol m ⁻²)	590.7 ± 132.7	554.3 ± 27.3	578.2 ± 58.9	476.1 ± 75.0	550.0 ± 8.6	683.6 ± 59.5
sulfate (mmol m ⁻²)	92.1 ± 14.6	17.8 ± 3.7	75.9 ± 28.0	30.0 ± 7.7	68.8 ± 4.0	32.0 ± 1.5
DIC (mol m ⁻²)	1.4 ± 0.4	1.3 ± 0.0	2.0 ± 0.2	0.9 ± 0.1	2.0 ± 0.1	1.8 ± 0.1
H ₂ (μmol m ⁻²)	8.4 ± 2.4	25.6 ± 3.1	44.2 ± 7.5	7.6 ± 2.9	29.3 ± 3.0	9.3 ± 1.9
**Ace (mmol m ⁻²)	11.3	30.7	10.6	9.2	13.8	24.0
DOC (mol m ⁻²)	2.1 ± 0.7	0.5 ± 7.2x10 ⁻³	0.7 ± 2.7x10 ⁻²	0.7 ± 4.3x10 ⁻²	0.6 ± 2.8x10 ⁻²	1.0 ± 0.2
Mn ²⁺ (mmol m ⁻²)	na	65.5 ± n/a	201.1 ± 27.9	114.5 ± 20.7	80.8 ± 1.7	167.7 ± 14.8
Fe ²⁺ (mmol m ⁻²)	na	59.3 ± 11.8	94.2 ± 17.4	120.3 ± 27.7	69.7 ± 15.4	110.3 ± 8.1
NH ₄ ⁺ (mmol m ⁻²)	120.8 ± 83.3	212.8 ± 44.6	324.7 ± 85.8	283.6 ± 49.6	244.0 ± 4.5	420.5 ± 103.4
NO _x (mmol m ⁻²)	20.1 ± 3.8	19.2 ± 5.8	14.2 ± 1.5	13.8 ± 1.8	27.7 ± 0.5	20.9 ± 1.0
PO ₄ ²⁻ (mmol m ⁻²)	0.6 ± 0.2	0.2 ± 0.1	0.4 ± 0.2	0.8 ± 0.5	1.8 ± 0.1	0.1 ± 0.0

Table 3.2. Seasonal variations in depth-integrated (0-40 cm) rates of hydrogenotrophic methanogenesis (bic-MOG), acetoclastic methanogenesis (ace-MOG), anaerobic oxidation of methane (AOM), and sulfate reduction (SR). All rates in $\text{mmol m}^{-2} \text{d}^{-1}$. Values represent the average of triplicate cores +/- the standard error of that average. Percent methane production from bicarbonate (% bic), ratio of methane consumption to methane production (AOM:MOG), and the ratio of methane consumption to sulfate reduction (AOM:SR) were calculated from these areal rates. na, data not available

Rates (in $\text{mmol m}^{-2} \text{d}^{-1}$)	January 2008	April 2008	August 2008	February 2009	July 2009	November 2009
bic-MOG	$0.4 \pm 1.4 \times 10^{-2}$	16.6 ± 0.8	2.2 ± 0.2	$0.4 \pm 1.9 \times 10^{-2}$	3.1 ± 0.4	2 ± 0.1
ace-MOG	$0.2 \pm 5.2 \times 10^{-3}$	$1.0 \pm 7.8 \times 10^{-3}$	1.6 ± 0.2	3.2 ± 0.5	7.6 ± 1.2	14.4 ± 0.5
AOM	10.1 ± 0.6	14.2 ± 0.4	13.2 ± 0.4	7.4 ± 1.6	2.5 ± 0.1	5.3 ± 1.0
AOG	$0.2 \pm 8.9 \times 10^{-3}$	1.6 ± 0.1	0.8 ± 0.2	$7.1 \times 10^{-2} \pm 3.8 \times 10^{-3}$	$0.3 \pm 4.3 \times 10^{-2}$	$0.2 \pm 3.6 \times 10^{-2}$
Ace Ox	$0.7 \pm 2.3 \times 10^{-2}$	1.8 ± 0.1	9.2 ± 0.8	$1.0 \pm 2.2 \times 10^{-2}$	15.6 ± 0.3	6.3 ± 1.2
SR	na	19.9 ± 0.5	16.2 ± 1.6	99.9 ± 6.6	358.8 ± 31.9	279.5 ± 18.3
AOM:MOG	23.5	0.8	3.6	2	0.2	0.4
SR:AOM	na	1.4	1.2	14.5	147.2	56.8

Table 3.3. Summary of IPL classes identified in the sediments of Hammersmith Creek and their probable sources. See text for abbreviations.

<i>IPL</i>	<i>Probable Source</i>	<i>References</i>
2, 3 Gly-AR	Archaea; methanotrophic and methanogenic archaea	Lipp et al. 2008; Rossel et al. 2011; Yoshinaga et al. 2011
PME-OH-AR	Archaea; Freshwater archaea	Koga et al. 1993; Yoshinaga et al. 2011; this study
PG-Uns(2)-OH-AR	Archaea, possibly cold-adapted archaea	Yoshinaga et al. 2011; this study
1 Gly-GDGT	Archaea; methanotrophic and methanogenic archaea	Schubotz et al. 2009; Yoshinaga et al. 2011
2, 3 Gly-GDGT	Methanotrophic and methanogenic archaea	Schubotz et al. 2009; Rossel et al. 2011; Yoshinaga et al. 2011
2, 3 Gly-OH-GDGT	Archaea, methanotrophs	Schubotz et al. 2009; Liu 2010.
PI-GDGT-Gly	Archaea, possibly cold-adapted archaea	this study

Table 3.4. Stable carbon isotopic signatures, in ‰, of archaeal and bacterial lipids in Hammersmith Creek, GA. Abbreviations: nd, not detected; na, data not available. * Calculated from DIC according to Mook et al. 1978

depth interval (cm)	January 2008			April 2008			August 2008			February 2009			July 2009			November 2009		
	0-3	6-9	15-20	0-3	6-9	15-20	0-3	6-9	15-20	0-3	6-9	15-20	0-3	6-9	15-20	0-3	6-9	15-20
<i>Archaeal Core Lipid</i>																		
phytane	-34.6	-31.3	-34.6	-35.7	-35.7	na	-30.0	-35.7	-32.1	-35.7	-32.2	na	-33.6	-33.0	na	-31.0	-32.4	na
biphytane 0	-38.9	-41.2	-49.1	-38.6	-38.2	na	-40.2	-40.4	-40.5	-39.7	-39.6	na	-40.7	-43.3	na	-41.6	-42.8	na
biphytane 1	-44.9	-50.8	-51.9	-44.1	-45.5	na	-45.1	-48.0	-49.7	-45.0	-44.7	na	-43.8	-48.5	na	-47.9	-46.5	na
biphytane 2	-52.1	-56.3	-56.1	-50.9	-52.2	na	-52.3	-51.8	-53.3	-52.6	-53.3	na	-52.8	-58.9	na	-59.5	-57.1	na
biphytane 3	nd	-31.2	-33.7	nd	nd	na	nd	-36.7	-33.3	nd	nd	na	-38.1	-33.4	na	-34.5	-34.0	na
<i>Fatty Acids</i>																		
aiC ₁₄	-29.8	-30.6	-31.9	-28.4	-29.5	-30.7	-30.4	-29.7	-31.8	-30.2	-29.3	-30.7	-31.7	-33.9	-32.4	-33.1	-33.0	-31.0
C ₁₄	-35.7	-35.8	-35.8	-34.2	-34.5	-35.6	-34.2	-33.6	-36.2	-34.4	-34.4	-35.6	-35.0	-36.5	-35.3	-37.0	-35.4	-35.2
iC ₁₅	-30.5	-30.0	-29.4	-26.4	-29.3	-29.9	-28.8	-29.7	-31.7	-29.9	-28.5	-29.9	-30.4	-30.2	-29.0	-30.7	-30.2	-29.1
aiC ₁₅	-31.0	-31.1	-32.2	-31.7	-30.3	-32.2	-30.6	-29.2	-32.5	-30.3	-30.7	-32.2	-29.9	-32.3	-31.4	-32.4	-31.3	-31.9
C ₁₅	-30.6	-30.5	-28.6	-30.2	-30.6	-30.0	-30.4	-31.3	-32.2	-28.2	-30.1	-30.0	-31.6	-32.9	-30.3	-34.3	-31.2	-30.3
iC ₁₆	-29.8	-30.8	-29.8	-27.7	-29.5	-29.4	-28.8	-27.6	-31.5	-29.6	-29.5	-29.4	nd	-31.6	-30.5	-31.2	-27.5	-31.9
C _{16:1w7}	-41.0	-40.6	-39.1	-36.6	-39.1	-38.1	-38.7	-36.5	-41.1	-38.1	-39.7	-38.1	-36.7	-40.5	-38.9	-42.5	-39.1	-41.5
C _{16:1w5}	-46.6	-44.5	-45.4	-45.8	-44.1	-45.1	-43.9	-41.2	-45.7	-43.3	-45.0	-45.1	-41.2	-46.3	-44.9	-45.7	-44.9	-48.5
C ₁₆	-36.4	-35.6	-35.4	-33.8	-34.5	-35.9	-35.2	-34.2	-35.9	-34.6	-35.1	-35.9	-34.9	-36.5	-35.6	-37.0	-36.1	-35.8
10meC ₁₆	-34.9	-33.5	-31.3	-29.7	-30.3	-30.1	-33.5	-31.1	-33.7	-33.7	-30.2	-30.1	-31.1	-31.6	-32.2	-34.7	-33.4	-30.0
iC ₁₇	-30.6	-30.8	-29.5	-29.8	-28.9	-30.0	-31.4	-29.9	-31.7	-30.3	-29.4	-30.0	-30.2	-30.4	-30.6	-44.4	-31.4	-29.6
aC ₁₇	-25.4	-28.0	-29.1	-27.0	-26.3	-29.6	-27.4	-25.7	-30.6	-30.1	-27.1	-29.6	-26.3	-29.1	-31.5	-34.6	-27.0	-28.9
C _{17:1}	-32.8	-32.5	-31.6	-32.4	-31.5	-31.7	-33.2	-31.3	-32.9	-31.4	-31.4	-31.7	-30.2	-33.1	-33.8	-34.3	-33.1	-32.3
C ₁₇	-33.5	-32.3	-31.3	-32.3	-30.6	-31.0	-31.7	-30.8	-32.8	-31.9	-31.0	-31.0	-31.5	-34.6	-33.6	-33.3	-32.0	-30.4
C _{18:2}	-35.5	-34.8	-32.6	-28.7	-33.6	-30.3	-32.7	-32.4	-32.6	-31.6	-33.6	-30.3	-33.5	-33.4	-30.5	-32.5	-35.0	-32.5
C _{18:1w9}	-30.0	-30.4	-28.6	-26.6	-29.2	-29.4	-30.2	-29.9	-31.2	-29.0	-28.8	-29.4	-30.9	-29.9	-29.4	-30.0	-30.5	-30.0
C _{18:1w7}	-39.3	-39.5	-39.1	-37.3	-38.1	-38.8	-37.7	-36.4	-39.4	-38.1	-38.1	-38.8	-37.5	-39.4	-38.6	-40.5	-40.6	-40.5
C ₁₈	-32.8	-31.7	-30.9	-29.9	-30.4	-30.2	-31.5	-30.3	-32.2	-31.4	-30.8	-30.2	-30.9	-32.3	-31.3	-31.5	-31.8	-31.5
<i>Geochemical Species</i>																		
methane	-72.2	-69.9	-70.9	-66.4	-66.9	-68.7	-62.0	-61.7	-65.5	-67.1	-65.4	-67.9	-64.6	-61.5	-65.2	-62.0	-61.5	-62.5
DIC	-14.8	-15.0	-11.8	-10.7	-9.9	-8.5	-18.0	-12.9	-2.4	-14.3	-9.6	-2.0	-14.0	-1.2	4.6	-4.9	-1.2	4.2
CO ₂ *	-24.0	-24.6	-16.6	-19.2	-18.4	-16.9	-25.9	-20.8	-10.4	-27.8	-23.1	-15.5	-21.9	-21.0	-3.3	-13.4	-7.5	-4.3
acetate	nd	nd	-32.4	-31.3	-31.3	-25.5	-26.9	-28.9	-29.9	nd	-26.7	-29.3	-35.1	-28.8	-33.0	-30.7	-28.8	-28.5
POC	-25.5	-26.3	-26.9	-25.6	-25.3	-26.6	-25.9	-25.3	-26.5	-26.1	-26.0	-26.3	-26.4	-26.7	-26.6	-26.8	-26.7	-26.6

Table 3.5. Seasonal variation in the residence times of porewater acetate (in days) and hydrogen (in minutes) in top 40 cm with respect to relevant sources and sinks measured during the study. See methods for details. Acetate sinks: Acetate oxidation (Ace Ox), acceoclastic methanogenesis (Ace-MOG), sulfate reduction (SR). Acetate sources: homoacetogenesis (AOG). Hydrogen sinks: hydrogenotrophic methanogenesis (bic-MOG) and homoacetogenesis (AOG), sulfate reduction (SR).

Season	Turnover times for acetate (days)			Turnover times for hydrogen (minutes)				
	due to Ace Ox	due to Ace-MOG	due to SR	due to AOG	due to bic-MOG	due to AOG	due to SR	due to AOM
Winter 2008	16.1	26.3	<i>na</i>	56.3	30.3	60.7	<i>na</i>	1.2
Spring 2008	17	30.7	1.5	19.2	2.2	23.7	1.9	2.6
Summer 2008	1.2	6.6	<1	13.2	2828.9	79.6	3.9	4.8
Winter 2009	9.2	2.9	<1	130.1	27.3	153.7	<1	1.5
Summer 2009	0.9	1.8	<1	45.9	13.6	140.8	<1	16.9
Fall 2009	3.8	1.7	<1	120.2	6.7	67.0	<1	2.5

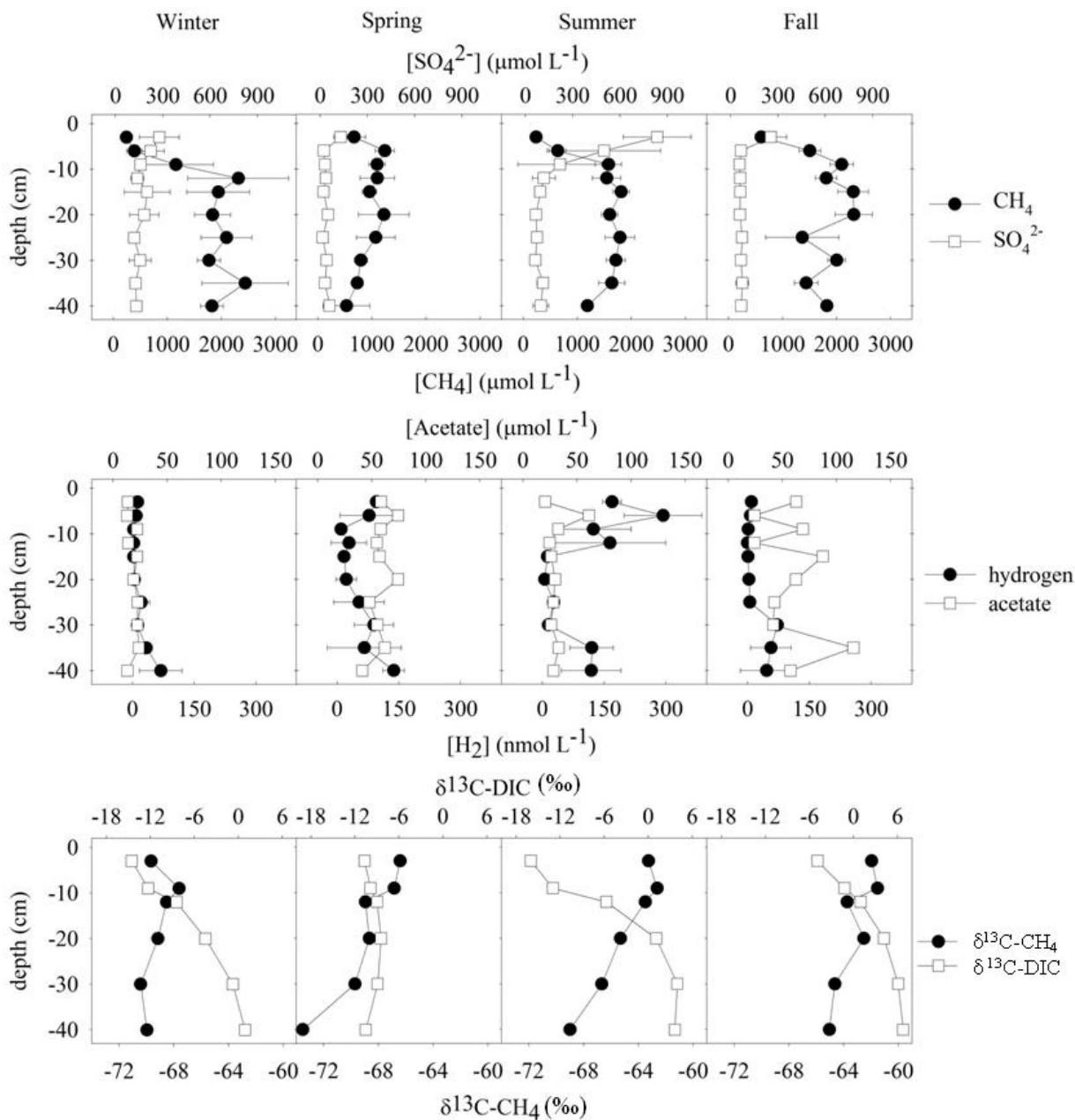


Figure 3.1. Seasonal variations in porewater geochemistry in the sediments of Hammersmith Creek, GA. Porewater concentrations are an average of replicate sediment cores ($n=3-6$) and error bars represent the standard error of that mean. Values for $\delta^{13}\text{C-CH}_4$ and $\delta^{13}\text{C-DIC}$ represent averages of duplicate measurements. Values for winter and summer are from two consecutive years (2008-2009) and values for spring and fall are from a single season (2008 for spring and 2009 for fall). Abbreviations: CH_4 , methane, SO_4^{2-} , sulfate, $\delta^{13}\text{C-CH}_4$ stable isotope composition of methane, $\delta^{13}\text{C-DIC}$, stable isotopic composition of dissolved inorganic carbon.

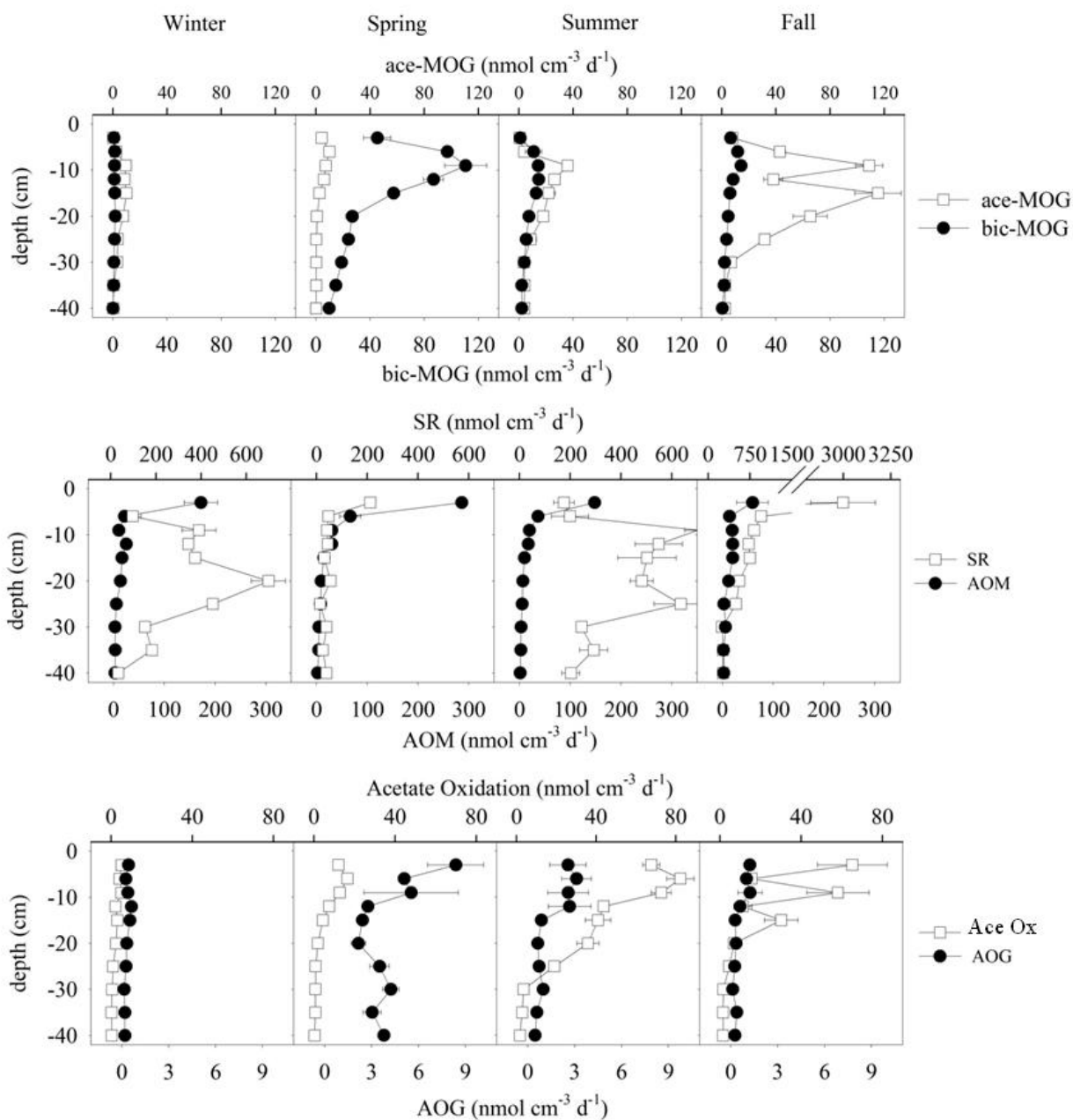


Figure 3.2. Seasonal variations of microbial activities in the sediments of Hammersmith Creek, GA. Shown are depth profiles of microbial rates of methane production from $\text{H}^{14}\text{CO}_3^-$ (bic-MOG), and $^{14}\text{CH}_3\text{COO}^-$ (ace-MOG), anaerobic oxidation of methane (AOM), sulfate reduction (SR), acetate production from $\text{H}^{14}\text{CO}_3^-$ (AOG), and acetate oxidation (Ace Ox). Values are an average of replicate sediment cores ($n=3-6$) and error bars represent the standard error of that mean. Values for winter and summer are from two consecutive years (2008-2009) and values for spring and fall are from a single season (2008 for spring and 2009 for fall).

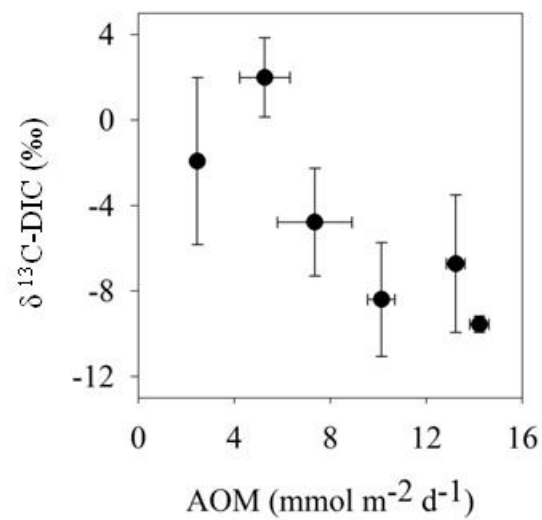


Figure 3.4. Depth-averaged stable carbon isotopic signatures of DIC ($\delta^{13}\text{C-DIC}$) with areal rates of anaerobic methane oxidation (AOM). Values are shown as an average of triplicate cores and error bars represent the standard error of that average.

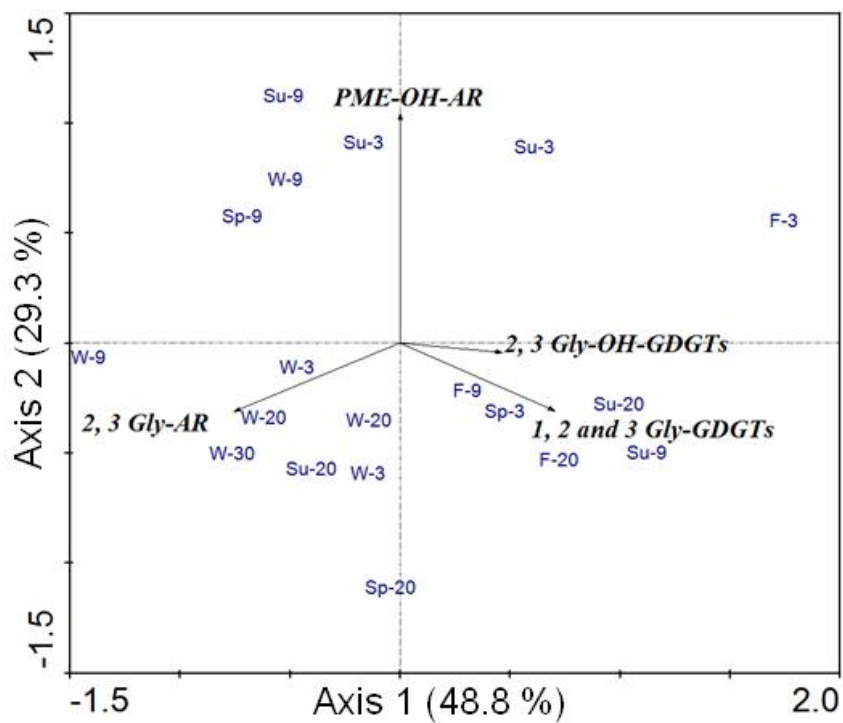


Figure 3.5. PCA plot showing the distribution of archaeal IPLs. Individual samples are labeled in blue according to the scheme season-depth (cm). The direction and length of the arrows for each species represents the direction and rate of increase in the ordination space.

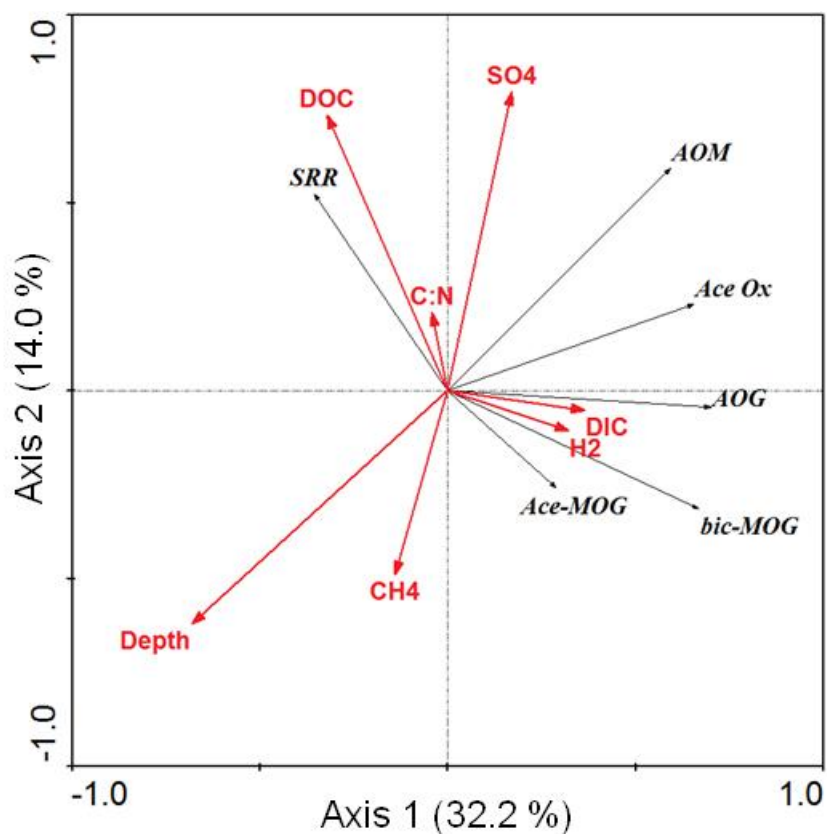


Figure 3.6. RDA biplot showing the relation of microbial rate activities (in black) and those geochemical variables (in red) which explain the most variability as determined via forward selection with monte carlo significance testing. The direction and length of the arrows for the rates and variables represent the direction and rate of increase in the ordination space.

Abbreviations: CH₄, methane; H₂, hydrogen, DIC, dissolved inorganic carbon, SO₄, sulfate; C:N, ratio of carbon to nitrogen; DOC, dissolved organic carbon; Ace-MOG, acetoclastic methanogenesis; bic-MOG, hydrogenotrophic methanogenesis; AOG, homoacetogenesis; Ace Ox, acetate oxidation; AOM, anaerobic oxidation of methane; SRR, sulfate reduction.

CHAPTER 4

SEASONAL PATTERNS OF METHANE CYCLING IN FLORIDA AND MAINE PEAT WETLANDS

K. E. A. Segarra¹, F. Schubotz², V. Samarkin¹, M. Y. Yoshinaga³, V. Heuer³,
K.-U. Hinrichs³, and S. B. Joye^{1*}.

To be submitted to *Geochimica et Cosmochimica Acta*

* Corresponding Author

1 Department of Marine Sciences, University of Georgia, Athens, GA

2 MARUM Center for Marine Environmental Sciences and Department of Geosciences,
University of Bremen, 28359 Bremen, Germany

3 Department of Earth, Atmospheric and Planetary Sciences, MIT, Cambridge, MA

ABSTRACT

Peat wetlands are a major source of methane to the atmosphere and the final stages of organic matter degradation in these ecosystems are thought to be dominated by methanogenesis. Methane cycling in peatlands may be influenced by interactions with other terminal metabolizers, substrate availability, and community structure. Seasonal changes in these factors were explored in two peat wetlands in distinct climate regimes, Florida and Maine. Both peats displayed different seasonal variations in carbon cycling with high rates of sulfate reduction (SR) and anaerobic oxidation of methane (AOM) in the winter months. Methane production rates increased from the winter to summer and in Maine, this increase was associated with a shift in the dominant methanogenic precursor from hydrogen with carbon dioxide to acetate. Though the evidence was not conclusive, all AOM activity may be supported by SR in these peatlands. Both SR and AOM effectively limit the methane emissions from these peatlands through competitive interactions with methanogens and the consumption of large fractions of the methane produced from acetate and hydrogen. Intact polar lipid (IPL) biomarkers revealed a diverse community of archaea and bacteria which were dominated by IPLs associated with methane cycling and SR. However, seasonal variations in carbon flow were not reflected by changes in the IPL composition. In contrast to marine-based AOM studies, corroborating lipids depleted in ^{13}C were not detected. Additionally, the major shifts in methanogenic pathways were not reflected in the stable carbon isotopes of methane. In highly dynamic settings such as peat wetlands, the isotopic signal of individual processes may be obscured by multiple 'background' processes which likely dilute the carbon

isotope pool. Studies that evaluate the role of AOM in wetlands using lipid and isotope-based approaches may underestimate its importance.

1. INTRODUCTION

Though they occupy a small fraction of the Earth's surface, wetlands are the single largest source of methane (CH_4) to the atmosphere (BROOK et al., 2008). CH_4 has a heat trapping potential over 23 times that of carbon dioxide (CO_2) and as such is the second-most important greenhouse gas in the atmosphere (FORSTER, 2007). CH_4 emissions from wetlands have been implicated in past (CHAPPELLAZ et al., 1993; SEVERINGHAUS and BROOK, 1999; SMITH et al., 2004), contemporary (WORTHY et al., 2000), and future (GEDNEY et al., 2004) variations in the global CH_4 budget. Since peatlands comprise nearly 40% of global wetlands (as estimated by BRIDGHAM et al., 2006), CH_4 cycling in peatlands plays a crucial role in the global CH_4 budget and, in turn, global climate change.

The two major substrates for methanogenesis (MOG) are acetate, which is fermented to CH_4 and CO_2 by acetoclastic methanogens, and CO_2 , which is reduced with hydrogen during hydrogenotrophic MOG (ZEIKUS, 1977). Previous studies identified a temperature-driven shift in the relative importance of these methanogenic pathways, with acetoclastic MOG dominant at lower temperature and hydrogenotrophic MOG dominant at higher temperature (CHIN and CONRAD, 1995; CONRAD et al., 1987; FEY and CONRAD, 2000; SCHULZ and CONRAD, 1996; SCHULZ et al., 1997). However, this shift was documented only in rice-paddy soils and lake sediments, environments where acetoclastic MOG typically dominates CH_4 production (ROTHFUSS and CONRAD, 1993; SCHULZ and CONRAD, 1996; YAO and CONRAD, 1999). The dominant pathway of CH_4 production in

peatlands is considered to be hydrogenotrophic MOG (CHASAR et al., 2000; DUDDLESTON et al., 2002; HINES et al., 2001; HORNIBROOK et al., 2000; LANSDOWN et al., 1992), although acetoclastic MOG may dominate under some conditions (GALAND et al., 2005; KELLER and BRIDGHAM, 2007; METJE and FRENZEL, 2007; SVENSSON, 1984). Few studies have examined the seasonal, potentially temperature-related variations in methanogenic pathways in peatlands (AVERY et al., 1999; AVERY et al., 2003; SVENSSON, 1984). In the face of global climate change, it is imperative to determine how methanogenic carbon cycling in peatlands is affected by temperature and other climate-related factors.

The analysis of intact polar membrane lipids (IPLs) provides a culture-independent profile of the living biomass in a single analytical window (STURT et al., 2004): bulk biomass, the relative contribution of archaea and bacteria, and the diversity of these two microbial groups are simultaneously quantified. Genetic-based techniques such as FISH and *q*PCR may suffer from primer (TESKE and SORENSEN, 2007) and/or extraction method biases (LIPP et al., 2008). In contrast, IPL analyses provide a fingerprint of the viable microbial community with relatively little sample preparation.

Intact or intact-derived lipid biomarkers have been characterized previously in peat environments (LIU et al., 2010; SUNDH et al., 1995; WEIJERS et al., 2004); however, those studies examined only particular aspects of the microbial community, such as the intact, branched GDGTs produced by bacteria (LIU et al., 2010; WEIJERS et al., 2004) or PLFAs (produced only by eukaryotes and bacteria; SUNDH et al., 1995). Intact archaeal lipids have been relatively uncharacterized in peat environments. Additionally, few simultaneous investigations of methanogenic carbon cycling and microbial community

structure in peatlands are available (JUOTTONEN et al., 2008; KOTSYURBENKO et al., 2004; METJE and FRENZEL, 2007) The present study is the first to combine IPL profiling and microbial rate measurements to describe CH₄ cycling in peat wetlands. The combined analysis of IPLs with the stable carbon isotopic analysis of their apolar derivatives is a powerful tool for tracing carbon flow in aquatic environments. However, this approach has been applied in only a few studies (OBA et al., 2006; SCHUBOTZ et al., 2011a) compared to those studies which have coupled stable carbon isotopic analysis with non-polar lipid biomarkers (HINRICHS et al., 1999; JAHNKE et al., 2001; ORCUTT et al., 2005; PANCOST and SINNINGHE DAMSTÉ, 2003).

Though the anaerobic oxidation of CH₄ (AOM) has been extensively studied in marine environments (as reviewed in REEBURGH, 2007), the process is far less chronicled in freshwater systems (ELLER et al., 2005; PANGANIBAN et al., 1979; SCHUBERT et al., 2011). Though the mechanism remains unclear, it is believed that sulfate is the major oxidant of CH₄ in marine systems (HINRICHS and BOETIUS, 2002), where AOM is performed by a consortium of sulfate-reducing bacteria (SRB) and anaerobic methanotrophic archaea (ANME) archaea (KNITTEL and BOETIUS, 2009; ORPHAN et al., 2001). In freshwater systems, however, multiple electron acceptors have been linked to AOM including sulfate (SCHUBERT et al., 2011), nitrate/nitrite (DEUTZMANN and SCHINK, 2011; RAGHOEBARSING et al., 2006), iron (SIVAN et al., 2011), and manganese (ZEHNDER and BROCK, 1980).

CH₄ oxidation is an important process in peatlands, although most previous work has been largely focused on aerobic CH₄ oxidation (DUNFIELD et al., 1993; HARRISS et al., 1982; TOPP and PATTEY, 1997; YAVITT et al., 1990; YAVITT et al., 1988). There are

fewer studies of AOM in peatlands (POZDNYAKOV et al., 2011; SMEMO and YAVITT, 2007; SMEMO and YAVITT, 2011). Because the ratio of CH₄ production to CH₄ consumption directly controls CH₄ emissions from wetlands, understanding the seasonal controls on MOG and AOM in peatlands warrant further inquiry.

The goal of the study was to identify the seasonal controls on CH₄ cycling in two peatlands which experience distinct annual temperature ranges. Porewater geochemistry and rates of terminal metabolic processes (e.g. MOG, AOM, SR and homoacetogenesis) were measured in the winter and summer at each site. Evaluation of the lipid biomarkers provided seasonal estimates of microbial biomass as well as the composition of the bacterial and archaeal communities. Comparison of the stable carbon isotopic signatures of CH₄, its immediate precursors, and of the microbial lipids afforded a different understanding of carbon cycling than the directly measured rates of terminal metabolism. Here, we identified seasonal changes in carbon flow, including high rates of AOM and SR. Biomarkers for SRB and archaea composed a major portion of the viable lipid profile, yet, isotopic evidence for methanotrophy was limited.

2. METHODS

2.1 Site Description

Samples were collected from two peat wetlands from distinct biogeographical provinces: in the Florida Everglades (West Indian province) and in Acadia National Park (Acadian province). The study site in Acadia National Park is located on the north side of Mt. Desert Island, Maine. Samples were collected in Aunt Betsey's Brook (44°24' N 68°18' W), a freshwater creek which runs into the Fresh Meadow, then Northeast Creek, and eventually into Thomas Bay. The site, hereafter simply referred to as 'Maine', was

visited in late winter (March) and again in late summer (August) 2009. Peat was collected from the unvegetated creek bed which is permanently inundated with freshwaters ranging from 0-2 PSU. A 3-10 cm layer of ice which had formed over the brook in the winter of 2009 was manually removed from the sampling area before cores were taken. The surrounding marsh is dominated by *Spartina pectinata*, *Scirpus acutus*, and *Typha*. The peat in Maine contained an average of 18% C with an average C:N (wt:wt) of 17.

The study site in Florida is adjacent to Shark River Slough site 3 (SRS-3; 25°5'N, 80°9' W) within the Florida Coastal Everglades LTER domain. The peat at SRS-3 is approximately 1 meter thick, lies atop a bed of marl, and contained an average of 52% C with an average C:N (by weight) of 15. The marsh at SRS-3 is dominated by *Cladium jamaicense* interspersed with *Eleocharis* and *Panicum*, though no living macrophytes were present in the peat sampled. While the everglades are typified by a distinct wet (May to November) and dry (December to April) season, SRS-3 remains inundated throughout the year. Samples were collected from 'Florida' in September 2009 and January 2010.

2.2 Sample Collection and Geochemical Analyses

Several replicate cores (~40 cm in length) were collected from the unvegetated peats of Florida and Maine using a Russian peat corer. For geochemical analyses, triplicate cores were sectioned in the field into 10 depth intervals of 3 or 5 cm to a maximum depth of 40 cm. As the sections were extruded from the corer each horizon was immediately sub-sampled for dissolved gases and porosity. For CH₄ analysis, a 6 cm³ peat sample was taken from each subcore with a cut-off plastic syringe. These plugs were immediately preserved in a helium-purged serum vial containing 3 mL 2N NaOH (to halt

biological activity) and sealed with a blue, butyl-rubber stopper and a crimp seal. Samples were stored at room temperature until analysis on a GC-FID. For hydrogen analysis, a separate 6 cm³ peat sample was collected into a helium-purged gas vial and sealed with a blue, butyl-rubber stopper. These vials were then re-purged with helium in the field, transported back to the laboratory, and incubated at *in situ* temperature for 5 days for determination of steady-state hydrogen concentration (HOEHLER et al., 1998) using a Peak Performer RGA (Peak Laboratories®). A 1 cm³ sample was collected into tarred glass vials for porosity determination (JOYE et al., 2004). After these three subsamples were collected in the field, the remaining peat from each horizon was placed into a plastic sampling bag, purged several times with ultra-high-purity argon, sealed in a Mylar® bag which was also purged with ultra-high-purity argon, and transported back to the laboratory at *in situ* temperature.

The porewater from the peat in each horizon was extracted into an argon-purged syringe using a mechanical squeezer and argon-purged squeezer cups (JOYE et al., 2004). A portion of this extracted porewater was preserved for dissolved inorganic carbon (DIC) analysis by injecting 5 mL of porewater into a helium-purged gas vial containing 200 µL of hydrochloric acid and was fitted with a blue, butyl-rubber stopper and crimp seal. The liberated CO₂ in the headspace was analyzed using a GC-FID outfitted with a methanizer after the vial was shaken vigorously.

A 10 mL aliquot of the porewater was 0.2 µm filtered (to halt microbial activity) and stored frozen for dissolved organic carbon (DOC), volatile fatty acid (VFA), nitrite, and nitrate analysis. Another 10 mL aliquot was 0.2 µm filtered and preserved for sulfate, chloride, phosphate, iron (II), and manganese (II) by addition of 100 µL concentrated

trace-metal grade nitric acid. A 2 mL sample was preserved for ammonium with 200 μ L phenol reagent and analyzed spectrophotometrically (SOLORZANO, 1969). A 2 mL sample for hydrogen sulfide (HS) was preserved by adding 200 μ L 20% zinc acetate to 2 mL of pore water and analyzed according to Cline (1969). Concentrations of DOC were determined with a Shimadzu[®] TOC-V. Concentrations of nitrite (NO_2^-) were determined colorimetrically (PARSONS et al., 1984). An Antek Instruments model 745 vanadium reduction manifold and model 7050 nitric oxide detector was used to determine concentrations of NO_x (nitrite + nitrate). Concentrations of nitrate (NO_3^-) were determined as the difference between NO_x and NO_2^- . Sulfate and chloride were analyzed via ion chromatography with a Dionex[®] ICS-2000 ion chromatograph. Dissolved iron (II) and manganese (II) were analyzed colorimetrically using the methods of Stookey (1970) and Armstrong (1979), respectively. Phosphate concentrations were determined colorimetrically (STRICKLAND and PARSONS, 1972). Concentrations of VFAs were determined using high-performance liquid chromatography (HPLC; ALBERT and MARTENS, 1997).

2.3 Microbial Activity Assays

Three additional cores were collected for microbial rate measurements. The same depth horizons were sub-sampled for geochemistry and activity. Several subsamples from each horizon were collected in to a cut-end glass Hungate tubes and sealed with a moveable black butyl rubber stopper at one end and a black butyl rubber septa and open-hole screw cap at the other. These tubes were transported back to the laboratory and stored at *in situ* temperature for 24 hours before beginning radiotracer incubations. Microbial activities were calculated as volume-specific ($\text{nmol cm}^{-3} \text{d}^{-1}$) and as depth-

integrated ($\text{mmol m}^{-2} \text{d}^{-1}$) rates [via trapezoidal integration of the volume-specific rates in the top 40 cm of sediment]. All rates were porosity corrected when appropriate. Killed-controls were incubated in parallel for each process within each depth interval so that live samples could be corrected for the ‘background’ activity. Rates of hydrogenotrophic MOG (bic-MOG; $^{14}\text{CH}_4$ from $\text{H}^{14}\text{CO}_3^-$) and acetoclastic MOG (ace-MOG; $^{14}\text{CH}_4$ from $^{14}\text{CH}_3\text{COO}^-$) were performed, processed, and calculated using the methods of Orcutt et al. (2005). The average activity of the $\text{H}^{14}\text{CO}_3^-$ tracer was 2.3×10^7 . The average activity of the added $^{14}\text{CH}_3\text{COO}^-$ was 9.8×10^6 DPM with a specific activity of 45-60 mCi mmol^{-1} . Rates of acetate oxidation ($^{14}\text{CO}_2$ from $^{14}\text{CH}_3^{14}\text{COO}^-$, 7.7×10^6 DPM, 45-60 mCi mmol^{-1}) were determined using methods similar to Orcutt et al. (2010) with the following differences: The distillation proceeded for 1 hour during which samples were heated to a low boil and the acid used to liberate the $^{14}\text{CO}_2$ in the sample was sulfuric rather than hydrochloric. No base traps were used and instead the $^{14}\text{CO}_2$ vapor was trapped into a 15 mL centrifuge tube with 2 mL of Carbosorb. The entirety of this volume was transferred to a glass 7 mL scintillation vial before counting. Rates of acetate oxidation were calculated as in Orcutt et al. (2010).

Rates of homoacetogenesis (AOG), the production of ^{14}C -acetate from $\text{H}^{14}\text{CO}_3^-$, were determined in the same incubations as bic MOG. Following MOG processing, samples were spiked with 5 mL of 20% zinc acetate. The samples were transferred to 125 mL flasks and connected to a soxhlet device and condenser. Samples were brought to a low boil for 45 minutes to separate the volatile fatty acids (VFAs; including acetate) from the rest of the organics and these VFAs were subsequently collected into the soxhlet reservoir. After separation, the condensate from the soxhlet reservoir was transferred to a

50 mL centrifuge tube and 1% of the final volume was mixed with Scintisafe Gel in a 20 mL glass vial and counted with a scintillation counter. Recovery rates of acetate standards averaged 97%. Rates of homoacetogenesis were calculated:

$$\text{AOG} = [\text{DIC}] \times \alpha_{\text{AOG}} \times \frac{a^{14}\text{C-Acetate}}{\text{time} \times a\text{H}^{14}\text{CO}_3^-} \quad (1)$$

Here, [DIC] is the concentration of dissolved inorganic carbon in the porewater (mM), α_{AOG} is the isotope fractionation factor for homoacetogenesis (1.12; GELWICKS et al., 1989), time is the incubation time in days, $a^{14}\text{C-Acetate}$ is the activity of the product, and $a\text{H}^{14}\text{CO}_3^-$ is the activity of the injected tracer. Rate samples for SR were prepared identically and methods of tracer addition, product recovery, remaining substrate recovery, activity measurements, and calculations were identical to those of Orcutt et al. (2010; adapted from CANFIELD et al. 1986 and FOSSING AND JORGENSEN 1989).

2.4 Lipid Extraction and IPL analysis

For lipid analyses, a combined peat sample was created by combining equal portions of peat from the duplicate core horizons used for porewater analyses. Between 3 and 7 grams of each peat sample were extracted using a modified Bligh and Dyer protocol as described by Sturt et al. (2004) and Lipp and Hinrichs (2009). An aliquot of 50-66% of the resulting total lipid extracts was separated using preparative HPLC with a preparative LiChrospher Diol-100 column (250x10 mm, 5 μm , Alltech, Germany) using the same parameters as Kellermann et al.(2012) except that only 2 fractions were collected: polar and apolar. These two fractions were checked using LC-MS (see protocol below) to ensure good separation. IPLs within the polar fraction were analyzed using a high-pressure liquid chromatography system coupled to a ThermoFinnigan LCQ DecaXP Plus ion-trap mass spectrometer via electrospray interface (HPLC-ESI-MSⁿ)

system using conditions described previously (SCHUBOTZ et al., 2009; STURT et al., 2004). Identification of bacterial and archaeal IPLs was based on mass spectral interpretation (ROSSEL et al., 2011; ROSSEL et al., 2008; SCHUBOTZ et al., 2009; STURT et al., 2004; YOSHINAGA et al., 2011). Concentrations of IPLs were determined using a comparison of the response of the various lipid classes against an injection standard (C₁₉-PC) and corrected by relative response factors of the injection standard relative to different IPL standards which were run in parallel (SCHUBOTZ et al., 2011a).

2.5 Stable Isotope Analyses

Stable carbon isotope (¹³C) measurements were performed on porewater CH₄, DIC, acetate, and lactate, particulate organic carbon (POC), and microbial core lipids. All isotope ratios are reported in δ¹³C notation (‰) relative to the Vienna Pee Dee Belemnite Standard.

2.5.1 Geochemical Isotope Analysis

Stable carbon isotope compositions of CH₄ (δ¹³C-CH₄) and dissolved inorganic carbon (δ¹³C-DIC) were analyzed at the Center for Applied Isotope Studies at the University of Georgia with a Thermo Scientific Delta V Plus IRMS. Prior to isotopic analysis, CH₄ and carbon dioxide were separated with an Agilent HP 6890 gas chromatograph on a Carboxen 1006 Plot column with a helium carrier at 100 °C interfaced with a Thermo Scientific Delta V Plus GC combustion module. Stable carbon isotope composition of particulate organic carbon (POC) was determined with an elemental analyzer coupled to an IRMS. Sediment samples were dried at 60 °C and ground with a mortar and pestle prior to analysis and the triplicate sediment horizons were combined.

Samples were weighed into silver capsules and fumed with concentrated HCl to remove inorganic carbon.

Carbon isotope compositions of the volatile fatty acids (VFAs) acetate and lactate were analyzed by irm-LC/MS as reported previously (HEUER et al., 2006; HEUER et al., 2010). The analysis involved separation of VFAs by HPLC (ThermoFinnigan Surveyor HPLC) combined with chemical oxidation of the effluents using the ThermoFinnigan LC IsoLink interface (KRUMMEN et al., 2004) and subsequent inline transfer of the resulting CO₂ into an irm-MS (ThermoFinnigan Delta Plus XP). As a modification of the original approach (HEUER et al., 2006), we used an optimized chromatographic method consisting of a VA300/7.8 Nucleogel Sugar 810H column (300 mm length; 7.8 mm i.d.; Macherey-Nagel) equipped with a guard column (CC30/4 Nucleogel Sugar 810H; 30 mm length; Macherey-Nagel), and 5 mM phosphoric acid as mobile phase with a flow rate of 300-400 $\mu\text{L}\cdot\text{min}^{-1}$. The column was kept at room temperature.

2.5.2 Core-lipid Characterization and Isotopic Composition

Intact-derived, apolar derivatives of IPLs were analyzed to determine their relative abundances and stable carbon isotopic composition. The stable carbon isotopic signatures ($\delta^{13}\text{C}$) of individual core lipids were determined with a ThermoFinnigan GC coupled to a ThermoFinnigan Delta-plus SP IRMS via GC-combustion interface III to a HP Series GC (SCHUBOTZ et al., 2011a). The precision of replicate analysis (n=2) of selected samples was better than 1%. Prior to compound-specific $\delta^{13}\text{C}$ analysis, apolar derivatives of the IPLs were produced using standard protocols and analyzed with a GC-FID for quantification and with a GC-MS for identification of compounds. The methods used for each lipid class are briefly described below.

Polar lipid fatty acids (PLFAs) and polar neutral lipids were obtained via saponification of an aliquot of the polar TLE using methods described previously (ELVERT et al., 2003; SCHUBOTZ et al., 2011a). The PLFA and neutral products were stored in n-hexane at -20°C until derivatization and analysis by GC-FID. The PLFA products were derivatized with BBr₃ and analyzed as fatty acid methyl esters (FAMES) with GC-FID (JAHNKE et al., 2002). FAME concentrations were determined by comparison on their responses with an internal standard added prior to saponification (10-methyl-C₁₈). The neutral lipid fractions (alcohols, monoacyl glycerol esters or MAGEs, and diacyl glycerol ester or DAGEs) were derivatized with bis-(trimethylsilyl)trifluoroacetamide (BSTFA) at 70°C for 1 hr. Apolar derivatives of ether-bound IPLs were obtained using the ether-cleavage protocol (JAHNKE et al., 2002; SCHUBOTZ et al., 2011a). The ether-based products (phytanes and biphytanes) were stored in n-hexane at -20°C until analysis on the GC-IRMS without derivitization. Core lipids of intact GDGTs were produced by acid hydrolysis and quantified with an HPLC system coupled to a ion trap mass spectrometer via an electrospray ionization (ESI) source (Liu, 2011).

2.6 Statistics

Site and seasonal related differences in measured porewater geochemistry and microbial activities were determined with Kruskal-Wallis one-way analysis of variance test with post-hoc Mann-Whitney-Wilcoxon testing if significant differences were determined. Statistical dependence between variables was determined using Spearman's rank correlation coefficient. All significances were determined at the 0.05 level. The Kruskal-Wallis tests, Mann-Whitney-Wilcoxon tests, and Spearman's rank correlations were all performed in SPSS for Windows (version 15.0, SPSS Inc., Chicago).

Ordination techniques were used to relate measured environmental variables, microbial activities, IPL composition, and stable carbon isotopic compositions of relevant geochemical species and microbial lipids. All ordination analyses were performed with the statistical package CANOCO for Windows 4.5 (Microcomputer Power, Ithaca, NY). The IPL data was divided into two groups (archaeal and bacterial sources) and then Hellinger transformed (LEGENDRE and GALLAGHER, 2001; RAMETTE, 2007); all other data was log transformed ($X'=\log[X+10]$) prior to analysis. Rare IPL categories which occurred in only a few samples were not used in the ordination and where appropriate, highly similar IPL classes were combined (e.g. DPG with lyso-DPG or all betaine lipid classes were combined). Within CANOCO all species were centered and standardized. We employed an indirect linear method (principle components analysis; PCA) with a scaling focus on sample distances to explore the distribution of individual samples and their relation to various biogeochemical variables. We used canonical redundancy analysis (RDA) with a focus on species correlations to explore multiple correlations among our data sets. Forward selection with monte carlo permutation test (499 permutations, significance level $p=0.05$) was used to select minimal sets of variables which significantly explained variation in the data for each RDA. Some variables were included as passive variables and were not used in the actual analysis, but included in the plot to aid interpretation. These are noted in the figure captions where appropriate.

3. RESULTS

3.1 Porewater and sediment characteristics

CH₄ concentrations ranged from 11 to 789 $\mu\text{mol L}^{-1}$ in Florida and from 4 to 1170 $\mu\text{mol L}^{-1}$ in Maine. Depth-integrated CH₄ concentrations in the top 20 cm of peat were

statistically indistinguishable between the two sites (Fig. 4.1). Temperature varied significantly with season at both sites, and temperatures were higher in Florida than in Maine ($p < 0.05$; Table 4.1). Despite the seasonality observed in CH_4 concentration, there was no seasonal variation in the concentration of major methanogenic substrates, hydrogen, DIC, or acetate, at either site (Table 4.1; $p < 0.05$). Hydrogen concentrations were positively correlated with temperature in both Maine ($\rho = 0.36$) and Florida ($\rho = 0.48$).

Sulfate concentration ranged from $30 \mu\text{mol L}^{-1}$ to 1.59 mmol L^{-1} , were significantly higher in summer than in winter at both sites (Fig. 4.1; $p < 0.05$), and were positively correlated with temperature in Florida ($\rho = 0.74$) and Maine ($\rho = 0.51$). Sulfide concentrations were low (max of $8 \mu\text{mol L}^{-1}$) and although sulfide did not vary on a seasonal basis, concentrations were significantly higher in Maine than in Florida ($p < 0.05$; Table 4.1). Dissolved organic carbon (DOC) concentration was significantly higher in Maine than in Florida ($p < 0.05$), although seasonal variation in concentration was only observed in Florida ($p < 0.05$; Table 4.1). Concentrations of total dissolved iron and manganese were significantly higher in Maine than in Florida ($p < 0.05$; Table 4.1). Total dissolved iron concentrations were significantly higher in summer than in winter in Florida ($p < 0.05$; Table 4.1). Manganese concentrations were significantly higher in winter than summer in Maine ($p < 0.05$; Table 4.1). Concentrations of dissolved nitrogen species (nitrate, nitrite, and ammonium) were statistically indistinguishable between the two sites ($p < 0.05$; Table 4.1). Nitrate was significantly higher in the winter in both Maine and Florida ($p < 0.05$) and nitrite was significantly higher in the summer in Florida ($p < 0.05$). No seasonal variability was observed in ammonium concentrations. Phosphate concentrations were significantly higher in Maine, where concentrations were

significantly higher in the winter than summer ($p < 0.05$; Table 4.1). Finally, ratios of dissolved inorganic nitrogen (nitrate+nitrite+ammonium) to dissolved phosphate (N:P) were significantly higher in Florida than in Maine ($p < 0.05$) but no seasonal variability was observed at either site (Table 4.1).

3.2 Microbial Activities

Rates of CH_4 production from both radiolabeled acetate ($^{14}\text{CH}_3\text{COO}^-$) and bicarbonate ($\text{H}^{14}\text{CO}_3^-$) were significantly higher in the summer at both sites (Table 4.2; $p < 0.05$). Rates of total CH_4 production (sum of ace and bic MOG) ranged from < 0.1 to $12 \text{ nmol cm}^{-3} \text{ d}^{-1}$ in Maine and were positively correlated with temperature ($\rho = 0.75$). In Florida these rates ranged from < 0.1 to $39 \text{ nmol cm}^{-3} \text{ d}^{-1}$ and were also positively correlated with temperature ($\rho = 0.37$). At both sites rates of total MOG generally decreased with depth (Fig. 4.2 A and F). There were distinct seasonal variations in methanogenic pathways in Maine and Florida: In Maine, the contribution of bic-MOG ranged from 4 to 99% (Fig. 4.2) with a significant seasonal decrease in this contribution in top 20 cm of 53% between winter and summer (Table 4.2; $p < 0.05$). In Florida the contribution of bic-MOG was generally lower than in Maine and ranged from 1 to 98% with a significantly lower contribution in the top 20 cm of peat in the summer than in the winter (Table 4.2; $p > 0.05$). When pooled together, there was a significant negative correlation between temperature and the contribution of bic-MOG (Fig. 4.3; $\rho = -0.86$).

Rates of AOM ranged from < 0.1 to $103 \text{ nmol cm}^{-3} \text{ d}^{-1}$ in Florida and from < 0.1 to $80 \text{ nmol cm}^{-3} \text{ d}^{-1}$ in Maine with maximum rates observed in the surface peat horizons at both sites (Fig. 4.2 C and H). While there was no significant variation in AOM rates in Maine, rates were significantly higher in winter than summer in Florida (Table 4.2;

$p < 0.05$). AOM was negatively correlated with temperature at both sites ($\rho = -0.39$ in Maine and $\rho = -0.75$ in Florida). Rates of AOM were not correlated with any of the following species at either site: sulfate, nitrate, nitrite, dissolved total iron, or dissolved manganese. CH_4 concentrations and AOM rates were inversely correlated at both sites ($\rho = -0.53$ for Florida and $\rho = -0.49$ for Maine; $p < 0.05$).

The high rates of AOM led to significant seasonal imbalance between CH_4 production from acetate and bicarbonate and anaerobic methanotrophy. In the summer in Maine the production of MOG to AOM was balanced, but in the winter there was far more anaerobic CH_4 consumption than CH_4 production (Table 4.2; $p < 0.05$). In Florida the seasonal difference between MOG and AOM was even greater with extremely high ratios of AOM:MOG in the winter and much lower rates of AOM than MOG in the summer (Table 4.2; $p < 0.05$).

Despite low porewater concentrations of sulfate, SR rates were high at both sites (Fig. 2 D and I). There were seasonal variations in the rates of SR in Florida, where rates were significantly higher in the winter than summer ($p < 0.05$), and in Maine, where rates were higher in the summer ($p < 0.05$). Rates of SR and AOM were highly correlated in Florida ($\rho = 0.86$) and Maine ($\rho = 0.55$), though SR rates exceeded rates of AOM at all sampling points (Table 4.2). Rates of SR were also inversely correlated with CH_4 concentration at both sites ($\rho = -0.52$ and -0.37 in Florida and Maine, respectively).

Rates of AOG ranged from < 0.1 to $4 \text{ nmol cm}^{-3} \text{ d}^{-1}$ in Florida (Fig. 4.2 E) and from < 0.1 to $7.8 \text{ nmol cm}^{-3} \text{ d}^{-1}$ in Maine (Fig. 4.2 J). Rates of AOG in Maine exceeded those in Florida on a depth-integrated basis (Table 4.2; $p < 0.05$). While there was no significant seasonal variation in AOG rates at either site, AOG rates significantly

exceeded rates of MOG in the winter at both sites while MOG rates were significantly higher than AOG in the winter (Table 4.2; $p > 0.05$).

Rates of acetate oxidation ranged from 0.4 to 19 $\text{nmol cm}^{-3} \text{d}^{-1}$ in Florida and were significantly higher than rates in Maine, which ranged from <0.1 to 3.2 $\text{nmol cm}^{-3} \text{d}^{-1}$ (Table 4.2; $p < 0.05$). Rates of acetate oxidation were correlated with SR at both sites ($\rho = 0.63$ and 0.81 at Florida and Maine, respectively).

3.3 Intact Membrane Polar Lipids

Total IPL concentration, which provides an index of viable microbial biomass, ranged from 1.1 to 16.0 $\mu\text{g g dry peat}^{-1}$ in Maine with a similar range in Florida, 1.8 to 12.0 $\mu\text{g g dry peat}^{-1}$ (Fig. 4.4). Florida IPL concentrations varied with depth (Fig. 4.4 A and B). In Maine, IPL concentrations decreased with depth (Fig. 4.4 C and D). IPL concentrations displayed some seasonal variation: concentrations of total IPLs were higher in the summer, especially in Florida (statistics not performed due to low sample size).

In Florida between 42 and 89% of the total identified IPL classes were categorized as archaeal in origin, with archaeol (AR) and isoprenoidal glycerol dialkyl glycerol tetraether (GDGT) as main core lipid structures and different glycosidic or phosphate-based head groups (Fig. 4.4). Similar archaeal IPLs were detected in Maine, although the contribution was generally lower (4 to 45%). The contribution of archeal lipids to the IPL pool increased with depth at both sites, but did not vary on a seasonal basis.

The composition of archaeal IPLs was distinct between the two sites: Florida peats were dominated by isoprenoidal GDGTs with 2 to 3 sugar as head groups (2 and 3

Gly-GDGT) while Maine generally contained more archaeol-based IPLs, particularly 2 Gly-AR. The diversity in archaeal-sourced IPLs was highest in Maine, where a total of 9 different archaeal IPLs were detected with a general increase of diversity with depth. In addition to archaeol and GDGTs, their hydroxylated counterparts, namely hydroxyarchaeol (OH-AR) and the newly identified hydroxy-GDGTs (OH-GDGT; Liu, 2011) were found with phosphatidyl-(*N*)-methylethanolamine (PME) and sugars as head groups, respectively. The most prevalent glyco-OH-GDGT we identified in this study was 2Gly-OH-GDGT which occurred in both Florida and Maine peats at all depths in concentrations up to 760 ng g⁻¹ dry peat in Florida and 40 ng g⁻¹ dry peat in Maine. There were three other glyco-OH-GDGTs: 3Gly-OH-GDGT and dihydroxy-GDGT with 2 and 3 sugars,(2, 3Gly-OH-GDGT) which were identified in only a single sample (Maine, summer, 25-30 cm) in low quantities (max of 90 ng g⁻¹ dry peat) along with a phosphoglyco-GDGT, namely phosphatidylinositol-monoglycosyl-GDGT (PI-GDGT-Gly). The structures and characteristic mass-spectra of these archaeal IPLs have been reported elsewhere (LIPP and HINRICHS, 2009; LIU, 2011; YOSHINAGA et al., 2011). The ring distribution of the isoprenoidal GDGT core lipids was highly similar in both Florida and Maine (appendix I). Both were dominated by acyclic GDGT, followed by GDGT with 1 and 2 rings, which were present in almost equal amounts, and very low relative amounts of GDGT with 3 rings and crenarchaeol, a tentative marker for ammonium oxidizing crenarchaea (SINNINGHE DAMSTÉ et al., 2002).

The remaining IPL classes, which were comprised of different types of phospholipids, glycolipids and aminolipids, could be largely assigned to bacterial origins though a few may be attributed to eukaryotic detritus (see text below). Since the turnover

of phospholipids in both aerobic and anaerobic sediments occurs on very short timescales, between days to weeks (HARVEY et al., 1986; LOGEMANN et al., 2011; WHITE et al., 1979), the majority of phospholipids in the anoxic peats could be confidently assigned to bacterial sources. A bacterial origin of the observed phospholipids is further corroborated by the presence of dietherglycerol (DEG), and mixed acyletherglycerol (AEG) as core lipids, which have been to date only found among bacteria (RÜTTERS et al., 2001; STURT et al., 2004). Six types of different phospholipid head groups were identified, the two most dominant being phosphatidylethanolamine (PE) and PME, followed by diphosphatidylglycerol (DPG) and lyso-DGP and smaller amounts of phosphatidylglycerol (PG), phosphatidylcholine (PC) and phosphatidyl-(*N,N*)-dimethylethanolamine (PDME). The most common phospholipids in Maine were PE and PME with AEG or diacylglycerol (DAG) side chains. These phospholipids were found at all depth horizons and ranged from 0.4 to 1.7 $\mu\text{g g}^{-1}$ dry peat for PE/PME-AEGs and from <0.1 to 1.9 $\mu\text{g g}^{-1}$ dry peat for PE/PME-DAGs. These two lipid classes were only found in the upper peat horizons in the summer peats of Florida. PG-DAG was identified in only a single, surface sample in Florida. PE-DEG was detected in all analyzed samples, in concentrations up to 0.6 $\mu\text{g g}^{-1}$ dry peat in Maine and up to 1.9 $\mu\text{g g}^{-1}$ dry peat in Florida where also some PME-DEG were detected. Phosphatidylethanolamine-Cer (PE-Cer), a phospholipid with a sphingosine core, was found in Maine, where it co-eluted with small amounts of PME-Cer and ornithine lipids. PE-Cer decreased in concentration with depth and ranged from 50 ng to 1.2 $\mu\text{g g}^{-1}$ dry peat. In Florida, PE-Cer was found in the surface peats of the summer at a concentration of 490 ng g^{-1} dry peat. An unknown IPL type, tentatively identified as a phospholipid was detected in all peat samples. The

mass spectra of these compounds, which elute after PE and shortly before PC, indicated both a loss of a PE head group (loss of $m/z=141$) as well as a minor fragment of $m/z=184$, which is characteristic for PC-containing molecules (STURT et al., 2004). This compound will be referred to throughout this text as a PE+PC mix.

Glycolipids with DAG core structures and glucuronic acid (1GlyA), diglycosyl (2Gly) and sulfonoquinovosyl (SQ) head groups were found only in Maine peats, with the highest concentrations in the surface horizons. 2Gly-DAG and SQ-DAG were only detected in the 0-3 cm surface layers in Maine and GlyA-DAG decreased 10 fold from around 200 ng g^{-1} dry peat in the surface to 20 ng g^{-1} dry peat in the deeper layers. 2 Gly-DAG and SQ-DAG are common glycolipids found in photosynthetic membranes (Holzl and Dormann, 2007; Wada and Murata, 1998) and are likely sourced from photosynthetic algae and/or cyanobacteria in the surface layers of the peat. Their presence in the deeper layers is surprising and points either to an additional bacterial source, for instance some gram positive bacteria are known to produce GlyA-DAG (HOLZL and DORMANN, 2007) or to a slower degradation of glycolipids in anaerobic environments

Two types of aminiolipids were detected in both Maine and Florida, betaine lipids (BLs) and ornithine lipids (OL). While BLs have to date only been found in photosynthetic organisms, mainly algae and some anoxygenic phototrophic bacteria, OLs are believed to be exclusively synthesized by bacteria (GEIGER et al., 2010). The BLs identified in Maine included 1,2-diacylglyceryl-3-(*O*-carboxyhydroxymethylcholine (DGCC), diacylglyceryl-hydroxymethyl-(*N,N,N*-trimethyl)- β -alanine(DGTA), and diacylglyceryl-(*N,N,N*)-trimethylhomoserine (DGTS) and decreased substantially with depth. We could not differentiate between DGTA and DGTS, because they fragment

similarly in the mass spectrometer and we did not have cultures for retention time comparison. In Florida, DGTS and DGTA occurred only in the surface peat horizons, in larger amounts in the summer ($1.9 \mu\text{g g}^{-1}$ dry peat) than in the winter ($0.5 \mu\text{g g}^{-1}$ dry peat). In Maine and Florida, OLS were present in every sample analyzed. In Maine, OLS were the single most abundant IPL with the highest concentrations found in the top peat horizon (maximum of $5.8 \mu\text{g g}^{-1}$ dry peat).

In Florida another type of GDGTs were found, namely branched GDGT, which are ubiquitously found in soil environments (HOPMANS et al., 2004; SCHOUTEN et al., 2000; WEIJERS et al., 2006b; WEIJERS et al., 2007). Unlike their isoprenoidal, archaeal-sourced counterparts (KATES, 1978), branched GDGTs are believed to be bacterial in origin (WEIJERS et al., 2006a), and recently Acidobacteria were identified as a bacterial source organism (SINNINGHE DAMSTÉ et al., 2011). Until recently, however, intact, polar branched GDGTs had not yet been detected. In Florida we identified an intact branched GDGT with glycuronic acid (GluA-br-GDGT) as main head group, which has been previously observed in peats from Germany and Sweden (LIU et al., 2010; PETERSE et al., 2011). It was present in every analyzed peat horizon in concentrations ranging between 39 and 260 ng g^{-1} dry peat. Core lipid analysis revealed the presence of branched GDGTs in both Florida and Maine peats throughout all depths (not shown). The main core lipids of the branched GDGTs were the 4-methyl branched and the 5-methyl branched GDGT. Concentrations of the branched core GDGTs ranged around 100 ng g^{-1} dry peat in Florida and 60 ng g^{-1} dry peat in Maine. These slightly lower concentrations in Maine together with a higher abundance and diversity of bacterial IPLs could explain the non-detection of the intact branched GDGTs in Maine peats.

The polar-lipid derived fatty acid composition in both Florida and Maine peats is dominated by odd-carbon numbered and branched fatty acids in addition to the generic microbial biomarkers of C_{16:0} and C_{14:0} (appendix II). The relative abundance of these fatty acids displayed little variation with depth or season. Absolute abundance of fatty acids decreased in a similar manner as the respective IPLs, in Maine they decreased about a ten-fold from surface to deeper layers and in Florida no real trends with depth were obvious.

3.4 Stable carbon isotopes

The stable carbon isotopic composition of CH₄ varied between the two sites, with more depleted CH₄ observed in Florida (Table 4.3). In Maine and Florida the ¹³C values of CH₄ gradually decreased with depth, though there was little variation between winter and summer values (Fig. 4.5). Isotope values for DIC were stable with depth and season in Florida. In contrast, δ¹³C DIC values increased markedly with depth in the peats of Maine. Values for δ¹³C POC were very similar between the two sites and varied little with depth or season. Acetate values were generally more depleted in ¹³C relative to POC and lactate (when detectable) at both sites. In Maine, the influence of AOM on the isotopic composition of CH₄ and DIC was clear (Fig. 4.6): δ¹³C-CH₄ was inversely correlated with δ¹³C-DIC (ρ=-0.7, p<0.05) and positively correlated with rates of AOM (ρ=0.7; p<0.05). There were no significant correlations in Florida.

Phytanes and biphytanes released by ether-cleavage of the polar lipid fraction of the TLE varied in isotopic composition (Table 4.3). Phytane, derived from phytanyl glycerol ethers of archaeol and hydroxyarchaeol, ranged in δ¹³C from -36 to -30‰ in Florida and from -28 to -30‰ in Maine: phytane isotopic signatures were slightly less

depleted in Florida than in Maine. Biphytanes with 0 up to 3 rings derived from GDGTs demonstrated a larger range in isotopic composition. Biphytane-0, derived partially from GDGT-0, and biphytane-3, derived exclusively from crenarchaeol, were the least depleted GDGT-sourced lipids, with a range from -37 to -32 ‰. Biphytanes 1 and 2, derived from GDGT-1,-2 and -3 were the most depleted archaeal lipids in the peats of both Florida and Maine, though those in Maine (-62 to -47 ‰) were more depleted than in Florida (-43 to -36‰). Although no statistical relationship was determined between AOM and the $\delta^{13}\text{C}$ of biphytanes 1 and 2, there is a clear influence of CH_4 oxidation on these two core lipids (Fig. 4.7). In Maine, biphytanes 1 and 2 generally increased in ^{13}C content with depth, with little variation between the winter and summer. Otherwise, there were no clear variations within the isotopic composition of specific core lipids with site, depth, or season.

There was relatively little variation in $\delta^{13}\text{C}$ of most of the bacterial core lipids (Table 4.3). The most depleted bacterial lipids were the unsaturated fatty acids $\text{C}_{16:1\omega 7}$, $\text{C}_{16:1\omega 5}$, and $\text{C}_{18:1\omega 7}$. The lowest $\delta^{13}\text{C}$ values measured were -46 ‰ in Florida ($\text{C}_{16:1\omega 5}$) and -50 ‰ in Maine (also for $\text{C}_{16:1\omega 5}$) in surface peats in the winter at both sites. The isotopic composition of monoalkylglycerolethers (MAGEs), derived from AEG phospholipids and dialkylglycerolethers (DAGEs), derived from DEG phospholipids, varied little between site or season with an overall range of -35 to -28 ‰.

3.5 Ordinations

In order to more fully understand the dynamics of seasonal carbon cycling within the microbial community of these peats, we examined multiple aspects of our data set using PCA and RDA. The first ordination analysis was limited to geochemical

characteristics and microbial activity (Fig. 4.8 A and B). The PCA of the various activities (Fig. 8A) indicated a clear seasonal distinction between microbial activity in the winter and summer of Florida, with winter samples grouped tightly together along axis 1 which is correlated with high rates of AOM, SR, acetate oxidation, and high ratios of CH₄ oxidation relative to production. There was a much less pronounced separation of the winter and summer samples in Maine.

We examined the relationship between microbial activities and measured geochemical constituents (site geochemistry, temperature, and depth) using an RDA (Fig. 4.8B). Using forward selection, we identified those variables which best explain the variation in the radiotracer rate data. The two RDA axes represented 55.8% of the variation in the microbial activity data and the selected parameters explained 94% of the variation in the relationship between the species and environmental variables. The contribution of bic-MOG to total CH₄ production (% bic) was negatively correlated with temperature and increased with depth. CH₄ production from both substrates increased together and appear unrelated to SR and AOM. SR was uncorrelated with sulfate availability and well correlated with rates of AOM and acetate oxidation, as well as acetate availability.

The distribution of bacterial IPLs in Maine and Florida was distinct, as indicated by the clear separation of samples from the two sites in the PCA diagram (Fig. 4.9). The direction of the arrows for the various IPL classes suggests relationships among the species. For example, DPG/lyso DPG, 1,2, Gly-DAG, and PC-DAG all plotted together which suggests a similar source or sources that share the same environmental niche. They are all present in relatively low amounts throughout the peat core. Most of the

phospholipids with PE and PME head groups, regardless of their core composition, plotted together with the betaine lipids: PE-Cer, PE, PME-AEG, and PE, PME-DAG. The novel PE+PC mix IPL, PE-DEG, and the intact branched GDGT did not plot with other IPLs classes, suggesting a distinct source for these three IPLs.

In contrast to the bacterial IPLs, the archaeal IPL composition of Maine and Florida were similar and do not separate according to site or season in the PCA (Fig. 4.10A). Redundancy analysis with the archaeal IPL composition and relevant geochemical parameters (Fig. 4.10B) indicated that the selected parameters (rates of MOG and AOM, in addition to CH₄ concentrations, N:P, and temperature) explained most (98%) of the variation in the archaeal IPL distribution and environmental variable relationship. The two RDA axes explained 54.2% of the variation in the archaeal IPL composition. The direction of the archaeol-based arrow indicated a source unique from the GDGT-based IPLs, which is correlated with CH₄ production. 2, 3Gly-OH-GDGTs and 2 Gly-GDGT plotted in the same direction along with increasing CH₄ concentrations. Unlike 2 Gly-GDGT, 3 Gly-GDGT correlated with temperature and the direction of the arrows for 2 and 3 Gly-GDGT suggest independent sources for these two IPL classes.

PCA of the isotopic composition of archaeal phytanes and biphytanes indicated distinct compositions for Maine and Florida samples with little seasonal distinction within the sites (Fig. 4.11). The isotopic composition of biphytanes 1 and 2 were correlated and had a distinct isotopic composition from other biphytanes and phytane.

The PCA of the isotopic composition of bacterial fatty acids shows a slight seasonal distinction between the summer and winter samples in Maine but not in Florida (Fig. 4.12A). However, the majority of the Maine samples separate from Florida within

the ordination space. The RDA axes represent 33% of the variation in the isotopic composition of bacterial core lipids and 57% of the variation in the relationship between the isotopic composition of the bacterial core lipids and geochemical species (Fig. 4.12B). The stable isotopic composition of branched bacterial fatty acids *ai*-C_{17:0}, *ai*-C_{15:0}, and *i*-C_{16:0} were correlated together with the ¹³C content of CH₄. The isotopic composition of the core lipids C_{18:ω7} and *i*-C_{15:0} correlated together and with the ¹³C content of DIC. Though not included in the RDA, the direction of the passively-displayed AOM arrow suggested an influence of AOM on the C_{18:ω7}, *i*-C_{15:0}, and DIC isotopic compositions.

4. DISCUSSION

Peatlands are the largest natural source of CH₄ to the atmosphere (BARTLETT and HARRISS, 1993; CICERONE and OREMLAND, 1988) and are generally regarded as methanogenic environments. Though the peats of Maine and Florida maintained considerable reservoirs of CH₄ during the study, direct rate measurements revealed that rates of bic- and ace-MOG were exceeded by rates of SR (Table 4.1). In addition to high SR, these peats supported substantial AOM activity, which exceeded CH₄ production in the top 20 cm of peat in the winter months. Higher rates of MOG in the summer led to considerably lower AOM:MOG ratios. The IPL composition of these peat wetlands revealed a viable microbial community dominated by SRB and CH₄-cycling archaea. However, isotope and lipid analyses did not reflect seasonal variations in carbon cycling, and surprisingly, no distinct signal for anaerobic methanotrophy was evident in any measured bacterial or archaeal lipids. These and other unique aspects of this study are discussed below.

4.1 Freshwater peats sustain high sulfate reduction rates

Although sulfate concentrations are typically low in peatlands (BLODAU et al., 2007; VILE et al., 2003; this study), the importance of SR has been documented in some systems (KELLER and BRIDGHAM, 2007; VILE et al., 2003; WATSON and NEDWELL, 1998; WIEDER et al., 1990). In accord with these previous findings, rates of SR in Maine and Florida exceeded rates of any other terminal metabolism measured (ace-MOG, bic-MOG, and AOG) in the top 20 cm of peat (Table 4.2). These SR rates are high but within the range reported for peatlands (WATSON and NEDWELL, 1998). Our data does not preclude the importance of other terminal electron accepting processes such as metal reduction and denitrification. The reduction of nitrate, though known to occur in the Everglades and other peat systems (GORDON et al., 1986; URBAN et al., 1988), is not known to be a major contributor to anaerobic carbon mineralization in peats (KELLER and BRIDGHAM, 2007). The low porewater concentrations of Mn(II) and Fe(II) suggest that metal reduction was not a major process of organic matter degradation, as observed in other peat wetlands (BLODAU et al., 2002). However, rapid recycling of these trace metals could support substantial rates of iron and manganese reduction (THAMDRUP et al., 1994). Thus, without further constraint on the carbon flow in these peats we cannot determine the contribution of sulfate reduction to total anaerobic carbon mineralization.

High SR rates in concert with relatively low sulfate concentrations (< 1 mM) resulted in turnover times of < 1 to 4 days for sulfate in the top 20 cm. This relatively rapid turnover and the low sulfate stocks at both sites suggest a tight coupling between SR and the reoxidation of reduced sulfur species, as observed in other peatlands (WIEDER and LANG, 1988). This reoxidation may occur in the uppermost peat layers, which are

exposed to oxygen (KNORR and BLODAU, 2009) or via anoxic mechanisms such as humic quinone shuttles (SCOTT et al., 1998).

Diverse populations of SRB have been identified in peats (STEGER et al., 2011), including those capable of acetate-oxidation (PESTER et al., 2010). Rates of acetate oxidation and SR were positively correlated, as were concentrations of acetate and SR (Fig. 4.8B), suggesting a link between sulfate and acetate cycling. Acetate-fueled SR could account for all acetate oxidation in the top 20 cm of peat at both sites, resulting in an acetate turnover times on the order of a few hours in the top 20 cm of peat. Alternatively, hydrogen consumption by autotrophic SRBs could result in a hydrogen turnover time of mere seconds in the top 20 cm of peat. Acetate and hydrogen demand from MOG were orders of magnitude lower than these estimates, with turnover times on the order of weeks and minutes, respectively. The substrate(s) of the SRBs in the peats of FL and ME were not explicitly determined in this study. In addition to acetate and hydrogen, other volatile fatty acids and alcohols are used by sulfate reducers, as well as more complex compounds, and some SRBs may even produce acetate as an end product (ODUM AND SINGLETON, 1993).

The reduction of sulfate, if available, typically predominates over MOG (ACHTNICH et al., 1995; KRISTJANSSON et al., 1982) as sulfate-reducers may outcompete methanogens for substrates (LOVLEY and KLUG, 1983). In other peat ecosystems, the addition of sulfate decreased potential MOG rates (WATSON and NEDWELL, 1998; YAVITT and LANG, 1990) and CH₄ emissions (GAUCI et al., 2002). Inhibition of MOG by sulfate was overcome by the addition of acetate and hydrogen to peat incubations

(YAVITT and LANG, 1990), suggesting that methanogens and sulfate reducers compete for these two substrates in peat soils.

The relative activity of MOG and SR in these peats indicated that SR likely limited CH₄ production. This limitation of MOG may even limit CH₄ emissions, as lower CH₄ fluxes are a demonstrated consequence of sulfate addition in peatlands (Dise and Verry, 2001) and rice paddies (Schütz et al., 1989). Coastal wetlands, such as those in the Florida Everglades or coastal Maine, are particularly sensitive to sea-level rise due to their proximity to the sea and low elevations (Cahoon et al., 2006). Increased sulfate availability to these environments via salt water intrusion is likely to result in lower CH₄ emissions from these ecosystems. The control of CH₄ emissions from peat wetlands through the competition with sulfate reducers has important implications for global climate change and future CH₄ budgets.

4.3 Importance of AOM in peat wetlands

Rates of AOM were high (in excess of 50 nmol cm⁻³ d⁻¹ in some cases) and are among the first ever reported for these environments (SMEMO and YAVITT, 2007). While aerobic CH₄ oxidation in peat has been documented extensively (KELLY et al., 1992; NEDWELL and WATSON, 1995; TOPP and PATTEY, 1997), until recently (SMEMO and YAVITT, 2007; SMEMO and YAVITT, 2011), AOM was thought to be inconsequential in peat environments (Segers, 1998). Both phylogenetic and isotopic techniques have been used as indicators of AOM in freshwater settings (CROWE et al., 2011; ELLER et al., 2005; SCHUBERT et al., 2011; TAKEUCHI et al., 2011), although few direct measurements of AOM in freshwater environments have been reported (DEUTZMANN and SCHINK, 2011; IVERSEN et al., 1987; SMEMO and YAVITT, 2007; ZEHNDER and BROCK, 1980). Smemo

and Yavitt (2011) estimated that AOM may consume an average of 41 Tg of CH₄ in northern wetlands each year, thereby reducing potential CH₄ emissions. In Florida and Maine, rates of AOM often exceeded acetoclastic and hydrogenotrophic CH₄ production, suggesting that AOM is indeed an important control of CH₄ emissions from these wetlands. These results highlight the potentially large role AOM plays in peat CH₄ cycling, an area of study which warrants further attention.

In marine settings, AOM is widespread and believed to be coupled to sulfate-reduction (VALENTINE, 2002). However, a growing body of research concerning sulfate-independent AOM has linked nitrate (ETTWIG et al., 2010; ETTWIG et al., 2008; RAGHOEBARSING et al., 2006), iron (BEAL et al., 2009; SIVAN et al., 2011; ZEHNDER and BROCK, 1980), and manganese (Beal et al., 2009; Zehnder and Brock, 1980) to the oxidation of CH₄. However, reports on the effect of various electron acceptors on AOM in freshwater environments are inconsistent (BOON and LEE, 1997; DEUTZMANN and SCHINK, 2011; SCHINK, 1997; SMEMO and YAVITT, 2007; ZEHNDER and BROCK, 1980). PCA revealed a correlation between AOM and SR were correlated with PCA (Fig. 4.8B) and the peat horizons harboring maximum activity of both processes often coincided (Fig. 4.2). All measured AOM activity could be supported by the high rates of SR which exceeded rates of AOM at both sites. The presence of IPLs which have been previously ascribed to SRB and ANMEs from seep communities (ROSSEL et al., 2011) supports a typical sulfate-fueled AOM mechanism (see discussion below). Although further investigation is needed to determine whether sulfate is the electron acceptor for CH₄ in these peatlands, our results suggest the feasibility of sulfate-dependent AOM in freshwater wetlands.

4.4 Seasonal carbon cycling

Reports of the predominance of ace- or bic-MOG in peatlands is variable (DUDDLESTON et al., 2002; GALAND et al., 2005; HORNIBROOK et al., 1997), and the response of peat-dwelling methanogens to seasonal and temperature changes is unclear (KOTSYURBENKO et al., 2004; SVENSSON, 1984). As observed in other peats (Nedwell and Watson 1995), rates of total CH₄ production increased with temperature between winter and summer (Fig. 4.2). Interestingly, total CH₄ production was highest in Maine, despite the relatively lower in situ temperature compared to Florida. A seasonal switch in MOG pathways was only observed in Maine (Table 4.2); however, the data from both sites show a decrease in the contribution of bic- MOG with temperature (Fig. 4.3). These seasonally-related changes in carbon flow are in contradiction to reports from lake sediments and rice paddy soils, where rates of bic-MOG increased with temperature (CHIN and CONRAD, 1995; SCHULZ and CONRAD, 1996; SCHULZ et al., 1997). This contrast in temperature response between peat wetlands and these other environments was unexpected and suggests that CH₄ cycling in peatlands is distinct from these other freshwater systems.

The distinct seasonal patterns in MOG in Florida and Maine may be attributed to competitive interactions among other metabolic processes. SR and AOG decreased between winter and summer, as MOG increased. Homoacetogens are known to outcompete methanogens for hydrogen at low temperatures (CONRAD and BABEL, 1989; KOTSYURBENKO et al., 2001). In freshwater environments such as rice paddy soils and lake sediments, interspecies competition for hydrogen may affect a temperature-related shift in methanogenic pathways (CHIN and CONRAD, 1995). In this study AOG

proceeded at rates higher than bic-MOG at both low (winter) and high (summer) temperatures, suggesting homoacetogens may outcompete hydrogenotrophic methanogens for hydrogen at a wider temperature range than in other freshwater environments.

The importance of AOG relative to CH₄ production did vary seasonally, although this was driven by decreasing rates of AOG and increasing rates of ace-MOG between the winter and summer samplings. In Florida, rates of acetate oxidation to CO₂ also displayed pronounced seasonal variation. This seasonal switch in acetate-consuming and acetate-producing processes was not associated with changes in the acetate pool, however, suggesting that other sources and sinks of acetate must be acting in concert to maintain consistent porewater acetate concentrations. In addition to the production of acetate from CO₂ and hydrogen, fermentation and some SRB may also contribute to the acetate pool (Schink, 1997; Sørensen et al., 1981). These acetogenic processes in combination with AOG likely support the acetate-consuming processes in these peats.

As discussed above, sulfate-reducers in these peats likely utilize acetate as a substrate, although other electron donors may also be used. Sulfate-reducers typically outcompete acetoclastic methanogens for substrate (SCHÖNHEIT et al., 1982). The lower summer SR rates may lead to more available acetate concentrations to support higher rates of ace-MOG. This would suggest seasonal substrate-limitation of acetoclastic methanogens, which in turn limits seasonal CH₄ production. Such a mechanism does not explain the fairly stable acetate concentration profiles, which never approached zero (Fig. 4.1). Higher summer sulfate concentrations belie any substrate limitation for SRB in the summer (Fig. 4.1), especially providing the evidently high affinity for freshwater sulfate

reducers (INGVORSEN and JØRGENSEN, 1984; PESTER et al., 2010). Seasonal declines in SR activity have been linked to carbon limitation of SRB at higher temperatures due to a decoupling between the production of substrates by fermentation and sulfate reduction (Weston and Joye 2005). SRB utilizing non-acetate substrates may experience similar seasonal limitations in these peats.

In addition to competitive interactions among methanogens, SRB, and homoacetogens, the relative importance of ace-MOG and bic-MOG may be influenced by the methods used in this study. The acetate tracer used in these studies provided both labeled and unlabeled or ‘cold’ acetate to the incubations. Acetate tracer additions inflated background acetate concentrations by an average of 20 $\mu\text{mol L}^{-1}$. This increase may have stimulated the acetate-consuming community which would overestimate rates of ace-MOG and acetate oxidation. A stimulatory effect of the added acetate would be exacerbated if portions of the in situ acetate pool were recalcitrant and therefore unavailable to the microbial community, as demonstrated in previous experiments (Parkes et al., 1984). An immobile acetate pool may also explain the relatively stable acetate concentrations over seasons where changes in acetate-cycling processes were observed. Future experiments with non-radioactive substrate additions are planned to elucidate the effect of substrate availability on methanogenic carbon cycling in these peats.

4.4 Distribution of IPL biomarkers

4.4.1 Bacterial IPLs – Previous IPL assignments in combination with PCA were used to identify sources of the non-archaeal IPLs (Table 4.4; Fig. 4.9). As stated above most of the phospholipids detected below depletion of oxygen could be confidently assigned to

anaerobic bacterial sources as phospholipids were shown to degrade rapidly in active anoxic sediments (Harvey et al., 1986; Logemann et al., 2011; White et al., 1979). The most abundant phospholipids PE- and PME-DAG are widespread among bacteria (Goldfine, 1984; Kates, 1964). While PE-DAG is present in almost all gram-negative and some gram-positive bacteria (Oliver and Colwell, 1973), PME-DAG is more restricted to members of the alpha- and gammaproteobacteria, bacterioides-flavobacteria and some gram-positive bacteria (Sohlenkamp et al., 2003). Sources for PME-DAG could be denitrifying (Goldfine and Hagen, 1968) or fermenting bacteria. PE-DAG, together with PG-DAG and DPG are the main IPLs found in all SRBs investigated to date (Makula and Finnerty, 1975; Rütters et al., 2001; Sturt et al., 2004). The presence of PG-DAG, which was found only in the surface sediments of Florida in winter, together with PE-DAG and DPG may explain the extremely high rates of SR in the winter in Florida (Table 4.2). Also, the dominance of saturated and branched C₁₅ and C₁₇ fatty acids further points to the presence of abundant SRBs (Taylor and Parkes, 1983) in the Florida peats, as does the prevalence of AEG and DEG phospholipids, which have been linked to SRB sources in previous studies, focusing on marine AOM sites (Rossel et al., 2008; Schubotz et al., 2011a; Sturt et al., 2004). The dominance of diether and mixed ether/ester-based lipids (up to 70% of total bacterial IPLs), and lack or normal PE and PME-DAGs in Florida in the winter season is particularly striking and may point to a seasonal adaptation in the bacterial membranes in the peats. The presence of unique bacterial IPLs in Florida is underlined by the abundant presence of the intact branched GluA-br-GDGT, which comprised between 2 to 35% of total IPLs, with higher abundances in winter (Fig. 4.4). The unique presence of GlyA-br-GDGT and PE-DEG in Florida might be one of the

main reasons these IPLs are negatively correlated with the other PE-containing lipids and indicate a different bacterial source to these (Fig. 4.9). GlyA-br-GDGT can be tentatively assigned to Acidobacteria based on recent findings (Sinninghe Damsté et al., 2011), but the mesophilic source for PE-DEG in soils and sediments is still unclear, because besides from Myxobacteria (Caillon et al., 1983), bacterial diethers are only known to be synthesized by thermophilic organisms (e.g. Sturt et al., 2004).

The PE+PC Mix, which is an as of yet unidentified IPL cannot be further assigned to specific sources other than anaerobic bacteria.

Lipids containing PE headgroups with Cer, AEG, and DAG side chains, which were abundantly detected in Maine, were correlated in the PCA (Fig. 4.9), suggesting a similar bacterial source for these IPLs or a common suite of environmental drivers. Likely sources for PE-DAG and PE-AEG are SRBs (Rütters et al., 2001), as stated above the presence of SRBs is also reflected in the fatty acid composition comprised of branched C₁₅ and C₁₇ fatty acids, which were also found as diacylglyceride fragments of these phospholipids (not shown).

Lipids, such as betaine lipids and glycolipids, which are typically associated with photosynthetic algae and cyanobacteria were either limited to the surface sediments (BLs in Maine and SQ-DAG) or decreased substantially with depth (BLs in FL, PC-DAG, 2Gly-DAG), as would be expected for photosynthetic organisms. The presence of BL and GlyA-DAG throughout the entire core in Maine could be assigned to either a preferential preservation of these IPLs or to alternative bacterial sources. Bacteria which are known to synthesize the BL, or encode the genes to do so, are mainly found among the alphaproteobacteria, particularly in plant associated bacteria and planctomycetes (Geiger

et al., 2011). Therefore it is feasible that anaerobic bacteria could be the producers of BL in the deeper peat layers in Maine and would also explain their correlation with PE and PME-DAGs in the PCA analysis (Fig. 4.9).

The ornithine lipids in the Florida and Maine peats are likely produced by sulfur-cycling bacteria (SCHUBOTZ et al., 2009; SHIVELY and KNOCHE, 1969) or plant-associated bacteria of the gamma or alphaproteobacteria (López-Lara et al., 2003). Low sulfate concentrations (Table 4.1) in these peats necessitate sulfur oxidation to resupply the high rates of SR (Table 4.2) measured throughout the study. The high contribution of OL and other lipids sourced from SRB to the IPL pool highlights the importance of sulfur cycling in these two peatlands.

4.4.2 Sources of Archaeal IPLs –The contribution of archaea was relatively high in these peats, especially in Florida. High contributions of archaeal IPLs (up to 36%) to the total IPL pool have been reported in other peat ecosystems (LIU et al., 2010). Specific source assignment of archaeols and GDGTs to particular archaea is not straightforward as these lipids are produced by nearly all members of Archaea (KOGA and MORII, 2005; KOGA et al., 1993). Previous field studies of archaeal IPLs relied on supplemental genetic data and/or environmental context to identify the source organisms (ROSSEL et al., 2011; ROSSEL et al., 2008; SCHUBOTZ et al., 2009). The PCA and RDA of the archaeal lipids aided in the interpretation of these IPL sources. Glycosidic archaeols, such as 2 and 3Gly-AR, and phosphohydroxyarchaeols (e.g. PME-OH-AR) have been ascribed to both methanogenic and methantrophic archaea in environmental samples (ROSSEL et al., 2011; SCHUBOTZ et al., 2011b). Many cultured methanogens produce both archaeol and hydroxyarchaeol (KOGA et al., 1993; STURT et al., 2004; SUNAMURA et al., 1999) and

concentrations of 2 and 3 Gly-AR correlated with total MOG in the RDA (Fig. 4.10). In these peats we assign archaeol and hydroxyarchaeol as methanogenic biomarkers. 2 and 3 Gly-GDGT in deep marine sediments is associated with anaerobic methanotrophy (ROSSEL et al., 2011; SCHUBOTZ et al., 2011b; YOSHINAGA et al., 2011). However, the ordination plots suggest distinct sources for these two IPLs. 2 Gly-GDGT, which has been ascribed to type 1 anaerobic methanotrophs (ANMEs; Rossel et al., 2011), was found at all depths and correlated with CH₄ concentration (Fig. 4.10). However, 3 Gly-GDGT only appeared in the lower peat horizons in Maine and was correlated with temperature and N:P ratios but not with CH₄ or MOG. 2 Gly-GDGT is therefore likely produced by methanotrophic archaea while 3 Gly-GDGT may have a distinct source, potentially heterotrophic archaea. The correlation of glycohydroxy-GDGTs with CH₄ concentrations and concentrations of other methanotrophic IPLs (2 Gly-GDGT) indicate an anaerobic methanotrophic source. Previous studies have ascribed these lipids to generic archaea as well as those involved in CH₄ cycling (SCHUBOTZ et al., 2009). The importance of AOM in Maine and Florida is supported by the detection of IPLs which have been previously found in ANME-dominated settings (Rossel et al., 2011; Rossel et al., 2008; Yoshinaga et al., 2011).

4.5 Seasonal Variation in Microbial Community Structure

In arctic peatlands, increased temperature resulted in higher rates of MOG with few changes in the archaeal community structure (Juottonen et al., 2008; Metje and Frenzel, 2005; Metje and Frenzel, 2007). Conversely, studies set in rice paddy soils, which contain similar methanogenic groups as peatlands (GALAND et al., 2005), demonstrated changes in the archaeal community with temperature (CHIN et al., 1999;

FEY and CONRAD, 2000). An increase in methanogenic archaea over the rest of the archaeal community with temperature may also explain the higher MOG rates in the summer at both sites without a corresponding increase in methanogenic substrates. However, there were no clear increases in methanogenic IPLs (e.g. 2Gly-AR and 2Gly-GDGT) between the two seasons. Arctic peat slurries at 20°C harbored a higher contribution of sequences belonging to known methanogens than slurries at 5°C (HOJ et al., 2007). Among those methanogens, the proportion of *Methanobacteria*, which exclusively utilizes CO₂-type substrates, decreased with temperature while the fraction of *Methanosarcina* and *Methanosaeta*, both capable of acetoclastic growth, increased during summer (HOJ et al., 2007). A similar seasonal increase in the proportion of acetoclastic methanogens over hydrogenotrophic methanogens in the peats of this study may explain the decrease in the contribution of bic-MOG to total CH₄ production. However, as members of these groups produce similar lipids (DE ROSA et al., 1986), such a shift is not evident in the IPL data. Though seasonal changes may have occurred in the microbial communities of Florida and Maine, no such changes were evident in the IPL biomarker data.

Previous studies have had mixed success linking microbial activities with biomass estimates. Enhanced MOG potential was not associated with changes in the size (as measured by *q*PCR) or structure of the archaeal community in a boreal mire (JUOTTONEN et al., 2008). Similar findings in Chinese wetlands were reported by Liu et al. (2011). High cell-specific rates may lead to high ecological importance of certain microbial groups, though they may occupy small fractions of the total community (PESTER et al.,

2010). Thus, the seasonal variation in microbial activities we documented at both sites may not have been accompanied by changes in the community.

4.6 Comparison of Isotopic Evidence with Microbial Activities

4.6.1 Seasonal variations in methanogenic pathways

The two dominant pathways of CH₄ production generally produce isotopically distinct CH₄: the carbon fractionation factors between the substrate and produced CH₄ are higher for bic-MOG than the acetoclastic pathway and therefore typically results in more depleted CH₄ (GELWICKS et al., 1994; KRZYCKI et al., 1987; WHITICAR et al., 1986). This distinct fractionation has been used to identify the major pathways of CH₄ formation in peats and other methanogenic settings (AVERY et al., 1999; KRÜGER et al., 2002; MARTENS et al., 1986). While few studies have compared the isotopic composition of CH₄ and its substrates (e. g. acetate and CO₂; HEUER ET AL., 2010), many studies have relied upon the isotopic signature of CH₄ alone to identify the methanogenic precursors (BURKE et al., 1988; KELLY et al., 1992; MARTENS et al., 1986).

In this study we compared the actual activities of bic- and ace-MOG with isotope geochemistry and found that the dominant pathways of CH₄ production in these peats are not reflected in the stable isotope composition of CH₄ (Fig. 4.5). We calculated the expected isotopic signature of CH₄ based on the relative contribution of acetate and bicarbonate-based MOG using the isotopic composition of acetate and CO₂ in porewaters (Table 4.3) and assuming a fractionation factor of 1.021 for ace-MOG (GELWICKS et al., 1994; KRZYCKI et al., 1987) and 1.073 for bic- MOG (LANSDOWN et al., 1992). Actual $\delta^{13}\text{C}$ values of CH₄ were 14 ‰ lighter to 33 ‰ heavier than values expected based on the relative rates of acetate and bicarbonate-based MOG (data not shown). In Maine the

expected $\delta^{13}\text{C-CH}_4$ values were generally heavier than the measured $\delta^{13}\text{C-CH}_4$ values in the summer and vice versa in the winter. In Florida expected values were all more negative than the expected CH_4 signatures. The depleted isotopic signatures of CH_4 alone, without the context of methanogenic activities and substrate compositions, suggests a purely hydrogenotrophic source in both peat sites (Fig. 4.5; WHITICAR et al., 1986). And yet, in Florida, where $\delta^{13}\text{C-CH}_4$ values remain highly depleted throughout the year, the dominant pathway of CH_4 production was ace-MOG (Table 4.2). In Maine the seasonal importance of ace-MOG was not accompanied by a shift in $\delta^{13}\text{C}$ of CH_4 .

This disagreement between radiotracer rate analyses and isotope-based inferences of methanogenic cycling could be attributed to several factors. One likely explanation is the use of non-competitive substrates such as methanol and methylated amines (KING et al., 1983). CH_4 produced from substrates other than acetate and CO_2 would dilute the isotope signal of CH_4 and obfuscate patterns arising from acetoclastic and hydrogenotrophic pathways. In other peat-based studies, the importance of alternative substrates is variable. The addition of methanol or methylated amines in mesocosms from Appalachian peat did not stimulate CH_4 production (YAVITT and LANG, 1990). However, MOG was fueled by methanol and formate in microcosms with moderately acidic peat (WÜST et al., 2009). CH_4 produced from alternative substrates would rectify the seasonal imbalance of CH_4 consumption via AOM over production observed in the top 20 cm of peat at both sites (Table 4.2).

Another explanation for the discrepancy between the expected and measured CH_4 signatures could be a methodological artifact. As discussed above, the contribution of acetoclastic CH_4 production may have been overestimated by our methods which

somewhat inflated the background concentrations of acetate and stimulate the methanogen community. Rates of ace-MOG are calculated with the in situ concentration of acetate, which may not be entirely labile (Wellsbury and Parkes, 1995). Such methodological biases would not be reflected in the stable isotope pool, which provides a time-integrated signal of dominating processes.

Anaerobic methanotrophy, a process of confirmed importance in these peats, effectively inflates the $\delta^{13}\text{C}$ values of CH_4 through the preferential consumption of lighter CH_4 (Whiticar, 1999). The influence of AOM on the $\delta^{13}\text{C}$ values of CH_4 and DIC is evident in Maine (Fig. 4.6) may explain why the expected CH_4 values in the surface winter samples were 14 ‰ lighter than the measured CH_4 values. It is thus impossible to determine the importance of alternative substrates in these peats. The mismatch in expected and measured $\delta^{13}\text{C}$ - CH_4 values is likely due to the influence of AOM and perhaps additional influence from other methanogenic pathways. Our findings caution against the use of stable isotopes alone to elucidate the dominant pathways of CH_4 production in systems where multiple processes simultaneously affect the stable carbon isotopic signature of CH_4 and its precursors.

4.6.2 Isotopic Evidence for AOM: Bacterial and Archaeal Biomarkers

Evidence indicates that sulfate-dependent AOM is performed by ANME archaea and SRB (HINRICHS et al., 2000; ORPHAN et al., 2001; PERNTHALER et al., 2008), which cooperate syntrophically to oxidize CH_4 (BOETIUS et al., 2000). Based on previous studies (HINRICHS et al., 1999; HINRICHS et al., 2000) which pioneered the use of lipid-biomarkers to identify sites of AOM-SR coupling, highly depleted microbial lipids have been used as a diagnostic for CH_4 -fueled microbial communities (Elvert et al., 1999;

Niemann and Elvert, 2008; Orcutt et al., 2005; Pancost et al., 2001; Pancost and Sinninghe Damsté, 2003; Rossel et al., 2008). Highly depleted (relative to CH₄) archaeal lipids such as archaeol, hydroxyarchaeol, and GDGTs have been identified in cold seeps (ORCUTT et al., 2005; PANCOST et al., 2001), marine sediments (HINRICHS and BOETIUS, 2002; HINRICHS et al., 1999), and brine pools. A few specific branched and cyclic fatty acids have been indicated as biomarkers of SRB involved in AOM (NIEMANN and ELVERT, 2008) and are found in isotopically depleted form in AOM-dominated communities (ELVERT et al., 2003; ORCUTT et al., 2005) .

Despite high rates of AOM and the influence of CH₄ oxidation on the isotopic composition of DIC and CH₄, no isotopic evidence for AOM was present in the lipids at either site. Diagnostic lipids of methanotrophic archaea are usually highly depleted in ¹³C with signatures 40-50 ‰ lower than CH₄ (PANCOST and SINNINGHE DAMSTÉ, 2003). However, such isotopic evidence is entirely from the marine realm, and typically based in ‘unique’ settings such as cold seeps (HINRICHS et al., 2000; ORCUTT et al., 2005; PANCOST et al., 2001), hydrate-rich sediments (ELVERT et al., 2003), mud volcanoes (PANCOST and SINNINGHE DAMSTÉ, 2003), and an asphalt volcano (SCHUBOTZ et al., 2011a). In this study the lowest δ¹³C values for any archaeal lipids was -62 ‰. Is it possible that these depleted signals in archaeal lipids could have been created without any methanotrophic activity?

The isotopic composition of the lipids of *Methanosarcina barkeri*, a typical methanogen found in wetland peats (CADILLO-QUIROZ et al., 2008), depends upon the type and availability of the substrate (LONDRY et al., 2008). Depending upon growth conditions, *Methanosarcina barkeri* produces an observed fractionation between

substrate and lipids from a relative enrichment in ^{13}C of 6.6 ‰ to a depletion to up 52.2 ‰ (LONDRY et al., 2008). If we assume fractionations between the dissolved CO_2 and DIC according to Mook et al. (1974; Table 4.3), the most depleted lipids of hydrogenotrophic methanogens in these peats would likely be in the range of -53 ‰ (Florida) to -65 ‰ (Maine). The most negative signatures resulting from ace-MOG would be -43‰ in Florida and -37 ‰ in Maine. The use of alternative methanogenic substrates (e.g. methanol and trimethylamine; OREMLAND and POLCIN, 1982; WHITMAN et al., 1992) could result in even more depleted lipids (LONDRY et al., 2008; SUMMONS et al., 1998). However, we can neither estimate the isotopic composition of these alternative substrates nor their importance as a methanogenic substrate in the peats of Florida and Maine, though some previous reports suggested methanol and trimethylamine are not important in CH_4 cycling in peat (YAVITT and LANG, 1990). Regardless, the $\delta^{13}\text{C}$ of the phytanes and biphytanes in these peats are well within the range of a pure methanogenic source.

These comparisons assume that the methanogens within these peats, including those which produce GDGTs, fractionate their lipids similarly to *M. barkeri*. Methanogenic archaea typically produce GDGTs without rings (biphytane-0) as opposed to ANME archaea (e.g. ANME 1) which contain biphytanes derived from GDGT-0, GDGT-1, and GDGT-2 (BLUMENBERG et al., 2004; KOGA AND MORII, 2005). This aligns with the isotopic composition of the biphytanes in these peats, which became increasingly depleted with between 0 and 2 cyclopentane rings (Table 4.3), suggesting an increasing contribution of archaeal methanotrophs. Schubotz et al. (2011a) also observed increased depletion with an increase in the number of cyclopentane rings. The observed

influence of AOM on the $\delta^{13}\text{C}$ of biphytanes with 1 and 2 rings (Fig. 4.7) further supports at least a partial methanotrophic source for these core lipids. The highest depletions also occurred in the surface peat horizons, where maximum AOM activity was measured (Fig. 4.2).

Crenarchaeol (which produces biphytane-3 upon ether cleavage) is produced by crenarchaeota (SINNINGHE DAMSTÉ et al., 2002), are typically heterotrophic archaea in sediment settings (BIDDLE et al., 2006; SCHUBOTZ et al., 2011a). Heterotrophic processes typically result in a fractionation between lipid and bulk POC of only a few ‰ (HAYES, 2001). The heterotrophic isotope signal of BP-3 isotope does not appear to correlate with any other archaea core lipids (Fig. 4.11), suggesting that phytane and biphytanes 0-2 are influenced by other isotopic sources. The isotopic compositions of the archaeal lipids in the peats of this study are likely sourced from a complicated mixture of methanogens, methanotrophs, and generic autotrophic and heterotrophic bacteria. An AOM-biomarker signal is likely diluted by other archaeal processes which utilized substrates enriched in ^{13}C , as would be expected for peat wetlands which constantly receive substantial inputs of fresh organic material.

As with the archaeal lipids, there were no highly depleted bacterial lipids detected in these peats. The most depleted bacterial lipids ($\text{C}_{16:1\omega 7}$, $\text{C}_{16:1\omega 5}$, and $\text{C}_{18:1\omega 7}$) have all been suggested as biomarkers for SRB associated with AOM (ELVERT et al., 2003; NIEMANN and ELVERT, 2008). Their relatively lower $\delta^{13}\text{C}$ values compared to the rest of the bacterial community suggest a methanotrophic influence. As with the archaeal lipid signatures of this study, a more robust methanotrophic signal was likely obscured by autotrophic and heterotrophic sulfate-reduction which produce less depleted lipids

(LONDRY et al., 2004). It should also be noted that AOM in these environments could be mediated by one or more groups of organisms whose lipids were not detected by our methods.

4. 7 Conclusions

Although peat wetlands are typically considered methanogenic, SR dominated over MOG in these two peat wetlands. High AOM activity, which may be linked to SR, and CH₄ production displayed opposite seasonal trends which led to high ratios of AOM:MOG in the winter and low AOM:MOG ratios in the summer. Our results demonstrate that SR, in addition to AOM, limit the eventual emission of CH₄ from peatlands, either through the inhibition of MOG or the consumption of CH₄ before it diffuses to the atmosphere. Substantial rates of AOG highlight its importance as a terminal metabolic process in peat. Large contributions of intact polar lipids representative of SRB and anaerobic methanogens reinforces the significance of these processes in Maine and Florida peats. However, seasonal shifts in microbial carbon cycling were not accompanied by changes in the microbial intact lipid composition. Isotopic analyses did not support microbial activity measurements: shifts in the methanogenic pathways were not reflected in the $\delta^{13}\text{C}$ of CH₄ and lipids displaying a distinct methanotrophic isotope signature were not detected.

Wetlands are highly dynamic settings that receive large inputs of organic matter and support diverse metabolic activity. In such environments it may be difficult to isolate isotopic signals of particular microbial processes. Our findings suggest that the importance of AOM in these settings should not be evaluated with isotopic approaches alone. AOM in freshwater systems is a burgeoning area of research with implications for

global change. A better understanding of AOM in freshwater systems is paramount to a better understanding of the global CH₄ budget and its role in past and present climate perturbations.

ACKNOWLEDGMENTS

The authors thank E. King, C. Culbertson, F. Tobias, E. Gaiser, and the FCE-LTER for support in the field. Analytical assistance was provided by J. Lipp, X. Prieto, M. Elvert, and K. Hunter. External methane isotope standards were kindly provided by J. Chanton. This work was financially supported by an award from the National Science Foundation (DEB 0717189).

REFERENCES

- Achnich, C., Bak, F., and Conrad, R. (1995) Competition for electron donors among nitrate reducers, ferric iron reducers, sulfate reducers, and methanogens in anoxic paddy soil. *Biology and Fertility of Soils* **19**, 65-72.
- Albert, D. B. and Martens, C. S. (1997) Determination of low-molecular-weight organic acid concentrations in seawater and pore-water samples via HPLC. *Marine Chemistry* **56**, 27-37.
- Armstrong, P. B., Lyons, W. B., and Gaudette, H. E. (1979) Application of Formaldoxime Colorimetric Method for the Determination of Manganese in the Pore Water of Anoxic Estuarine Sediments. *Estuaries* **2**, 198-201.
- Avery, G. B., Jr., Shannon, R. D., White, J. R., Martens, C. S., and Alperin, M. J. (1999) Effect of seasonal changes in the pathways of methanogenesis on the d13C values of pore water methane in a Michigan peatland. *Global Biogeochem. Cycles* **13**, 475-484.

- Avery, G. B., Shannon, R. D., White, J. R., Martens, C. S., and Alperin, M. J. (2003) Controls on methane production in a tidal freshwater estuary and a peatland: methane production via acetate fermentation and CO₂ reduction. *Biogeochemistry* **62**, 19-37.
- Bartlett, K. B. and Harriss, R. C. (1993) Review and assessment of methane emissions from wetlands. *Chemosphere* **26**, 261-320.
- Beal, E. J., House, C. H., and Orphan, V. J. (2009) Manganese- and Iron-Dependent Marine Methane Oxidation. *Science* **325**, 184-187.
- Biddle, J. F., Lipp, J. S., Lever, M. A., Lloyd, K. G., Sørensen, K. B., Anderson, R., Fredricks, H. F., Elvert, M., Kelly, T. J., Schrag, D. P., Sogin, M. L., Brenchley, J. E., Teske, A., House, C. H., and Hinrichs, K.-U. (2006) Heterotrophic Archaea dominate sedimentary subsurface ecosystems off Peru. *Proceedings of the National Academy of Sciences of the United States of America* **103**, 3846-3851.
- Blodau, C., Mayer, B., Peiffer, S., and Moore, T. R. (2007) Support for an anaerobic sulfur cycle in two Canadian peatland soils. *J. Geophys. Res.* **112**, G02004.
- Blodau, C., Roehm, C. L., and Moore, T. R. (2002) Iron, sulfur, and dissolved carbon dynamics in a northern peatland. *Archiv für Hydrobiologie* **154**, 561-583.
- Blumenberg, M., Seifert, R., Reitner, J., Pape, T., and Michaelis, W. (2004) Membrane lipid patterns typify distinct anaerobic methanotrophic consortia. *Proceedings of the National Academy of Sciences of the United States of America* **101**, 11111-11116.
- Boetius, A., Ravenschlag, K., Schubert, C. J., Rickert, D., Widdel, F., Gieseke, A., Amann, R., Jørgensen, B. B., Witte, U., and Pfannkuche, O. (2000) A marine

microbial consortium apparently mediating anaerobic oxidation of methane.

Nature **407**, 623-626.

Boon, P. I. and Lee, K. (1997) Methane oxidation in sediments of a floodplain wetland in south-eastern Australia. *Letters in Applied Microbiology* **25**, 138-142.

Bridgham, S. D., Patrick Megonigal, J., Keller, J. K., Bliss, N. B., and Trettin, C. (2006) The Carbon Balance of North American Wetlands. *Wetlands* **26**, 889-916.

Brook, E., Archer, D., Dlugokencky, E., Frohling, S., and Lawrence, D. (2008) Potential for abrupt changes in atmospheric methane, *Abrupt Climate Change. A report by the U.S. Climate Change Science Program and the Subcommittee on Global Change Research.* . U.S. Geological Survey, Reston, VA.

Burke, R. A., Martens, C. S., and Sackett, W. M. (1988) Seasonal variations of D/H and ¹³C/¹²C ratios of microbial methane in surface sediments. *Nature* **332**, 829-831.

Cadillo-Quiroz, H., Yashiro, E., Yavitt, J. B., and Zinder, S. H. (2008) Characterization of the Archaeal Community in a Minerotrophic Fen and Terminal Restriction Fragment Length Polymorphism-Directed Isolation of a Novel Hydrogenotrophic Methanogen. *Applied and Environmental Microbiology* **74**, 2059-2068.

Cahoon, D. R., Hensel, P. F., Spencer, T., Reed, D. J., McKee, K. L., and Saintilan, N. (2006) Coastal Wetland Vulnerability to Relative Sea-Level Rise: Wetland Elevation Trends and Process Controls Wetlands and Natural Resource Management. In: Verhoeven, J. T. A., Beltman, B., Bobbink, R., and Whigham, D. F. (Eds.). Springer Berlin Heidelberg.

- Canfield, D. E., Raiswell, R., Westrich, J. T., Reaves, C. M., and Berner, R. A. (1986)
The use of chromium reduction in the analysis of reduced inorganic sulfur in
sediments and shales. *Chemical Geology* **54**, 149-155.
- Chappellaz, J., Blunier, T., Raynaud, D., Barnola, J. M., Schwander, J., and Stauffert, B.
(1993) Synchronous changes in atmospheric CH₄ and Greenland climate between
40 and 8 kyr BP. *Nature* **366**, 443-445.
- Chasar, L. S., Chanton, J. P., Glaser, P. H., Siegel, D. I., and Rivers, J. S. (2000)
Radiocarbon and stable carbon isotopic evidence for transport and transformation
of dissolved organic carbon, dissolved inorganic carbon, and CH₄ in a northern
Minnesota peatland. *Global Biogeochem. Cycles* **14**, 1095-1108.
- Chin, K.-J. and Conrad, R. (1995) Intermediary metabolism paddy soil and the influence
of temperature. . *FEMS microbiology ecology* **18**, 85-102.
- Chin, K.-J., Lukow, T., and Conrad, R. (1999) Effect of Temperature on Structure and
Function of the Methanogenic Archaeal Community in an Anoxic Rice Field Soil.
Applied and Environmental Microbiology **65**, 2341-2349.
- Cicerone, R. J. and Oremland, R. S. (1988) Biogeochemical aspects of atmospheric
methane. *Global Biogeochem. Cycles* **2**, 299-327.
- Cline, J. D. (1969) Spectrophotometric Determination of Hydrogen Sulfide in Natural
Waters. *Limnology and Oceanography* **14**, 454-458.
- Conrad, R. and Babbel, M. (1989) Effect of dilution on methanogenesis, hydrogen
turnover and interspecies hydrogen transfer in anoxic paddy soil. *FEMS
Microbiology Letters* **62**, 21-27.

- Conrad, R., Schütz, H., and Babel, M. (1987) Temperature limitation of hydrogen turnover and methanogenesis in anoxic paddy soil. *FEMS Microbiology Letters* **45**, 281-289.
- Crowe, S. A., Katsev, S., Leslie, K., Sturm, A., Magen, C., Nomosatryo, S., Pack, M. A., Kessler, J. D., Reeburgh, W. S., Roberts, J. A., González, L., Douglas Haffner, G., Mucci, A., Sundby, B., and Fowle, D. A. (2011) The methane cycle in ferruginous Lake Matano. *Geobiology* **9**, 61-78.
- De Rosa, M., Gambacorta, A., and Gliozzi, A. (1986) Structure, biosynthesis, and physicochemical properties of archaebacterial lipids. *Microbiological Reviews* **50**, 70-80.
- Deutzmann, J. S. and Schink, B. (2011) Anaerobic Oxidation of Methane in Sediments of an Oligotrophic Freshwater Lake (Lake Constance). *Appl. Environ. Microbiol.*, AEM.00340-11.
- Dise, N. and Verry, E. (2001) Suppression of peatland methane emission by cumulative sulfate deposition in simulated acid rain. *Biogeochemistry* **53**, 143-160.
- Duddleston, K., Kinney, M., Kiene, R., and Hines, M. (2002) Anaerobic microbial biogeochemistry in a northern bog: acetate as a dominant metabolic end product. *Global Biogeochem. Cycles* **16**.
- Dunfield, P., Knowles, R., Dumont, R., and Moore, T. R. (1993) Methane production and consumption in temperate and subarctic peat soils: Response to temperature and pH. *Soil Biology and Biochemistry* **25**, 321-326.

- Eller, G., Känel, L., and Krüger, M. (2005) Cooccurrence of Aerobic and Anaerobic Methane Oxidation in the Water Column of Lake Plußsee. *Applied and Environmental Microbiology* **71**, 8925-8928.
- Elvert, M., Boetius, A., Knittel, K., and Jørgensen, B. B. (2003) Characterization of Specific Membrane Fatty Acids as Chemotaxonomic Markers for Sulfate-Reducing Bacteria Involved in Anaerobic Oxidation of Methane. *Geomicrobiology Journal* **20**, 403-419.
- Elvert, M., Suess, E., and Whiticar, M. J. (1999) Anaerobic methane oxidation associated with marine gas hydrates: superlight C-isotopes from saturated and unsaturated C20 and C25 irregular isoprenoids. *Naturwissenschaften* **86**, 295-300.
- Ettwig, K. F., Butler, M. K., Le Paslier, D., Pelletier, E., Mangenot, S., Kuypers, M. M. M., Schreiber, F., Dutilh, B. E., Zedelius, J., de Beer, D., Gloerich, J., Wessels, H. J. C. T., van Alen, T., Luesken, F., Wu, M. L., van de Pas-Schoonen, K. T., Op den Camp, H. J. M., Janssen-Megens, E. M., Francoijs, K.-J., Stunnenberg, H., Weissenbach, J., Jetten, M. S. M., and Strous, M. (2010) Nitrite-driven anaerobic methane oxidation by oxygenic bacteria. *Nature* **464**, 543-548.
- Ettwig, K. F., Shima, S., Van De Pas-Schoonen, K. T., Kahnt, J., Medema, M. H., Op Den Camp, H. J. M., Jetten, M. S. M., and Strous, M. (2008) Denitrifying bacteria anaerobically oxidize methane in the absence of Archaea. *Environmental Microbiology* **10**, 3164-3173.
- Fey, A. and Conrad, R. (2000) Effect of Temperature on Carbon and Electron Flow and on the Archaeal Community in Methanogenic Rice Field Soil. *Appl. Environ. Microbiol.* **66**, 4790-4797.

- Forster, P., V. Ramaswamy, P. Artaxo, T. Berntsen, R. Betts, D.W. Fahey, J. Haywood, J. Lean, D.C. Lowe, G. Myhre, J. Nganga, R. Prinn, G. Raga, M. Schulz and R. Van Dorland. (2007) Changes in Atmospheric Constituents and in Radiative Forcing. In: Solomon, S., D. Qin, M. Manning, Z. Chen, M. Marquis, K.B. Averyt, M. Tignor and H.L. Miller (Ed.), *Climate Change 2007: The Physical Science Basis. Contribution of Working Group I to the Fourth Assessment Report of the Intergovernmental Panel on Climate Change*. Cambridge University Press, Cambridge, United Kingdom.
- Fossing, H. and Jørgensen, B. B. (1989) Measurement of bacterial sulfate reduction in sediments: Evaluation of a single-step chromium reduction method. *Biogeochemistry* **8**, 205-222.
- Galand, P. E., Fritze, H., Conrad, R., and Yrjala, K. (2005) Pathways for Methanogenesis and Diversity of Methanogenic Archaea in Three Boreal Peatland Ecosystems. *Appl. Environ. Microbiol.* **71**, 2195-2198.
- Gauci, V., Dise, N. B., and Fowler, D. (2002) Controls on suppression of methane flux from a peat bog subjected to simulated acid rain sulfate deposition. *Global Biogeochem. Cycles* **16**, 4.1-4.12.
- Gedney, N., Cox, P. M., and Huntingford, C. (2004) Climate feedback from wetland methane emissions. *Geophys. Res. Lett.* **31**, L20503.
- Geiger, O., Sohlenkamp, C., and López-Lara, I. M. (2010) Formation of Bacterial Membrane Lipids: Pathways, Enzymes, Reactions
Handbook of Hydrocarbon and Lipid Microbiology. In: Timmis, K. N. (Ed.). Springer Berlin Heidelberg.

- Gelwicks, J. T., Risatti, J. B., and Hayes, J. M. (1989) Carbon isotope effects associated with autotrophic acetogenesis. *Organic Geochemistry* **14**, 441-446.
- Gelwicks, J. T., Risatti, J. B., and Hayes, J. M. (1994) Carbon isotope effects associated with acetoclastic methanogenesis. *Appl. Environ. Microbiol.* **60**, 467-472.
- Goldfine, H. (1984) Bacterial membranes and lipid packing theory. *Journal of Lipid Research* **25**, 1501-7.
- Goldfine, H. and Hagen, P. O. (1968) N-methyl groups in bacterial lipids. *J. Bacteriol.* **95**, 367-375.
- Gordon, A. S., Cooper, W. J., and Scheidt, D. J. (1986) Denitrification in Marl and Peat Sediments in the Florida Everglades. *Applied and Environmental Microbiology* **52**, 987-991.
- Harriss, R. C., Sebacher, D. I., and Day, F. P. (1982) Methane flux in the Great Dismal Swamp. *Nature* **297**, 673-674.
- Harvey, H. R., Fallon, R. D., and Patton, J. S. (1986) The effect of organic matter and oxygen on the degradation of bacterial membrane lipids in marine sediments *Geochimica et Cosmochimica Acta* **50**, 795-804.
- Hayes, J. M. (2001) Fractionation of Carbon and Hydrogen Isotopes in Biosynthetic Processes. *Reviews in Mineralogy and Geochemistry* **43**, 225-277.
- Heuer, V., Elvert, M., Tille, S., Krummern, M., Mollar, X. P., Hmelo, L., and Hinrichs, K.-U. (2006) Online d13C analysis of volatile fatty acids in sediment/porewater systems by liquid chromatography-isotope ratio mass spectrometry. *Limnology and Oceanography: Methods* **4**, 346-357.

- Heuer, V. B., Krüger, M., Elvert, M., and Hinrichs, K.-U. (2010) Experimental studies on the stable carbon isotope biogeochemistry of acetate in lake sediments. *Organic Geochemistry* **41**, 22-30.
- Hines, M., Duddleston, K., and Kiene, R. (2001) Carbon flow to acetate and C1 compounds in northern wetlands. *Geophys. Res. Lett.* **28**, 4251-4254.
- Hinrichs, K.-U. and Boetius, A. (2002) The anaerobic oxidation of methane: new insights in microbial ecology and biogeochemistry. *Ocean Margin Systems*.
- Hinrichs, K.-U., Hayes, J. M., Sylva, S. P., Brewer, P. G., and DeLong, E. F. (1999) Methane-consuming archaeobacteria in marine sediments. *Nature* **398**, 802-805.
- Hinrichs, K.-U., Summons, R. E., Orphan, V., Sylva, S. P., and Hayes, J. M. (2000) Molecular and isotopic analysis of anaerobic methane-oxidizing communities in marine sediments. *Organic Geochemistry* **31**, 1685-1701.
- Hoehler, T. M., Alperin, M. J., Albert, D. B., and Martens, C. S. (1998) Thermodynamic control on hydrogen concentrations in anoxic sediments. *Geochimica et Cosmochimica Acta* **62**, 1745-1756.
- Hoj, L., Olsen, R. A., and Torsvik, V. L. (2007) Effects of temperature on the diversity and community structure of known methanogenic groups and other archaea in high Arctic peat. *ISME J* **2**, 37-48.
- Holz, G. and Dormann, P. (2007) Structure and function of glycolipids in plants and bacteria. *Progress in lipid research* **46**, 225-43.
- Hopmans, E. C., Weijers, J. W. H., Schefuß, E., Herfort, L., Sinninghe Damsté, J. S., and Schouten, S. (2004) A novel proxy for terrestrial organic matter in sediments

- based on branched and isoprenoid tetraether lipids. *Earth and Planetary Science Letters* **224**, 107-116.
- Hornibrook, E. R. C., Longstaffe, F. J., and Fyfe, W. S. (1997) Spatial distribution of microbial methane production pathways in temperate zone wetland soils: Stable carbon and hydrogen isotope evidence. *Geochimica et Cosmochimica Acta* **61**, 745-753.
- Hornibrook, E. R. C., Longstaffe, F. J., and Fyfe, W. S. (2000) Evolution of stable carbon isotope compositions for methane and carbon dioxide in freshwater wetlands and other anaerobic environments. *Geochimica et Cosmochimica Acta* **64**, 1013-1027.
- Ingvorsen, K. and Jørgensen, B. B. (1984) Kinetics of sulfate uptake by freshwater and marine species of *Desulfovibrio*. *Archives of Microbiology* **139**, 61-66.
- Iversen, N., Oremland, R. S., and Klug, M. J. (1987) Big Soda Lake (Nevada). 3. Pelagic Methanogenesis and Anaerobic Methane Oxidation. *Limnology and Oceanography* **32**, 804-814.
- Jahnke, L. L., Eder, W., Huber, R., Hope, J. M., Hinrichs, K.-U., Hayes, J. M., Des Marais, D. J., Cady, S. L., and Summons, R. E. (2001) Signature Lipids and Stable Carbon Isotope Analyses of Octopus Spring Hyperthermophilic Communities Compared with Those of Aquificales Representatives. *Applied and Environmental Microbiology* **67**, 5179-5189.
- Jahnke, L. L., Embaye, T., and Summons, R. E. (2002) Lipid biomarkers for methanogens in hypersaline cyanobacterial mats for Guerro Negro, Baja California Sur. In: NASA (Ed.).

- Joye, S. B., Boetius, A., Orcutt, B. N., Montoya, J. P., Schulz, H. N., Erickson, M. J., and Lugo, S. K. (2004) The anaerobic oxidation of methane and sulfate reduction in sediments from Gulf of Mexico cold seeps. *Chemical Geology* **205**, 219-238.
- Juottonen, H., Tuittila, E.-S., Juutinen, S., Fritze, H., and Yrjala, K. (2008) Seasonality of rDNA- and rRNA-derived archaeal communities and methanogenic potential in a boreal mire. *ISME J* **2**, 1157-1168.
- Kates, M. (1964) Bacterial lipids. *Advances in lipid research* **2**, 17-90.
- Kates, M. (1978) The phytanyl ether-linked polar lipids and isoprenoid neutral lipids of extremely halophilic bacteria. *Progress in the Chemistry of Fats and other Lipids* **15**, 301-342.
- Keller, J. K. and Bridgham, S. D. (2007) Pathways of Anaerobic Carbon Cycling across an Ombrotrophic-Minerotrophic Peatland Gradient. *Limnology and Oceanography* **52**, 96-107.
- Kellermann, M. Y., Schubotz, F., Elvert, M., Lipp, J. S., Birgel, D., Prieto-Mollar, X., Dubilier, N., and Hinrichs, K.-U. (2012) Symbiont–host relationships in chemosynthetic mussels: A comprehensive lipid biomarker study. *Organic Geochemistry* **43**, 112-124.
- Kelly, C. A., Dise, N. B., and Martens, C. S. (1992) Temporal variations in the stable carbon isotopic composition of methane emitted from Minnesota peatlands. *Global Biogeochem. Cycles* **6**, 263-269.
- King, G. M., Klug, M. J., and Lovley, D. R. (1983) Metabolism of Acetate, Methanol, and Methylated Amines in Intertidal Sediments of Lowes Cove, Maine. *Applied and Environmental Microbiology* **45**, 1848-1853.

- Knittel, K. and Boetius, A. (2009) Anaerobic Oxidation of Methane: Progress with an Unknown Process. *Annual Review of Microbiology* **63**, 311-334.
- Knorr, K.-H. and Blodau, C. (2009) Impact of experimental drought and rewetting on redox transformations and methanogenesis in mesocosms of a northern fen soil. *Soil Biology and Biochemistry* **41**, 1187-1198.
- Koga, Y. and Morii, H. (2005) Recent Advances in Structural Research on Ether Lipids from Archaea Including Comparative and Physiological Aspects. *Bioscience, Biotechnology, and Biochemistry* **69**, 2019-2034.
- Koga, Y., Nishihara, M., Morii, H., and Akagawa-Matsushita, M. (1993) Ether polar lipids of methanogenic bacteria: structures, comparative aspects, and biosyntheses. *Microbiological Reviews* **57**, 164-182.
- Kotsyurbenko, O. R., Chin, K.-J., Glagolev, M. V., Stubner, S., Simankova, M. V., Nozhevnikova, A. N., and Conrad, R. (2004) Acetoclastic and hydrogenotrophic methane production and methanogenic populations in an acidic West-Siberian peat bog. *Environmental Microbiology* **6**, 1159-1173.
- Kotsyurbenko, O. R., Glagolev, M. V., Nozhevnikova, A. N., and Conrad, R. (2001) Competition between homoacetogenic bacteria and methanogenic archaea for hydrogen at low temperature. *FEMS microbiology ecology* **38**, 153-159.
- Kristjansson, J. K., Schönheit, P., and Thauer, R. K. (1982) Different K_{m} values for hydrogen of methanogenic bacteria and sulfate reducing bacteria: An explanation for the apparent inhibition of methanogenesis by sulfate. *Archives of Microbiology* **131**, 278-282.

- Krüger, M., Eller, G., Conrad, R., and Frenzel, P. (2002) Seasonal variation in pathways of CH₄ production and in CH₄ oxidation in rice fields determined by stable carbon isotopes and specific inhibitors. *Global Change Biology* **8**, 265-280.
- Krummen, M., Hilkert, A. W., Juchelka, D., Duhr, A., Schlüter, H.-J., and Pesch, R. (2004) A new concept for isotope ratio monitoring liquid chromatography/mass spectrometry. *Rapid Communications in Mass Spectrometry* **18**, 2260-2266.
- Krzycki, J. A., Kenealy, W. R., DENiro, M. J., and Zeikus, J. G. (1987) Stable Carbon Isotope Fractionation by *Methanosarcina barkeri* during Methanogenesis from Acetate, Methanol, or Carbon Dioxide-Hydrogen. *Appl. Environ. Microbiol.* **53**, 2597-2599.
- Lansdown, J. M., Quay, P. D., and King, S. L. (1992) CH₄ production via CO₂ reduction in a temperate bog: A source of ¹³C-depleted CH₄. *Geochimica et Cosmochimica Acta* **56**, 3493-3503.
- Legendre, P. and Gallagher, E. (2001) Ecologically meaningful transformations for ordination of species data. *Oecologia* **129**, 271-280.
- Lipp, J. S. and Hinrichs, K.-U. (2009) Structural diversity and fate of intact polar lipids in marine sediments. *Geochimica et Cosmochimica Acta* **73**, 6816-6833.
- Lipp, J. S., Morono, Y., Inagaki, F., and Hinrichs, K.-U. (2008) Significant contribution of Archaea to extant biomass in marine subsurface sediments. *Nature* **454**, 991-994.
- Liu, D. Y., Ding, W. X., Jia, Z. J., and Cai, Z. C. (2011) Relation between methanogenic archaea and methane production potential in selected natural wetland ecosystems across China. *Biogeosciences* **8**, 329-338.

- Liu, X.-L. (2011) Glycerol ether lipids in sediments: sources, diversity and implications
University of Bremen.
- Liu, X.-L., Leider, A., Gillespie, A., Gröger, J., Versteegh, G. J. M., and Hinrichs, K.-U. (2010) Identification of polar lipid precursors of the ubiquitous branched GDGT orphan lipids in a peat bog in Northern Germany. *Organic Geochemistry* **41**, 653-660.
- Logemann, J., Graue, J., Koster, J., Engelen, B., Rullkotter, J., and Cypionka, H. (2011) A laboratory experiment of intact polar lipid degradation in sandy sediments. *Biogeosciences* **8**, 2547-2560.
- Londry, K. L., Dawson, K. G., Grover, H. D., Summons, R. E., and Bradley, A. S. (2008) Stable carbon isotope fractionation between substrates and products of *Methanosarcina barkeri*. *Organic Geochemistry* **39**, 608-621.
- Londry, K. L., Jahnke, L. L., and Des Marais, D. J. (2004) Stable Carbon Isotope Ratios of Lipid Biomarkers of Sulfate-Reducing Bacteria. *Appl. Environ. Microbiol.* **70**, 745-751.
- López-Lara, I. M., Sohlenkamp, C., and Geiger, O. (2003) Membrane Lipids in Plant-Associated Bacteria: Their Biosyntheses and Possible Functions. *Molecular Plant-Microbe Interactions* **16**, 567-579.
- Lovley, D. R. and Klug, M. J. (1983) Sulfate Reducers Can Outcompete Methanogens at Freshwater Sulfate Concentrations. *Applied and Environmental Microbiology* **45**, 187-192.
- Makula, R. A. and Finnerty, W. R. (1975) Isolation and characterization of an ornithine-containing lipid from *Desulfobivrio gigas*. *Journal of Bacteriology* **123**, 523-529.

- Martens, C., Blair, N., Green, C., and Des Marais, D. (1986) Seasonal variations in the stable carbon isotopic signature of biogenic methane in a coastal sediment. *Science* **233**, 1300-1303.
- Metje, M. and Frenzel, P. (2005) Effect of Temperature on Anaerobic Ethanol Oxidation and Methanogenesis in Acidic Peat from a Northern Wetland. *Applied and Environmental Microbiology* **71**, 8191-8200.
- Metje, M. and Frenzel, P. (2007) Methanogenesis and methanogenic pathways in a peat from subarctic permafrost. *Environmental Microbiology* **9**, 954-964.
- Mook, W. G., Bommerson, J. C., and Staverman, W. H. (1974) Carbon isotope fractionation between dissolved bicarbonate and gaseous carbon dioxide. *Earth and Planetary Science Letters* **22**, 169-176.
- Nedwell, D. B. and Watson, A. (1995) CH₄ production, oxidation and emission in a U.K. ombrotrophic peat bog: Influence of SO₄²⁻ from acid rain. *Soil Biology and Biochemistry* **27**, 893-903.
- Niemann, H. and Elvert, M. (2008) Diagnostic lipid biomarker and stable carbon isotope signatures of microbial communities mediating the anaerobic oxidation of methane with sulphate. *Organic Geochemistry* **39**, 1668-1677.
- Oba, M., Sakata, S., and Tsunogai, U. (2006) Polar and neutral isopranyl glycerol ether lipids as biomarkers of archaea in near-surface sediments from the Nankai Trough. *Organic Geochemistry* **37**, 1643-1654.
- Odum, J. M. and Singleton, R. (1993) *The Sulfate-reducing bacteria: Contemporary perspectives* Springer-Verlag, New York.

- Oliver, J. D. and Colwell, R. R. (1973) Extractable Lipids of Gram-Negative Marine Bacteria: Phospholipid Composition. *Journal of Bacteriology* **114**, 897-908.
- Orcutt, B., Boetius, A., Elvert, M., Samarkin, V., and Joye, S. B. (2005) Molecular biogeochemistry of sulfate reduction, methanogenesis and the anaerobic oxidation of methane at Gulf of Mexico cold seeps. *Geochimica et Cosmochimica Acta* **69**, 4267-4281.
- Orcutt, B. N., Joye, S. B., Kleindienst, S., Knittel, K., Ramette, A., Reitz, A., Samarkin, V., Treude, T., and Boetius, A. (2010) Impact of natural oil and higher hydrocarbons on microbial diversity, distribution, and activity in Gulf of Mexico cold-seep sediments. *Deep Sea Research Part II: Topical Studies in Oceanography* **57**, 2008-2021.
- Oremland, R. S. and Polcin, S. (1982) Methanogenesis and Sulfate Reduction: Competitive and Noncompetitive Substrates in Estuarine Sediments. *Applied and Environmental Microbiology* **44**, 1270-1276.
- Orphan, V. J., Hinrichs, K.-U., Ussler, W., III, Paull, C. K., Taylor, L. T., Sylva, S. P., Hayes, J. M., and Delong, E. F. (2001) Comparative Analysis of Methane-Oxidizing Archaea and Sulfate-Reducing Bacteria in Anoxic Marine Sediments. *Appl. Environ. Microbiol.* **67**, 1922-1934.
- Pancost, R. D., Hopmans, E. C., and Sinninghe Damsté, J. S. (2001) Archaeal lipids in Mediterranean cold seeps: molecular proxies for anaerobic methane oxidation. *Geochimica et Cosmochimica Acta* **65**, 1611-1627.

- Pancost, R. D. and Sinninghe Damsté, J. S. (2003) Carbon isotopic compositions of prokaryotic lipids as tracers of carbon cycling in diverse settings. *Chemical Geology* **195**, 29-58.
- Panganiban, A. T., Jr, Patt, T. E., Hart, W., and Hanson, R. S. (1979) Oxidation of methane in the absence of oxygen in lake water samples. *Appl. Environ. Microbiol.* **37**, 303-309.
- Parkes, R. J., Taylor, J., and Jørck-Ramberg, D. (1984) Demonstration, using *Desulfobacter sp.*, of two pools of acetate with different biological availabilities in marine pore water. *Marine Biology* **83**, 271-276.
- Parsons, T. R., Maita, Y., and Lalli, C. (1984) *A manual of chemical and biological methods for seawater analysis*. Pergamon Press, Oxford Oxfordshire.
- Pernthaler, A., Dekas, A. E., Brown, C. T., Goffredi, S. K., Embaye, T., and Orphan, V. J. (2008) Diverse syntrophic partnerships from deep-sea methane vents revealed by direct cell capture and metagenomics. *Proceedings of the National Academy of Sciences* **105**, 7052-7057.
- Pester, M., Bittner, N., Deevong, P., Wagner, M., and Loy, A. (2010) A 'rare biosphere' microorganism contributes to sulfate reduction in a peatland. *ISME J* **4**, 1591-1602.
- Peterse, F., Hopmans, E. C., Schouten, S., Mets, A., Rijpstra, W. I. C., and Sinninghe Damsté, J. S. (2011) Identification and distribution of intact polar branched tetraether lipids in peat and soil. *Organic Geochemistry* **42**, 1007-1015.

- Pozdnyakov, L., Stepanov, A., and Manucharova, N. (2011) Anaerobic methane oxidation in soils and water ecosystems. *Moscow University Soil Science Bulletin* **66**, 24-31.
- Raghoebarsing, A. A., Pol, A., van de Pas-Schoonen, K. T., Smolders, A. J. P., Ettwig, K. F., Rijpstra, W. I. C., Schouten, S., Damste, J. S. S., Op den Camp, H. J. M., Jetten, M. S. M., and Strous, M. (2006) A microbial consortium couples anaerobic methane oxidation to denitrification. *Nature* **440**, 918-921.
- Ramette, A. (2007) Multivariate analyses in microbial ecology. *FEMS microbiology ecology* **62**, 142-160.
- Reeburgh, W. S. (2007) Oceanic Methane Biogeochemistry. *Chemical Reviews* **107**, 486-513.
- Rossel, P. E., Elvert, M., Ramette, A., Boetius, A., and Hinrichs, K.-U. (2011) Factors controlling the distribution of anaerobic methanotrophic communities in marine environments: Evidence from intact polar membrane lipids. *Geochimica et Cosmochimica Acta* **75**, 164-184.
- Rossel, P. E., Lipp, J. S., Fredricks, H. F., Arnds, J., Boetius, A., Elvert, M., and Hinrichs, K.-U. (2008) Intact polar lipids of anaerobic methanotrophic archaea and associated bacteria. *Organic Geochemistry* **39**, 992-999.
- Rothfuss, F. and Conrad, R. (1993) Thermodynamics of methanogenic intermediary metabolism in littoral sediment of Lake Constance. *FEMS microbiology ecology* **12**, 265-276.

- Rütters, H., Sass, H., Cypionka, H., and Rullkotter, J. (2001) Monoalkylether phospholipids in the sulfate-reducing bacteria *Desulfosarcina variabilis* and *Desulforhabdus amnigenus*. *Archiv für Hydrobiologie* **176**, 435-442.
- Schink, B. (1997) Energetics of syntrophic cooperation in methanogenic degradation. *Microbiol. Mol. Biol. Rev.* **61**, 262-280.
- Schönheit, P., Kristjansson, J. K., and Thauer, R. K. (1982) Kinetic mechanism for the ability of sulfate reducers to out-compete methanogens for acetate. *Archives of Microbiology* **132**, 285-288.
- Schouten, S., Hopmans, E. C., Pancost, R. D., and Damsté, J. S. S. (2000) Widespread occurrence of structurally diverse tetraether membrane lipids: Evidence for the ubiquitous presence of low-temperature relatives of hyperthermophiles. *Proceedings of the National Academy of Sciences* **97**, 14421-14426.
- Schubert, C. J., Vazquez, F., Lösekann-Behrens, T., Knittel, K., Tonolla, M., and Boetius, A. (2011) Evidence for anaerobic oxidation of methane in sediments of a freshwater system (Lago di Cadagno). *FEMS microbiology ecology* **76**, 26-38.
- Schubotz, F., Lipp, J. S., Elvert, M., and Hinrichs, K.-U. (2011a) Stable carbon isotopic compositions of intact polar lipids reveal complex carbon flow patterns among hydrocarbon degrading microbial communities at the Chapopote asphalt volcano. *Geochimica et Cosmochimica Acta* **75**, 4399-4415.
- Schubotz, F., Lipp, J. S., Elvert, M., Kasten, S., Mollar, X. P., Zabel, M., Bohrmann, G., and Hinrichs, K.-U. (2011b) Petroleum degradation and associated microbial signatures at the Chapopote asphalt volcano, Southern Gulf of Mexico. *Geochimica et Cosmochimica Acta* **75**, 4377-4398.

- Schubotz, F., Wakeham, S. G., Lipp, J. S., Fredricks, H. F., and Hinrichs, K.-U. (2009) Detection of microbial biomass by intact polar membrane lipid analysis in the water column and surface sediments of the Black Sea. *Environmental Microbiology* **11**, 2720-2734.
- Schütz, H., Holzapfel-Pschorn, A., Conrad, R., Rennenberg, H., and Seiler, W. (1989) A 3-Year Continuous Record on the Influence of Daytime, Season, and Fertilizer Treatment on Methane Emission Rates From an Italian Rice Paddy. *J. Geophys. Res.* **94**, 16405-16416.
- Schulz, S. and Conrad, R. (1996) Influence of temperature on pathways to methane production in the permanently cold profundal sediment of Lake Constance. *FEMS microbiology ecology* **20**, 1-14.
- Schulz, S., Hidetoshi, M., and Conrad, R. (1997) Temperature dependence of methane production from different precursors in a profundal sediment (Lake Constance). *FEMS microbiology ecology* **22**, 207-213.
- Scott, D. T., McKnight, D. M., Blunt-Harris, E. L., Kolesar, S. E., and Lovley, D. R. (1998) Quinone Moieties Act as Electron Acceptors in the Reduction of Humic Substances by Humics-Reducing Microorganisms. *Environmental Science & Technology* **32**, 2984-2989.
- Segers, R. (1998) Methane Production and Methane Consumption: A Review of Processes Underlying Wetland Methane Fluxes. *Biogeochemistry* **41**, 23-51.
- Severinghaus, J. P. and Brook, E. J. (1999) Abrupt Climate Change at the End of the Last Glacial Period Inferred from Trapped Air in Polar Ice. *Science* **286**, 930-934.

- Shively, J. M. and Knoche, H. W. (1969) Isolation of an Ornithine-containing Lipid from *Thiobacillus thiooxidans*. *J. Bacteriol.* **98**, 829-830.
- Sinninghe Damsté, J. S., Rijpstra, W. I. C., Hopmans, E. C., Weijers, J. W. H., Foesel, B. U., Overmann, J., and Dedysh, S. N. (2011) 13,16-Dimethyl Octacosanedioic Acid (iso-Diabolic Acid), a Common Membrane-Spanning Lipid of Acidobacteria Subdivisions 1 and 3. *Applied and Environmental Microbiology* **77**, 4147-4154.
- Sinninghe Damsté, J. S., Schouten, S., Hopmans, E. C., van Duin, A. C. T., and Genevasen, J. A. J. (2002) Crenarchaeol. *Journal of Lipid Research* **43**, 1641-1651.
- Sivan, O., Alder, M., Pearson, A., Gelman, F., Bar-Or, I., John, S., and Eckert, W. (2011) Geochemical evidence for iron-mediated anaerobic oxidation of methane. *Limnology and Oceanography* **56**, 1536-1544.
- Smemo, K. A. and Yavitt, J. B. (2007) Evidence for Anaerobic CH₄ Oxidation in Freshwater Peatlands. *Geomicrobiology Journal* **24**, 583-597.
- Smemo, K. A. and Yavitt, J. B. (2011) Anaerobic oxidation of methane: an underappreciated aspect of methane cycling in peatland ecosystems? *Biogeosciences* **8**, 779-793.
- Smith, L. C., MacDonald, G. M., Velichko, A. A., Beilman, D. W., Borisova, O. K., Frey, K. E., Kremenetski, K. V., and Sheng, Y. (2004) Siberian Peatlands a Net Carbon Sink and Global Methane Source Since the Early Holocene. *Science* **303**, 353-356.
- Sohlenkamp, C., López-Lara, I. M., and Geiger, O. (2003) Biosynthesis of phosphatidylcholine in bacteria. *Progress in lipid research* **42**, 115-162.

- Solorzano, L. (1969) Determination of Ammonia in Natural Waters by the Phenolhypochlorite Method. *Limnology and Oceanography* **14**, 799-801.
- Sørensen, J., Christensen, D., and Jørgensen, B. B. (1981) Volatile Fatty Acids and Hydrogen as Substrates for Sulfate-Reducing Bacteria in Anaerobic Marine Sediment. *Applied and Environmental Microbiology* **42**, 5-11.
- Steger, D., Wentrup, C., Braunegger, C., Deevong, P., Hofer, M., Richter, A., Baranyi, C., Pester, M., Wagner, M., and Loy, A. (2011) Microorganisms with Novel Dissimilatory (Bi)Sulfite Reductase Genes Are Widespread and Part of the Core Microbiota in Low-Sulfate Peatlands. *Applied and Environmental Microbiology* **77**, 1231-1242.
- Stookey, L. L. (1970) Ferrozine---a new spectrophotometric reagent for iron. *Analytical Chemistry* **42**, 779-781.
- Strickland, J. D. H. and Parsons, T. R. (1972) A manual of seawater analysis *Bulletin of the Fisheries Research Board Canada*, Ottawa.
- Sturt, H. F., Summons, R. E., Smith, K., Elvert, M., and Hinrichs, K.-U. (2004) Intact polar membrane lipids in prokaryotes and sediments deciphered by high-performance liquid chromatography/electrospray ionization multistage mass spectrometry—new biomarkers for biogeochemistry and microbial ecology. *Rapid Communications in Mass Spectrometry* **18**, 617-628.
- Summons, R. E., Franzmann, P. D., and Nichols, P. D. (1998) Carbon isotopic fractionation associated with methylotrophic methanogenesis. *Organic Geochemistry* **28**, 465-475.

- Sunamura, M., Koga, Y., and Ohwada, K. (1999) Biomass Measurement of Methanogens in the Sediments of Tokyo Bay Using Archaeol Lipids. *Marine Biotechnology* **1**, 562-568.
- Sundh, I., Borgå, P., Nilsson, M., and Svensson, B. H. (1995) Estimation of cell numbers of methanotrophic bacteria in boreal peatlands based on analysis of specific phospholipid fatty acids. *FEMS microbiology ecology* **18**, 103-112.
- Svensson, B. H. (1984) Different Temperature Optima for Methane Formation When Enrichments from Acid Peat Are Supplemented with Acetate or Hydrogen. *Applied and Environmental Microbiology* **48**, 389-394.
- Takeuchi, M., Yoshioka, H., Seo, Y., Tanabe, S., Tamaki, H., Kamagata, Y., Takahashi, H. A., Igari, S., Mayumi, D., and Sakata, S. (2011) A distinct freshwater-adapted subgroup of ANME-1 dominates active archaeal communities in terrestrial subsurfaces in Japan. *Environmental Microbiology* **13**, 3206-3218.
- Taylor, J. and Parkes, R. J. (1983) The Cellular Fatty Acids of the Sulphate-reducing Bacteria, *Desulfobacter* sp., *Desulfobulbus* sp. and *Desulfovibrio desulfuricans*. *Journal of General Microbiology* **129**, 3303-3309.
- Teske, A. and Sorensen, K. B. (2007) Uncultured archaea in deep marine subsurface sediments: have we caught them all? *ISME J* **2**, 3-18.
- Thamdrup, B., Fossing, H., and Jørgensen, B. B. (1994) Manganese, iron and sulfur cycling in a coastal marine sediment, Aarhus bay, Denmark. *Geochimica et Cosmochimica Acta* **58**, 5115-5129.
- Topp, E. and Pattey, E. (1997) Soils as sources and sinks for atmospheric methane. *Canadian Journal of Soil Science* **77**, 167-177.

- Urban, N. R., Eisenreich, S. J., and Bayley, S. E. (1988) The Relative Importance of Denitrification and Nitrate Assimilation in Midcontinental Bogs. *Limnology and Oceanography* **33**, 1611-1617.
- Valentine, D. (2002) Biogeochemistry and microbial ecology of methane oxidation in anoxic environments: a review. *Antonie van Leeuwenhoek* **81**, 271-282.
- Vile, M. A., Bridgham, S. D., and Wieder, R. K. (2003) RESPONSE OF ANAEROBIC CARBON MINERALIZATION RATES TO SULFATE AMENDMENTS IN A BOREAL PEATLAND. *Ecological Applications* **13**, 720-734.
- Wada, H. and Murata, N. (1998) Membrane lipids in cyanobacteria In: Siegenthaler, P.-A. and Murata, N. (Eds.), *Lipids in Photosynthesis: Structure, Function, and Genetics*. Kluwer Academic.
- Watson, A. and Nedwell, D. B. (1998) Methane production and emission from peat: the influence of anions (sulphate, nitrate) from acid rain. *Atmospheric Environment* **32**, 3239-3245.
- Weijers, J. W. H., Schouten, S., Hopmans, E. C., Genevasen, J. A. J., David, O. R. P., Coleman, J. M., Pancost, R. D., and Sinninghe Damsté, J. S. (2006a) Membrane lipids of mesophilic anaerobic bacteria thriving in peats have typical archaeal traits. *Environmental Microbiology* **8**, 648-657.
- Weijers, J. W. H., Schouten, S., Spaargaren, O. C., and Sinninghe Damsté, J. S. (2006b) Occurrence and distribution of tetraether membrane lipids in soils: Implications for the use of the TEX86 proxy and the BIT index. *Organic Geochemistry* **37**, 1680-1693.

- Weijers, J. W. H., Schouten, S., van den Donker, J. C., Hopmans, E. C., and Sinninghe Damsté, J. S. (2007) Environmental controls on bacterial tetraether membrane lipid distribution in soils. *Geochimica et Cosmochimica Acta* **71**, 703-713.
- Weijers, J. W. H., Schouten, S., van der Linden, M., van Geel, B., and Sinninghe Damsté, J. S. (2004) Water table related variations in the abundance of intact archaeal membrane lipids in a Swedish peat bog. *FEMS Microbiology Letters* **239**, 51-56.
- Wellsbury, P. and Parkes, R. J. (1995) Acetate bioavailability and turnover in an estuarine sediment. *FEMS microbiology ecology* **17**, 85-94.
- White, D. C., Davis, M., Nickels, J. S., King, J. D., and Bobbie, R. J. (1979) Determination of the sedimentary microbial biomass by extractible lipid phosphate. . *Oecologia* **40**, 51-62.
- Whiticar, M. J. (1999) Carbon and hydrogen isotope systematics of bacterial formation and oxidation of methane. *Chemical Geology* **161**, 291-314.
- Whiticar, M. J., Faber, E., and Schoell, M. (1986) Biogenic methane formation in marine and freshwater environments: CO₂ reduction vs. acetate fermentation—Isotope evidence. *Geochimica et Cosmochimica Acta* **50**, 693-709.
- Whitman, W. B., Bowen, T. L., and Boone, D. R. (1992) The methanogenic bacteria. In: Balows, A., Truper, H. G., Dworkin, M., Harder, W., and Schleifer, K.-H. (Eds.), *The Prokaryotes*. Springer-Verlag, Berlin.
- Wieder, R. and Lang, G. (1988) Cycling of inorganic and organic sulfur in peat from Big Run Bog, West Virginia. *Biogeochemistry* **5**, 221-242.
- Wieder, R. K., Yavitt, J. B., and Lang, G. E. (1990) Methane production and sulfate reduction in two Appalachian peatlands. *Biogeochemistry* **10**, 81-104.

- Worthy, D. E. J., Levin, I., Hopper, F., Ernst, M. K., and Trivett, N. B. A. (2000) Evidence for a link between climate and northern wetland methane emissions. *J. Geophys. Res.* **105**, 4031-4038.
- Wüst, P. K., Horn, M. A., and Drake, H. L. (2009) Trophic links between fermenters and methanogens in a moderately acidic fen soil. *Environmental Microbiology* **11**, 1395-1409.
- Yao, H. and Conrad, R. (1999) Thermodynamics of methane production in different rice paddy soils from China, the Philippines and Italy. *Soil Biology and Biochemistry* **31**, 463-473.
- Yavitt, J. B., Downey, D. M., Lancaster, E., and Lang, G. E. (1990) Methane consumption in decomposing Sphagnum-derived peat. *Soil Biology and Biochemistry* **22**, 441-447.
- Yavitt, J. B. and Lang, G. E. (1990) Methane production in contrasting wetland sites: Response to organic-chemical components of peat and to sulfate reduction. *Geomicrobiology Journal* **8**, 27-46.
- Yavitt, J. B., Lang, G. E., and Downey, D. M. (1988) Potential methane production and methane oxidation rates in peatland ecosystems of the Appalachian Mountains, United States. *Global Biogeochem. Cycles* **2**, 253-268.
- Yoshinaga, M. Y., Kellermann, M. Y., Rossel, P. E., Schubotz, F., Lipp, J. S., and Hinrichs, K.-U. (2011) Systematic fragmentation patterns of archaeal intact polar lipids by high-performance liquid chromatography/electrospray ionization ion-trap mass spectrometry. *Rapid Communications in Mass Spectrometry* **25**, 3563-3574.

Zehnder, A. J. B. and Brock, T. D. (1980) Anaerobic Methane Oxidation: Occurrence and Ecology. *Appl. Environ. Microbiol.* **39**, 194-204.

Zeikus, J. G. (1977) The biology of methanogenic bacteria. *Bacteriol. Rev.* **41**, 514-541.

Table 4.1. Seasonal comparison of geochemical species in the top 20 cm of Florida and Maine peat. All species are reported as areal concentrations except for N:P ratios which were calculated from these areal concentrations, and % organic carbon, C:N, pH, temperature, and salinity, which are reported as an average of measurements within the top 20 cm. All values are the average of triplicate cores \pm the standard error.

	Florida		Maine	
	<i>Winter</i>	<i>Summer</i>	<i>Winter</i>	<i>Summer</i>
methane (mmol m ⁻²)	44.1 \pm 26.1	105.0 \pm 20.5	88.8 \pm 12.3	28.2 \pm 6.6
hydrogen* (μ mol m ⁻²)	1.6 \pm 1.0	3.3 \pm 0.8	0.9 \pm 0.3	1.5 \pm 0.4
DIC (mol m ⁻²)	1.1 \pm 0.1	0.9 \pm 0.1	0.7 \pm 0.0	0.6 \pm 0.2
acetate (mmol m ⁻²)	3.7 \pm 0.8	3.0 \pm 1.2	3.0 \pm 0.6	3.2 \pm 0.7
sulfate (mmol m ⁻²)	16.1 \pm 2.9	76.1 \pm 17.9	30.8 \pm 3.6	76.7 \pm 8.6
sulfide (μ mol m ⁻²)	87.1 \pm 13.7	90.0 \pm 1.4	285 \pm 115	322 \pm 84.2
DOC (mol m ⁻²)	0.3 \pm 0.1	0.5 \pm 0.0	0.9 \pm 0.1	0.6 \pm 0.2
Fe _T (mmol m ⁻²)	0.04 \pm 0.01	0.18 \pm 0.03	0.61 \pm 0.23	0.41 \pm 0.04
Mn ²⁺ (mmol m ⁻²)	0.32 \pm 0.04	0.38 \pm 0.04	1.44 \pm 0.07	0.98 \pm 0.12
nitrate (mmol m ⁻²)	10.1 \pm 0.4	8.8 \pm 0.7	9.2 \pm 0.6	7.7 \pm 0.6
nitrite (mmol m ⁻²)	0.1 \pm 0.1	0.2 \pm 0.0	0.2 \pm 0.0	0.1 \pm 0.0
ammonium (mmol m ⁻²)	35.1 \pm 23.5	16.7 \pm 12.1	51.7 \pm 6.8	61.4 \pm 9.0
phosphate (mmol m ⁻²)	0.1 \pm 0.0	0.1 \pm 0.0	1.4 \pm 0.3	0.4 \pm 0.2
N:P	270.7 \pm 0.3	230.4 \pm 0.3	46.0 \pm 0.2	96.2 \pm 0.1
OC (%)	52.6 \pm 2.2	52.3 \pm 1.4	17.0 \pm 4.7	16.8 \pm 5.1
C:N	18.1 \pm 0.6	17.3 \pm 1.3	13.8 \pm 2.0	15.4 \pm 2.7
pH	7.5 \pm 0.2	7.6 \pm 0.3	6.8 \pm 0.4	7.2 \pm 0.2
temperature (°C)	14.7 \pm 2.3	30.3 \pm 0.6	2.2 \pm 0.7	17.7 \pm 0.2
salinity	1.1 \pm 0.4	0 \pm 0	0.7 \pm 0.9	0.9 \pm 0.6

Abbreviations: DIC, dissolved inorganic carbon; DOC, dissolved organic carbon, Fe_T, total dissolved iron, Mn²⁺, dissolved, reduced manganese; N:P, ratio of dissolved inorganic nitrogen to dissolved phosphate; OC, percent of organic carbon (by weight) in dry peat; C:N, ratio of carbon to nitrogen (by weight) in dry peat.

* Hydrogen was determined as steady state concentrations (see methods for details).

Table 4.2. Seasonal comparison of relevant microbial activities determined with radiotracers in the top 20 cm of Florida and Maine peat. All activities are reported as areal rates in $\mu\text{mol m}^{-2} \text{d}^{-1}$ and values are an average of triplicate cores \pm the standard error. Ratios and percentages were calculated with these areal rates and are reported as an average percent of ratio of triplicate cores \pm the standard error.

	Florida		Maine	
	Winter	Summer	Winter	Summer
bic-MOG	7.2 \pm 0.8	30 \pm 2.4	117 \pm 4	192 \pm 30
ace-MOG	18.1 \pm 6.8	473 \pm 43.5	43 \pm 5	745 \pm 77
totalMOG	25 \pm 9.4	503 \pm 45.9	161 \pm 3	937 \pm 94
% bic	25.6 \pm 5.7	5.9 \pm 0.1	73 \pm 3	20.4 \pm 2.6
AOM	4120 \pm 700	11.7 \pm 6.8	889 \pm 201	651 \pm 61.9
SR	4.8x10 ⁵ \pm 6.3x10 ³	1.9 x 10 ⁴ \pm 2.7x10 ⁴	9.6x10 ³ \pm 1x10 ³	6.3x10 ⁴ \pm 1.34x10 ⁴
AOM:totalMOG	142 \pm 26	3.1x10 ⁻² \pm 1.2x10 ⁻²	5.6 \pm 1.4	0.8 \pm 0.1
SR:AOM	3400 \pm 250	100 \pm 16	20 \pm 3	170 \pm 32
AOG	144 \pm 10	159 \pm 63	502 \pm 54	370 \pm 30
AOG:MOG	4 \pm 0.1	0.2 \pm 0.1	3 \pm 0.3	0.4 \pm 0.1
Ace Ox	2060 \pm 170	950 \pm 64	143 \pm 9	222 \pm 42

Abbreviations: bic-MOG, hydrogenotrophic methanogenesis; ace-MOG, acetoclastic methanogenesis; total MOG, total methanogenesis calculated as the sum of bic-MOG and ace-MOG; % bic, contribution of hydrogenotrophic methanogenesis to total methane production; AOM, anaerobic oxidation of methane; SR, sulfate reduction; Ace Ox, acetate oxidation, AOG, homoacetogenesis.

Table 4.3. Stable carbon isotopic signatures, in $\delta^{13}\text{C}$ (‰), of archaeal and bacterial lipids and relevant geochemical species in the peats of Florida and Maine with season and depth. Isotope values are an average based on n=1-2 measurements for lipids and n=3 for geochemical species which were derived from triplicate cores. Abbreviations: DIC, dissolved inorganic carbon; POC, particulate organic carbon, nd, not determined due to low signal/resolution on GC-IRMS.

depth interval (cm)	FLORIDA						MAINE					
	Winter			Summer			Winter			Summer		
	0-3	6-9	15-20	0-3	6-9	15-20	0-3	6-9	15-20	0-3	6-9	15-20
<i>Archaeal Lipids</i>												
phytane	-35.7	-35.7	-30.0	-31.7	-32.6	-35.7	-28.3	-30.0	-29.2	-29.1	-29.2	-29.9
biphytane 0	-34.6	-34.0	-32.9	-35.9	-35.5	-32.1	-34.3	-36.7	-30.8	-35.2	-36.1	-34.9
biphytane 1	-37.8	-36.8	-38.6	-36.8	-37.7	-36.3	-47.5	-47.3	-45.2	-52.0	-47.3	-46.6
biphytane 2	-42.1	-40.5	-42.3	-43.3	-41.7	-40.4	-60.6	-57.9	-48.1	-61.9	-57.9	-57.8
biphytane 3	-33.7	-35.1	-35.1	-31.9	-34.0	-36.8	nd	-32.5	-32.4	-31.6	-32.5	-33.0
<i>Bacterial Lipids</i>												
<i>ai</i> C ₁₄	-34.4	-31.6	-32.8	-32.6	-30.9	nd	-33.8	-30.9	-31.6	-32.6	-32.6	-31.3
C ₁₄	-35.2	-33.8	-36.2	-35.3	-36.0	-36.2	-34.8	-34.4	-34.4	-33.5	-35.0	-34.6
<i>i</i> C ₁₅	-31.4	-31.0	-31.7	-30.8	-30.4	-29.7	-32.3	-29.3	-31.5	-29.6	-30.0	-29.3
<i>ai</i> C ₁₅	-36.1	-34.3	-34.6	-34.6	-34.3	-33.5	-32.9	-32.8	-33.2	-33.7	-34.0	-34.2
C ₁₅	-29.7	-30.2	-32.3	-32.1	-31.7	-30.0	-32.7	-29.6	-30.6	-29.2	-30.2	-29.2
<i>i</i> C ₁₆	-33.1	-32.1	-32.1	-32.9	-31.4	nd	-31.2	-31.0	-30.7	-31.3	-32.2	-31.3
C _{16,1007}	-41.7	-37.3	-34.3	-37.6	-35.8	nd	-41.7	-34.6	-33.6	-33.0	-37.0	-37.1
C _{16,1005}	-46.2	-43.9	-33.4	nd	nd	nd	-49.5	-39.2	-44.7	-36.1	-33.8	-47.0
C ₁₆	-33.4	-32.3	-33.7	-34.1	-34.8	-34.6	-35.9	-34.0	-33.5	-32.1	-33.5	-33.1
10meC ₁₆	na	-34.2	-35.5	-31.3	na	nd	-37.3	-30.3	-36.6	-30.4	-32.1	-32.2
<i>i</i> C ₁₇	-34.6	-29.8	-31.3	-30.0	-28.7	nd	-35.2	-31.2	-30.9	-30.5	-32.2	-30.1
aC ₁₇	-33.6	-34.1	-34.9	-31.6	-32.3	nd	-27.9	-29.5	-30.5	-28.4	-32.7	-33.2
C _{17:1}	-34.3	nd	nd	nd	nd	nd	-39.5	nd	nd	nd	nd	nd
C ₁₇	-33.6	-33.6	-34.2	-33.6	-33.7	nd	-34.5	-33.0	-31.0	nd	-31.5	-30.1
C _{18:2}	-23.9	-25.6	-25.8	-27.6	-25.6	nd	-28.7	-19.8	-29.5	nd	nd	-23.8
C _{18:1005}	-29.2	-30.9	-32.2	-32.3	-32.3	-31.5	-32.7	-29.3	-31.9	-28.3	nd	-30.1
C _{18:1007}	-38.3	-35.2	-38.0	-36.3	-36.8	nd	-40.3	-36.2	-34.4	-37.4	-31.9	-35.1
C ₁₈	-30.9	-31.7	-33.1	-32.9	-33.4	-34.8	-34.6	-32.1	-32.6	-31.6	-32.3	-30.7
C ₁₆ & C ₁₇ MAGEs ¹	-31.4	-30.2	-33.0	-32.6	-31.5	-31.5	-30.3	-31.8	-31.4	-32.4	-34.8	-34.8
C ₃₀ DAGEs ²	nd	-30.0	-31.6	-28.2	-31.3	-29.2	-31.0	-30.1	-31.7	-30.0	-30.0	-30.0
<i>Geochemical Species</i>												
methane	-80.5	-76.6	-87.6	-75.5	-73.2	-87.5	-70.4	-71.9	-76.1	-73.1	-73.1	-77.4
CO ₂ (g) ³	2.5	3.3	2.5	2.3	2.2	2.6	-9.2	-6.3	-2.4	-3.5	-2.7	0.3
acetate	nd	-37.1	-37.9	-37.7	-33.0	-29.3	nd	-32.2	-32.1	-29.9	-24.9	-29.2
lactate	nd	-30.9	-30.3	nd	nd	nd	-26.8	-28.8	-32.1	-17.4	-19.7	-25.4
POC	-25.9	-25.6	-26.1	-26.3	-26.0	-25.8	-26.9	-26.8	-27.2	-26.8	-26.8	-27.3

1. Weighted average of $\delta^{13}\text{C}$ values for saturated and unsaturated C₁₆ and C₁₇ monoalkylglycerol ethers (MAGEs)
2. Weighted average of $\delta^{13}\text{C}$ saturated and unsaturated C₃₀ dialkylglycerol ethers (DAGEs)
3. Isotopic composition of dissolved CO₂ calculated from $\delta^{13}\text{C}$ -DIC with *in situ* temperature according to Mook et al. (1979).

Table 4.4. Summary of IPL classes identified at each site and the assigned source organisms for each IPL. For abbreviations, interpretations, and references refer to the text.

<i>Site</i>	<i>IPL Class</i>	<i>Depths found</i>	<i>Probable biological source</i>	
Maine and Florida	2 Gly-AR	all depths	Archaea , methanogens	
	2 Gly-GDGT	all depths	Archaea, ANME-1 and methanogens	
	3Gly-GDGT	FL: all depths, ME: lower depths	Archaea, heterotrophs	
	2Gly-OH-GDGT	all depths	Archaea, methanotrophs	
	Betaine Lipid: DGTS/DGTA	FL: surface only ME: decrease with depth	Photosynthetic algae and unknown anaerobic bacteria	
	PE-Cer	FL: surface only ME: decrease with depth	Anaerobic bacteria	
	PE-DEG	all depths	SRB, Myxobacteria	
	PE, PME-AEG	FL: summer only; all depths ME: all depths	SRB	
	PE,PME-DAG	FL: summer; surface	SRB, Acidobacteria, anaerobic bacteria	
	PC-DAG	ME: decrease with depth	Photosynthetic algae and anaerobic bacteria	
	OL	decrease with depth	Plant-associated bacteria	
	PE+PC Mix	decrease with depth	Anaerobic bacteria	
	Maine Only	PME-OH-AR	all	Archaea; methanogens; freshwater archaea
		3Gly-OH-GDGT	lower depths	Archaea; methanotrophs
		2,3Gly-2OH-GDGT	lower depths	Archaea; methanotrophs
PI-GDGT-Gly		lower depths	Archaea; methanotrophs	
2 Gly-DAG		decreases with depth	Photosynthetic algae and anaerobic bacteria	
GlyA-DAG		surface	Anaerobic bacteria	
SQ-DAG		surface only	Cyanobacteria	
Betaine Lipids: DGCC		surface only	Photosynthetic algae and anaerobic bacteria	
DPG, lysoDPG		decrease with depth	SRB, anaerobic bacteria	
Florida Only		PG-DAG	winter, surface only	SRB, anaerobic bacteria
	GluA-br-GDGT	all depths	Acidobacteria	

Appendix I. Relative abundances of polar-derived core GDGTs in the peats of Florida and Maine.

depth interval (cm)	FLORIDA				MAINE						
	Winter	Summer	Winter	Summer	Winter	Summer	Winter	Summer			
	0-3	6-9	15-20	0-3	6-9	15-20	0-3	6-9	15-20		
GDGT-0	50	50	46	45	46	50	65	50	52	53	55
GDGT-1	9	10	11	12	10	9	8	13	11	11	11
GDGT-2	16	17	20	20	21	15	7	11	8	8	7
GDGT-3	25	23	22	23	23	25	20	25	27	26	27
Crenarchaeol	<1	<1	<1	<1	<1	<1	<1	<1	2	1	2
									1	2	1

Appendix II. Relative abundances of selected polar-derived fatty acid biomarkers in the peats of Florida and Maine. *bd*: below detection

depth interval (cm)	FLORIDA						MAINE					
	<i>Winter</i>			<i>Summer</i>			<i>Winter</i>			<i>Summer</i>		
	0-3	6-9	15-20	0-3	6-9	15-20	0-3	6-9	15-20	0-3	6-9	15-20
<i>Fatty Acids</i>												
<i>aiC</i> ₁₄	1	2	1	2	1	2	2	1	4	2	1	3
<i>C</i> ₁₄	8	11	13	11	16	20	9	8	15	5	10	8
<i>iC</i> ₁₅	4	6	3	3	2	4	3	4	4	6	3	4
<i>aiC</i> ₁₅	6	4	3	4	3	3	6	5	3	7	5	4
<i>C</i> _{15:0}	3	5	5	4	4	4	3	3	5	3	3	2
<i>iC</i> ₁₆	5	3	3	3	2	3	3	4	3	4	3	4
<i>C</i> _{16:1ω7}	3	1	1	5	1	2	4	2	2	7	2	3
<i>C</i> _{16:1ω5}	1	<1	<1	<i>bd</i>	<i>bd</i>	<i>bd</i>	1	1	<1	1	4	1
<i>C</i> _{16:0}	34	31	34	33	31	35	38	37	39	31	43	40
10 <i>meC</i> ₁₆	<i>bd</i>	1	1	1	1	<i>bd</i>	2	3	1	3	3	3
<i>iC</i> ₁₇	2	3	2	1	1	2	1	2	1	2	1	1
<i>aC</i> ₁₇	2	2	2	1	1	1	2	2	1	1	2	3
<i>C</i> _{17:1}	2	<i>bd</i>	<i>bd</i>	<i>bd</i>	<i>bd</i>	<i>bd</i>	1	1	<i>bd</i>	2	<i>bd</i>	<i>bd</i>
<i>C</i> _{17:0}	3	3	3	2	2	3	2	1	2	2	2	3
<i>C</i> _{18:2}	1	3	3	2	3	2	4	3	3	3	1	3
<i>C</i> _{18:1ω9}	5	10	13	16	16	3	7	9	4	7	3	5
<i>C</i> _{18:1ω7}	6	3	2	3	2	1	6	4	2	8	4	4
<i>C</i> _{18:0}	15	11	12	10	11	15	6	8	11	6	10	9

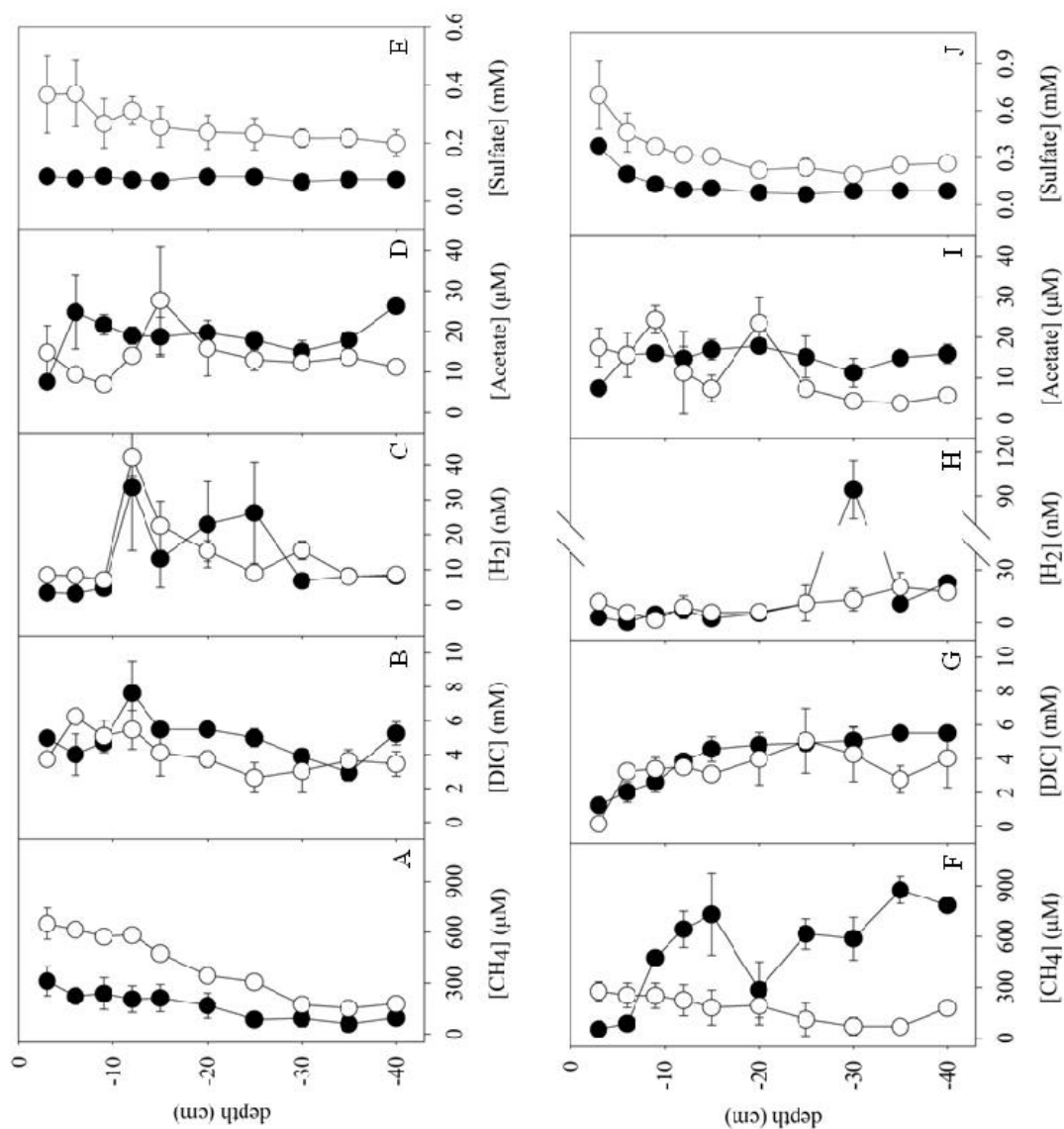


Figure 4.1. Depth profiles of porewater concentrations of relevant geochemical species in Florida (A-E) and Maine (F-J) in the winter (closed circles) and summer (open circles). The values for methane (A-F), DIC (B,G), hydrogen (C,H), acetate (D,I), and sulfate (E,J) are an average of replicate peat cores ($n=3$) and error bars represent the standard error of the mean. Note the difference scales between Florida and Maine for hydrogen and sulfate concentrations. Abbreviations used: CH₄, methane; DIC, dissolved inorganic carbon; H₂, hydrogen.

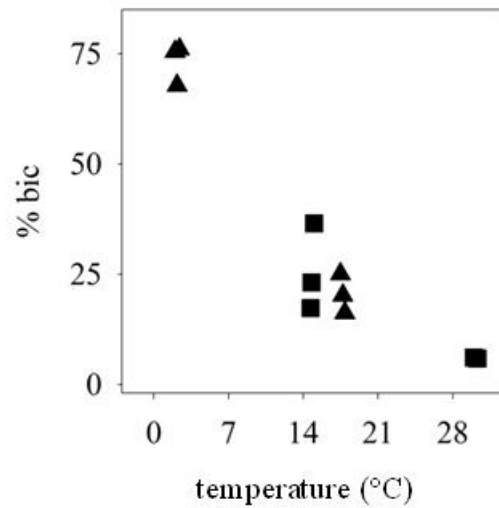


Figure 4.3. The contribution of hydrogenotrophic methanogenesis (% bic) to total methane production as measured with radiolabeled acetate and bicarbonate with temperature in Florida (squares) and Maine (triangles). Temperature and % bic were significantly correlated ($\rho=0.86$; $p<0.05$). Values of % bic were calculated with depth-integrated rates of methane production determined with radiotracers from triplicate cores at each site.

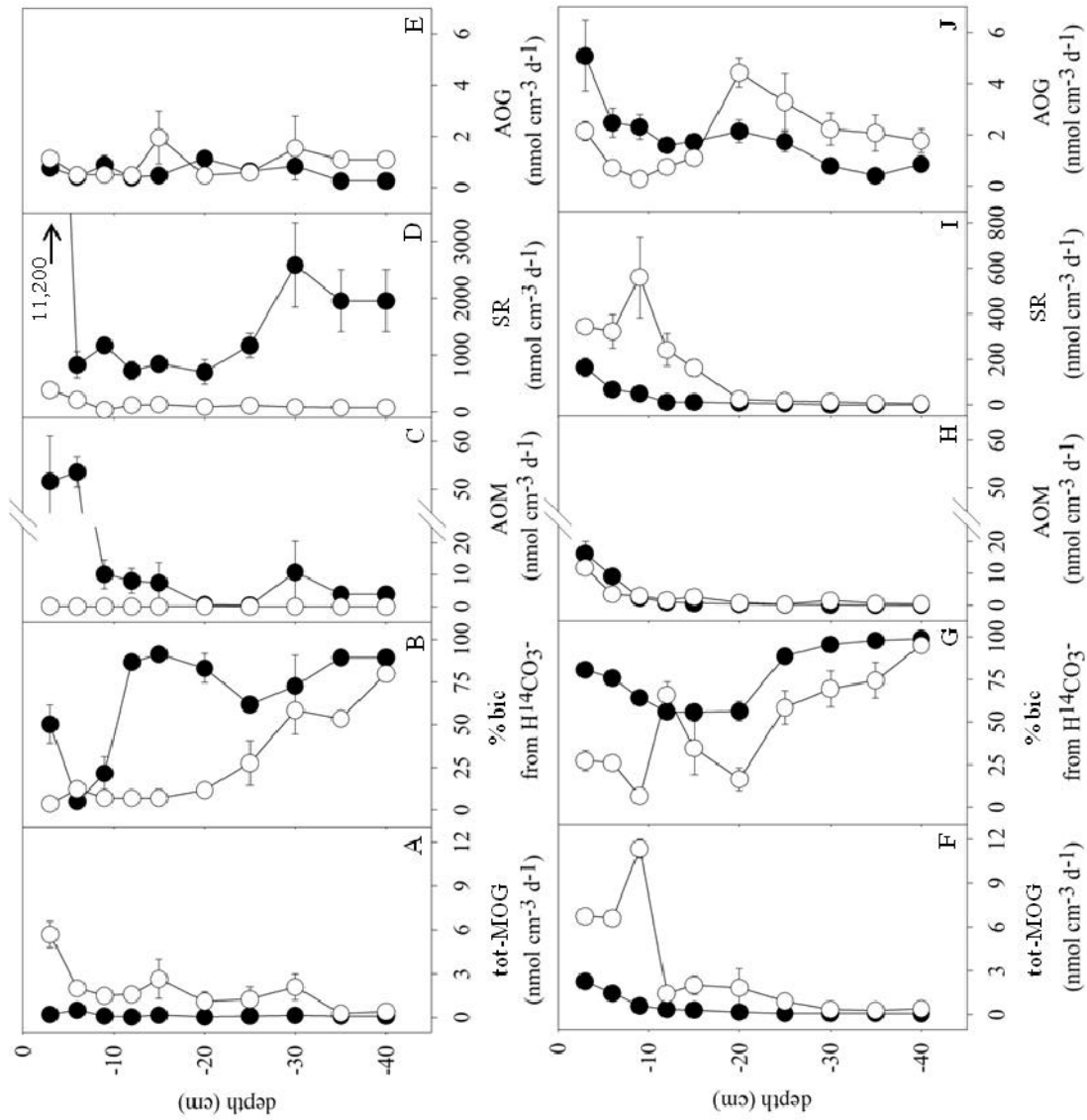


Figure 4.2. Depth profiles of microbial activities determined with radiotracers in the peats of Florida (A-E) and Maine (F-J) in the winter (open circles) and summer (closed circles). The values for total methane production* (tot-MOG; A, F), contribution of hydrogenotrophic methanogenesis to total methane production (% bic; B, G), anaerobic methane oxidation (AOM; C, H), sulfate reduction (SR; D, I), and homoacetogenesis (AOG; E, J) are a mean of replicate peat cores (n=3) and error bars represent the standard error of the mean. Note the difference scales between Florida and Maine for sulfate reduction.

* Total methane production was calculated as the sum of hydrogenotrophic and acetoclastic methanogenesis.

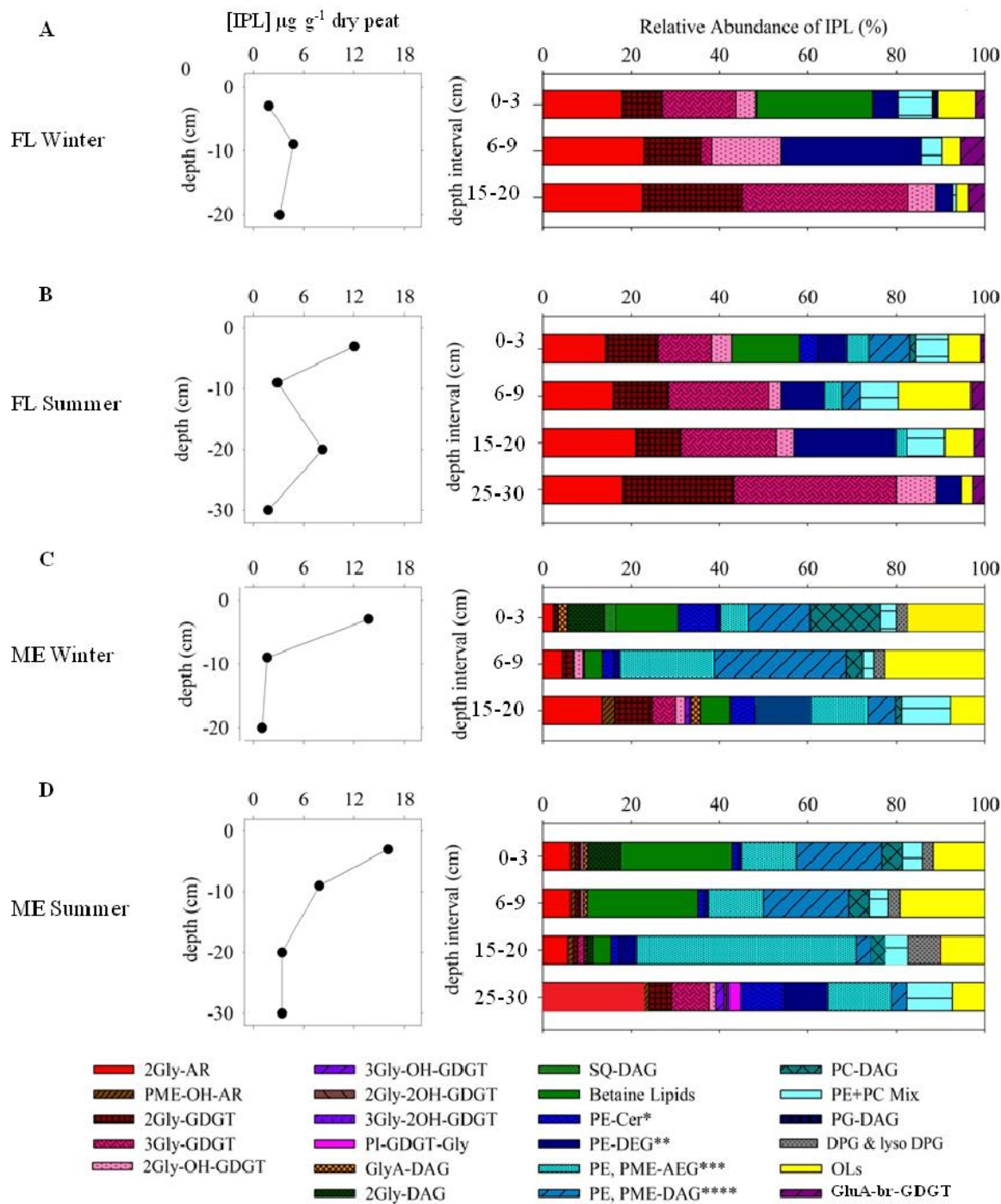


Figure 4.4. Concentration and relative abundance of IPLs in the peats of Florida in the winter (A) and summer (B) and of Maine in the winter (C) and summer (D). For abbreviations of IPLs see text. * In Maine contains some PME and OL ** may contain some PME-DEG in Maine *** may contain some PA-AEG in Maine **** may contain some PDME-DAG in Maine

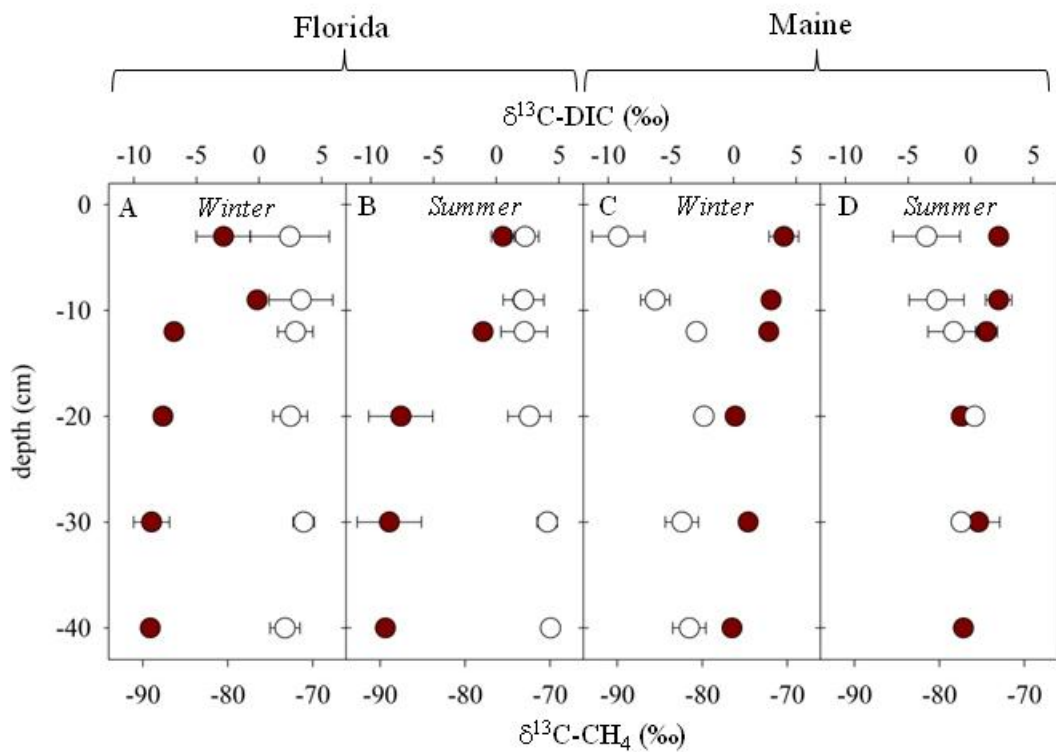


Figure 4.5 A-D. Depth profiles of stable carbon isotopic signatures ($\delta^{13}\text{C}$ in ‰) for methane (CH_4 ; red circles) and dissolved inorganic carbon (DIC; open circles) in the winter and summer of Florida (A-B) and Maine (C-D).

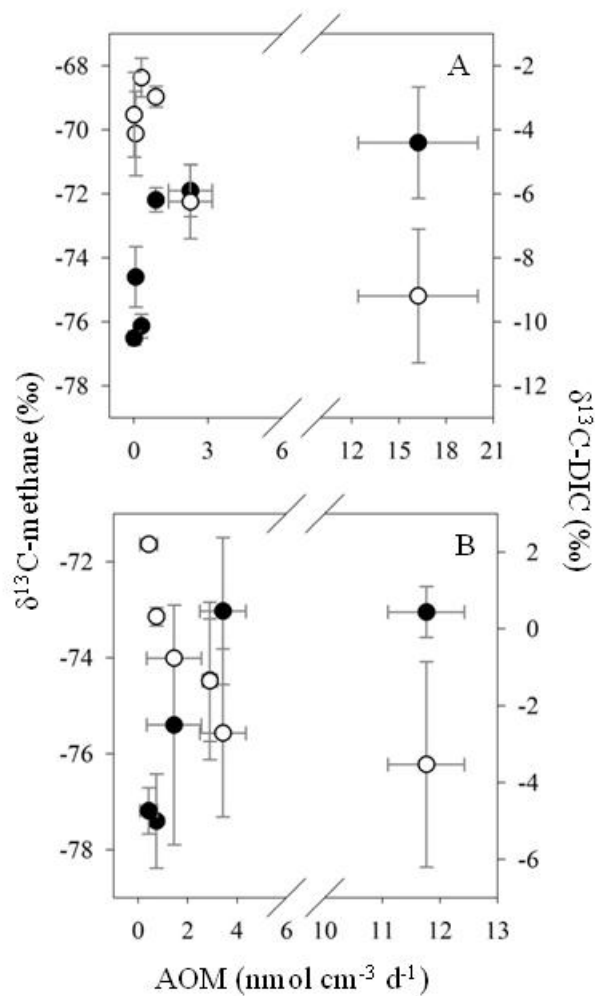


Figure 4.6. Stable carbon isotopic signatures ($\delta^{13}\text{C}$) of methane (black circles) and DIC (open circles) with rates of AOM in the winter (A) and summer (B) in Maine. Values represent the mean of replicate cores ($n=3$) and the error bars represent the standard error of the mean.

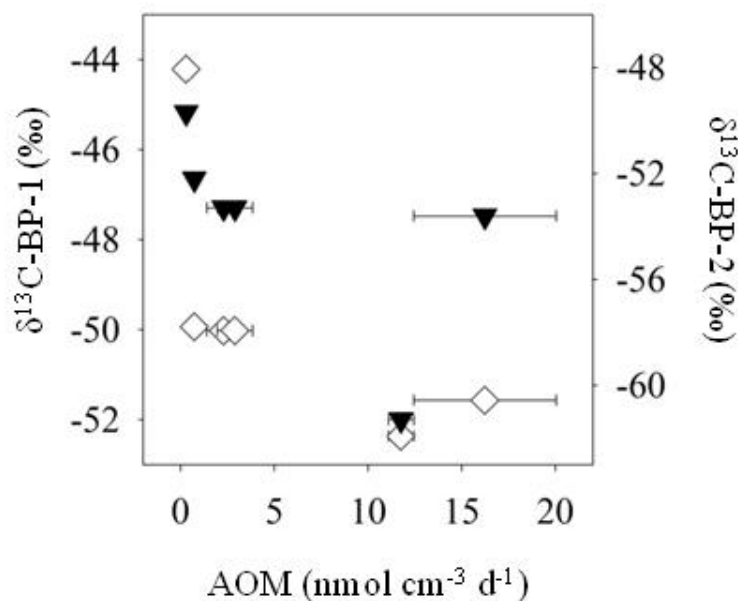


Figure 4.7. Stable carbon isotopic signatures ($\delta^{13}\text{C}$) of biphytane 1 (BP-1; black triangles) and biphytane-2 (BP-2; open diamonds) with rates of AOM in Maine. AOM rates are a mean of replicate cores ($n=3$) and the error bars represent the standard error of the mean. Values of $\delta^{13}\text{C}$ for biphytanes are a single measurement from pooled replicate cores. Data are from both winter and summer samplings.

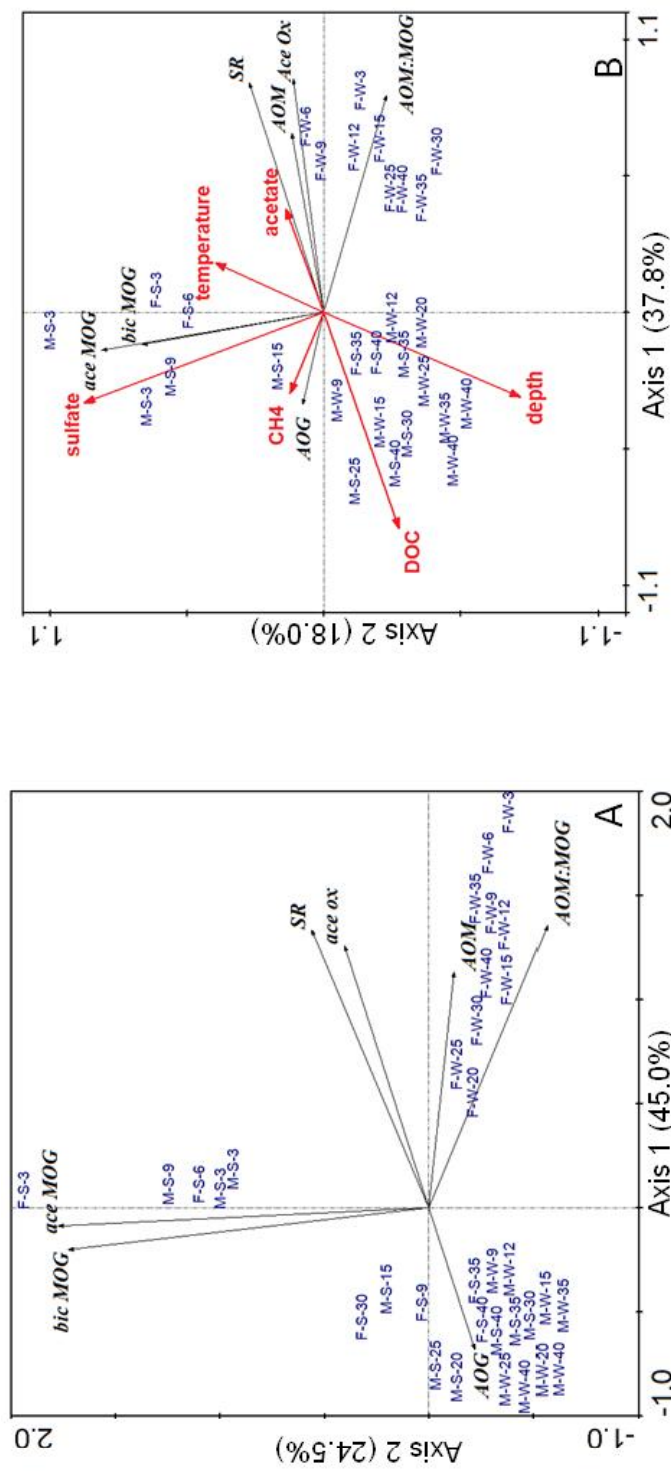


Figure 4.8 A and B. PCA plot displaying the distribution of microbial activities (A) and an RDA biplot (B) depicting the relation of those activities to environmental variables (red arrows) which explain the most variability as determined via forward selection with monte carlo testing in the peat of Florida ('F') and Maine ('M') in the winter ('W') and summer ('S'). Individual samples are labeled in blue according to site-season-depth in cm and those with 30% or better fit are shown. The direction and length of the arrows for each species (black arrows) and environmental variables (red arrows) represents the direction and rate of increase in the ordination space. ace.MOG, methane produced from $^{14}\text{CH}_3\text{COO}^-$; bic.MOG, methane produced from $\text{H}^{14}\text{CO}_3^-$; AOG, acetate produced from $\text{H}^{14}\text{CO}_3^-$; % bic. percent of methane produced from $\text{H}^{14}\text{CO}_3^-$; AOM, anaerobic methane oxidation, ace ox, acetate oxidation, SR, sulfate reduction.

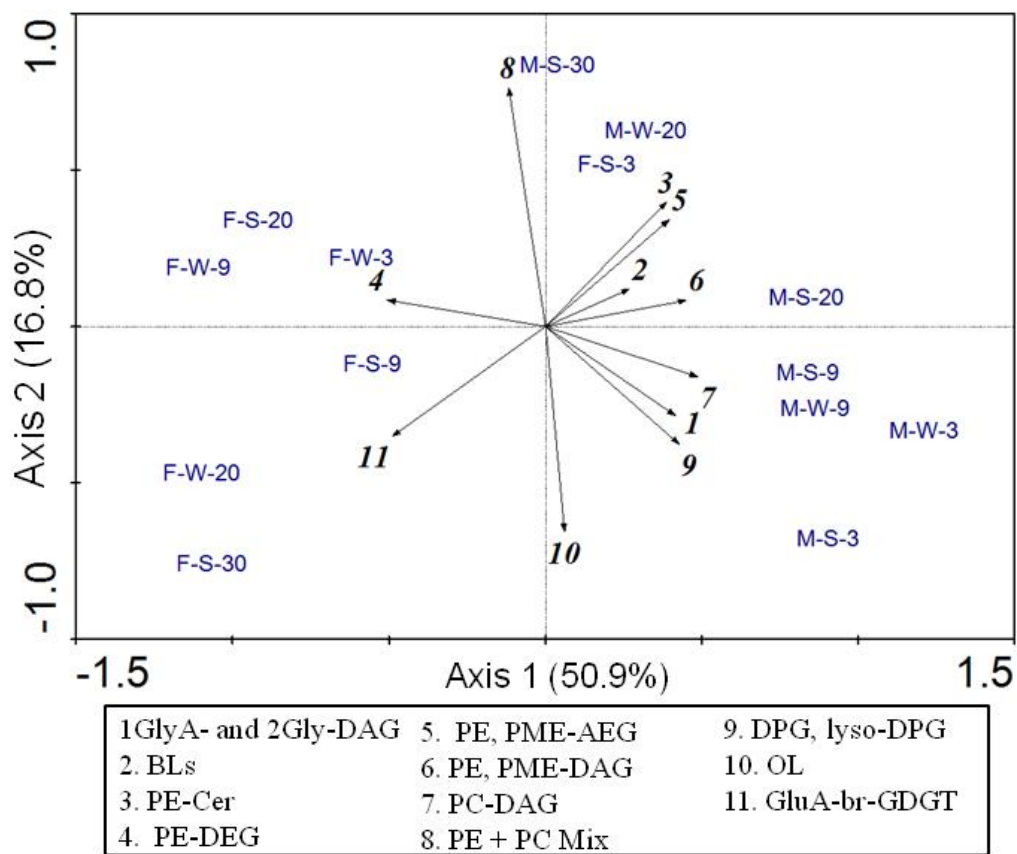


Figure 4.9. PCA plot showing the distribution of bacterial IPLs in the peats of Florida (F) and Maine (M) in the winter (W) and summer (S). Individual samples are labeled in blue according to the scheme site-season-depth in cm. The direction and length of the arrows for each species represents the direction and rate of increase in the ordination space.

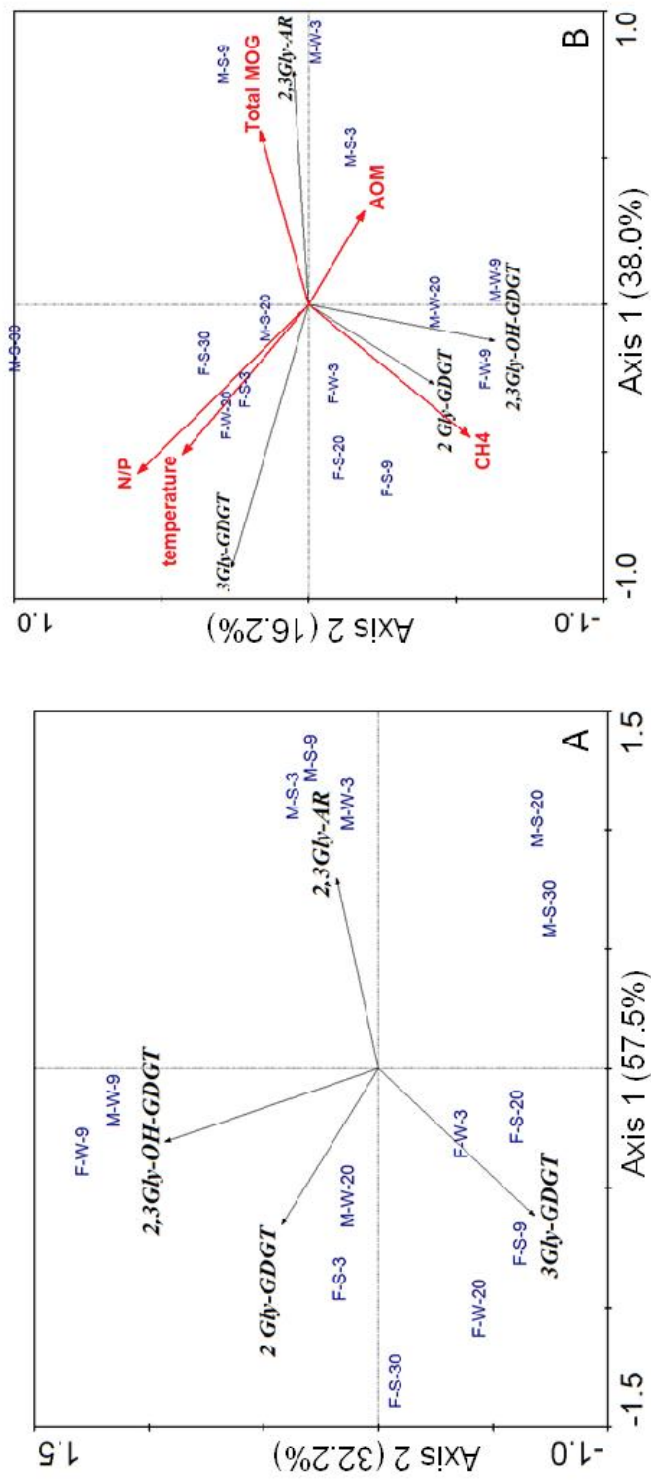


Figure 4.10. PCA plot displaying the distribution of archaeal IPLs (A) and an RDA biplot (B) displaying the relation of those IPLs to environmental variables and microbial activities (red arrows) which explain the most variability as determined via forward selection with Monte Carlo testing. The direction and length of the arrows for species and environmental variables represents the direction and rate of increase in the ordination space. Individual samples are labeled in blue according to the scheme: site-season-depth in cm. W, winter; S, summer; F, Florida; M, Maine; N.P., ratio of dissolved inorganic nitrogen to dissolved phosphate; Total MOG, methane produced from $^{14}\text{CH}_3\text{COO}^-$ and $\text{H}^{14}\text{CO}_3^-$; AOM, anaerobic oxidation of methane. For full names of individual IPLs see text.

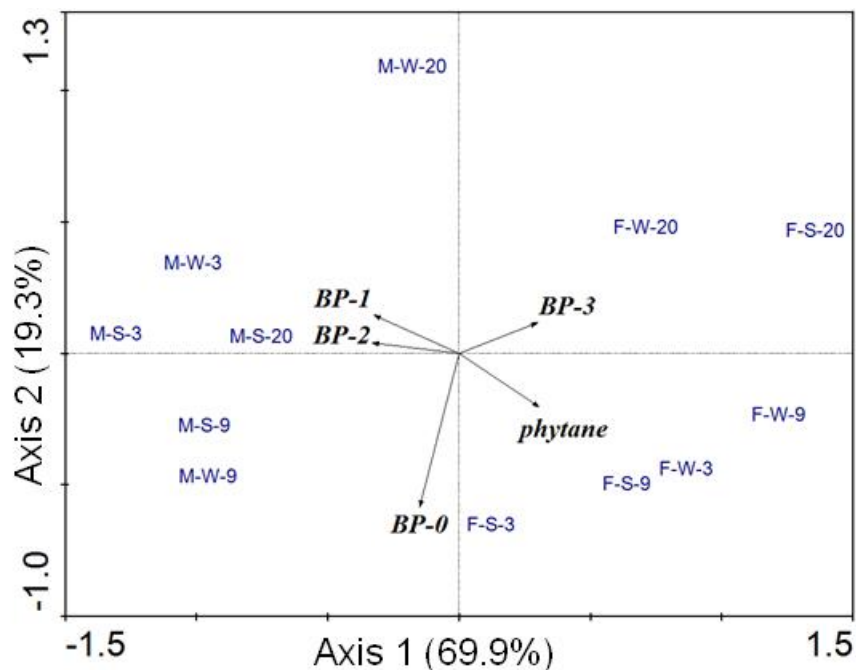


Figure 4.11. PCA plot displaying the distribution of the stable carbon isotopic signatures of intact-derived archaeal core lipids. Individual samples are labeled in blue according to site-season-depth in cm. The direction and length of the arrows for species represent the direction and rate of increasing depletion in the ordination space. Individual samples are labeled in blue according to the scheme site-season-depth in cm. BP-X, biphytane with 0, 1, 2, or 3 rings.

CHAPTER 5

IMPACT OF ELECTRON ACCEPTOR AVAILABILITY ON THE ANAEROBIC OXIDATION OF

METHANE IN COASTAL

FRESHWATER AND BRACKISH INTERTIDAL SEDIMENTS

Running title: *AOM in coastal freshwater and brackish sediments*

Katherine Segarra, Christopher Comerford, Julia Slaughter, and Samantha B. Joye^{*}

In preparation for *Geochimica Cosmochimica Acta*

Department of Marine Sciences, The University of Georgia, Athens, GA 30602

*Corresponding Author: Dr. Samantha Joye, Room 220 Marine Sciences Building,
Athens GA, USA, 30602-3636; tel: 706-542-5893; fax: 706-542-5888; electronic mail:
mjoye@uga.edu

ABSTRACT

Methane, a powerful greenhouse gas, is both produced and consumed in anoxic coastal sediments via microbial processes. Although the anaerobic oxidation of methane (AOM) is almost certainly an important process in coastal freshwater and salt marsh sediments, the factors that control the rates and pathways of AOM in these habitats are poorly understood. Here, we present the first direct measurements of AOM activity in freshwater (0 psu) and brackish (25 psu) intertidal sediments. Despite disparate sulfate concentrations, both environments supported high rates of AOM. Higher sulfate reduction (SR) rates were measured in the freshwater site, and SR at both sites was of sufficient magnitude to support the observed AOM activity. In the laboratory, long-term incubations of freshwater and brackish intertidal sediments amended with sulfate, nitrate, manganese oxide (birnessite) or iron oxide (ferrihydrite or ferric citrate), or unamended (control), were kept under a methane headspace to evaluate the impact(s) of electron acceptor availability on potential AOM rates. In these experiments, sulfate-dependent AOM was more important in brackish slurries than in the freshwater slurries. Maximum AOM rates in both freshwater and brackish sediments occurred in the ferric citrate amendments, which exhibited the highest rates of acetate and hydrogen production, substrates that could stimulate AOM. The addition of ferrihydrite, manganese oxides, and nitrate significantly lowered AOM rates relative to the control, although high ratios of AOM relative to SR rates in these treatments indicated that the two processes were decoupled in those treatments. This study provides further evidence for sulfate-independent AOM and demonstrates that both freshwater and brackish coastal sediments

support high rates of anaerobic methanotrophy, likely coupled to electron acceptors other than sulfate.

1. INTRODUCTION

Methane is a powerful greenhouse gas with a heat-trapping potential more than 20 times that of carbon dioxide (Blake and Rowland, 1988). Microbially-mediated processes produce and consume methane in anoxic sediments, thus playing a pivotal role in regulating Earth's climate. About 90% of methane produced in marine sediments is oxidized by microorganisms before it reaches the water surface (Reeburgh, 1996; Reeburgh, 2007), although this percentage varies widely among systems. Though coastal regions comprise a small area of the Earth's surface, coastal wetlands emit 40 to 160 Tg of methane per year to the atmosphere, accounting for 7 to 30 percent of global annual methane flux (Anselman and Crutzen, 1989; Dentener et al., 2003). Despite the importance of methane cycling in shallow coastal habitats, no direct measurements of the anaerobic oxidation of methane (AOM) are available. Thus, the factors that regulate AOM here are unknown. Projected increases in mean sea level may cause dramatic shifts in the biogeochemical functioning of coastal marshes through changes in salinity and the availability of electron acceptors such as iron and sulfate (Mitsch and Gosselink, 2007; Weston et al., 2011). It is thus crucial to investigate the factors that influence AOM rates in freshwater and brackish intertidal sediments to understand the present day – and future – methane cycle in these habitats.

Many aspects of the physiological mechanism of AOM in aquatic systems remain enigmatic. Coupling between sulfate reduction (SR) and AOM has been suggested in a variety of marine environments (Boetius et al., 2000; Iversen and Jorgensen, 1985;

Treude et al., 2003). Sulfate-linked AOM was first proposed in 1974 based on non-conservative concentration profiles of methane and sulfate in marine sediments, which suggested simultaneous consumption of methane and sulfate in the sulfate-methane transition zone (SMTZ; Barnes and Goldberg, 1976; Martens and Berner, 1974; Reeburgh, 1976). The process of sulfate-mediated AOM is proposed to involve a consortial relationship between methanotrophic archaea and sulfate-reducing bacteria via syntrophic transfer of a redox intermediate (Hoehler et al., 1994). Molecular phylogenetic and biomarker analyses suggest that the microorganisms responsible for AOM, namely the anaerobic methanotrophic archaea of the ANME-1, ANME-2, or ANME-3 clades, are close relatives of methanogenic archaea (Boetius et al., 2000; Hinrichs et al., 1999; Orphan et al., 2001). These ANMEs are proposed to oxidize methane via ‘reverse methanogenesis’ (Hoehler et al., 1994), a hypothesis that is supported by the discovery of a nearly complete set of genes necessary for methane production in ANME-1 and -2 (Hallam et al., 2004; Pernthaler et al., 2008).

However, attempts to constrain the reaction mechanism for AOM have been elusive. Inhibitor studies with 2-bromoethanesulfonate (BES), an analogue for the key enzyme methyl-coenzyme M reductase of the methanogenic pathway and a known inhibitor of methanogenesis (MOG; Oremland and Capone, 1988), have generated conflicting results. While some experiments showed partial or complete inhibition of AOM by BES (Nauhaus et al., 2005; Zehnder and Brock, 1980), others demonstrated no effect of BES on AOM (Alperin and Reeburgh, 1985; Orcutt et al., 2008). It therefore remains unclear whether AOM and MOG share the same biochemical mechanism.

Furthermore, studies of AOM typically report rates of AOM and/or SR but rarely consider the possibility of contemporaneous MOG. Several species of methanogenic archaea can concurrently oxidize methane while producing it, though the rate of methane oxidation is small relative to the MOG rate (Moran et al., 2007; Zehnder and Brock, 1979). Multiple environmental surveys and laboratory experiments reveal the opposite trend: contemporaneous AOM and MOG, with MOG rates occurring at a fraction of the AOM rate (Orcutt et al., 2005; Orcutt et al., 2008; Orcutt et al., 2010). At present, it is unclear how AOM and MOG are connected in the environment, whether the processes are reversible, and if so, whether this reversibility is due to microbial energetics or random enzyme activity.

Although there are disparate findings on the effect of sulfate and sulfate reduction on AOM, sulfate is still considered the most important electron acceptor for AOM in marine sediments (Knittel and Boetius, 2009; Thauer, 2010). Other electron acceptors may also be important. Net coupling of SR and AOM is exergonic under standard state conditions. However, methane oxidation coupled to the reduction of manganese, iron, nitrate, or nitrite yields at least 10 times more energy. These alternative electron acceptors for AOM were explored previously (Mason, 1977; Thalasso et al., 1997; Zehnder and Brock, 1980) and reexamined recently (Beal et al., 2009; Raghoebarsing et al., 2006). Nitrite reduction coupled to AOM is mediated by a single bacterium, *Candidatus Methyloirabilis oxyfera*, (Ettwig et al., 2010; Ettwig et al., 2008), that is able to oxidize methane using molecular oxygen produced during anaerobic nitrite dismutation (Ettwig et al., 2010). However, AOM coupled to denitrification has only been documented in long-term enrichments of sediment from polluted canals and lake sediments (Ettwig et al., 2008;

Raghoebarsing et al., 2006), and it is not clear whether this process is widespread in the environment (Deutzmann and Schink, 2011). In addition to nitrite and sulfate, manganese- and iron-stimulated AOM was documented in long-term incubations of seafloor methane-seep sediments (Beal et al., 2009). The recent documentation of AOM under sulfate-free conditions (Ettwig et al., 2010) has challenged the canonical coupling between AOM and SR and shown that AOM can be carried out by a single microorganism. Given the influence of methanotrophy on the global methane budget, examinations of coupling between all potential electron acceptors and AOM are warranted.

Shallow coastal sediments are constantly replenished with terrestrially sourced electron acceptors such as nitrate and iron oxides, making them ideal environments for studying AOM coupled to non-sulfate electron acceptors. In this study we evaluated the importance of AOM in the intertidal sediments of two coastal environments. To understand and identify the factors that might regulate methane cycling in these two settings, we evaluated rates of AOM and SR and geochemical patterns and examined potential couplings between AOM and potential inorganic electron acceptors through long-term incubations of sediment slurries. Geochemical analyses and rate measurements of AOM, SR, and MOG identified the possible electron acceptors for AOM. We expected the potential AOM rates to vary depending on the baseline conditions. In slurries with sediment from Dover Bluff, a highly sulfidic salt marsh, we expected the highest rates of potential AOM to be supported by sulfate reduction. For Hammersmith Creek, a freshwater marsh, we expected potential AOM rates to be supported by iron and/or nitrate reduction.

2. MATERIALS AND METHODS

2.1. Site Descriptions

The two study sites in coastal Georgia were characterized by different salinities and *in situ* sulfate concentrations (Table 5.1). Dover Bluff (DB), a salt marsh site located along Umbrella Creek (31°00' N, 81°31'W), a tributary of the Satilla River, had porewater salinities between 21 and 28 PSU. Hammersmith Creek (HC) is a freshwater tidal creek (porewater salinity of 0-1 PSU; 31°20' N, 81°28'W) that feeds into the Altamaha River.

2.2. Field Sample Collection, Processing, and Analysis

Several replicate cores, 40 cm in length and 7.5 cm in diameter, were collected from the unvegetated, intertidal zones of DB and HC in July of 2009 and stored at *in situ* temperature (20 °C) until processing. Three replicate cores from each site were processed to obtain baseline porewater and solid phase data; cores were extruded and sectioned at 3-5 cm intervals under a stream of argon to minimize oxygen exposure. Multiple subsamples were collected from each depth interval: a 6 cm³ sediment plug was collected and preserved for methane (CH₄) analysis in a helium-purged 20 mL glass headspace vial containing 2 mL of 2 mol L⁻¹ NaOH and crimp-sealed with a butyl rubber stopper. Methane was analyzed subsequently using a Shimadzu GC-2014 gas chromatograph equipped a flame-ionization detector and a CarbosphereTM column. A subsample (1 cm³) was placed in a tared weigh-dish for porosity determination (Joye et al., 2004). Another 3 cm³ of sediment was collected for hydrogen (H₂) analysis (Hoehler et al., 1994) using a Peak Performer 1 reduced-gas analyzer (Peak Laboratories[®]). The remaining sediment from each depth was transferred to an argon-purged Reeburgh-type squeezer cup (Joye et

al., 2004; Reeburgh, 1967). Porewater was expressed using a mechanical squeezer, collected in an argon-purged syringe, and filtered (0.2 μm) to halt microbial activity. A 10 mL volume of porewater was preserved for sulfate, chloride, phosphate, iron (II), and manganese (II) by addition of 100 μL concentrated trace-metal grade nitric acid. Samples for hydrogen sulfide (HS^-) concentration determination were preserved by adding 100 μL 20% zinc acetate per mL of pore water and analyzed according to Cline (1969). Samples for ammonium were preserved with 200 μL phenol reagent per mL of pore water (Solorzano, 1969). Samples for nitrate and nitrite analysis were stored frozen. Samples (1-2 mL) for dissolved inorganic carbon (DIC) analysis were collected and preserved by adding 0.5 mL of 15 mmol/L sodium molybdate in 50% phosphoric acid and 0.5 mL of saturated cupric sulfate in gas tight glass tubes fitted with a butyl rubber stopper and screw cap. The CO_2 in the headspace of tube was then analyzed using a Licor LI-840A $\text{CO}_2/\text{H}_2\text{O}$ analyzer after vigorous shaking. Sulfate and chloride were analyzed via ion chromatography (IC) with a Dionex ICS-2000 RFIC. Dissolved iron (II) and manganese (II) were quantified colorimetrically (Armstrong et al., 1979; Stookey, 1970). Combined NO_x ($= \text{NO}_2^- + \text{NO}_3^-$) was analyzed with an Antek Instruments model 745 vanadium reduction manifold and model 7050 nitric oxide detector. Nitrite was determined colorimetrically (Parsons et al. (1984). Nitrate was determined by difference ($= \text{NO}_x - \text{NO}_2^-$). Salinity was measured on unfiltered, extracted porewater using a refractometer and was confirmed by IC chloride analysis.

Triplicate intact sediment cores were sectioned into 3 cm depth intervals and approximately 6 cm^3 of sediment was subsampled into a 20 mL cut-end glass Hungate tube to determine rates of microbial activity (Orcutt et al., 2005). For AOM, triplicate

sub-samples from each depth were injected with 10.8 kBq of dissolved $^{14}\text{CH}_4$ tracer and incubated for 24 hours at *in situ* temperature. Base killed-controls were incubated in parallel for each depth interval and experiments were terminated and samples processed according to Joye et al. (1999). The rate of AOM was calculated using standard equations (Bowles et al., 2011; Orcutt et al., 2005).

SR rate samples were prepared identically and methods of tracer addition, product recovery, remaining substrate recovery, and activity measurements were from Orcutt et al. (2010; adapted from Canfield et al., 1986 and Fossing and Jorgensen, 1989). Killed-controls were incubated in parallel for each depth interval and rates were calculated as described previously (Orcutt et al., 2005). Rates were calculated using *in situ* concentrations of methane and sulfate, which were measured shortly after sample collection from parallel (cold) samples. Rates of AOM and SR are presented as volume-specific ($\text{nmol cm}^{-3} \text{ d}^{-1}$) and as areal ($\text{mmol m}^{-2} \text{ d}^{-1}$) [via trapezoidal integration of the volume-specific rates in the top 12 cm of sediment] rates.

2.3. Slurry Preparation and Maintenance

Manipulated slurry experiments commenced within 2 weeks of sediment collection. The top 12 cm of several replicate cores were combined and homogenized gently by hand in an argon-filled glove bag and then mixed with sterile ($0.2 \mu\text{m}$) filtered anoxic, artificial porewater (APW) in a ratio of 1 part sediment to 3 parts APW (final volume = 650 mL). The APW recipes mimicked the *in situ* geochemistry. The APW for the freshwater slurries contained $57 \mu\text{mol L}^{-1}$ potassium chloride, $100 \mu\text{mol L}^{-1}$ magnesium chloride, $323 \mu\text{mol L}^{-1}$ calcium chloride, 2 mmol L^{-1} sodium bicarbonate, $500 \mu\text{mol L}^{-1}$ ammonium chloride, and $30 \mu\text{mol L}^{-1}$ potassium phosphate. The APW for the

brackish slurries contained 5.7 mmol L⁻¹ potassium chloride, 12.6 mmol L⁻¹ magnesium chloride, 900 µmol L⁻¹ calcium chloride, 9 mmol L⁻¹ sodium bicarbonate, 2 mmol L⁻¹ ammonium chloride, 125 µmol L⁻¹ potassium phosphate, and 345 mmol L⁻¹ sodium chloride.

Potential electron acceptors for AOM such as SO₄²⁻, nitrate (NO₃⁻), and manganese and iron oxides were excluded from the APW and all glassware used in the experiment was trace metal clean. After slurring the sediment, the bottles were sealed with a butyl rubber stopper that was secured with an open-top screw cap. After being sealed, the headspace of each slurry was purged with ultra-high purity (UHP) argon and incubated in the dark at 20 °C for 4 weeks to lower background concentrations of sulfate and H₂S. Slurries were purged with argon every 3-5 days to remove H₂S in the headspace and gently inverted each day to re-suspend the sediment. Reducing the background sulfate concentration in the brackish slurries to less than 100 µmol L⁻¹ required dilution of the aqueous phase, which was achieved by allowing the sediment to settle out of suspension, removing 25% of the sediment-free overlying water, and replacing it with the same volume of sulfate-free, argon-purged APW. A total of 3 dilutions were carried out in the first week of the pre-incubation period.

After H₂S and sulfate concentrations were below 1 and 50 µmol L⁻¹, respectively, the experiment commenced. The slurries were amended with one of five different electron acceptors by adding 50 mL of an anoxic stock solution to achieve desired initial concentrations for the various treatments: ferrihydrite (an iron (III) oxyhydroxide; 10 mmol L⁻¹ iron (III) equivalent), ferric citrate (10 mmol L⁻¹ iron (III) equivalent), sulfate - SO₄²⁻ (1 mmol L⁻¹ in HC/fresh slurries or 10 mmol L⁻¹ in DB/brackish slurries), nitrate -

NO_3^- (1 mmol L^{-1}), and birnessite (a mixed valence manganese(IV)/manganese(III) oxide; 10 mmol L^{-1} manganese (IV) equivalent). The concentration of these additions were chosen to provide adequate increase background levels of the various species within ecological limits. Except for the ferrihydrite and birnessite, which were produced in the laboratory, all reagents were ACS grade. Two-line ferrihydrite and birnessite were prepared immediately before addition according to published protocols (Cornell and Schwertmann, 2003; Golden et al., 1986). Ferrihydrite was purified via dialysis and added to the slurries in solution. Birnessite was purified via centrifuging and dialysis, freeze-dried, and added to the slurries as a fine powder. Controls were treated similarly but were not supplemented with an additional electron acceptor. Each experimental addition was performed in triplicate. After the amendments were made, the headspace of each slurry was purged with 100% UHP CH_4 . Initial slurry CH_4 concentrations were approximately $340 \mu\text{mol L}^{-1}$ slurry in the DB and $480 \mu\text{mol L}^{-1}$ slurry in the HC slurries but were higher at all subsequent time points after headspace methane reached equilibrium with the porewater. Throughout the experiment the slurry bottles were maintained at $20 \text{ }^\circ\text{C}$ in the dark and were inverted gently four times every 24 hours to resuspend the sediment.

Slurries were monitored throughout the incubation period to maintain concentrations of the electron acceptors and methane (see below). The concentration of sulfate and nitrate were re-amended as needed (see Results). The metal-enriched slurries were re-amended on day 99. The methane headspace was replaced with 100% UHP methane after every sampling.

2.4. Slurry Sub-sampling and Geochemistry

The slurries were sampled for full geochemical characterization on day zero and again on days 21, 42, 71, 132, and 181. At each sampling point the slurries were placed in an argon-purged glove bag, opened, and sampled via tygon tubing attached to a syringe. Each bottle was inverted several times to suspend the sediment and then 45 mL of homogenized slurry was removed and distributed as follows: 5 mL into a headspace-free Hungate tube, 20 mL into a centrifuge tube, and 20 mL into a syringe with a gas-tight stop-cock. The slurries were resealed, removed from the glove bag, the headspace re-purged with 100 % UHP methane, and replaced in the dark at 20° C. The Hungate tube and centrifuge tubes were centrifuged at 2000 rpm for 10 minutes. The supernatant of the Hungate tube (1-2 mL; unfiltered) was collected with a needle and syringe and preserved and analyzed for DIC analysis (as described for porewater samples). A portion of the supernatant in the centrifuge tube was 0.2 µm filtered, preserved, and analyzed for sulfide, nitrite, dissolved organic carbon, and ammonium, as described for porewater samples. The remaining volume of this supernatant was filtered and preserved for sulfate, nitrate, dissolved iron(II), manganese(II), and phosphate analysis by preserving with concentrated hydrochloric acid (10 µL acid per mL of sample). All analyses (nitrate, nitrite, sulfate, phosphate, DOC, etc.) were conducted as described above for pore water samples. A sample for volatile fatty acids (VFA) was 0.2 µm filtered and frozen until quantification using a Dionex Ultimate HPLC (Albert and Martens, 1997). The remaining sediment in the centrifuge was scooped into plastic sampling bags with an acid-cleaned spatula, purged with argon, and immediately frozen for subsequent solid-phase metal analyses (see Electronic Annex EA 1). The syringe containing homogenized slurry was subsampled for CH₄, H₂, porosity, and pH, as described previously.

2.5. Slurry Microbial Activity Measurements

Rates of AOM were assayed at each time point using methods similar to those used for the intact sediment cores. Sub-samples were transferred to rate tubes, sealed, injected with 0.95 kBq $^{14}\text{CH}_4$ tracer, and incubated for 24 hours. The procedures for terminating the incubations, recovering product, and calculating the rates were identical to those described previously. Rates of SR were assayed days 0, 21, 71, 132, and 181 in the sulfate-amended slurries and on days 0 and 181 for the remaining treatments, as described above for sediment core sub-samples.

At the end of the experiment (day 181), rates of MOG were evaluated using radiotracers to determine importance of methane production relative to methane oxidation. Rates of hydrogenotrophic MOG (bi-MOG; $^{14}\text{CH}_4$ from $\text{H}^{14}\text{CO}_3^-$) and acetoclastic MOG (ace-MOG; $^{14}\text{CH}_4$ from $[\text{1-C}]-^{14}\text{CH}_3\text{COO}^-$) were prepared identically to those for measurement of AOM and SR rates. MOG rates from both substrates were processed and calculated using the methods of Orcutt et al. (2005). The incubation temperature was the same as those for AOM and SR slurry rate measurements. Killed-controls (slurries amended with 100 μM NaOH) run simultaneously with the live incubations of MOG confirmed that no abiotic methane production occurred.

2.6. Calculations

The increase in dissolved and adsorbed reduced iron and manganese concentration with time was used to estimate iron and manganese reduction rates. Using the concentration difference between the final two time points, the following equation was employed to calculate the rate in $\text{nmol g dry sediment}^{-1} \text{d}^{-1}$:

$$R = (\Delta M^2+_{\text{D}} + \Delta M^2+_{\text{A}} + \Delta M^2+_{\text{C}})/(\Delta t) \quad (1)$$

Where ΔM^2+_{D} is the change in concentration of dissolved, reduced iron or manganese in $\text{nmol g dry sediment}^{-1}$, ΔM^2+_{A} is the change in concentration of adsorbed, reduced iron or manganese in $\text{nmol g dry sediment}^{-1}$, ΔM^2+_{C} is the change in concentration of reduced iron or manganese in the carbonate mineral phase in $\text{nmol g dry sediment}^{-1}$, and Δt is the change in time in days. Dissolved metal concentrations were converted from $\mu\text{mol L}^{-1}$ slurry to $\text{nmol g dry sediment}^{-1}$ using the moisture content and weight of dry sediment of the slurries. As all treatment replicates were combined for solid phase analysis, average concentrations of dissolved metal were used in the calculation and the rates reflects an average rate for the triplicates.

The Gibbs free energy yields associated with the various pathways of methane oxidation examined in this study, as well as hydrogenotrophic MOG, were calculated under *in situ* conditions in the top 12 cm and under experimental conditions in the slurries according to the following equation:

$$\Delta G_{\text{rxn}} = \Delta G^{\circ} + RT \times \ln \left(\Pi a^y_{\text{products}} / \Pi a^z_{\text{reactants}} \right) \quad (2)$$

where ΔG_{rxn} is the Gibbs free energy of the reaction under *in situ* or experimental conditions, ΔG° is the standard Gibbs free energy (calculated from Stumm and Morgan, 1996), R is the gas constant, and T is the temperature in Kelvin. Π_{products} and $\Pi_{\text{reactants}}$ are the mathematical products of the activities of the of products and reactants, respectively. The powers y and z represent the stoichiometric coefficients of the products and reactants, respectively.

An *in situ* ΔG_{rxn} was calculated for discrete depth horizons using the *in situ* concentrations of relevant species and *in situ* temperature within each horizon. Experimental ΔG_{rxn} calculations were performed with experimental temperatures and

concentrations of relevant species in each slurry treatment after 181 days (time final). In those cases where the concentration of a species was below detection limit, sulfide was assumed to be 1 nmol L⁻¹; nitrate was assumed to be 1 μmol L⁻¹; nitrite was assumed to be 0.1 μmol L⁻¹; and dissolved iron(III) was assumed to be 0.01 μmol L⁻¹. Dinitrogen gas (N₂) was not measured but saturated concentrations were assumed (Weiss, 1970). This assumption likely over-estimated [N₂] which would under-estimate energy yields for AOM coupled to nitrate or nitrite reduction.

An estimated energy gain from AOM coupled to various electron acceptors in the slurries was calculated by multiplying the Gibbs free energy yield calculated for a given process by the rate of AOM in the slurry:

$$\Delta G_{\text{rxn}} \times \text{rate of AOM} = \text{estimated energy gain} \quad (3)$$

Data from the final time point was used for rates of AOM and free-energy calculations.

The contribution of AOM to the total pool of DIC was calculated using the following equation:

$$\% \text{ DIC from AOM} = \frac{\text{AOM rate} \times \text{time} \times 100}{\Delta \text{DIC}} \quad (4)$$

Here, ΔDIC is the change in DIC between days 0 and 181. We assumed 1 mole of DIC was produced from the oxidation of 1 mole of methane. Concentrations were porosity corrected.

2.7. Statistics

To identify significant differences within and among the treatments over time, a repeated measures analysis was followed by Tukey HSD post-hoc testing. To determine

significant differences at a single time point ANOVAs were performed with Tukey HSD post-hoc testing. Significances were evaluated at the 0.05 level.

3. RESULTS

3.1. Environmental Measurements

The two study sites exhibited distinct patterns of pore water geochemistry and microbial activity (Fig. 5.1 and Table 5.1). The sulfate concentrations at DB decreased with depth from 12 mmol L^{-1} at the sediment-water interface to $500 \text{ } \mu\text{mol L}^{-1}$ at 18 cm (Fig. 5.1). In contrast, surface sulfate concentrations at HC were $<1 \text{ mmol L}^{-1}$, decreasing to $<100 \text{ } \mu\text{mol L}^{-1}$ at 9 cm (Fig. 5.1). Methane concentrations increased with depth at both sites but concentrations were much higher at HC (Fig. 5.1). Although the concentrations of methane and sulfate differed significantly between the two sites, the SMTZ occupied the same depth horizon (Fig. 5.1). At DB, sulfide concentration increased with depth to a maximum of 6 mmol L^{-1} whereas sulfide concentrations at HC were $<1 \text{ } \mu\text{mol L}^{-1}$. Hydrogen concentration was higher at HC, up to 215 nmol L^{-1} , than DB, up to 44 nmol L^{-1} . Concentrations of DIC and DOC increased with depth at DB, although DIC concentrations were higher, up to 30 mmol L^{-1} . DIC concentrations were much lower at HC, ranging from 4 to 7 mmol L^{-1} . At HC, DOC concentrations showed little variation with depth, ranging between 1 and 2 mmol L^{-1} . Porewater concentrations of nitrate, dissolved reduced iron (Fe^{2+}) and dissolved reduced manganese (Mn^{2+}) were higher at HC (Fig. 5.1). Nitrite, however, was higher at DB. Despite these differences in porewater geochemistry, rates of AOM were comparable between the two sites (Fig. 5.1) and SR rates exceeded AOM rates at all depths.

Biogeochemical differences between HC and DB in the top 12 cm are summarized in Table 5.1. Areal rates of AOM were indistinguishable between the two sites (Table 5.1) while rates of SR were roughly 20 times higher at HC, despite higher sulfate concentrations at DB. Integrated rates of SR exceeded AOM rates at both sites. Concentrations of methane, dissolved, reduced iron and manganese, nitrate, and hydrogen were significantly higher at HC (Table 5.1). Concentrations of nitrite, dissolved inorganic carbon, and sulfide and salinity were significantly higher at DB (Table 5.1). DOC concentration and pH were similar between sites.

3.2. Thermodynamics

The differences in the pore water geochemistry within the SMTZ at the two sites influenced the thermodynamics of methane oxidation and production (Table 5.2). Sulfate-dependent methane oxidation was significantly more favorable at HC, despite significantly higher sulfate concentrations at DB. The energy yield for AOM coupled to other terminal electron acceptors was similar between sites (Table 5.2). The most favorable electron acceptor for methane oxidation under *in situ* conditions was nitrite. Although the standard state energy yields are quite similar for methane oxidation coupled to aqueous and solid-phase iron, the *in situ* energy yields for aqueous iron were much higher than for solid-phase iron. Energy yields for hydrogenotrophic MOG were indistinguishable between the two sites and were much lower than the estimated energy yields for methane oxidation.

3.3. Slurry Geochemistry

The experimental slurries were sub-sampled 6 times during the 181-day incubation. Porewater methane concentrations were constant after 41 days. Average concentrations

were 881 nmol CH₄ cm⁻³ in the DB slurries and 1088 nmol CH₄ cm⁻³ in the HC slurries (data not shown). Concentrations of sulfate and nitrate were monitored closely in the sulfate- and nitrate-amended slurries to ensure that concentrations of each species remained elevated. In the case of the nitrate-amended slurries, nitrite concentrations were also monitored because nitrite is toxic to many microorganisms at high concentrations (> 50 μM; BOLLAG and HENNINGER, 1978; KLÜBER and CONRAD, 1998; ZUMFT, 1993). Nitrate was added to the nitrate-amended slurries when nitrate concentrations dropped below 250 μmol L⁻¹ nitrate and when nitrite concentrations were < 10 μmol L⁻¹. Throughout the time-course incubation, nitrite concentrations increased shortly (days) after nitrate addition. Initially nitrate amendments were made every 2-3 weeks. After about 100 days, nitrate and nitrite consumption rates decreased and nitrate re-amendment was less frequent (every 3-5 weeks). At this point the maximum nitrate concentration was adjusted from 1 mmol L⁻¹ to 500 μmol L⁻¹ in order to avoid spikes in nitrite concentration.

Sulfate consumption patterns were less dynamic than nitrate consumption patterns. Sulfate concentrations were monitored and re-amended when sulfate concentrations were < 7.5 mmol L⁻¹ in the DB sulfate slurries and < 500 μmol L⁻¹ in the HC sulfate slurries. On average, sulfate was resupplied to the sulfate-treated slurries every 6-8 weeks (data not shown).

Sulfate concentrations remained significantly higher in the sulfate-amended slurries than the other treatments (Figs. 2A and 2G; *p*>0.05). In the nitrate and birnessite treatments, however, sulfate concentrations increased significantly throughout the experiment and were significantly higher than those observed in the controls despite the

fact that no sulfate was added. For DB, sulfate concentrations peaked at 6 mmol L⁻¹ and 3 mmol L⁻¹ in the nitrate and birnessite treatments, respectively. For HC, these maxima were 727 μmol L⁻¹ and 423 μmol L⁻¹. For DB, the average sulfate concentrations in the control, ferrihydrite, and ferric citrate slurries were 25, 13, and 25 μmol L⁻¹, respectively; for HC, these concentrations were 16, 5, and 19 μmol L⁻¹ (Figs. 5.2A, G).

Sulfide concentrations were significantly higher in the DB sulfate-amended slurries (up to 2.3 mmol L⁻¹) than the control slurries (Table 5.3; $p < 0.05$). All other DB treatments had significantly lower sulfide concentrations than the control. No significant treatment effects were observed in the sulfide concentrations in the HC slurries.

Dissolved inorganic carbon (DIC) concentrations varied significantly with time and treatment (Figs. 5.2B, H). At the end of the experiment, maximum DIC concentrations were observed in the ferric citrate-amended slurries at both sites ($p < 0.05$). In HC slurries, final DIC concentrations in the sulfate and nitrate treatments were significantly higher than the control ($p < 0.05$). For both sites, birnessite addition significantly lowered DIC concentrations relative to the control ($p < 0.05$).

The pH of the slurries mirrored the DIC content: slurries with the highest DIC content had the lowest pH and vice versa. The slurry pH ranged from 7.1 to 8.7 for DB (Fig. 5.2C) and from 6.9 to 9.5 for HC (Fig. 5.2I). For both sites, the lowest pH values were recorded in the ferric citrate slurries and the highest values in the birnessite slurries ($p < 0.05$).

Hydrogen was most variable in the ferric citrate amended slurries (Figs. 5.2D, J). Sharp increases in hydrogen concentrations up to 51 nmol L⁻¹ occurred after the initial amendment with ferric citrate and again after the second addition. Hydrogen

concentrations in the ferric citrate slurries were significantly higher than the other treatments throughout the experiment in both DB and HC ($p < 0.05$). The other amended slurries had hydrogen concentrations less than or equal to the control throughout the experiment.

Although dissolved organic carbon (DOC) concentrations decreased significantly with time in all slurries, the largest decrease was observed in the ferric citrate treatments ($p < 0.05$; Figs. 5.2E, K). In the ferric citrate slurries, DOC concentrations were extreme, starting at 72 mM but decreasing rapidly to ≤ 1 mM in 40 (HC) to 70 (DB) days. DOC concentrations in the other slurries varied to a much smaller degree, with an average concentration of 0.9 mmol L^{-1} in DB and 1 mmol L^{-1} in HC. Control acetate concentrations of 2 mmol L^{-1} (DB) and 1 mmol L^{-1} (HC slurries), respectively, were only statistically different the ferric citrate treatments (Fig. 5.2F, L).

Dissolved phosphate concentrations were significantly lower in the metal- and nitrate-amended slurries than the control (Table 5.3; $p < 0.05$). For HC, the addition of sulfate increased the phosphate concentrations relative to the control by a factor of 2 ($p < 0.05$).

Only the nitrate-amended slurries had nitrate concentrations that were significantly different from the control ($p < 0.05$; Table 5.3). Nitrate addition resulted in sharp, temporary increases in nitrite concentrations; significantly higher nitrite concentrations were observed in the nitrate-amended slurries throughout the experiment at both sites ($p < 0.05$) although nitrite concentrations were only slightly inflated to the control at the end of the experiment (Table 5.3). Average ammonium concentrations in the DB sulfate, nitrate, and birnessite slurries were 1.74 , 1.92 , and 1.82 mmol L^{-1} ,

respectively. These concentrations were significantly elevated relative to the DB control slurries, which had an average ammonium concentration of 1.64 mmol L^{-1} ($p < 0.05$; data not shown). Ammonium concentrations were lower in the HC slurries (data not shown). Average concentrations in the ferrihydrite (0.59 mmol L^{-1}) and nitrate (0.67 mmol L^{-1}) slurries were significantly elevated relative to the control (0.55 mmol L^{-1} ; $p < 0.05$).

The highest Fe^{2+} concentrations were observed in the ferric citrate treatments (Table 5.3), with maximum concentrations observed at the time points following the two additions of ferric citrate (data not shown). After 181 days, dissolved Fe^{2+} concentrations remained significantly higher in the ferric citrate slurries than the other treatments for both sites (Table 5.3; $p < 0.05$). In DB slurries, Fe^{2+} concentrations increased over time in the ferrihydrite-amended slurries (data not shown) and were significantly higher than the control after 181 days (Table 5.3; $p < 0.05$). No such increase or differences were observed in the HC slurries.

Concentrations of Mn^{2+} increased significantly over time in the DB birnessite-amended slurries (data not shown); the maximum concentration ($474 \text{ } \mu\text{mol L}^{-1}$) was observed after 181 days (Table 5.3). In HC slurries, the highest dissolved Mn^{2+} concentrations were observed at the end of the experiment in the control (Table 5.3).

The solid-phase partitioning of iron and manganese minerals varied over the course of the experiment compared to the control (see electronic annex; EA 1). The addition of trace-metals to the slurries resulted in significantly higher contributions of easily reduced Mn (with birnessite) or Fe (with ferric citrate and ferrihydrite) in those treatments than in the control for both sites. Over time, the pool of easily reducible manganese or iron decreased and the proportion of iron or manganese in the reduced

phases (adsorbed and carbonates) increased throughout the experiment in both the DB and HC slurries. At the end of the experiment the proportion of reduced iron and manganese in the metal-amended slurries was significantly higher than the control in the slurries from both sites ($p < 0.05$).

The addition of trace metals to the slurries all resulted in significantly higher rates of iron reduction (in the cases of ferrihydrite and ferric citrate) and manganese reduction (in the birnessite) relative to the control for both sites ($p < 0.05$). Iron and manganese reduction rates were below detection in the controls of HC and DB. In contrast, iron reduction rates in the ferrihydrite treatments were 13.8 (DB) $\text{nmol g dry sediment}^{-1} \text{ d}^{-1}$ and 1.8 (HC) $\mu\text{mol g dry sediment}^{-1} \text{ d}^{-1}$. In the ferric citrate slurries, these rates were 3.5 (DB) and 1.6 (HC) $\mu\text{mol g dry sediment}^{-1} \text{ d}^{-1}$. Manganese reduction rates in the birnessite slurries were very similar between the two sites: the rate for DB was 3.2 $\mu\text{mol g dry sediment}^{-1} \text{ d}^{-1}$ while the rate in HC was 3.4 $\mu\text{mol g dry sediment}^{-1} \text{ d}^{-1}$.

3.4. Anaerobic Oxidation of Methane

Potential AOM rates increased throughout the incubation in all treatments and the largest differences between treatments were observed at the end of the experiment (Figs. 5.3A and B). For HC, AOM rates ranged from 0.3 to 32.2 $\text{nmol CH}_4 \text{ cm}^{-3} \text{ slurry d}^{-1}$ and for DB, the range was 0.1 to 10.4 $\text{nmol CH}_4 \text{ cm}^{-3} \text{ slurry d}^{-1}$. In the first 132 days of the experiment, only the ferric citrate treatment had higher AOM rates than the control in the HC slurries (Fig. 5.3A). For DB, the sulfate-treated slurries maintained the highest rates of AOM for the first 71 days and then at 132 days, rates of AOM in the ferric citrate and sulfate slurries were identical (Fig. 5.3B). After 181 days of incubation, average potential AOM rates ranged from 2.4 ± 0.2 to $9.9 \pm 0.3 \text{ nmol CH}_4 \text{ cm}^{-3} \text{ d}^{-1}$ in DB slurries, and from

3.6 ± 0.1 to 30.9 ± 0.6 nmol CH₄ cm⁻³ d⁻¹ in HC slurries (Table 5.4). In DB slurries, the addition of both ferric citrate and sulfate resulted in significantly higher rates than the control ($p < 0.05$; Table 5.4). AOM rates were significantly lower in the DB sediments amended with birnessite ($p < 0.05$). In HC slurries, the ferric citrate slurries also produced the highest rates of AOM while the addition of sulfate, ferrihydrite, nitrate and birnessite significantly lowered AOM rates relative to the control (Table 5.4; $p < 0.05$).

A significant positive relationship was observed for AOM rates and acetate concentration at DB ($R^2 = 0.98$; $p < 0.05$; Fig. 5.4) but not at HC. No patterns were observed between bulk DOC concentration and AOM rates (data not shown). Slurries with the highest AOM rates had the highest H₂ concentration; when plotted together there was a site-dependent logarithmic increase in AOM rate with H₂ concentrations (Fig. 5.5).

3.5. Sulfate Reduction (SR)

Despite the higher sulfate concentrations in DB than HC in the sulfate-amended treatments (Fig. 5.2), potential SR rates were similar between the sites (Fig. 5.6). Rates of SR increased linearly over time in the sulfate-amended slurries of HC (max: 24 nmol SO₄²⁻ reduced cm⁻³ slurry d⁻¹) and DB (max: 25 nmol SO₄²⁻ cm⁻³ slurry d⁻¹; $p < 0.05$); rates between sites were not significantly different.

After 181 days, SR varied significantly among the various treatments in the slurries of HC and DB (Table 5.4). In the DB sediments, SR rates were higher in the ferric citrate and sulfate treatments than the control ($p < 0.05$). Surprisingly, SR rates in the ferric citrate treatment were higher than those in the sulfate treatment (Table 5.4; $p < 0.05$) despite lower sulfate concentration (Figs. 5.2A and G). In the incubations with HC sediment, SR was highest in the sulfate-amended slurries, followed by the control (Table

5.4). Addition of other electron acceptors (nitrate, ferrihydrite, birnessite, and ferric citrate) significantly lowered SR rates relative to the control ($p < 0.05$).

The ratios of AOM to SR (AOM:SR) were higher in the HC slurries than the DB slurries (Table 5.4). The ratios of AOM:SR in DB treatments ranged from an average of 0.3 to 34 and from 0.7 to 143 in the HC slurries. Notably, the ratio of AOM:SR in the sulfate amended treatments was always less than 1, while the ratio was always greater than 1 in the treatments with ferrihydrite, nitrate, and birnessite.

3.6. Methanogenesis Rates (MOG)

At the end of the experiment, rates of MOG were assayed in subsamples from all 36 slurries. MOG rates ranged from below detection to $106.5 \text{ nmol cm}^{-3} \text{ d}^{-1}$ and were highest in the ferric citrate-amended slurries ($p < 0.05$; Table 4). Rates of MOG were lower than the control in the ferrihydrite and sulfate-amended slurries at both sites and were not detectable in the nitrate and birnessite treatments. The majority of the methane was produced from acetate except in the control slurries of HC. No methane production was detected in the killed controls.

For those treatments displaying both AOM and MOG potential, the ratio of AOM to MOG (AOM:MOG) rates at 181 days ranged from 0.4 to 16.6. This ratio was never equal to or close to 1 for any of the treatments. The highest ratios were observed in the sulfate- and ferrihydrite-amended slurries of both sites (Table 5.4). The lowest ratios of AOM:MOG were calculated for the ferric citrate slurries in which methane production exceeded methane oxidation (AOM:MOG of 0.4 for both DB and HC; Table 5.4). Methane production also exceeded methane oxidation in the control slurries of DB.

4. Discussion

Both freshwater and brackish coastal intertidal sediments supported substantial and comparable rates of AOM, despite the different geochemical characteristics. Enrichments with freshwater and brackish tidal creekbank sediments amended with various electron acceptors and high methane concentrations revealed interesting and surprising patterns in the microbial potential for AOM. The results suggest that coastal wetland sediments support high rates of AOM coupled to electron acceptors other than sulfate. Long-term slurry experiments indicated that AOM was coupled to the reduction of multiple electron acceptors, such as nitrate and ferric iron oxides, in addition to sulfate, and that the degree of this coupling between the oxidation of methane and reduction of these different species is influenced by relative substrate availability. The addition of some electron acceptors (namely nitrate and manganese) resulted in the accumulation of sulfate in the slurries indicating the stimulation of anaerobic sulfide oxidation. Surprisingly, the production of sulfate in the nitrate and birnessite treatments did not stimulate SR and AOM and SR were conspicuously uncoupled in these treatments.

4.1. In situ Rates and Geochemistry

Rates of AOM in coastal intertidal sediments of DB and HC were comparable to or higher than those observed previously in coastal subtidal marine sediments (Table 5.1; DEVOL, 1983; IVERSEN and BLACKBURN, 1981; IVERSEN and JORGENSEN, 1985) although lower than those generally reported for deep-sea, methane-rich cold seep sediments (Bowles et al., 2011; Joye et al., 2004; Orcutt et al., 2010; Treude et al., 2003). Although sulfate concentrations were higher in DB sediments, the SMTZ occurred at roughly the same depth at both sites (Fig. 5.1). Not surprisingly, methane concentrations were much

lower in the salty sediments (Fig. 5.1), where sulfate-reducers typically outcompete methanogens for substrates (Capone and Kiene, 1988). Rates of AOM at HC were well above the few measurements of AOM available for freshwater environments (max = 0.08 nmol cm⁻³ d⁻¹; Deutzmann and Schink, 2011).

In situ rates of SR were high enough to support all methane oxidation in all depth intervals at both sites (Table 5.1); however, SR and AOM were not correlated consistently at depth (Fig. 5.1), suggesting that these two processes were not necessarily linked and that some of the SR was fueled by endogenous organic matter. Iron oxides, manganese oxides, and/or nitrate, which were all present at higher concentrations at HC than at DB, may serve as alternate electron acceptors for AOM (Beal et al., 2009; Raghoebarsing et al., 2006) and may explain the similar rates of AOM between the two study sites despite the differences in sulfate concentrations. The *in situ* oxidation of methane coupled to nitrate, nitrite, iron, or manganese reduction was significantly more thermodynamically favorable than AOM coupled to SR (Table 5.2). Despite the distinct geochemistry of each site, the thermodynamics of AOM were comparable.

Our results highlight the importance of AOM in both fresh and brackish intertidal sediments, where the process of AOM has largely been overlooked. High SR rates do not necessarily indicate sulfate-dependent AOM, as alternative electron acceptors were plentiful in the porewaters of the freshwater site. Additionally, the oxidation of methane with alternative electron acceptors (e.g. nitrate, iron, and manganese) was more thermodynamically favorable than with sulfate. Slurry experiments with known enrichment of single electron acceptor were employed to elucidate the mechanisms of AOM in the fresh and brackish sites, which appear to be distinct.

4.2. Slurry Results

Identifying the oxidant(s) for methane in environmental samples is not straightforward. Sulfate-independent AOM has been directly measured only in long-term enrichments of eutrophic sediment and sludge (HU et al., 2009; RAGHOEBARSING et al., 2006). Such enrichments provide a powerful way to study the response of communities to various environmental conditions and such laboratory manipulation experiments have been used to examine mechanisms of AOM for decades (Alperin and Reeburgh, 1985; Beal et al., 2011; Beal et al., 2009; Ettwig et al., 2010; Ettwig et al., 2008; Mason, 1977; Orcutt et al., 2008; Thalasso et al., 1997; Zehnder and Brock, 1980). We employed long-term enrichments to evaluate the response of two different microbial communities to variable dominant terminal electron acceptor regimes. While the conditions in enrichment slurries are undeniably different than those *in situ*, the amendments provide the opportunity to evaluate the impacts of different oxidants across treatments simultaneously.

Potential AOM rates were higher in the freshwater HC slurries than in the brackish DB slurries (Table 5.4), although *in situ* rates were comparable between the two sites (Table 5.1). Given the high methane concentrations in the slurries ($>500 \mu\text{mol L}^{-1}$), it is unlikely that methane availability limited AOM. A more likely explanation is that differences in microbial community composition or physiology or electron acceptor availability regulated AOM rates. The response of AOM to the various slurry amendments, as well as comparisons with rates of SR and MOG are discussed below.

4.2.1. AOM Coupled to Sulfate Reduction

Sulfate amendment to DB sediments generated higher rates of AOM compared to the control throughout the experiment (Fig. 5.3), consistent with previous studies of AOM coupled to SR in marine sediments (Nauhaus et al., 2002; Treude et al., 2003). In contrast, amendment of HC sediment with sulfate resulted in lower AOM rates compared to the control (Table 5.4), suggesting that sulfate inhibited the freshwater sediment AOM community. Hansen et al. (1998) also observed a negative effect of sulfate on AOM rates in coastal marine sediments while others documented stimulation of net methane oxidation by sulfate in subtidal marine sediments (Hoehler et al., 1994). However, recent work in freshwater lake sediments did not report stimulation of AOM by sulfate (Deutzmann and Schink, 2011). The AOM:SR ratio was <1 in the sulfate-amended slurries at both sites, indicating that SR exceeded AOM and all observed AOM could be coupled to SR, as observed in some marine sediments (Bowles et al., 2011; Joye et al., 2004; Orcutt et al., 2005) and *in situ* at DB and HC (Fig. 5.1). However, SR in excess of AOM shows clearly that some SR is fueled by endogenous organic carbon other than methane. The contrasting response in AOM and SR in the sulfate-amended freshwater slurries suggests that these two processes were independent. Thus, although all AOM in HC sediments (both *in situ* and in the control and sulfate-amended slurries) could conceivably be supported by SR (AOM:SR < 1), the decrease in AOM rates with the addition of sulfate relative to the control suggests that the freshwater community utilizes a non-sulfate electron acceptor.

At the end of the experiment, SR rates in the two sulfate amended treatments were indistinguishable (Table 5.4), even though the sulfate concentrations differed by almost an order of magnitude (Figs. 5.2A, G). These slurry results and those of the profile cores

indicate that low (μM level) sulfate concentrations do not translate into lower SR rates but they do require rapid, efficient reduced sulfur oxidation and/or enhanced sulfate supply via bioirrigation or bubble-induced mixing (Bowles et al., 2011). Furthermore, sulfide recycling must play an important role in regulating sulfate reduction activity in these habitats, as observed previously at Gulf of Mexico cold seeps (Bowles et al., 2011). Tidal pumping may also provide additional sulfate to the intertidal sediments of HC (DEBORDE et al., 2008; DEBORDE et al., 2010). It is possible that a combination of these physical and biological processes act in concert to sustain the high rates of *in situ* sulfate reduction in these sediments, especially in the low-sulfate environment of HC.

4.2.2. AOM Coupled to Other Electron Acceptors

To evaluate how much of the observed AOM could be coupled to SR in the slurries, we compared rates of AOM and SR: if all the observed AOM activity was linked solely to SR, the AOM:SR ratio should be 1. The observed ratios of AOM:SR, which ranged from 0.3 to 143, suggest that AOM was coupled to other electron acceptors in some of the non-sulfate amendments. Amendment of ferric citrate to HC sediments resulted in highest AOM rates and AOM rates exceeded SR rates by a factor of 2, indicating that at least 50% of the AOM was SR-independent (Table 5.4). Very high AOM:SR ratios in the birnessite, ferrihydrite, and nitrate treatments of HC sediments indicated that despite suppressed rates of AOM relative to the controls, AOM was essentially independent of SR in those treatments. In DB slurries, the highest potential AOM rates were also observed in the ferric citrate treatments but it is not clear that this AOM was independent of SR because SR rates were high enough to account for the observed AOM. However, the AOM:SR in the ferrihydrite, birnessite, and especially the

nitrate slurries of DB, indicated sulfate-independent AOM. These results are consistent with previous enrichment experiments that showed AOM could be coupled to birnessite, ferrihydrite, and sulfate reduction in long-term enrichments of methane-seep sediments (Beal et al., 2009). Those authors also reported that AOM rates coupled to SR were several times higher than AOM coupled to birnessite or ferrihydrite reduction (Beal et al., 2009). However, Beal et al. (2009) did not measure SR or AOM rates using radiotracer, making comparisons with the data presented here difficult. Other *in vitro* experiments with enriched ANME communities from marine sediments showed no AOM without sulfate, regardless of addition of other electron acceptors, including MnO₂, ferrihydrite, ferric citrate, nitrate, or elemental sulfur (Nauhaus et al., 2005). The data presented here show that while AOM rates coupled to alternative substrates may be lower than AOM coupled to SR, there is significant potential for sulfate-independent AOM in these intertidal sediments.

Lower rates of AOM are not necessarily indicative of the metabolic efficiency of the organism(s) mediating the process. Although AOM rates in the nitrate treatments were among the lowest, the energy gained from AOM coupled to denitrification was much higher than AOM coupled to SR in the slurries. Estimated energy gain calculations revealed that AOM coupled to nitrate reduction in the nitrate-amended slurries was between 5 (fresh) and 16 (brackish) times higher than AOM coupled to SR in the sulfate-amended (see methods for details; data not shown). Similarly, in the birnessite treatments, although absolute rates of AOM coupled to manganese reduction were lower, this process could generate 3 (fresh) to 6 (brackish) times more energy than sulfate-based AOM. Ultimately, these and previous findings (Beal et al., 2009; Deutzmann and Schink,

2011) suggest that AOM coupled to other electron acceptors is likely widespread and that the dominant mechanism may be site- and microbial community- specific and that the pathway is influenced by *in situ* environmental conditions (e.g. availability of various oxidants).

The ratio of AOM:SR was not dependent upon sulfate concentrations. For example, the concentrations of sulfate in the nitrate and sulfate treatments were inflated relative to the control after 181 days (Figs. 5.2A and G), yet AOM in the nitrate slurries was largely independent of SR (Table 5.4). Although sulfate was available in these treatments, likely through anaerobic sulfide oxidation coupled to nitrate reduction, SR was likely inhibited thermodynamically by nitrate availability (Achnich et al., 1995), resulting in sulfate accumulation and low SR rates. Generation of sulfate through anaerobic oxidation of solid phase metal sulfides, likely coupled to nitrate reduction, is not widely reported but appears to be important in both freshwater and brackish sediments. During the early stages of the enrichment, NO_x had both biological (denitrification) and abiotic (sulfide oxidation) sinks. As solid phase iron sulfides were oxidized and consumed, the associated abiotic NO_x demand decreased (Garcia-Gil and Golterman, 1993) such that NO_x consumption later in the experiment reflected solely biological consumption, which is what was observed.

4.2.3. Methane Production vs. Oxidation

The mechanism of ‘reverse methanogenesis’ for AOM was first proposed by Zehnder and Brock (1979) and is supported by more recent work (Shima and Thauer, 2005). Pure cultures of methanogens oxidize trace amounts of methane during active MOG (Moran et al., 2005; Zehnder and Brock, 1979). It has been suggested that ANME

archaea are involved in methane production as well as oxidation, although whether the observed activity reflects metabolic purpose versus spurious enzymatic back reaction remains unclear (Alperin and Hoehler, 2009; Orcutt et al., 2005; Orcutt et al., 2008). In the studies which have simultaneously measured MOG and AOM (Hansen et al., 1998; Hoehler et al., 1994; Joye et al., 2009; Meulepas et al., 2010; Moran et al., 2005; Orcutt et al., 2005; Orcutt et al., 2008; Orcutt et al., 2010; Zehnder and Brock, 1979; Zehnder and Brock, 1980), contemporaneous methane production was observed with AOM. The consistent finding of contemporaneous AOM and MOG indicated that the two processes may be mechanistically linked, at least in marine sediments.

However, our results suggest that AOM may occur in the absence of MOG and that these two processes are likely independent in these coastal sediments. AOM and MOG could be mediated by the same organism, but the artificially high methane concentrations in the slurries thermodynamically made methane production unfavorable. Considering the thermodynamics of the reactions, neither hydrogenotrophic nor acetoclastic MOG were favorable in the slurries except in the ferric citrate treatment (which experienced accumulation of the two substrates DIC and acetate; data not shown). While some slurries demonstrated co-occurrence of MOG and AOM at roughly the same order of magnitude (Table 5.4), other treatments (i.e. nitrate and birnessite) did not display any measurable methane production. These findings support one of two scenarios: either AOM and MOG are completely independent *or* the linkage between MOG and AOM is dependent upon experimental/environmental conditions and/or the microbial community.

The highest MOG rates occurred in unamended or ferric citrate amended slurries, while MOG appeared to be inhibited by amendment with ferrihydrite, birnessite, nitrate, and sulfate (Table 5.4). Thermodynamically, metal oxide, sulfate and nitrate respiration processes are more favorable than either MOG or homoacetogenesis (Hoehler et al., 1998) and methanogenesis is typically inhibited when more favorable electron acceptors are available (Acht nich et al., 1995; Chidthaisong and Conrad, 2000; Lovley and Klug, 1983; Westermann and Ahring, 1987). Therefore, the observance of maximum rates of AOM and MOG in the ferric citrate slurries is likely coincidental: high concentrations of acetate, DIC, and hydrogen stimulated MOG and offset any inhibition of MOG by iron oxides. This is consistent with previous studies that showed inhibition of methanogens by other terminal metabolisms, e.g. iron reduction, could be overcome by addition of hydrogen and acetate (Acht nich et al., 1995; Winfrey and Zeikus, 1977). After ferric citrate, the second highest rates of MOG were measured in the control slurries of both sites, which also displayed some of the highest contributions of hydrogenotrophic MOG to total methane production. We suspect other autotrophic/fermentative metabolic processes, such as homoacetogenesis, were also higher in the control slurries than the slurries enriched in electron acceptors, which likely supported other processes such as metal, sulfate, and nitrate reduction at the expense of MOG and other autotrophic processes. Thus, the lower MOG rates in the other slurry treatments were likely due to competition with other terminal metabolisms.

Phylogenetic studies in sulfate-replete environments indicated assemblages of sulfate-reducing bacteria and ANMEs (closely related to methanogens) conduct AOM (Knittel et al., 2005; Pernthaler et al., 2008). However, Ettwig et al. (2008; 2009)

successfully identified a new microorganism, *M. oxyfera*, a NC10 bacterium, that couples the reduction of nitrite to the oxidation of methane (Ettwig et al., 2010) demonstrating that AOM can be carried out by a single type of bacteria, independent of archaea. Similar NC10 microorganisms were linked to sulfate-independent AOM in Lake Constance sediments (Deutzmann and Schink, 2011). These comparisons of sulfate-dependent AOM communities with those of sulfate-independent AOM indicate that the reliance of AOM on MOG may depend upon the microbial community and availability of electron acceptors. It is possible that sulfate-dependent AOM involves archaea that could either produce or consume methane as a function of the thermodynamic forcing. In contrast, sulfate-independent AOM (i.e. nitrite-dependent AOM) could be carried out exclusively by bacteria and therefore would be completely independent of methane production. While this mechanistic dichotomy is plausible, it seems the simplest explanation – AOM and MOG are mechanistically separate processes – is the most likely situation.

4.2.4. Impact of Hydrogen and Acetate on AOM

Acetate and hydrogen have both been proposed as intermediates in sulfate-dependant AOM, wherein the methane oxidizing partner of the consortium produces one of these substrates for consumption by the sulfate-reducing partner (Hoehler et al., 1994; Valentine and Reeburgh, 2000). Thermodynamically, higher concentrations of these species should inhibit AOM rates if they are indeed the intermediate transferred during syntrophic methane oxidation. Surprisingly, the highest rates of AOM coincided with the highest concentrations of hydrogen and acetate (Figs. 5.4 and 5.5). Further, a significant linear relationship was observed between acetate concentrations and AOM rates in DB slurries. The relationship was much weaker for the HC slurries, suggesting that distinct

physiological populations of methanotrophs carried out AOM at the two sites. The addition of both hydrogen and acetate stimulated methane consumption in lake sediments and sludge (Zehnder and Brock, 1980). In experiments with deep-water cold seep sediments, Orcutt et al. (2008) reported significant increases in AOM rates with the addition of acetate, although this was not observed in shallow-water cold seep sediments. These findings, in combination with our results, do not implicate an acetate or hydrogen intermediate in the AOM process. Although the mechanism is unclear and admittedly counter-intuitive, low-molecular weight substrates such as acetate and hydrogen appear to stimulate AOM activity. The positive effect of acetate and hydrogen concentrations on AOM rates may suggest a more complicated mechanism than simply supplying substrates for methane oxidizers and/or their possible syntrophic partners.

4.2.5. Other Terminal Metabolic Processes

The addition of ferric citrate provided both a possible electron acceptor (soluble Fe(III)) and a labile carbon source (citrate) to the slurries. The significantly higher hydrogen and DIC concentrations (Fig. 5.2), as well as the pronounced DOC consumption and acetate production in the ferric citrate treatments of both sites, indicated that ferric citrate addition stimulated the total microbial activity. Surprisingly, the rates of AOM in the ferric citrate treatments accounted for an average of 6 % and 23 % of the increase in the DIC pool in DB and HC slurries, respectively. Given the difference in rates of AOM between the ferric citrate and ferrihydrite-amended slurries, one might infer that the addition of a labile carbon source resulted in higher rates of AOM, which is surprising. As observed previously (Orcutt et al., 2008; Zehnder and Brock, 1980), we propose the higher concentrations of acetate and hydrogen in the ferric citrate treatments

led to higher rates of AOM (Figs. 5.4 and 5.5). While we also documented enhanced iron reduction in these slurries relative to the control, further work is needed to isolate the influences of labile DOC, H₂, versus easily reducible iron sources on rates of AOM. The high rates of SR in the ferric citrate treatments may have been stimulated by the inflated H₂ and acetate concentrations in those slurries, both of which are known substrates of sulfate reducers (Canfield et al., 2005 and references therein). The high rates of SR despite low sulfate concentrations in the ferric citrate slurries require that reduced sulfur oxidation be an important process in these slurries. Tight sulfur redox coupling would provide a mechanism for resupplying sulfate to sulfate reducers (Bowles et al., 2011).

The increase in sulfate over time in the nitrate and birnessite amended slurries strongly suggests the oxidation of reduced solid phase sulfur species coupled to reduction of nitrate and Mn oxides (Aller and Rude 1988). The production of sulfate coupled to the reduction of nitrate and solid-phase Mn has been previously reported (Dannenberg et al., 1992; Lovley and Phillips, 1994). Brunet and Garcia-Lil (1996) reported the coupling of denitrification and dissimilatory nitrate reduction to ammonium to the oxidation of reduced sulfur species in nitrate-amended slurries. The steady nitrate consumption and sulfate and ammonium production in all nitrate-amended slurries suggests a similar mechanism occurring in these experiments. Several bacterial groups are capable of manganese- and/or nitrate-reduction coupled to sulfur oxidation, including a variety of sulfate reducers (Dannenberg et al., 1992; Lovley and Phillips, 1994), denitrifiers (Friedrich and Mitrenga, 1981), and metal-reducing bacteria (Nealson and Saffarini, 1994). In this experiment, the sulfur source was likely solid-phase sulfides as dissolved sulfide remained low or below detection throughout the experiment. Although sulfate was

an available electron acceptor for AOM in these slurries, AOM and SR were decoupled and AOM was more likely linked to nitrate/nitrite or Mn reduction (Table 5.4). The bacteria that mediate NO_x or Mn reduction can outcompete sulfate reducers for substrates (Acht nich et al., 1995; Hoehler et al., 1998), which likely repressed SR in these treatments. Furthermore, both nitrate and manganese reduction are more thermodynamically favorable processes than sulfate reduction whether coupled to AOM (Table 5.2) or to organic matter degradation (Schink 1997). NO_x and Mn-supported sulfide oxidation is a potential mechanism for replenishing sulfate in sediments with sufficient concentrations of these two electron acceptors which may in turn fuel SR activity once Mn and/or NO_x are exhausted. The oxidation of solid-phase sulfides by Mn-oxides or nitrate is an uncommonly reported process (Aller and Rude, 1988) but clearly warrants further study in coastal sediments.

4.3. Conclusions

A greater understanding of methane cycling in coastal wetlands is paramount to predicting the contribution of these wetlands to global methane fluxes under changing environmental conditions. Here, we report the first direct measurements of AOM in intertidal sediments. We demonstrate that both freshwater and brackish sediments support substantial rates of AOM. The regulation of AOM was explored by varying electron acceptor concentrations in enrichment experiments. The results suggest that AOM is controlled by a variety of factors, many of which are likely environment-specific. Based on the results from long-term enrichments, the addition of labile carbon with iron increased rates of AOM in both freshwater and brackish sediments, while sulfate-dependent AOM was more important in brackish settings. The individual roles of soluble

iron species and labile organic carbon on AOM rates remain unclear and warrant future study. Appreciable rates of AOM together with high AOM:SR ratios in slurries treated with nitrate, ferrihydrite, and birnessite suggest AOM was coupled to the reduction of nitrate/nitrite, amorphous solid iron(III), and solid manganese(IV) and was independent of sulfate and sulfate reduction. Sulfate-independent AOM was energetically more favorable than sulfate-dependent AOM both *in situ* and in the experimental slurries. Although rates of AOM linked to alternative electron acceptors were lower than AOM coupled to SR, the energy gain associated with sulfate-independent AOM were several times higher. We also documented AOM in the absence of MOG from bicarbonate or acetate, indicating independent mechanisms for these two processes, at least in sediments with low sulfate concentrations and SR rates. These results suggest that AOM in freshwater and brackish sediments may proceed through distinct pathways, with sulfate-dependent AOM of greater import in brackish sediments. Furthermore, the biogeochemical controls of AOM in deep-sea sediments are likely distinct from those operating in coastal sediments, which typically receive a greater influx of organic carbon and electron acceptors. Future studies should examine the effects of different labile carbon sources, hydrogen, and iron minerals on rates of AOM in both shallow brackish and freshwater settings.

Electronic Annex 1: Methods and Results of Solid-Phase Iron and Manganese Extractions for Slurries

Methods

At each time point adsorbed and dissolved iron(II) and manganese(II) were extracted from a 1 cm³ volume of slurried sediment with a buffered Ferrozine reagent and analyzed using flame atomic absorption spectrometry on a Perkin Elmer AAnalyst 400 (Hyacinthe et al., 2006). The concentration of the adsorbed species was determined as the difference between the concentration of the dissolved iron or manganese (II) and the total concentration of iron or manganese in the extracts. At the end of the experiment frozen sediments from the control, ferrihydrite, ferric citrate, and birnessite treatments from sampling days 0, 71, 132, and 181 were subjected to a sequential extraction of solid-phase iron and manganese following the methods of (Poulton and Canfield, 2005). All solid-phase calculations were corrected for porosity.

The solid-phase partitioning of iron and manganese minerals varied over the course of the experiment. Since the total iron and manganese content of the initial sediment differed between the two sites and because we added significant amounts of both iron and manganese oxides to some of the experimental treatments, we present the solid-phase mineralogy as a percent of the total mineral present in tables EA1 and EA2. Adsorbed Fe(II) content increased over time in the ferrihydrite and ferric-citrate amended slurries such that the % adsorbed iron was significantly higher in these two treatments than the control for both sites at the end of the experiment (Tables EA1 and EA2; $p < 0.05$). The proportion of adsorbed Mn(II) to total Mn was significantly higher than the control in the birnessite-amended slurries for DB but not for HC ($p < 0.05$). The proportion

of iron carbonates generally increased over time in the iron-amended slurries of both sites and was significantly higher than the control for both sites ($p < 0.05$). The amount of manganese in the carbonate fraction increased significantly during the experiment in all HC slurries and only in the birnessite-amended slurries of DB. At the termination of the experiment, 96 % and 87 % of the Mn(II) in the birnessite amendments was present in the carbonate fraction of the DB and HC slurries, respectively (Tables EA1 and EA2).

ACKNOWLEDGEMENTS

This research was funded by the US National Science Foundation (DEB 0717189 to SBJ). We thank Charles Schutte and Daniel Saucedo for assistance with sample collection; the GCE-LTER program for logistical support; Marshall Bowles and Vladimir Samarkin for help with radiotracer assays; Tom Maddox for use of analytical equipment; and, Beth Orcutt and Eric King for providing comments that improved the paper.

REFERENCES

- Achtnich, C., Bak, F., and Conrad, R. (1995) Competition for electron donors among nitrate reducers, ferric iron reducers, sulfate reducers, and methanogens in anoxic paddy soil. *Biology and Fertility of Soils* **19**, 65-72.
- Albert, D. B. and Martens, C. S. (1997) Determination of low-molecular-weight organic acid concentrations in seawater and pore-water samples via HPLC. *Marine Chemistry* **56**, 27-37.
- Aller, R. C. and Rude, P. D. (1988) Complete oxidation of solid phase sulfides by manganese and bacteria in anoxic marine sediments. *Geochimica et Cosmochimica Acta* **52**, 751-765.
- Alperin, M. J. and Hoehler, T. M. (2009) Anaerobic methane oxidation by archaea/sulfate-reducing bacteria aggregates: 1. Thermodynamic and physical constraints. *Am J Sci* **309**, 869-957.
- Alperin, M. J. and Reeburgh, W. S. (1985) Inhibition Experiments on Anaerobic Methane Oxidation. *Appl. Environ. Microbiol.* **50**, 940-945.

- Anselman, I. and Crutzen, P. J. (1989) Global distribution of natural freshwater wetlands and rice paddies, their net primary productivity, seasonality and possible methane emissions. . *Journal of Atmospheric Chemistry*, 307-359.
- Armstrong, P. B., Lyons, W. B., and Gaudette, H. E. (1979) Application of Formaldoxime Colorimetric Method for the Determination of Manganese in the Pore Water of Anoxic Estuarine Sediments. *Estuaries* **2**, 198-201.
- Barnes, R. O. and Goldberg, E. D. (1976) Methane production and consumption in anoxic marine sediments. *Geology* **4**, 297-300.
- Beal, E. J., Claire, M. W., and House, C. H. (2011) High rates of anaerobic methanotrophy at low sulfate concentrations with implications for past and present methane levels. *Geobiology* **9**, 131-139.
- Beal, E. J., House, C. H., and Orphan, V. J. (2009) Manganese- and Iron-Dependent Marine Methane Oxidation. *Science* **325**, 184-187.
- Blake, D. R. and Rowland, F. S. (1988) Continuing Worldwide Increase in Tropospheric Methane, 1978 to 1987. *Science* **239**, 1129-1131.
- Boetius, A., Ravenschlag, K., Schubert, C. J., Rickert, D., Widdel, F., Gieseke, A., Amann, R., Jorgensen, B. B., Witte, U., and Pfannkuche, O. (2000) A marine microbial consortium apparently mediating anaerobic oxidation of methane. *Nature* **407**, 623-626.
- Bollag, J.-M. and Henninger, N. M. (1978) Effects of nitrite toxicity on soil bacteria under aerobic and anaerobic conditions. *Soil Biology and Biochemistry* **10**, 377-381.

- Bowles, M. W., Samarkin, V. A., Bowles, K. M., and Joye, S. B. (2011) Weak coupling between sulfate reduction and the anaerobic oxidation of methane in methane-rich seafloor sediments during ex situ incubation. *Geochimica et Cosmochimica Acta* **75**, 500-519.
- Brunet, R. C. and Garcia-Gil, L. J. (1996) Sulfide-induced dissimilatory nitrate reduction to ammonia in anaerobic freshwater sediments. *FEMS microbiology ecology* **21**, 131-138.
- Canfield, D. E., Kristensen, E., and Thamdrup, B. (2005) *Aquatic Geomicrobiology*. . Elsevier, Amsterdam.
- Canfield, D. E., Raiswell, R., Westrich, J. T., Reaves, C. M., and Berner, R. A. (1986) The use of chromium reduction in the analysis of reduced inorganic sulfur in sediments and shales. *Chemical Geology* **54**, 149-155.
- Capone, D. G. and Kiene, R. P. (1988) Comparison of Microbial Dynamics in Marine and Freshwater Sediments: Contrasts in Anaerobic Carbon Catabolism. *Limnology and Oceanography* **33**, 725-749.
- Chidthaisong, A. and Conrad, R. (2000) Turnover of glucose and acetate coupled to reduction of nitrate, ferric iron and sulfate and to methanogenesis in anoxic rice field soil. *FEMS microbiology ecology* **31**, 73-86.
- Cline, J. D. (1969) Spectrophotometric Determination of Hydrogen Sulfide in Natural Waters. *Limnology and Oceanography* **14**, 454-458.
- Cornell, R. M. and Schwertmann, U. (2003) *The Iron Oxides: structure, properties, reactions, occurrences and uses, 2nd Edition*. . Wiley-VCH, Weinheim.

- Dannenberg, S., Kroder, M., Dilling, W., and Cypionka, H. (1992) Oxidation of H₂, organic compounds and inorganic sulfur compounds coupled to reduction of O₂ or nitrate by sulfate-reducing bacteria. *Archives of Microbiology* **158**, 93-99.
- Deborde, J., Anschutz, P., Auby, I., Glé, C., Commarieu, M.-V., Maurer, D., Lecroart, P., and Abril, G. (2008) Role of tidal pumping on nutrient cycling in a temperate lagoon (Arcachon Bay, France). *Marine Chemistry* **109**, 98-114.
- Deborde, J., Anschutz, P., Guérin, F., Poirier, D., Marty, D., Boucher, G., Thouzeau, G., Canton, M., and Abril, G. (2010) Methane sources, sinks and fluxes in a temperate tidal Lagoon: The Arcachon lagoon (SW France). *Estuarine, Coastal and Shelf Science* **89**, 256-266.
- Dentener, F., Van Weele, M., Krol, M., Houweling, S., and Van Velthoven, P. (2003) Trends and inter-annual variability of methane emissions derived from 1979-1993 global CTM simulations. *Atmospheric Chemistry and Physics* **3**, 73-88.
- Deutzmann, J. S. and Schink, B. (2011) Anaerobic Oxidation of Methane in Sediments of an Oligotrophic Freshwater Lake (Lake Constance). *Appl. Environ. Microbiol.*, AEM.00340-11.
- Devol, A. H. (1983) Methane Oxidation Rates in the Anaerobic Sediments of Saanich Inlet. *Limnology and Oceanography* **28**, 738-742.
- Ettwig, K. F., Butler, M. K., Le Paslier, D., Pelletier, E., Mangenot, S., Kuypers, M. M. M., Schreiber, F., Dutilh, B. E., Zedelius, J., de Beer, D., Gloerich, J., Wessels, H. J. C. T., van Alen, T., Luesken, F., Wu, M. L., van de Pas-Schoonen, K. T., Op den Camp, H. J. M., Janssen-Megens, E. M., Francoijs, K.-J., Stunnenberg, H.,

- Weissenbach, J., Jetten, M. S. M., and Strous, M. (2010) Nitrite-driven anaerobic methane oxidation by oxygenic bacteria. *Nature* **464**, 543-548.
- Ettwig, K. F., Shima, S., Van De Pas-Schoonen, K. T., Kahnt, J., Medema, M. H., Op Den Camp, H. J. M., Jetten, M. S. M., and Strous, M. (2008) Denitrifying bacteria anaerobically oxidize methane in the absence of Archaea. *Environmental Microbiology* **10**, 3164-3173.
- Ettwig, K. F., van Alen, T., van de Pas-Schoonen, K. T., Jetten, M. S. M., and Strous, M. (2009) Enrichment and Molecular Detection of Denitrifying Methanotrophic Bacteria of the NC10 Phylum. *Appl. Environ. Microbiol.* **75**, 3656-3662.
- Fossing, H. and Jørgensen, B. B. (1989) Measurement of bacterial sulfate reduction in sediments: Evaluation of a single-step chromium reduction method. *Biogeochemistry* **8**, 205-222.
- Friedrich, C. G. and Mitrenga, G. (1981) Oxidation of thiosulfate by *Paracoccus denitrificans* and other hydrogen bacteria. *FEMS Microbiology Letters* **10**, 209-212.
- Garcia-Gil, L. J. and Golterman, H. L. (1993) Kinetics of FeS-mediated denitrification in sediments from the Camargue (Rhône delta, southern France). *FEMS microbiology ecology* **13**, 85-91.
- Golden, D. C., Dixon, J. B., and Chen, C. C. (1986) Ion exchange, thermal transformations, and oxidizing properties of birnessite. *Clays and Clay Minerals* **34**, 511-520.

- Hallam, S. J., Putnam, N., Preston, C. M., Detter, J. C., Rokhsar, D., Richardson, P. M., and DeLong, E. F. (2004) Reverse Methanogenesis: Testing the Hypothesis with Environmental Genomics. *Science* **305**, 1457-1462.
- Hansen, L. B., Finster, K., Fossing, H., and Iversen, N. (1998) Anaerobic methane oxidation in sulfate depleted sediments: effects of sulfate and molybdate additions. *Aquatic Microbial Ecology* **14**, 195-204.
- Hinrichs, K.-U., Hayes, J. M., Sylva, S. P., Brewer, P. G., and DeLong, E. F. (1999) Methane-consuming archaeobacteria in marine sediments. *Nature* **398**, 802-805.
- Hoehler, T. M., Alperin, M. J., Albert, D. B., and Martens, C. S. (1994) Field and laboratory studies of methane oxidation in an anoxic marine sediment: Evidence for a methanogen-sulfate reducer consortium. *Global Biogeochem. Cycles* **8**, 451-463.
- Hoehler, T. M., Alperin, M. J., Albert, D. B., and Martens, C. S. (1998) Thermodynamic control on hydrogen concentrations in anoxic sediments. *Geochimica et Cosmochimica Acta* **62**, 1745-1756.
- Hu, S., Zeng, R. J., Burow, L. C., Lant, P., Keller, J., and Yuan, Z. (2009) Enrichment of denitrifying anaerobic methane oxidizing microorganisms. *Environmental Microbiology Reports* **1**, 377-384.
- Hyacinthe, C., Bonneville, S., and Van Cappellen, P. (2006) Reactive iron(III) in sediments: Chemical versus microbial extractions. *Geochimica et Cosmochimica Acta* **70**, 4166-4180.
- Iversen, N. and Blackburn, T. H. (1981) Seasonal Rates of Methane Oxidation in Anoxic Marine Sediments. *Appl. Environ. Microbiol.* **41**, 1295-1300.

- Iversen, N. and Jorgensen, B. B. (1985) Anaerobic Methane Oxidation Rates at the Sulfate-Methane Transition in Marine Sediments from Kattegat and Skagerrak (Denmark). *Limnology and Oceanography* **30**, 944-955.
- Joye, S. B., Boetius, A., Orcutt, B. N., Montoya, J. P., Schulz, H. N., Erickson, M. J., and Lugo, S. K. (2004) The anaerobic oxidation of methane and sulfate reduction in sediments from Gulf of Mexico cold seeps. *Chemical Geology* **205**, 219-238.
- Joye, S. B., Connell, T. L., Miller, L. G., Oremland, R. S., and Jellison, R. S. (1999) Oxidation of Ammonia and Methane in an Alkaline, Saline Lake. *Limnology and Oceanography* **44**, 178-188.
- Joye, S. B., Samarkin, V. A., Orcutt, B. N., MacDonald, I. R., Hinrichs, K.-U., Elvert, M., Teske, A. P., Lloyd, K. G., Lever, M. A., Montoya, J. P., and Meile, C. D. (2009) Metabolic variability in seafloor brines revealed by carbon and sulphur dynamics. *Nature Geosci* **2**, 349-354.
- Kelley, C. A., Martens, C. S., and III, W. U. (1995) Methane dynamics across a tidally flooded riverbank margin. *Limnology and Oceanography* **40**, 1112-1129.
- Klüber, H. D. and Conrad, R. (1998) Effects of nitrate, nitrite, NO and N₂O on methanogenesis and other redox processes in anoxic rice field soil. *FEMS Microbiology Ecology* **25**, 301-318.
- Knittel, K. and Boetius, A. (2009) Anaerobic Oxidation of Methane: Progress with an Unknown Process. *Annual Review of Microbiology* **63**, 311-334.
- Knittel, K., Losekann, T., Boetius, A., Kort, R., and Amann, R. (2005) Diversity and Distribution of Methanotrophic Archaea at Cold Seeps. *Appl. Environ. Microbiol.* **71**, 467-479.

- Lovley, D. R. and Klug, M. J. (1983) Methanogenesis from Methanol and Methylamines and Acetogenesis from Hydrogen and Carbon Dioxide in the Sediments of a Eutrophic Lake. *Appl. Environ. Microbiol.* **45**, 1310-1315.
- Lovley, D. R. and Phillips, E. J. P. (1994) Novel Processes for Anaerobic Sulfate Production from Elemental Sulfur by Sulfate-Reducing Bacteria. *Appl. Environ. Microbiol.* **60**, 2394-2399.
- Martens, C. S. and Berner, R. A. (1974) Methane Production in the Interstitial Waters of Sulfate-Depleted Marine Sediments. *Science* **185**, 1167-1169.
- Mason, I. (1977) Methane as a Carbon Source in Biological Denitrification. *Journal (Water Pollution Control Federation)* **49**, 855-857.
- Meulepas, R., Jagersma, C., Khadem, A., Stams, A., and Lens, P. (2010) Effect of methanogenic substrates on anaerobic oxidation of methane and sulfate reduction by an anaerobic methanotrophic enrichment. *Applied Microbiology and Biotechnology* **87**, 1499-1506.
- Mitsch, W. J. and Gosselink, J. G. (2007) *Wetlands, 4th Ed.* . John Wiley & Sons, Inc. , New York.
- Moran, J. J., House, C. H., Freeman, K. H., and Ferry, J. G. (2005) Trace methane oxidation studied in several Euryarchaeota under diverse conditions. *Archaea* **1**, 303-309.
- Moran, J. J., House, C. H., Thomas, B., and Freeman, K. H. (2007) Products of trace methane oxidation during nonmethyltrophic growth by Methanosarcina. *J. Geophys. Res.* **112**, G02011.

- Nauhaus, K., Boetius, A., Krüger, M., and Widdel, F. (2002) In vitro demonstration of anaerobic oxidation of methane coupled to sulphate reduction in sediment from a marine gas hydrate area. *Environmental Microbiology* **4**, 296-305.
- Nauhaus, K., Treude, T., Boetius, A., and Krüger, M. (2005) Environmental regulation of the anaerobic oxidation of methane: a comparison of ANME-I and ANME-II communities. *Environmental Microbiology* **7**, 98-106.
- Nealson, K. H. and Saffarini, D. (1994) Iron and manganese in anaerobic respiration: environmental significance, physiology, and regulation. . *Annual Reviews of Microbiology* **48**, 311-343.
- Orcutt, B., Boetius, A., Elvert, M., Samarkin, V., and Joye, S. B. (2005) Molecular biogeochemistry of sulfate reduction, methanogenesis and the anaerobic oxidation of methane at Gulf of Mexico cold seeps. *Geochimica et Cosmochimica Acta* **69**, 4267-4281.
- Orcutt, B., Samarkin, V., Boetius, A., and Joye, S. B. (2008) On the relationship between methane production and oxidation by anaerobic methanotrophic communities from cold seeps of the Gulf of Mexico. *Environmental Microbiology* **10**, 1108-1117.
- Orcutt, B. N., Joye, S. B., Kleindienst, S., Knittel, K., Ramette, A., Reitz, A., Samarkin, V., Treude, T., and Boetius, A. (2010) Impact of natural oil and higher hydrocarbons on microbial diversity, distribution, and activity in Gulf of Mexico cold-seep sediments. *Deep Sea Research Part II: Topical Studies in Oceanography* **57**, 2008-2021.

- Oremland, R. S. and Capone, D. G. (1988) Use of 'specific' inhibitors in biogeochemistry and microbial ecology. *Advances in Microbial Ecology* **10**, 285-383.
- Orphan, V. J., Hinrichs, K.-U., Ussler, W., III, Paull, C. K., Taylor, L. T., Sylva, S. P., Hayes, J. M., and Delong, E. F. (2001) Comparative Analysis of Methane-Oxidizing Archaea and Sulfate-Reducing Bacteria in Anoxic Marine Sediments. *Appl. Environ. Microbiol.* **67**, 1922-1934.
- Parsons, T. R., Maita, Y., and Lalli, C. (1984) *A manual of chemical and biological methods for seawater analysis*. Pergamon Press, Oxford Oxfordshire.
- Pernthaler, A., Dekas, A. E., Brown, C. T., Goffredi, S. K., Embaye, T., and Orphan, V. J. (2008) Diverse syntrophic partnerships from deep-sea methane vents revealed by direct cell capture and metagenomics. *Proceedings of the National Academy of Sciences* **105**, 7052-7057.
- Poulton, S. W. and Canfield, D. E. (2005) Development of a sequential extraction procedure for iron: implications for iron partitioning in continentally derived particulates. *Chemical Geology* **214**, 209-221.
- Raghoebarsing, A. A., Pol, A., van de Pas-Schoonen, K. T., Smolders, A. J. P., Ettwig, K. F., Rijpstra, W. I. C., Schouten, S., Damste, J. S. S., Op den Camp, H. J. M., Jetten, M. S. M., and Strous, M. (2006) A microbial consortium couples anaerobic methane oxidation to denitrification. *Nature* **440**, 918-921.
- Reeburgh, W. S. (1967) An Improved Interstitial Water Sampler. *Limnology and Oceanography* **12**, 163-165.
- Reeburgh, W. S. (1976) Methane consumption in Cariaco Trench waters and sediments. *Earth and Planetary Science Letters* **28**, 337-344.

- Reeburgh, W. S. (1996) "Soft spots" in the global methane budget. In: Lindstrom, M. E. and Tabita, F. F. (Eds.), *Microbial growth on Cl compounds*. Kluwer Academic Publishers, Dordrecht.
- Reeburgh, W. S. (2007) Oceanic Methane Biogeochemistry. *Chemical Reviews* **107**, 486-513.
- Shima, S. and Thauer, R. K. (2005) Methyl-coenzyme M reductase and the anaerobic oxidation of methane in methanotrophic Archaea. *Current Opinion in Microbiology* **8**, 643-648.
- Solorzano, L. (1969) Determination of Ammonia in Natural Waters by the Phenolhypochlorite Method. *Limnology and Oceanography* **14**, 799-801.
- Stookey, L. L. (1970) Ferrozine---a new spectrophotometric reagent for iron. *Analytical Chemistry* **42**, 779-781.
- Stumm, W. and Morgan, J. J. (1996) *Aquatic chemistry: Chemical equilibria and rates in natural waters*. Wiley, New York.
- Thalasso, F., Vallecillo, A., García-Encina, P., and Fdz-Polanco, F. (1997) The use of methane as a sole carbon source for wastewater denitrification. *Water Research* **31**, 55-60.
- Thauer, R. K. (2010) Functionalization of Methane in Anaerobic Microorganisms. *Angewandte Chemie International Edition* **49**, 6712-6713.
- Treude, T., Boetius, A., Knittel, K., Wallmann, K., and Jørgensen, B. B. (2003) Anaerobic oxidation of methane above gas hydrates at Hydrate Ridge, NE Pacific Ocean. *Marine Ecology Progress Series* **264**, 1-14.

- Valentine, D. L. and Reeburgh, W. S. (2000) New perspectives on anaerobic methane oxidation. *Environmental Microbiology* **2**, 477-484.
- Weiss, R. F. (1970) The solubility of nitrogen, oxygen and argon in water and seawater. *Deep Sea Research and Oceanographic Abstracts* **17**, 721-735.
- Westermann, P. and Ahring, B. K. (1987) Dynamics of Methane Production, Sulfate Reduction, and Denitrification in a Permanently Waterlogged Alder Swamp. *Appl. Environ. Microbiol.* **53**, 2554-2559.
- Weston, N., Vile, M., Neubauer, S., and Velinsky, D. (2011) Accelerated microbial organic matter mineralization following salt-water intrusion into tidal freshwater marsh soils. *Biogeochemistry* **102**, 135-151.
- Winfrey, M. R. and Zeikus, J. G. (1977) Effect of sulfate on carbon and electron flow during microbial methanogenesis in freshwater sediments. *Appl. Environ. Microbiol.* **33**, 275-281.
- Zehnder, A. J. and Brock, T. D. (1979) Methane formation and methane oxidation by methanogenic bacteria. *J. Bacteriol.* **137**, 420-432.
- Zehnder, A. J. B. and Brock, T. D. (1980) Anaerobic Methane Oxidation: Occurrence and Ecology. *Appl. Environ. Microbiol.* **39**, 194-204.
- Zumft, W. G. (1993) The biological role of nitric oxide in bacteria. *Archives of Microbiology* **160**, 253-264.

Table 5.1. Comparison of relevant biogeochemical parameters within the SMTZ (top 12 cm) of sediments from Dover Bluff (DB) and Hammersmith Creek (HC) in July 2009. All activities and species are reported as areal rates/concentrations except for pH and salinity which are reported as an average within the top 20 cm. All values are the average of triplicate cores +/- the standard error.

Activity	DB	HC
AOM ($\mu\text{mol m}^{-2} \text{d}^{-1}$)	2.1 \pm 1.0	1.7 \pm 0.1
SR ($\mu\text{mol m}^{-2} \text{d}^{-1}$)	7.3 \pm 0.01	143.5 \pm 66.0
Species	DB	HC
methane (mmol m^{-2})	65.9 \pm 4.1	106.8 \pm 5.7
sulfate (mmol m^{-2})	709.1 \pm 116.6	38.5 \pm 2.6
sulfide (mmol m^{-2})	216.8 \pm 6.3	3.0 $\times 10^{-2}$ \pm 1.0 $\times 10^{-2}$
[Mn ²⁺] (mmol m^{-2})	5.4 \pm 0.2	40.2 \pm 3.2
[Fe ²⁺] (mmol m^{-2})	1.4 \pm 0.1	2.3 \pm 0.4
nitrite (mmol m^{-2})	0.8 \pm 0.2	0.2 \pm 0.1
nitrate (mmol m^{-2})	2.7 \pm 0.3	6.6 \pm 0.1
hydrogen* ($\mu\text{mol m}^{-2}$)	4.7 \pm 0.4	12.5 \pm 2.3
[DIC] (mol m^{-2})	2.0 \pm 0.2	0.7 \pm 0.0
[DOC] (mol m^{-2})	0.4 \pm 0.0	0.3 \pm 0.0
salinity (psu)	22.5 \pm 1.9	0.0 \pm 0.0
pH	7.1 \pm 0.1	7.0 \pm 0.2

Abbreviations: SMTZ, sulfate-methane transition zone, AOM, anaerobic oxidation of methane determined via radio tracers, [Fe²⁺], dissolved reduced iron, [Mn²⁺], dissolved reduced manganese, [DIC], dissolved inorganic carbon, [DOC], dissolved organic carbon. * Hydrogen was determined as steady state concentrations (see methods for details).

Table 5.2. The Gibbs free energies (in kJ mol CH₄⁻¹) for the oxidation of methane with various electron acceptors and hydrogenotrophic methanogenesis. Values for the standard free energies were calculated using Stumm and Morgan (1996). The energy yields of reaction are given as an average of triplicate cores (0-12 cm) with the standard error and were calculated with the average *in situ* activities of the products and reactants (see methods for details).

Reaction	ΔG^0	ΔG_{rxn} in top 12 cm	
		DB	HC
<i>Sulfate</i> : CH ₄ + SO ₄ ²⁻ → HCO ₃ ⁻ + HS ⁻ + H ₂ O	-33	-30 ± 2	-46 ± 1
<i>Aqueous Fe(III)</i> : CH ₄ + 8 Fe ³⁺ + 3 H ₂ O → HCO ₃ ⁻ + 8 Fe ²⁺ + 9 H ⁺	-435	-754 ± 4	-761 ± 3
<i>Ferrihydrite</i> : CH ₄ + 8Fe(OH) ₃ + 15 H ⁺ → HCO ₃ ⁻ + 8 Fe ²⁺ + 21 H ₂ O	-571	-175 ± 8	-192 ± 8
<i>Birnessite</i> : CH ₄ + 4 MnO ₂ + 7 H ⁺ → HCO ₃ ⁻ + 4Mn ²⁺ + 5 H ₂ O	-790	-594 ± 4	-577 ± 2
<i>Nitrate</i> : 5 CH ₄ + 8 NO ₃ ⁻ + 3 H ⁺ → 5 HCO ₃ ⁻ + 4 N ₂ + 9 H ₂ O	-801	-762 ± 1	-767 ± 1
<i>Nitrite</i> : 3 CH ₄ + 8 NO ₂ ⁻ + 5 H ⁺ → 3 HCO ₃ ⁻ + 8 N ₂ + 7 H ₂ O	-1007	-872 ± 2	-867 ± 3
<i>Hydrogenotrophic MCG</i> : 4 H ₂ + HCO ₃ ⁻ + H ⁺ → CH ₄ + 3 H ₂ O	-57	-6 ± 1	-3 ± 4

Table 5.3. Concentrations of several dissolved species in slurries after 181 days (time final). Values represent the average of 3 slurries \pm the standard error. The concentrations of those species which were inflated by each treatment are bolded (e.g. enriched manganese concentrations in the birnessite treatments)

Site	Treatment	Sulfide ($\mu\text{mol L}^{-1}$)	Phosphate ($\mu\text{mol L}^{-1}$)	Fe ²⁺ ($\mu\text{mol L}^{-1}$)	Mn ²⁺ ($\mu\text{mol L}^{-1}$)	Nitrate ($\mu\text{mol L}^{-1}$)	Nitrite ($\mu\text{mol L}^{-1}$)
DB	Control	162.5 \pm 6.1	247.4 \pm 2.0	3.3 \pm 3	13.1 \pm 0.1	<i>bdl</i>	0.8 \pm 0.1
	Ferrihydrite	<i>bdl</i>	0.5 \pm 0.1	53.1 \pm 1.5	4.5 \pm 0.1	<i>bdl</i>	0.2 \pm 4.1 $\times 10^{-2}$
	Ferric Citrate	<i>bdl</i>	15.9 \pm 3.1	429.2 \pm 19.8	76.3 \pm 4.0	<i>bdl</i>	1.4 \pm 0.1
	Sulfate	1365.8 \pm 73.6	283.4 \pm 1.0	6.8 \pm 0.3	26.4 \pm 0.3	<i>bdl</i>	0.5 \pm 0.5
	Nitrate	<i>bdl</i>	136.1 \pm 1.5	1.6 \pm 0.1	4.3 \pm 0.2	564.7 \pm 2.9	3 \pm 0.1
	Birnessite	<i>bdl</i>	2.2 \pm 0.0	0.8 \pm 3 $\times 10^{-1}$	383.2 \pm 31.9	<i>bdl</i>	<i>bdl</i>
HC	Control	<i>bdl</i>	83.5 \pm 4.2	71.2 \pm 1.0	250.8 \pm 6.1	<i>bdl</i>	0.8 \pm 0.1
	Ferrihydrite	<i>bdl</i>	1.4 \pm 0.1	73.5 \pm 2.4	104.0 \pm 1.3	<i>bdl</i>	0.1 \pm 1.2 $\times 10^{-2}$
	Ferric Citrate	0.3 \pm 0.2	11.8 \pm 0.2	340.3 \pm 17.4	52.4 \pm 3.1	<i>bdl</i>	1.5 \pm 0.3
	Sulfate	1.8 \pm 0.3	161.3 \pm 1.4	50.5 \pm 0.5	72.9 \pm 1.8	0.2 \pm 0.1	1.7 \pm 0.2
	Nitrate	0.2 \pm 0.1	7.4 \pm 0.4	13.6 \pm 1.9	24.5 \pm 2.2	490 \pm 5.7	2.7 \pm 0.3
	Birnessite	<i>bdl</i>	21.4 \pm 0.4	42.7 \pm 1.9	33.4 \pm 0.3	3.9 \pm 0.8	4 \pm 0.1

Abbreviations: Fe²⁺, dissolved iron II; Mn²⁺, dissolved manganese II; *bdl*, below detection limit.

Table 5.4. Summary of rates of methane oxidation (AOM), methane produced from radiolabeled acetate and bicarbonate (MOG), and sulfate reduction (SR) in slurries after 181 days (time final). The percent of methane produced from acetate is given as an average percent and the ratio of AOM to MOG and to SR are reported as an average ratio. Rates are reported in mmol cm⁻³ slurry d⁻¹ and are reported as the average of 3 slurries ± the standard error. See methods for details.

Site	Treatment	AOM	MOG	% ace	SR	Ratio of AOM	
						:MOG	:SR
DB	control	4.9 ± 0.2	10.6 ± 1.9	69	6.5 ± 0.4	0.5	0.8
	ferrhydrite	3.9 ± 0.3	0.9 ± 0.3	92	1.4 ± 0.2	4.4	1.8
	ferric citrate	9.9 ± 0.3	22.1 ± 5.6	87	38.0 ± 1.4	0.4	0.3
	sulfate	6.6 ± 0.2	1.5 ± 0.4	50	25.1 ± 1.8	4.5	0.3
	nitrate	4.3 ± 0.1	<i>bdl</i>	<i>nc</i>	0.3 ± 0.1	<i>nc</i>	34.3
	bimessite	2.4 ± 0.2	<i>bdl</i>	<i>nc</i>	1.6 ± 0.1	<i>nc</i>	1.5
HC	control	26.6 ± 0.4	7.7 ± 2.7	28	17.2 ± 2.7	3.5	1.1
	ferrhydrite	12.4 ± 0.3	0.7 ± 0.2	100	0.2 ± 1.2x10 ⁻²	16.6	83.4
	ferric citrate	30.9 ± 0.6	85.7 ± 17.0	71	13.9 ± 0.5	0.4	2.3
	sulfate	15.5 ± 0.3	2.1 ± 1.1	79	23.6 ± 0.5	7.4	0.7
	nitrate	4.9 ± 0.2	<i>bdl</i>	<i>nc</i>	0.1 ± 1.2x10 ⁻²	<i>nc</i>	143.1
	bimessite	3.6 ± 0.1	<i>bdl</i>	<i>nc</i>	0.1 ± 8.8x10 ⁻³	<i>nc</i>	42.9

Abbreviations: *bdl*, below detection limit; *nc*, not calculated due to *bdl* values.

Table EAI. Total iron and manganese content in control and metal-amended DB slurries reported as $\mu\text{mol g dry sediment}^{-1}$ and the composition of solid-phase iron and manganese reported as a percent of the total extractable trace metal.

DB Treatment	time (days)	Iron				Manganese			
		Total	% Adsorbed	% Carbonate	% Easily Reduced	Total	% Adsorbed	% Carbonate	% Easily Reduced
Control	0	853.2	0.0	4.8	0.6	7.6	0.0	9.6	0.3
	71	1013.8	0.0	5.1	1.1	8.8	0.0	12.6	0.0
	132	925.7	0.0	4.3	1.0	7.7	0.0	10.2	0.7
	181	811.7	0.0	4.3	3.9	6.7	0.0	9.7	6.9
Ferrihydrite	0	1031.0	0.1	15.0	17.8	6.8	0.0	12.8	2.3
	71	871.1	0.1	23.9	9.5	6.7	0.1	12.8	2.2
	132	1154.3	0.1	23.6	22.3	5.7	0.0	14.8	1.8
	181	1646.9	0.1	14.9	20.0	7.2	0.0	7.8	3.0
Ferric Citrate	0	878.1	0.0	10.2	4.7	6.9	0.0	10.7	4.6
	71	920.4	0.1	16.1	3.0	6.8	0.0	10.7	3.3
	132	973.4	0.0	22.4	4.5	6.5	0.0	11.2	2.9
	181	1243.6	0.1	30.4	2.6	7.4	0.0	15.4	1.2
Birnessite	0	842.3	0.0	6.2	3.5	225.3	0.4	66.2	25.6
	71	853.7	0.0	5.6	3.1	297.3	1.4	82.7	9.7
	132	865.1	0.0	5.1	2.7	369.4	2.0	92.7	0.0
	181	773.9	0.0	7.7	0.0	463.0	2.6	94.6	0.0

Table E.A2. Total extractable iron and manganese content in control and metal-amended HC slurries reported as $\mu\text{mol g dry sediment}^{-1}$ and the composition of solid-phase iron and manganese reported as a percent of the total extractable trace metal.

-HC Treatment	time (days)	Iron				Manganese			
		Total	% Adsorbed	% Carbonate	% Easily Reduced	Total	% Adsorbed	% Carbonate	% Easily Reduced
Control	0	1066.1	0.1	15.6	5.3	77.2	9.5	51.3	0.0
	71	1272.4	0.1	13.9	6.5	77.2	9.9	59.5	0.0
	132	942.8	0.1	19.1	9.7	70.4	10.2	56.8	7.4
	181	1300.8	0.1	10.3	7.7	63.1	10.8	72.9	0.0
Ferrihydrite	0	1224.5	0.1	9.6	24.9	78.0	10.0	57.4	0.0
	71	1142.3	0.1	14.0	25.2	75.7	8.7	70.8	0.0
	132	1402.0	0.1	14.3	35.5	79.1	4.7	70.4	0.0
	181	1595.8	0.1	18.2	32.0	64.4	2.3	100.0	0.0
Ferric Citrate	0	792.0	0.0	10.3	17.7	59.2	0.0	51.6	0.0
	71	1029.1	0.0	15.8	16.6	61.9	1.1	72.5	0.0
	132	1001.2	0.1	21.8	22.7	59.1	0.2	79.4	0.0
	181	1277.7	0.1	23.0	12.4	60.2	0.0	81.8	0.0
Eriocassite	0	979.1	0.0	14.3	13.1	253.1	0.8	58.9	42.9
	71	813.2	0.0	17.2	8.2	232.9	0.1	79.7	1.6
	132	804.7	0.0	13.4	6.5	297.5	0.0	90.9	0.0
	181	800.1	0.0	13.0	8.6	492.4	0.1	87.0	0.0

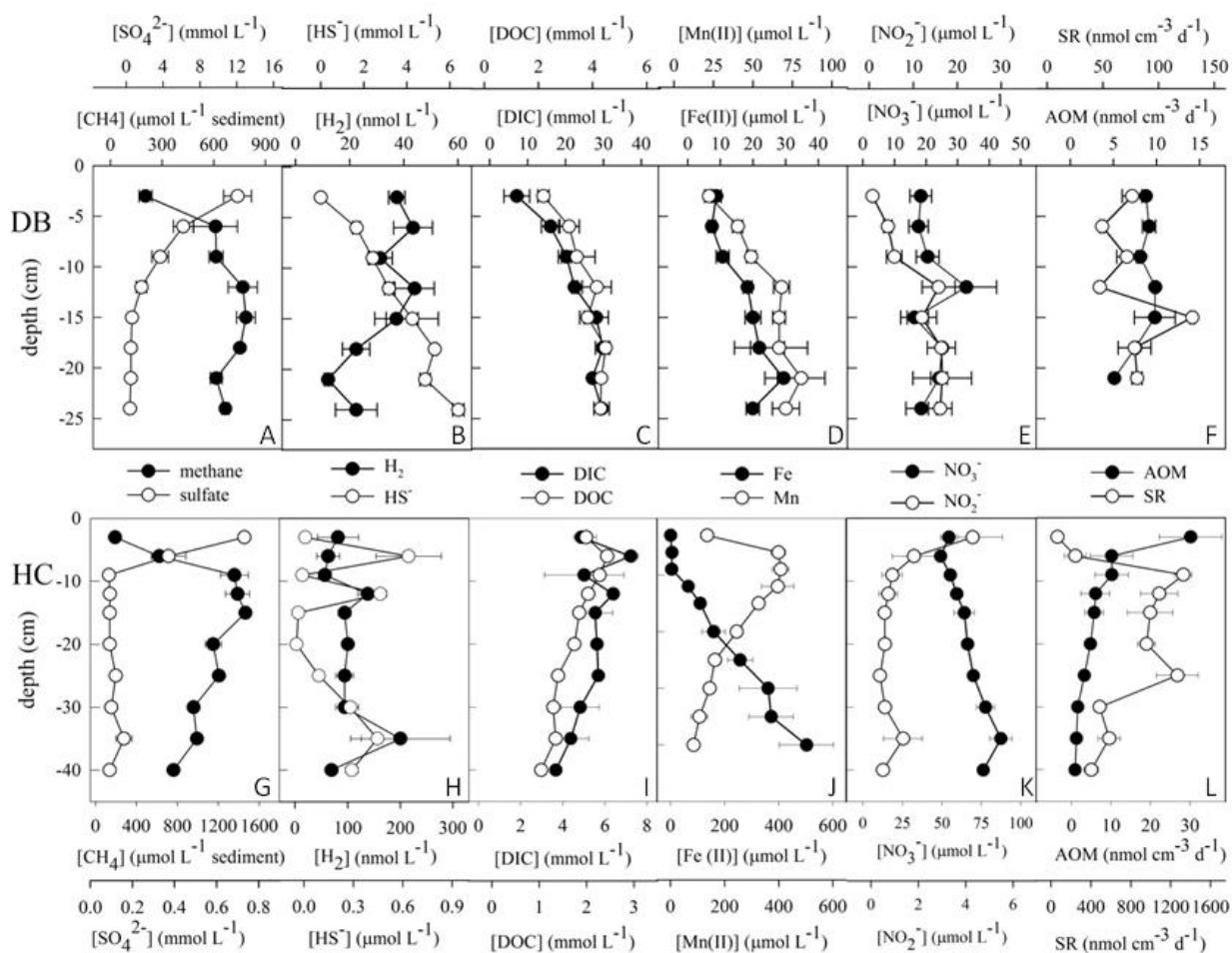


Fig. 5.1 A-L. Depth profiles of *in situ* sediment geochemistry and microbial activities at Dover Bluff (DB; A-F) and Hammersmith Creek (HC; G-L) in July 2009. Variables represented here are: methane and sulfate, A and G; sulfide and hydrogen, B and H; dissolved inorganic and organic carbon, C and I; dissolved, reduced manganese and iron, D and J; nitrate and nitrite, E and K; anaerobic oxidation of methane and sulfate reduction, F and L. Values are the average of replicate sediment cores (n=3) and error bars represent the standard error of the mean. Note the different scales between DB and HC for most parameters. Abbreviations used: CH₄, methane; SO₄²⁻, sulfate; HS⁻, hydrogen sulfide; DOC, dissolved organic carbon; DIC, dissolved inorganic carbon; Mn (II), dissolved manganese II; Fe (II), dissolved iron II; NO₂⁻, nitrite; NO₃⁻, nitrate; SR, sulfate reduction; AOM, anaerobic oxidation of methane. See text for details.

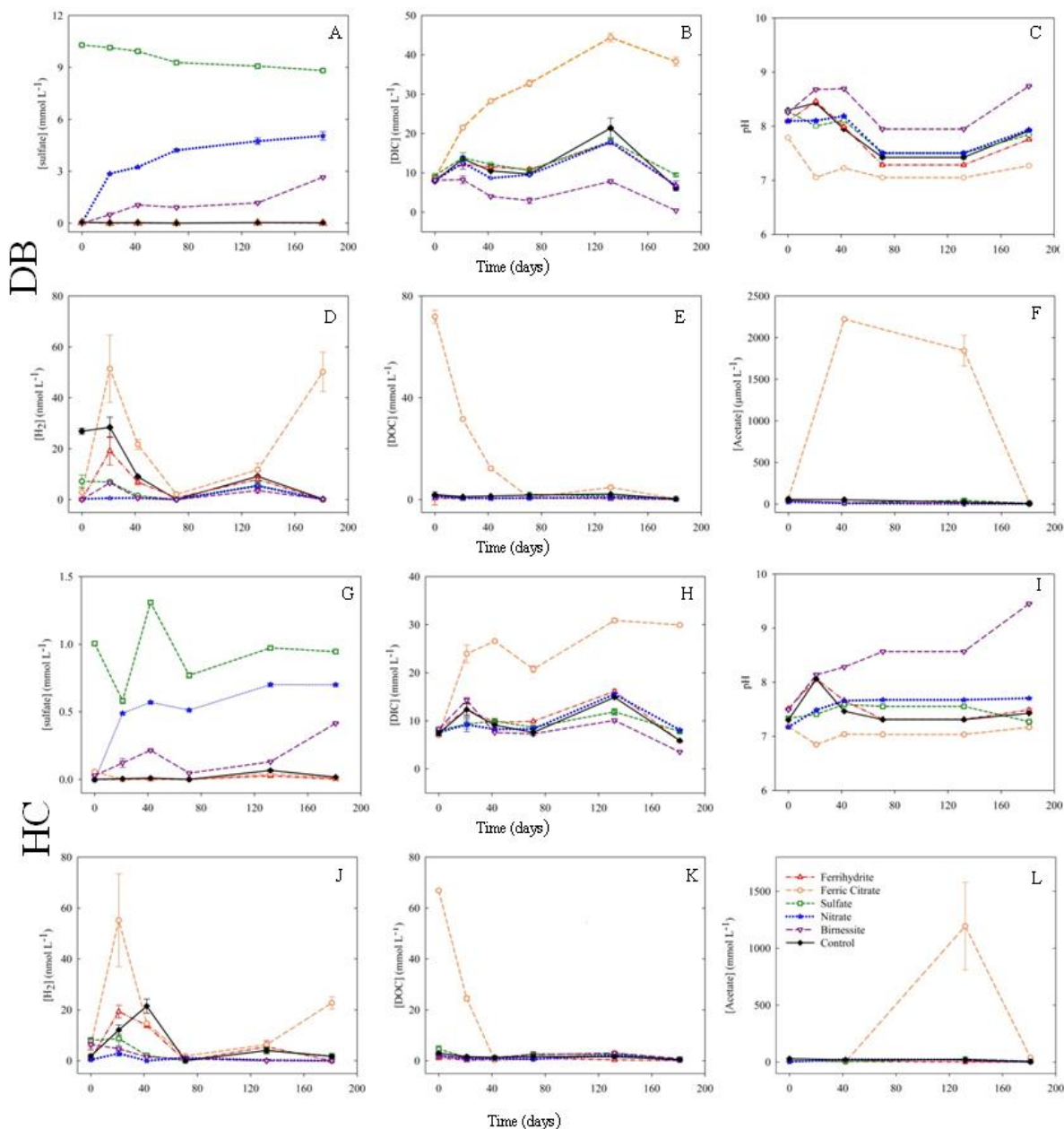
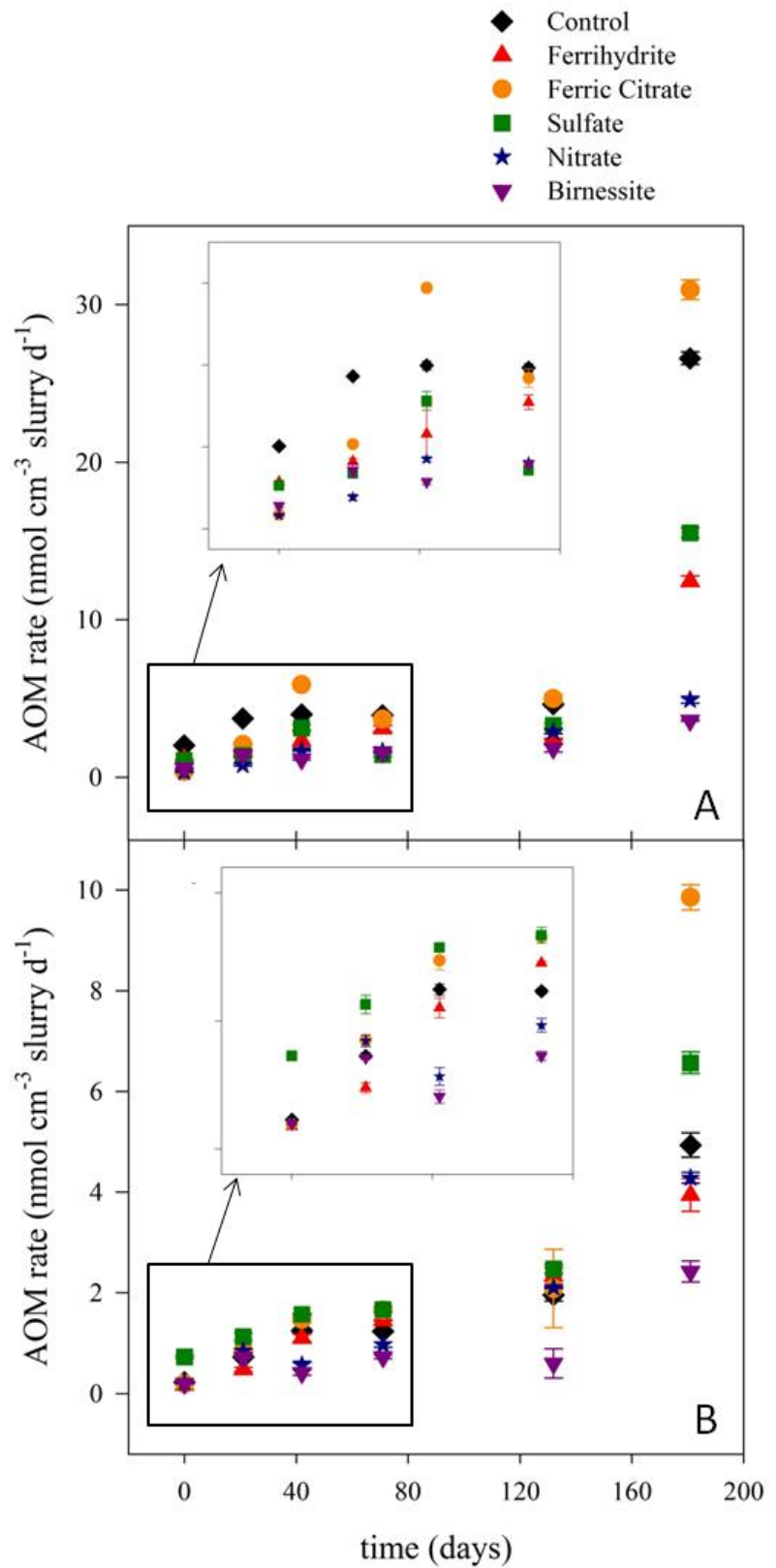


Fig. 5.2 A-L. Concentrations of sulfate (SO_4^{2-} ; A, G), dissolved inorganic carbon (DIC; B, H), the hydrogen ion as pH (C, I), dissolved hydrogen (H_2 ; D, J), dissolved organic carbon (DOC; E, K), and acetate (F, L) in DB (A-F) and HC (G-L) slurries during the experiment. Values are an average of triplicate slurries and error bars represent the standard error of those triplicates. Sulfate concentrations were monitored and re-amended as necessary in the sulfate-treated slurries (see text for details).

Fig. 5.3 A&B. Rates of anaerobic oxidation of methane (AOM) over time in slurries from HC (A) and DB (B) which were amended with various electron acceptors (key at top). Values are an average rate of 3 replicate slurries (minus a killed control) and error bars represent the standard error. In some cases the error bars are smaller than the symbol. The inserts provide detail for the first 80 days of the experiment.



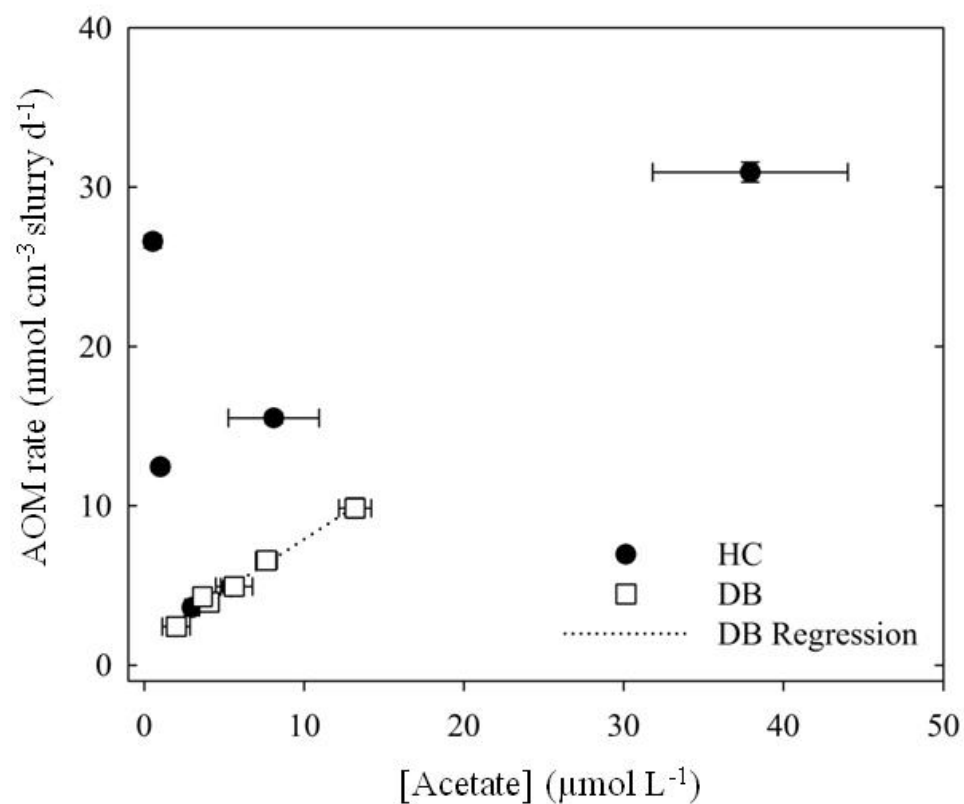


Fig. 5.4. Effect of acetate concentrations on rates of AOM in DB and HC slurries after 181 days. Values are an average of triplicate slurries and error bars represent the standard error. A linear fit is shown for DB data (dotted line) with an R^2 of 0.98 ($p < 0.05$).

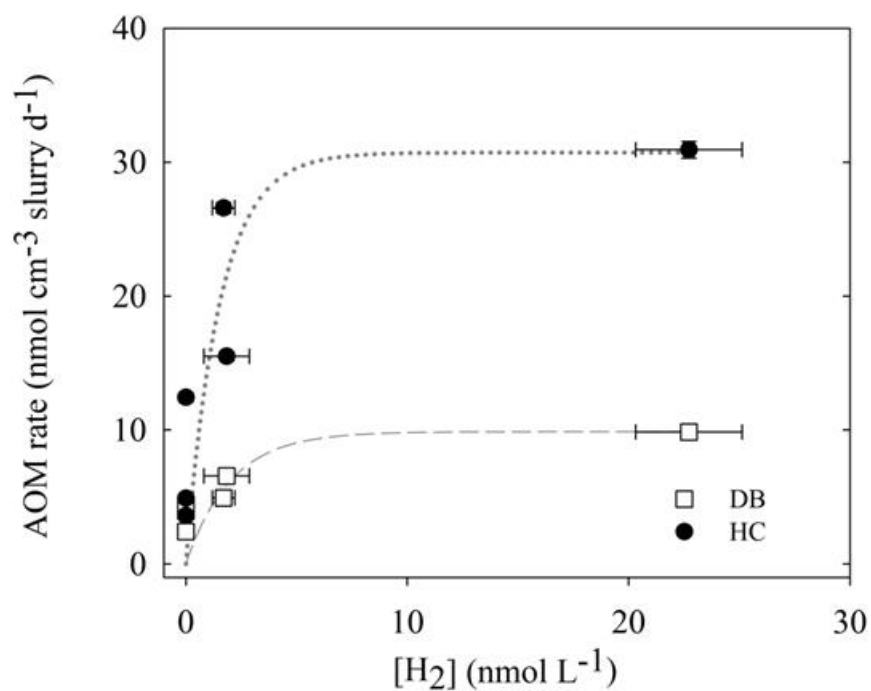


Fig. 5.5. Effect of hydrogen (H_2) concentrations on rates of anaerobic oxidation of methane in DB and HC slurries after 181 days. Values are an average of triplicate slurries and error bars represent the standard error. The dotted and dashed lines indicate a first-order exponential fit of the data for HC and DB, respectively.

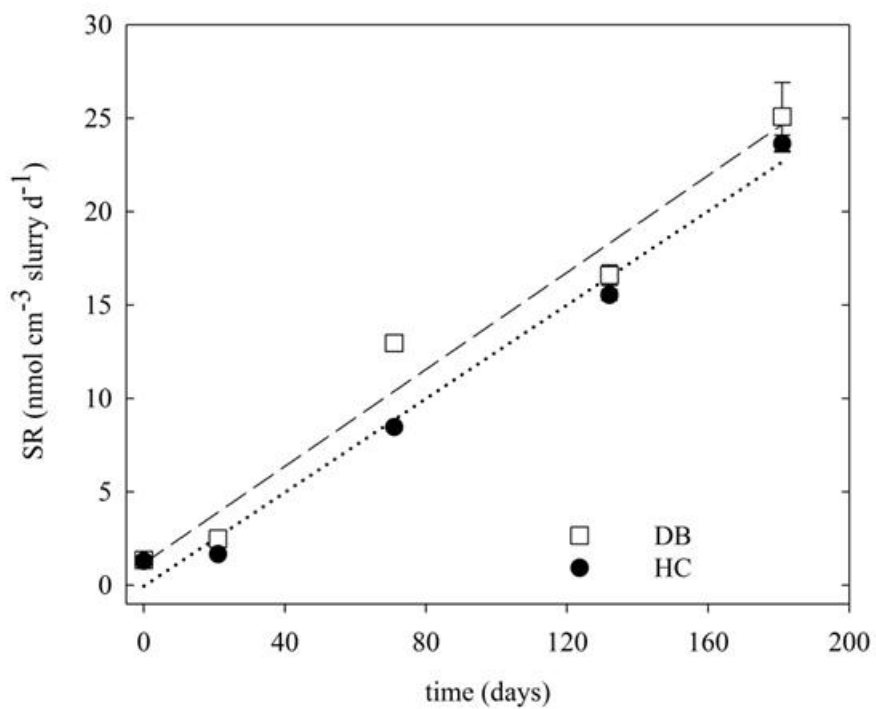


Fig. 5.6. Rates of sulfate reduction in sulfate treatments of the DB and HC slurries. Values are averaged rates of triplicate slurries and error bars represent the standard error. Linear fit lines are shown for DB (dotted line; $R^2 = 0.97$; $p < 0.05$) and HC (dashed line, $R^2 = 0.98$; $p < 0.05$).

CHAPTER 6

CONCLUSIONS AND OUTLOOK

The factors that control the production and consumption of methane, a major greenhouse gas, were explored in four separate studies. This dissertation advances the study of anaerobic carbon cycling in freshwater environments in a number of ways. 1) Although they represent a small area of the earth's surface, tidal, freshwater sediments may support high fluxes of methane to the atmosphere. 2) The methane budget in tidal, freshwater settings is seasonally variable and may be strongly influenced by tidal pumping of methane from adjacent sediments. 3) The anaerobic oxidation of methane (AOM) is an important process in some freshwater wetlands and sediments and is a major sink of methane in these environments. 4) Biomarker 'signatures' of AOM, which are common in marine settings, were not detected in any of the three freshwater environments examined in this dissertation. 5) The intact polar membrane lipids (IPLs) of the microbial community do not vary in concentration or composition in response to seasonal variations in microbial metabolism.

In *Chapter 2*, the seasonal controls on fluxes of methane from tidal, freshwater sediments were evaluated with field-based measurements and a 1D sediment model. Pronounced seasonal variations in methane emissions revealed an imbalance between *in situ* methane production and methane loss via flux from the top 40 cm of sediment column: Methane production was insufficient to support measured atmospheric fluxes. This methane deficit may be balanced by methane delivered to the system via tidal pumping. Modeled methane dynamics in these sediments corroborate this idea and methane input through lateral

advection is required to support the observed fluxes. Tidal freshwater wetlands, which represent a small area of the earth's surface, may serve as 'hot spots' in the global methane budget and many aspects of methane cycling in these environments are unique.

Chapters 3 and 4 of this dissertation challenged some previous assumptions governing freshwater carbon cycling. The importance of the anaerobic oxidation of methane (AOM) and sulfate reduction, two processes not traditionally associated with freshwater environments, were assessed in a freshwater sediment (*Chapter 3*) and two freshwater peatlands (*Chapter 4*). These chapters demonstrated that AOM and sulfate reduction may effectively limit methane emissions to the atmosphere either through its direct consumption (AOM) or through competitive interactions between methanogens and sulfate reducers. The rates of AOM detailed in these two chapters are among the first directly measured rates of AOM in freshwater environs. These rates of AOM may have been supported by sulfate reduction, which was found to be a more important terminal metabolism than methane production from acetate and bicarbonate. High contributions of both sulfate-reducing bacterial lipids and archaeal lipids associated with anaerobic methanotrophs to the IPL pool underscored the importance of these two processes. Yet, seasonal changes in microbial carbon flow were not reflected in the composition or concentrations of IPLs, suggesting that variations in carbon flow were not associated with changes in microbial biomass. Highly ¹³C depleted microbial lipids, which are often presented as a diagnostic for AOM in various settings, were not found in any of the freshwater environments studied in this dissertation. Isotopic evidence from freshwater wetland sediments (*Chapter 3*) and peat (*Chapter 4*) suggests that AOM dynamics in freshwater and marine ecosystems are dissimilar. As the

study of AOM extends beyond the marine realm, stable isotopic signatures of archaeal and bacterial biomarkers should be interpreted with caution.

The details regarding the process of AOM remain enigmatic. Laboratory-based manipulations which explored the mechanism of AOM in *Chapter 5* demonstrated that AOM in both freshwater and brackish sediments may be supported by sulfate reduction activity. Slurry incubations suggest that sulfate-independent AOM may occur in coastal sediments, though the importance of these processes remains unclear.

The reaction scheme, the organisms involved and their physiology, and the environmental factors controlling AOM are not well known. The importance of AOM has been demonstrated in marine sediments and now (*Chapters 3 and 4*) in freshwater wetlands. A greater understanding of this enigmatic process is necessary. The importance of AOM in other freshwater wetlands should be investigated. As these environments support high rates of methane flux to the atmosphere, it is critical to better constrain the role of this methane sink on a global scale. Climate predictions and methane budget models, which have previously ignored AOM as a methane sink in freshwater sediments, should be recalibrated to include the potentially strong influence of this process.

The seasonal controls on methanogenic carbon cycling in freshwater settings are complex. The response of peat wetlands to changes in temperature was in contradiction with previous findings in lake sediments and rice paddy soils. Future studies which seek to separate the effect of temperature, substrate availability, and microbial interactions may elucidate the individual roles of these variables. Some of the work presented in this dissertation conveys a connection between AOM and acetate cycling. The production of labile intermediates (e.g. acetate) through AOM may potentially provide substrates for

terminal metabolisms in freshwater sediments and peats. Such a mechanism would represent a previously overlooked pathway of carbon mineralization in freshwater sediments. As AOM activity in these settings may be quite high, as demonstrated in this work, the influence and seasonal controls of AOM on carbon cycling is a promising avenue of future research.